Regional corneal topographic responses in overnight orthokeratology and their influence on treatment zone decentration

Author:
Maseedupally, Vinod Kumar

Publication Date:
2013

DOI:
https://doi.org/10.26190/unsworks/16308

License:
https://creativecommons.org/licenses/by-nc-nd/3.0/au/
Link to license to see what you are allowed to do with this resource.

Downloaded from http://hdl.handle.net/1959.4/52849 in https://unsworks.unsw.edu.au on 2024-04-28

Regional corneal topographic responses in overnight orthokeratology and their influence on treatment zone decentration

Vinod Kumar Maseedupally ***B.S.Optom***

A thesis submitted in fulfilment of the requirements for admission to the degree of Doctor of Philosophy

School of Optometry and Vision Science

The University of New South Wales

Sydney, Australia

August 2013

ORIGINALITY STATEMENT

I hereby declare that this submission is my own work and to the best of my knowledge it contains no materials previously published or written by another person, or substantial portions of material which have been accepted for the award of any degree or diploma at UNSW or any other educational institution, except where due acknowledgement is made in the thesis. Any contribution made to the research by others, with whom I have worked at UNSW or elsewhere, is explicitly acknowledged in the thesis. I also declare that the intellectual content of this thesis is the product of my own work except to the extent of assistance from others in the project's design and conception or in style, presentation and linguistic expression is acknowledged.

Signed ……

Date ……

This thesis is dedicated to my father

Late Sri Subrahmanyam Maseedupally

‘Sometimes life hits you in the head with a brick. Don’t lose faith’

- *Steve Jobs*

ABSTRACT

Orthokeratology (OK) is a corneal reshaping procedure involving overnight wear of specialised rigid contact lenses, commonly prescribed for the correction of mild to moderate degrees of myopia associated with low degrees of astigmatism. Anecdotal clinical evidence has led to the currently accepted understanding that successful spherical OK lens fitting is limited to corneas with up to 1.50 DC of corneal toricity. Greater mismatch between the back surface of spherical OK lenses and the corneal surface with increasing corneal toricity is thought to be the main reason for this limitation. Toric OK lenses have recently been introduced, with the intention to improve lens alignment with the cornea and hence increase stability and success.

A successful OK lens fitting is characterised by a well-defined and centred treatment zone (TZ). TZ characteristics have been investigated for spherical OK lenses when fitted to eyes with minimal toricity, but the literature is sparse on the influence of higher degrees of corneal toricity on TZ characteristics. Further, there are no published reports on the performance of spherical and toric OK lenses on corneas with moderate amounts of corneal toricity. In the research reported in this thesis, possible corneal factors responsible for TZ decentration during spherical OK on eyes with minimal (< 1.50 DC) and moderate (1.50 to 3.50 DC) corneal toricity and also the performance of toric OK on eyes with moderately toric corneas were explored.

Based on previous reports of differing anterior ocular characteristics across ethnic groups, differences in corneal topography of East Asians and non-East Asians were investigated in relation to eyelid morphometry. Corneal topography was determined using the Medmont E300 corneal topographer. External eye photographs were captured by the Nikon D 5000 digital SLR camera, and were later exported into a customised MATLAB-based software program (i-Metrics) to quantify eyelid morphometric features. Using the raw corneal topographic data, the corneal shape in terms of corneal asphericity was determined across six different sectors, including supero-nasal, superior, supero-temporal, infero-temporal, inferior and infero-nasal sectors. Corneal shape was found to flatten at a faster rate in the nasal cornea compared with the temporal region, with no asymmetry found between superior and inferior sectors. The study also showed that corneal shape in terms of asphericity differed between East Asians and non-East Asians in a number of sectors, although only the superior sector showed a clinically significant difference. Several eyelid features including horizontal and vertical palpebral fissure widths, palpebral fissure slant, upper eyelid position, slope and curvature, lower eyelid slope and angle showed significant differences between East Asians and non-East Asians. However, when relationships between eyelid morphometry and corneal

shape were considered, only the influence of upper eyelid curvature on corneal shape was found to be different between the ethnic groups, with non-East Asians showing a stronger positive association with corneal spherical equivalent power than East Asians. The main conclusion from this study was that the nasal cornea was more prolate than the temporal cornea, suggesting that this asymmetry may have consequences for TZ decentration in OK lens wear.

A retrospective analysis was performed on data from a 2-week spherical OK lens-wearing study to understand whether the variation in normal corneal shape in minimally toric corneas influenced TZ centration. TZ diameter and centration were measured and assessed for association with sectorial corneal shape, and other corneal factors such as curvature along the principal corneal meridians and corneal toricity. It was found that after a single overnight wear the TZ tended to decentre away from the most prolate corneal region at baseline. This tendency was greater with longer duration of lens wear. Other corneal factors did not show a clinically relevant association with horizontal TZ decentration.

To investigate whether the decentred spherical OK lens after a single overnight wear in turn influences corneal shape in minimally toric corneas, further analysis was performed investigating corneal tangential curvature changes in four sectors (nasal, superior, temporal and inferior) and two zones, a central circular zone of 5 mm diameter and a para-central annular zone ranging between 5 and 8 mm diameter. Non-uniform corneal shape changes were found across sectors in the two different zones after spherical OK lens wear. These changes were more pronounced with longer duration of OK lens wear. Specifically it was shown that there was greater central flattening and para-central steepening in the temporal cornea when compared to the nasal cornea. These changes were consistent with temporal TZ decentration. Overall this study demonstrated that spherical OK lens wear tends to induce non-uniform corneal changes causing decentration of the TZ in minimally toric corneas.

To provide scientific evidence that fitting spherical OK lenses to highly toric corneas would lead to greater TZ decentration than when fitted to minimally toric corneas, a prospective study was conducted comparing these two groups. Spherical OK lenses on moderately toric corneas showed TZ decentration that was greater by 0.48 mm (p = 0.004, post hoc t-test) than when the same lens type was fit to minimally toric corneas. This confirmed the clinical opinion that fitting spherical lenses in eyes with greater than 1.50 DC of corneal toricity leads to poorer clinical outcomes.

To investigate whether TZ decentration could be reduced by altering the spherical OK lens fitting parameters, an alternative fitting approach was employed. This approach involved fitting moderately toric corneas with a modified lens sag height, analogous to the one-third fitting rule used when fitting conventional spherical rigid contact lenses to moderately toric corneas. The results showed no benefit of this alternative method over the conventional method.

In a small sample of four participants, the performance of toric OK lenses was investigated on moderately toric corneas in comparison to spherical OK lenses. The study showed a better quality TZ with toric OK lenses. An unexpected outcome was that the magnitude of TZ decentration was significantly greater in eyes fitted with toric OK lenses than when spherical OK lenses were used. However, the well defined TZ with distinct edges gave a dramatic improvement in unaided visual acuity. Other important observations of the study included that in some participants the refractive changes were not in agreement with corneal changes. Further studies using alternative corneal topographic analyses such as Zernike polynomials or Fourier analysis are required to explore if these methods are better in showing agreement between corneal and refractive outcomes.

From the series of studies reported in this thesis we were able to show that corneal shape parameters influence OK lens decentration, causing TZ decentration. Even though it might be assumed that spherical OK lenses show minimal lens and TZ decentration on minimally toric corneas, asymmetry in sectorial corneal asphericity affects TZ decentration. The decentred OK lens was also shown to induce non-uniform corneal changes with more pronounced central temporal flattening and para-central temporal steepening. It was also confirmed that fitting spherical OK lenses on moderately toric corneas leads to greater TZ decentration, suggesting the use of advanced OK lens designs such as toric OK lenses. Observations on a small number of participants with moderately toric corneas fitted with toric periphery OK lenses showed encouraging results, in particular enhanced definition of the TZ and a dramatic improvement in unaided visual acuity. This suggests that peripheral lens alignment is a critical factor in success of OK when fitting toric corneas.

ACKNOWLEDGEMENTS

Undertaking a PhD was my personal decision. However this journey would have not been possible without the encouragement, motivation and support that I received from my supervisors, friends and family.

Without hesitation, firstly I would like to acknowledge the support of my supervisor Professor Helen Swarbrick. She is certainly a human to understand a student before being a supervisor. She made tremendous contributions to this thesis work. I would like to thank you immensely for the knowledge you shared, time, advice, patience and the support you have given throughout my candidature. Your tender pat on my back was always a greatest motivation. I also feel very fortunate that you showed great confidence in me and helped me drive through this journey smoothly.

I would also like to thank my joint supervisor Dr. Paul Gifford who enormously contributed to this work. His knowledge on highly technical aspects of corneal topography and optics helped me drive through the bumpy road easily. The encouragement he provided in terms of setting timelines helped me to expedite my work all through the candidature. He also contributed greatly during thesis writing in ironing out the ripples of most written versions. I sincerely owe him for giving me the knowledge base required for scientific writing.

The encouragement I received from Dr Gullapalli N Rao, Prof Coen de Jong and Dr Savitri Sharma from LV Prasad Eye Institute, India were instrumental in laying a perfect path for doing this PhD.

It was indeed a great pleasure working with the famous Research in Orthokeratology (ROK) group, which included my supervisors, Helen O'Shea, Dr Ahmed Alharbi, Edward Lum, Dr Pauline Kang and Kathleen Watt. Edward Lum deserves a special mention for providing me his study data that contributed to two experimental chapters in this thesis work. His knowledge in industrial design helped him to discover dental floss as a sensible eyelid retractor used during corneal topography capture in initial experiments. In addition, discussions related to clinical outcomes after OK lens wear were useful in making important and timely decisions with regards to management. I simply do not hesitate to call him my 'big brother'. Discussions related to corneal topography and frequent proof reading of large portions of this thesis by Dr Pauline Kang were very useful in helping me succinctly express my scientific view points on various aspects of this research project.

Experts from Queensland University of Technology, Brisbane, Australia including Prof Michael Collins, Dr Scott Read, and Mr Brett Davis have generously shared their expertise in corneal topography and eyelid morphometry. I am very grateful to Dr Robert Iskander (Institute of Biomedical Engineering and Instrumentation, Wroclaw University of Technology, Wroclaw, Poland) for providing me the i-Metrics software to measure the eyelid morphometry parameters.

I would also extend my sincere thanks to Dr Isabelle Jalbert and Dr David Pye for their expert comments on my research work that guided me in setting the right protocols for various studies. Thanks to Thomas Naduvilath and Varghese for offering a help related to statistics without any hesitation.

The research presented in this thesis would not have been possible without the financial support from an Endeavour International Postgraduate Research Scholarship, a fund which I received from the Australian Government. Further support was received through the Australian Government ARC Linkage Project Scheme grant supported by industry partners Bausch & Lomb Boston (USA), BE Enterprises Pty, Lts and Capricornia Contact Lens Pty Ltd (Brisbane). I also would like to thank the Cornea and Contact Lens Society of Australia (CCLSA) for providing me with financial support in the form of a CCLSA research award.

Major support was obtained from contact lens companies during my PhD. BE Enterprises and Capricornia Contact Lens provided orthokeratology contact lenses used in various research studies reported in this thesis. Contact lens solutions were kindly donated by Bausch & Lomb, Australia. A special thanks to Ron Beerten, Procornea, the Netherlands for providing me with toric OK lenses and also sharing his experience in fitting toric OK lenses.

I also would like to thank my fellow postgraduate students who have helped me in various ways including participating in studies as participants and providing me with advice during my research work. IT personnel Brian Cheng and Ray Arnhold were my immediate contacts for fixing all computer and software related issues.

A special thanks to optometry undergraduate students Rajeev Naidu, Bingjie Wang and Dyana Sidawi who contributed greatly to one of the studies presented in this thesis (Chapter 5). I really appreciate their patience in recruiting study participants with a stipulated amount of astigmatism which indeed was a tough target, and in addition their time to sleep overnight at the laboratories to collect data on awakening. I also sincerely thank all the study participants for their participation in my study and for giving me their valuable time.

I would like to thank my Indian friends, Athira, Debarun, Jaya, Kalika, Krupa, Nagaraju, Manjula, Moneisha, Neeraj, Nisha, Parthasarathi, Ravi Chandra, Roopa, Rohit, Sailesh, Sameera, Sowba, Swagathika and Swetha. They have added the Indian spice to my life at Sydney. I certainly remember the happy times that we shared and fun we had together. Nagaraju and Roopa really made my life comfortable in Sydney in the early days of my PhD. Thanks to Manjula for clarifying all problems that I faced with statistics and SPSS. A special mention to Moneisha to bear with me all the times in listening to my research work, sharing her expertise in data sorting and statistics and also for sharing our unit on the campus. A special thanks also to Ravi Chandra for his ongoing support in unravelling some complicated mathematical issues and also for sowing the early seeds required for MATLAB programming, which was a great all time asset. I would also like to thank Maria Markoulli and Nikki for their friendly advice during my candidature.

I sincerely bow my head to my father who inspired me and taught me that nothing replaces education and thank him for laying the foundation of optometry in my life. I sincerely thank my mother Rukmini for her constant encouragement and love during my PhD candidature and also for tolerating absence of myself, my wife and my daughter. A great source of inspiration during my PhD candidature was my dearest brother Srikanth. I owe him a lot for shouldering the responsibilities of my family during my absence from India.

Of course this section cannot go without acknowledging my dearest wife Aarti, who is the real source of optimism and great moral support. I also feel so sorry for not spending enough quality time with her. I cannot imagine completing this thesis without her support and co-operation in really tough stages of my PhD. My dearest daughter Shailavi was a great source of happiness and certainly a stress reliever. Milestones of her growth will be remembered as contemporary with my PhD progress. I thank all my friends in India and abroad who contributed to my PhD in one or other way.

TABLE OF CONTENTS

LIST OF FIGURES

LIST OF TABLES

ABBREVIATIONS, ACRONYMS AND SYMBOLS USED IN THE THESIS

@	At the meridian
ASCII	American standard code for information interchange
ATR	Against-the-rule
BOZD	Back optic zone diameter
BOZR	Back optic zone radius
BPD	Back surface peripheral width of lens
BPR	Back surface peripheral radius
CCZ	Central circular zone
CF	Compression factor
CI	Confidence interval
CJ_{180}	Corneal power along 90/180 meridians
CJ_{45}	Corneal power along 45/135 meridians
CM	Corneal spherical equivalent power
cm	Centimetres
CRT	Corneal refractive therapy
CSC	Corneal sighting centre
D	Dioptres
DC	Dioptre cylinder
Dk	Oxygen permeability
Dk/t	Oxygen transmissibility
DV	Difference vector
e	eccentricity
EA	East Asian
FDA	Food and drug administration
flat K	Curvature along flatter corneal meridian
HEF	Horizontal eyelid fissure
HPFW	Horizontal palpebral fissure width
I	Inferior
IN	Infero-nasal
IT	Infero-temporal
J_{180}	Corneal power along 90/180 meridians

J_{45}	Corneal power along 45/135 meridians
K_f	Corneal curvature in dioptres along flatter corneal meridian
K_h	Radius of curvature along the horizontal corneal meridian in millimetres
K_v	Radius of curvature along the horizontal corneal meridian in millimetres
LE	Left eye
LogMAR	Logarithm of minimum angle of resolution
LOS	Line of sight
M	Spherical equivalent power
m	metres
MANOVA	Multivariate analysis of variance
mm	millimetres
Non-EA	non-East Asian
OBL	Oblique corneal toricity or oblique astigmatism
OK	Orthokeratology
PA	Palpebral aperture
P_a	Axial curvature (dioptres)
PASW	Predictive Analytics SoftWare
PCZ	Para-central annular zone
PEK	Photo electronic keratoscope
PMMA	Polymethyl methacrylate
P_R	Corneal refractive power
P_t	Corneal tangential curvature in dioptres
Q	Corneal asphericity
r	Correlation coefficient
r^2	Coefficient of determination
RE	Right eye
RGP	Rigid gas permeable
RM-ANOVA	Repeated measures analysis of variance
RMSE	Root mean square error
R_o	Apical curvature

r_s	Sagittal curvature
R_s	Corneal sagittal curvature in dioptres
r_t	Tangential curvature
S	Superior
Sag	Sagittal height
Sag_{fl}	Sagittal height along flatter meridian
Sag_{st}	Sagittal height along steeper meridian
SD	Standard deviation
SIA	Surgically induced astigmatism
Sim K	Simulated keratometry
SN	Supero-nasal
Sph-RGP	Spherical rigid gas permeable
SPSS	Statistical package for social sciences
ST	Supero-temporal
steep K	Curvature along steeper corneal meridian
TIA	Target induced astigmatism
TLT	Tear layer thickness
TMS	Topography Modelling System
TZ	Treatment zone
UNSW	University of New South Wales
VK	Videokeratoscopic (as in VK axis)
VM	Vinod Maseedupally (The chief investigator)
VN	Vertex normal
VST	Vision shaping treatment
WTR	With-the-rule

Note: The format used to represent the average of the data and its variation in this thesis was mean ± standard deviation (Mean ± SD).

CHAPTER 1 LITERATURE REVIEW

1.1 INTRODUCTION

Clear vision is the ultimate goal of correcting refractive errors. Methods by which refractive correction could be achieved include spectacles, contact lenses, refractive surgery and orthokeratology. Among these methods, orthokeratology stands apart because it corrects refractive errors by temporarily altering the corneal shape during overnight wear of specially designed contact lenses to avoid the need to wear vision correction during the day.

During its inception orthokeratology was referred to as the 'orthofocus' technique (Jessen 1962) but it has since been known under a number of different names including corneal reshaping, corneal refractive therapy (CRT), vision shaping treatment (VST) and overnight vision correction. The procedure is also referred to as 'ortho-k' or abbreviated to OK. In this thesis, the abbreviation OK will be used to refer to orthokeratology.

The definition of OK has been modified over time due to constant advances in the procedure. During the time when non-oxygen permeable rigid contact lenses were fitted with back optic zone radius flatter than that of the cornea, OK was defined as "the reduction, modification, or elimination of refractive anomalies by programmed application of contact lenses" (Swarbrick 2004a). According to our current understanding, OK can be defined as a procedure where a specially designed rigid contact lens is worn overnight for temporary correction of refractive errors by corneal reshaping. This special design of the lens is termed the 'reverse geometry' design, which is different from conventional rigid contact lens designs (Figure 1-1).

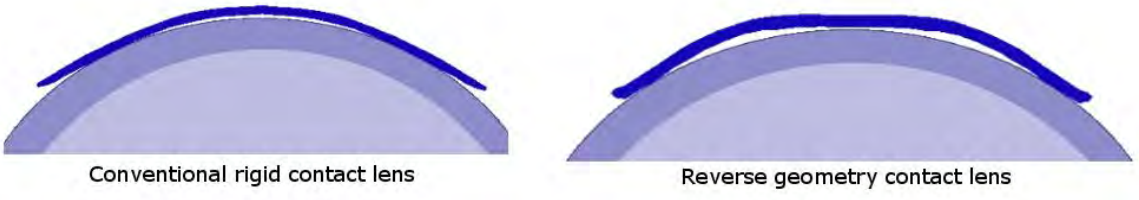

Figure 1-1. Illustration showing the lens profiles of a conventional rigid contact lens and a reverse geometry lens. The lens profiles are indicated in dark blue and the corneal surface in light purple. Note that the conventional rigid contact lens back surface has a relatively continuous curvature from the centre towards periphery whereas the lens back surface of the reverse geometry lens has a steepening curvature in the para-central region before the lens periphery lands on the cornea.

In conventional rigid contact lenses the central back surface of the contact lens closely matches the curvature of the central cornea while the curves towards the lens periphery are generated flatter than the central lens curvature in order to match the flatter corneal periphery. Conversely, 'reverse geometry' lenses have almost an opposite design where the central back surface is flatter than that of the central corneal curvature, and the mid-peripheral curves of the lens are steeper than the central lens curvature (Figure 1-1). When the reverse geometry lens is worn overnight, the special back surface design flattens the central cornea and steepens the para-central cornea. The corneal flattening in the centre is thought to be the major factor in the reduction of myopic refractive error (Mountford 1997b) and from the recent literature it has been proposed that the steepened para-central zone has a potential to modulate peripheral refraction and possibly act to control myopia progression (Smith et al. 2005, Charman et al. 2006, Walline et al. 2009, Queiros et al. 2010a, Kang and Swarbrick 2011, Kang and Swarbrick 2012).

The OK procedure is generally advocated for correcting myopic spherical refractive error with a modest upper limit of refractive astigmatism (Walline et al. 2004, Sorbara et al. 2005). It must be noted however that myopia and astigmatism often coexist (Fan et al. 2004), therefore frequently there is a need to correct not only spherical myopic refractive error but also associated astigmatism. Limited published literature is available describing the correction of astigmatism (1.50 to 2.00 DC) as the primary aim of spherical OK (Mountford and Pesudovs 2002, Hiraoka et al. 2004a, Cheung et al. 2009). Nevertheless, this information can be extracted from many myopic OK studies where a coincidental change in astigmatism has been reported (Fan et al. 1999, Tahhan et al. 2003a, Cheung and Cho 2004, Walline et al. 2004, Sorbara et al. 2005, Hiraoka et al. 2006, Cheung et al. 2007, Chan et al. 2008a). On the other hand, some case reports and large sample studies have been published in the recent past describing correction of moderate amounts of astigmatism (> 1.50 or 2.00 DC) using advanced toric OK lenses (Caroline and Andre 2009, Chan et al. 2009, Baertschi and Wyss 2010, Chen et al. 2012, Pauné et al. 2012).

The aim of this chapter is to give a detailed history regarding OK in general, in addition to various spherical OK lens fitting philosophies, correction of astigmatism using spherical OK lenses in previous studies, and current modalities for correcting lower and higher amounts of astigmatism. Since corneal shape is subjected to alteration during OK, a detailed account of the description of normal corneal shape will also be presented. Because the underlying aim of this thesis is to investigate ways to correct refractive astigmatism using OK lenses, a detailed

description of types of astigmatism and various ways to describe astigmatism will also be presented. Anecdotally, the decentration of OK lenses is considered as a major concern in correcting astigmatism greater than 1.50 DC, therefore an overview of decentration of spherical OK lenses will also be presented.

1.2 HISTORICAL OVERVIEW OF ORTHOKERATOLOGY

1.2.1 Traditional orthokeratology

Although currently the term OK relates to the procedure which involves wearing reverse geometry lens designs, traditional OK involved using non-oxygen permeable and non-reverse geometry rigid contact lenses which were typically fabricated in polymethyl methacrylate (PMMA) material.

The early concept of OK using conventional rigid contact lens designs was first described by Jessen in 1962 to which he gave the term 'orthofocus technique' (Jessen 1962). Jessen described that it was possible to correct myopia, hyperopia and astigmatism by deliberately altering corneal shape using rigid contact lenses manufactured in PMMA material. He suggested that fitting lenses flatter than corneal curvature could aid in myopic correction and lenses fitted steeper than corneal curvature would aid in hyperopic correction. In eye conditions with different keratometry readings in the principal meridians (corneal toricity), he emphasised the use of rigid lenses with varying lens curvature in the two meridians (toric lenses). To maintain the orientation of lenses in order to alter the curvature at the required meridian, a lens stabilisation method such as prism ballast was required (Jessen 1962, 1964).

An early problem that Jessen (1964) recognised was that fitting lenses with back optic zone radius flatter than that of corneal curvature often led to superior lens decentration, causing decentration of the lens-induced corneal flattening effect. In order to overcome this problem, Jessen suggested that the principle of a de Carle type bifocal, which was introduced in the late 1950s, could be reversed, so that rather than a central steepened area surrounded by flatter intermediate curves as is usually the case, the lens would instead have a flattened central curve surrounded by steeper intermediate curves. Jessen suggested that the steeper peripheral curves would promote lens centration, while the flat central base curve would flatten the cornea at the apex. Describing a similar technique, Fontana (1972) also suggested the use of a 'one piece bifocal' in order to reduce the induction of with-the-rule astigmatism which was noted with flat fitting conventional rigid contact lenses for OK.

Fitting rigid lenses with flatter base curves became a popular option for correcting myopia among a handful of early OK enthusiasts in the 1960s. However, flat fitting contact lenses were often associated with lens decentration and induction of astigmatism. At this time, Nolan (1972) recognised that fitting steep lenses could also bring about flattening of the cornea. With this entirely new concept, he presented a series of cases where there was no significant increase in refractive astigmatism, possibly because reduced lens decentration minimised induction of corneal toricity.

By late 1970s the OK procedure drew the attention of scientists and led to a number of controlled studies (Kerns 1976a, b, c, 1977a, b, c, d, 1978, Binder et al. 1980, Coon 1982, Brand et al. 1983, Polse et al. 1983a, Polse et al. 1983b, Coon 1984). The first of these studies was conducted by Kerns (Kerns 1976a, b, c, 1977a, b, c, d, 1978), who longitudinally followed volunteers for nearly three years. The study comprised three subject groups to whom spectacles, conventional rigid lenses and OK lenses were fitted. A relevant finding from the study was the induction of corneal toricity due to poor lens centration in OK wearers. Kerns (1978) reported that superior positioning of the OK lenses was believed to induce unwanted with-the-rule corneal toricity by an average of 0.82 DC.

The second controlled study by Binder et al. (1980) evaluated clinical responses in participants wearing OK lenses in comparison to conventional rigid contact lens wearers acting as controls for a period of 3 years. Their study also showed an increase in with-the-rule corneal toricity (vertical corneal meridian steeper than the horizontal meridian) in their OK lens wearers from an average of 0.10 DC before OK wear to an average of 0.90 DC after lens wear, whereas toricity decreased in the control group who wore conventional contact lenses from an average of 0.71 DC before lens wear to an average of 0.41 DC after lens wear. Binder et al. (1980) also concluded that the OK treatment responses in terms of visual acuity and refraction were predictable only in the initial 9 months of wear, after which responses were unpredictable. Their results were affected by significant drop-out of participants by the end of the study period in both groups.

On the other hand, the third controlled study, conducted by Polse et al. (1983a), found no induction of corneal toricity. An attempt to fit lenses with optimal centration in Polse's study, which was not the case with the earlier studies, offered a possible reason for not finding significant induction of corneal toricity. Finally, Coon (1982) investigated the Tabb technique, which used small diameter lenses with back optic zone radius steeper than corneal curvature along the flat meridian. No significant increase in corneal toricity was observed at

the end of the treatment in both OK wearing (0.02 ± 0.59 DC) and control groups (0.05 ± 0.83 DC). Again, better centration was thought to have been achieved due to the steeper base curve consequently leading to less induction of corneal toricity.

The general fitting methods of these early OK lenses involved choosing a lens with back optic zone radius flatter than the corneal curvature and progressively flattening the lens curvature over time until the desired myopic correction was achieved. However these studies also reported regression of myopic refractive error back to close to the levels measured at the pre-fitting stage after cessation of OK lens wear. For that reason, in order to maintain the OK effect the lenses were required to be worn at least 8 hours during the day time (Binder et al. 1980,Polse et al. 1983b); these lenses were called 'retainer lenses'.

Astigmatic correction using traditional OK was not given great attention at the time, as the primary concern was to obtain myopic reduction and also to determine the safety of these lenses. In the late 1990s Potts (1997) demonstrated in one case that steep fitting rigid lenses could bring about astigmatic reduction by sphericalisation of the cornea. In that particular astigmatic patient, the initial lens was fitted based on the 'one-third' rule, in which the lens was fitted with a back optic zone radius steeper by one third of the difference between the steep and flat corneal curvatures and the lens curvatures were progressively flattened during the aftercare visits. Using this technique, Potts demonstrated reduction of corneal toricity, which was 2.50 DC in the right eye and 2.75 DC in the left eye at baseline, to near spherical corneas at the end of treatment. Simultaneously a reduction of more than 2.00 DC was found in refractive astigmatism in both eyes. However, the lenses had to be worn for several hours during the day time to retain the effect of OK.

From these initial studies it can be concluded that lens centration was a problem with flat fitting rigid contact lenses, which to some extent was reduced by fitting lenses steeper than corneal curvature. However, despite the apparent advantage of improved centration, the concept of steep lens fitting to flatten the cornea was not widely adopted.

Although the OK procedure with rigid contact lenses was considered to be safe at that time (Polse et al. 1983a), only a few practitioners embraced this method of vision correction as a mainstream procedure in their contact lens practices due to several limitations. Primarily, the lenses had to be worn during the day time sometimes for several months for the OK effect to become evident. In order to preserve the refractive effect once it had been achieved a

'retainer' lens was required to be worn during the day time. Further, the amount of overall myopic refractive correction was unpredictable (Binder et al. 1980).

1.2.2 Accelerated orthokeratology

The OK procedure underwent a revolution during the early 1990s due to concurrent improvements in technology of lens fabrication and assessment of corneal shape. Improvements in the field of lens manufacturing in the form of computer controlled lathes enabled crafting of lens designs with peripheral curves that were steeper than the base curve, which became known as reverse geometry designs. At around the same time advances in instrumentation to record corneal topography allowed clinicians to visualise corneal shape beyond the central region (Klyce 1984, Dingeldein and Klyce 1988). These advances triggered interest among clinicians in OK on the basis that reverse geometry designs allowed improved stabilisation of flat fitting lenses, and the lenses could be fitted more accurately based on more detailed knowledge of corneal topography.

The first clinical use of reverse geometry contact lenses was reported by Wlodyga and Byrla (1989) followed three years later by Harris and Stoyan (1992). Both of these publications reported the use of reverse geometry lens designs manufactured by Contex Inc, USA. Alongside up to 6.00 D of myopia reduction, the authors also claimed correction of astigmatism of up to 3.00 DC associated with minimal induction of corneal toricity during lens wearing periods. The novel lens design with steeper peripheral curves was attributed as the reason for better centration of the lenses. Interestingly, the reverse geometry lens design concept was similar to that previously described by Jessen (1964) with his orthofocus technique.

Unlike OK with earlier conventional lenses, OK using reverse geometry lenses resulted in reduction of larger amounts of myopia over a short duration of lens wear therefore leading to the term 'accelerated OK'. However a major drawback that remained was that the lenses needed to be worn during the day time.

1.2.3 Overnight orthokeratology

The traditional and early accelerated OK approaches permitted lens wear only during the day time. The almost non-existent oxygen permeability (Dk) characteristics of PMMA and low-Dk (Brand et al. 1983) materials that were being used in rigid lenses of the time prevented overnight wear. Just 2 hours of day time use of PMMA contact lenses induced on an average 6% corneal swelling (Mandell and Polse 1971). Numerous experiments were conducted by

fitting air-tight goggles to expose eyes to various levels of oxygen concentration (Carney 1975, Mandell and Farrell 1980, Efron and Carney 1982, Benjamin and Hill 1985, Brennan et al. 1987, Benjamin and Hill 1988). These studies revealed a negative correlation between the oxygen concentration and corneal swelling response; in other words, higher levels of oxygen concentration led to lower amounts of corneal swelling. The outcomes of these experiments confirmed the concept that the cornea undergoes hypoxic stress during reduced oxygen supply, which may also occur during contact lens wear.

Day time short term and long term wear of PMMA contact lenses was also shown to have effects on the cornea. The short-term corneal changes due to PMMA contact lens wear included abnormal corneal epithelial fragility (O'Leary and Millodot 1981), corneal staining (Kline et al. 1979) and endothelial bleb response (Barr and Schoessler 1980). Long-term changes such as increased variation in endothelial cell size (polymegethism) (Schoessler and Woloschak 1981) and decreased corneal sensitivity (Millodot 1978) were also reported. These experiments raised the need for establishing the minimum oxygen requirements for the cornea to maintain no more than physiological overnight corneal swelling.

This discussion requires an understanding of the terms 'oxygen permeability' (Dk) and 'oxygen transmissibility' (Dk/t) to ease the explanation of the importance of oxygen levels reaching the cornea through different types of contact lenses. Oxygen permeability is indicated by Dk, and is defined as the permeability coefficient of a material factored by the rate at which the oxygen molecules move in the matrix of a given material (D) and the amount of oxygen dissolved in the material (k) (Fatt 1978). The units for Dk are barrers, and are expressed as 10^{-11} $cm^2/sec \times ml O_2/ml \times mm\ Hg$. Oxygen transmissibility, indicated as Dk/t, is the measurement of passage of oxygen through a contact lens of a specified thickness (t) in cm. The units for Dk/t are also barrers, and are expressed as 10^{-9} $cm/sec \times ml O_2/ml \times mm\ Hg$.

Continuous development in the field of contact lens materials during the 1980s and early 1990s led to the possibility of overnight lens wear. Particular attention was given to maximising the oxygen permeability of contact lens materials in order to avoid hypoxic effects associated with PMMA lens wear. A great amount of research was dedicated to discover the safe levels of oxygen transmissibility through contact lenses. The research culminated in the well known 'Holden and Mertz criteria' of oxygen transmissibility for safe daily and extended wear use of soft contact lenses. The criteria stated that, in order to maintain overnight corneal swelling to a physiological level of 4%, the Dk/t of the soft lens must be at least 87 barrers (Holden and Mertz 1984). Harvitt and Bonanno (1999) later found by using mathematical

corneal models that the minimum Dk/t value to avoid corneal anoxia (absence of oxygen) in the closed eye needed to be 125 barrers. Coincidentally at about the same time Sweeney (2003) proposed a modification to the Holden-Mertz criterion for overnight lens wear based on an overnight physiological oedema level of 3% (La Hood et al. 1988), and found that the critical Dk/t to limit oedema to this amount was 125 barrers. The introduction of silicone hydrogel contact lenses in 1998 added a whole new dimension to overnight use of contact lenses. The silicone hydrogel lens materials evolved from the combination of silicone materials that facilitate the transmission of high amounts of oxygen and hydrogel monomers which are good at providing flexibility and fluid transport. Many silicone hydrogel contact lenses possess Dk/t greater than critical levels required for overnight use. Overnight use of silicone hydrogel contact lenses has been shown to have eliminated clinical hypoxic signs associated with previously used low-Dk/t hydrogel contact lenses (Sweeney 2003).

Rigid gas permeable (RGP) contact lens materials were introduced in the early 1980s. The initial lens material (cellulose acetate butyrate, CAB) had a Dk of 8-10 barrers. But Sweeney and Holden (1983) suggested that the Dk of RGP materials should be at least 35 barrers to meet corneal oxygen requirements for overnight wear for a 0.15 mm thick lens. The quest for better oxygen permeable rigid contact lens materials for extended wear led to the evolution of siloxane and fluoro-siloxane methacrylates. RGP contact lenses fabricated from these materials had higher Dk/t and the clinical performance for extended wear was reasonably good and sometimes better than concurrently available hydrogel extended wear contact lenses (Henry et al. 1987, Fonn and Holden 1988, Polse et al. 1988, Young and Port 1992). By the early 2000s RGP contact lens materials with Dk as high as 175 (Menicon Z) were commercially available. The clinical performance was comparable and considered to be as safe as extended wear hydrogel contact lenses (Benjamin and Cappelli 2002, Gleason and Albright 2003). The Food and Drug Administration (FDA) approved RGP contact lenses manufactured in Menicon Z for 30-night continuous wear in July 2002 (Gleason and Albright 2003).

Harris and Stoyan (1992) proposed occasional overnight use of OK lenses to retain the effect of the myopic correction that resulted from the previous daily wear phase. Grant (1992) was the first to report that OK lenses in high Dk materials could instead be used exclusively on an overnight basis, without the need for daily wear or compromise of the overall OK effect. This marked the birth of overnight OK. Subsequently numerous reports on the efficacy and safety of overnight OK lens wear have been published (Mountford 1997b, Fan et al. 1999, Nichols et al. 2000, Rah et al. 2002, Alharbi and Swarbrick 2003, Cho et al. 2003, Joslin et al.

2003, Soni et al. 2003, Tahhan et al. 2003a, Hiraoka et al. 2004b, Owens et al. 2004, Walline et al. 2004, Berntsen et al. 2005, Maldonado-Codina et al. 2005, Sorbara et al. 2005, Soni and Nguyen 2006, Knappe et al. 2007, Lu et al. 2007a, b).

1.3 DETERMINATION OF CORNEAL SHAPE

Assessment of corneal shape is an important step during OK, not only at baseline where the corneal shape parameters are used to determine the required initial OK lens parameters, but also to monitor OK-induced changes to corneal shape. A thorough understanding of corneal shape and how it is measured and described is necessary to further understand OK lens fitting philosophies. This section gives an overview of methods involved in determining corneal shape, and also corneal shape classification and various factors that influence corneal shape.

1.3.1 Radius of curvature versus curvature

Before describing about various instruments used to determine corneal shape it is important to distinguish between the terms 'radius of curvature' and 'curvature' as these terms will be used throughout this thesis when describing corneal shape. Radius of curvature (r) is defined as the distance in millimetres (mm) along the normal at a point on a curved surface to the centre of curvature of that point. Curvature (P), on the other hand, is the reciprocal of radius of curvature of a curved surface in dioptres which is derived from the following formula:

$$P = \frac{n' - n}{r}$$

where n' and n are the refractive indices of the refractive element and air vacuum respectively. The radius of curvature (r) should be denoted in metres.

1.3.2 Instruments used for corneal shape determination

1.3.2.1 Keratometer

The keratometer is an ophthalmic device primarily used to determine central corneal shape. Primitive models of the keratometer were introduced as early as 1779 and a slightly improved version was described by Hermann von Helmholtz in 1853.

Keratometry relies on the reflective properties of the tear film that lies over the anterior corneal surface to act like a convex mirror. By measuring the image displacement of a known object separation, corneal curvature in the steep and flat principal corneal meridians

can be derived. The reflected object mire is projected approximately 3 mm from the corneal apex, meaning that the keratometer measures radius of curvature within this 3 mm central region. This is a fundamental limitation of the keratometer as far as its use during OK is concerned, because OK-induced corneal changes are not only limited to the central region but also extend towards the para-central region (Mountford 1997b, Alharbi and Swarbrick 2003, Lu et al. 2007b, Queiros et al. 2010b). Mandell (1966) suggested a different approach to assess corneal curvature beyond the central region. In this method he obtained peripheral corneal measurements by offering a series of peripheral fixation points. The measured values thus obtained required a correction factor for them to be accurate.

As far as peripheral corneal measurements during reverse geometry lens wear are concerned, Wlodyga and Bryla (1989) and later Harris and Stoyan (1992) emphasised the importance of para-central corneal curvature measurements. Wlodyga and Bryla stated that greater flatness of the temporal corneal curvature relative to the central cornea would predict a better flattening effect in the centre. Harris and Stoyan further added that the amount of myopic reduction after OK can be estimated to be equivalent to twice the difference between the central and temporal corneal curvatures. However the logic behind using temporal corneal curvature readings to estimate myopic reduction was not provided by the authors.

The keratometer is still routinely used in contact lens practice. For this reason some OK lens manufacturers rely on keratometry data for initial trial lens fitting purposes. Keratometry can be used to provide information on central corneal changes. However, this is of limited use for post-OK lens wear fitting assessment.

1.3.2.2 Keratoscopy and photokeratoscopy

While the keratometer provides quantitative information about the central region of the cornea, keratoscopy on the other hand provides qualitative information over a substantial corneal area. A typical keratoscope consists of a flat circular disc with a series of black and white concentric rings on the surface which are projected on the corneal surface. The earliest form of keratoscope is the hand held Placido disc (Levene 1965). The disc is held approximately 15 cm from the eye with its surface pattern projected on to the patient's cornea. After good alignment with the patient's eye the reflection of the concentric rings is viewed through a central hole fitted with a convex lens whose focal length is equal to the distance between the disc and the patient's eye. The concentric ring pattern reflected from the cornea is evaluated qualitatively for the presence of any distortion. The main limitation with the Placido disc assessment of corneal shape is that it does not give quantitative information.

In later years the Placido disc was modified to obtain quantitative information about corneal shape. The basic feature of the photokeratoscope is that a photograph of the reflected mire pattern from the cornea is recorded and these photographic images were later used for detailed analysis of corneal shape from the centre towards para-central regions (Ludlam et al. 1967, Sivak 1977). The photokeratoscopic-based corneal shape assessment was used by the early OK practitioners (Kerns 1976c, Freeman 1978, Binder et al. 1980, Grant 1980, Coon 1984).

1.3.2.3 Computerised videokeratoscopy (Placido disc-based devices)

The development of digital imaging alongside continued advances in computing power led to the development of the videokeratoscope towards the end of the 1980s (Klyce 1984, Maguire et al. 1987). Videokeratoscopes project a Placido disc pattern on to the cornea, the image of which is digitally captured and rapidly analysed to provide detailed corneal topography data. From the captured image, the computer determines the distance between rings of the reflected Placido disc image at various corneal locations. These distances are then matched with the mathematical geometry of the original Placido disc to determine the corneal slope at these corneal locations. The corneal slope values are processed further to calculate corneal elevation and corneal curvature by means of integration. The term 'corneal topographer' used in this thesis refers to a Placido disc-based videokeratoscope.

Studies that assessed the performance of Placido disc-based videokeratoscopes revealed a high accuracy on test surfaces (Tang et al. 2000) and also showed good repeatability on normal human corneas (Cho et al. 2002). However these devices are not without limitations. The central approximate 2 mm zone of the measured topography is prone to errors because the calculations in this area are based on only a few acquisition points (Belin and Ratliff 1996) and the data within this zone require extrapolation from these small number of points. In addition, several mathematical assumptions are made in determining the corneal dioptric powers displayed by the topographer (Roberts 1994b, Applegate and Howland 1995). Paraxial errors can also occur due to poor patient fixation and due to poor focussing of the instrument (Mandell 1996), although these paraxial errors can be reduced to some extent by averaging multiple measurements taken from the same eye (Zadnik et al. 1995). Furthermore the Placido disc corneal image may be partially obstructed by the nose and ocular adnexa such as the upper eyelid and the orbital rim, which can limit corneal topography capture towards nasal and superior regions of the cornea (Mandell 1996). The examiner can overcome this issue to a certain degree by instructing the patient to open their eyes as widely as possible or

by retracting the upper and lower eyelids in order to enlarge the acquisition area. The Medmont E300 corneal topographer (Medmont International Pty Ltd, Victoria, Australia) used for all of the experiments reported in this thesis further overcomes some of these problems by adopting a cone shaped Placido disk that allows closer positioning to the eye and thus avoiding obstruction from the nose and brow.

1.3.2.4 Non-Placido disc-based corneal shape determination

In order to overcome the limitations encountered with the Placido-based systems manufacturers have come up with alternative ways to measure corneal topography including scanning slit systems and Scheimpflug photography.

1.3.2.4.1 Scanning slit devices

The most widely recognised scanning slit device is the Orbscan (Bausch & Lomb, NY, USA) The initial design of the Orbscan incorporated only slit-scanning technology which involved projecting a series of illuminated slits across the cornea. The information captured from the projected slits was used to mathematically determine corneal surface elevation. This elevation data could be used to determine corneal thickness and surface curvature. The technology allowed the measurement of both anterior and posterior corneal curvature simultaneously. In the later designs (Orbscan II), the slit-scanning technology was combined with Placido disc image capture enabling the use of both technologies in one device. The anterior surface corneal topography is derived from the Placido disc image capture and the corneal thickness is derived from a narrow slit of light which is scanned across the cornea. The posterior surface topography is derived from combining the anterior topography data and the corneal thickness data. Despite this hybrid technology the Orbscan II is shown to have very poor repeatability in measuring anterior topography of human corneas in comparison to the Placido disc-based Medmont E300 corneal topographer (Cho et al. 2002).

1.3.2.4.2 Scheimpflug photography

Scheimpflug technology is incorporated into the Pentacam (Oculus Inc., Germany), Galilei Dual Scheimpflug Analyser (Ziemer Ophthalmics, Port, Switzerland), and Sirius (C.S.O., Firenze, Italy). Scheimpflug technology uses a rotating camera to image the front and back surface topography of the cornea. The devices also provide information about anterior segment structures such as the anterior chamber.

Studies that compared some corneal indices of the Pentacam with Placido disc-based devices revealed similar accuracy. Kawamorita et al. (2009) showed poor repeatability of the

Pentacam in measuring superior corneal axial curvature at 4 and 5 mm from the corneal centre compared with a Placido disc-based corneal topographer (Keratron, Opticon 2000 SpA, Italy). Chen and Lam (2009) investigated repeatability of corneal power vector components (M, J_0, J_{45}) derived from the simulated keratometry (Sim K) values (the steep and flat keratometry readings determined by a typical corneal topographer) calculated by the Pentacam and showed good repeatability, but found poor repeatability in measuring the superior corneal curvature (both axial and tangential) at as little as 2 mm from the corneal apex. Savini et al. (2009) demonstrated good agreement between the Pentacam and two Placido disc-based corneal topographers (TMS2 Topography System, Tomey, Germany; and Keratron) in measuring the Sim K values. However the authors advised caution in interpreting the results because although there was good statistical agreement between the Pentacam and the two corneal topographers, the 95% limits of agreement were approximately ± 1.00 D which is clinically a very wide range. Read et al. (2009) showed good agreement in the measurement of corneal power vector components (M, J_0, J_{45}) derived from the Pentacam and the Medmont E300 corneal topographer, but showed poor repeatability in the agreement of certain types of aberrations (trefoil and tetrafoil). Most of these studies have investigated the agreement or repeatability of just a few corneal parameters within the Pentacam device or between the Pentacam and the Placido disc-based corneal topographers. However, McAlinden et al. (2011) studied several corneal and anterior eye parameters to test the precision of the Pentacam device. The study showed good repeatability between several parameters but showed poor precision in the measurement of astigmatic axes, and anterior corneal tangential, axial and refractive power maps.

Whereas the Pentacam uses Scheimpflug photographic image analysis alone for determining anterior corneal parameters the Galilei Dual Scheimpflug Analyser also incorporates Placido disc based anterior corneal topography analysis with the aim to improve measurement accuracy. In a prospective study, Menassa et al. (2008) compared keratometry readings using the Galilei Dual Scheimpflug Analyser and the Orbscan II anterior segment analysis system in 85 eyes of 45 subjects. From the regression analysis the authors showed that the difference between the devices was not clinically significant. The authors also showed low inter- and intra-observer variation in the keratometry readings measured by Galilei and this variation was not significant in comparison to Orbscan II readings. In a different prospective study, Shirayama et al. (2009) compared corneal powers obtained from four different devices including the Galilei Dual Scheimpflug Analyser, the Humphrey Atlas (Carl Zeiss, Jena, Germany) a Placido disc-based corneal topographer, the IOLMaster (Zeiss,

Oberkochen, Germany) and a manual keratometer (Bausch & Lomb Inc, Rochester, New York, USA). The coefficient of variation for each device was lower than 0.22% and the intraclass correlation coefficients were higher than 0.99 for all devices. This suggested that repeated measurements taken by each device were highly reproducible and also comparable between devices. In a different study, Savini et al. (2011b) determined the repeatability of various anterior segment measurements in normal and post-refractive surgery eyes, to show high repeatability for the Galilei for all measured parameters.

The Sirius is similar to the Galilei in using a single Scheimpflug camera and Placido disc technique to measure various anterior eye biometrics. A series of 25 Scheimpflug images in different meridians is captured with a simultaneous top-view Placido disc. Savini et al. (2011a) assessed the repeatability of Sirius in unoperated, post-refractive surgery and keratoconic eyes. An intra-class correlation (ICC) of 0.99 was noted for most parameters in the three groups investigated, suggesting good repeatability. The ICC was lower than 0.99 when measuring anterior and posterior corneal asphericity in normal eyes and posterior corneal power and mean pupil power in keratoconus. In another study Savini et al (Savini et al. 2011c) compared anterior segment measurements taken with the Pentacam, two devices that incorporated a Scheimpflug camera with a Placido disc (Sirius and TMS-5) and a Placido disc corneal topographer (Keratron). Differences in Sim K values were found between the devices. The Keratron gave the highest values and Pentacam and Sirius the lowest values. Other parameters such as posterior corneal power and minimum corneal thickness were shown to be significantly different between the three Scheimpflug camera based devices leading to the authors expressing caution in using these devices interchangeably. In another study, intra-subject repeatability of several anterior segment measurements was evaluated including anterior and posterior corneal curvature, shape factor, white-to-white corneal diameter, central and minimal corneal thickness and anterior chamber depth (Montalbán et al. 2012). Several anterior segment parameters measured by Sirius were shown to be repeatable.

Most of these studies also suggested recording of multiple readings of corneal topography to improve the measurement precision of the measurements. In conclusion, the Scheimpflug devices are relatively new instruments and caution is advocated in analysing certain corneal parameters from these devices. Further validation may be necessary to consider these instruments suitable for mainstream clinical research and practice.

1.3.3 Corneal shape descriptors

Videokeratoscopes provide both qualitative and quantitative information about corneal shape. The qualitative information presented in the form of colour-coded maps generally provides an overview impression of corneal shape, but does not allow detailed analysis of optical characteristics of the cornea. Quantitative descriptors, on the other hand, allow corneal shape to be explored in a very detailed manner to the extent of understanding variations in shape within a given cornea and between the corneas of different individuals. In this section a detailed description of various mathematical descriptors and an overview of various corneal topography maps will be provided.

1.3.3.1 Mathematical descriptors of corneal shape

It is well known that human corneas tend to flatten from apex towards periphery (Townsley 1970, Mandell and St Helen 1971, Kiely et al. 1982, Guillon et al. 1986). Because of this flattening towards the periphery of the cornea, conic sections are considered as a suitable way to describe corneal shape (Lindsay et al. 1998). There are basically four types of conic sections including a circle, ellipse, parabola and hyperbola. Among these, the ellipse is considered as the closest approximation to describe corneal shape (Kiely et al. 1982). The two parameters by which a conic section can fully be described are apical curvature (R_o) and eccentricity (e). Various other indices describing the rate of change in corneal shape from centre to periphery and the relationships between them are described below.

1.3.3.1.1 Eccentricity (e)

The shape of an ellipse (Figure 1-2) can be described as a compressed circle which is symmetrical along its major ($2a$) and minor ($2b$) axes which are perpendicular to each other. An ellipse has prolate and oblate apices. The prolate apex is the sharp end present along the major axis where the surface tends to flatten away from the sharp apex. The oblate apex is the blunt end of the ellipse present along the minor axis where the surface tends to steepen away from the blunt apex.

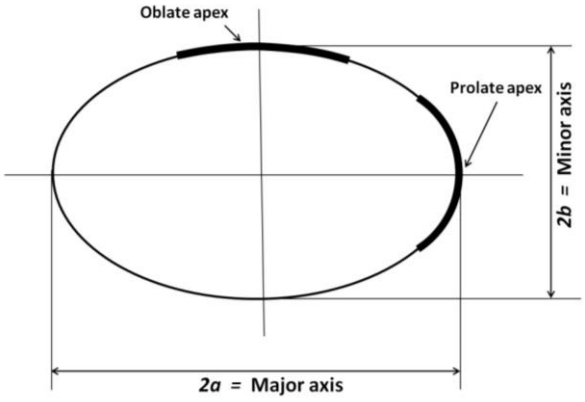

Figure 1-2. An ellipse showing prolate and oblate apices along the major (2a) and minor (2b) axes respectively.

The general form of the ellipse equation with the origin at the coordinate centre and where the major axis is horizontal (Larson and Hostetler 2007) is:

$$\frac{x^2}{a^2} + \frac{y^2}{b^2} = 1$$

As long as the lengths of the major and minor axes are known, one can determine the rate at which the surface tends to flatten away from the prolate apex using an index called eccentricity (e), from the equation:

$$e^2 = 1 - \left(\frac{b}{a}\right)^2$$

or

$$e = \sqrt{1 - \left(\frac{b}{a}\right)^2}$$

where a and b are semi-major and semi-minor axes of the ellipse respectively. Apical radius (R_o), which is the radius of curvature of the conic section at the prolate apex, can be calculated from these half-axes as (Burek and Douthwaite 1993):

$$R_o = \frac{b^2}{a}$$

Mathematically, the eccentricity e adequately describes the shape of a prolate ellipse but cannot describe the shape of an oblate ellipse. This is because for a prolate ellipse $a > b$ and the value under the square root gives a positive e value, but in the case of an oblate ellipse where $b > a$, the value under the square root becomes negative and the square root of a negative value leads to a complex result. Therefore eccentricity cannot be determined for an oblate end of the ellipse. This is the main limitation of using the eccentricity value. Alternative indices such as shape factor (p) or asphericity (Q) have been proposed to overcome this limitation (Guillon et al. 1986, Lindsay et al. 1998, Swarbrick 2004b).

1.3.3.1.2 Shape factor (p)

The shape factor (p) of an ellipse describes the amount by which the form of the ellipse deviates from being a perfect circle, or simply it indicates the rate at which the ellipse flattens or steepens as it deviates away from the apex of the ellipse (Douthwaite et al. 1999). The shape factor p can be determined from e^2 as

$$p = 1 - e^2$$

If shape factor p is greater than 1 then the ellipse is an oblate and if it is less than 1 then the ellipse is a prolate.

1.3.3.1.3 Asphericity (Q)

Another shape index that describes the rate at which the ellipse changes its shape from the apex to the periphery is asphericity (Q). This parameter is also related to e as:

$$Q = -e^2$$

When Q equals zero it describes a circle, a value greater than zero (thus a positive value) indicates an oblate ellipse and less than zero (thus a negative value) indicates a prolate ellipse. In this way the sign becomes the indicator of prolateness or oblateness of the ellipse and the magnitude of Q indicates the rate of steepening (for a positive Q) or flattening (for a negative Q) of the ellipse from the apex to the periphery. The major advantage of using Q over

p is that the prolate and oblate surfaces can be identified by the sign of Q. The types of conic section and their corresponding eccentricity, shape factor and asphericity values are given in Table 1-1.

Conic section	Eccentricity (e)	Shape factor (p)	Asphericity (Q)
Prolate ellipse	$0 < e < 1$	$0 < p < 1$	$-1 < Q < 0$
Circle	0	1	0
Oblate ellipse	Cannot be determined	> 1	> 0
Parabola	1	0	−1
Hyperbola	> 1	< 0	< −1

Table 1-1. Types of conic sections and their corresponding eccentricity (e), shape factor (p) and asphericity (Q) values.

1.3.3.2 Derivation of corneal asphericity (Q) or shape factor (p)

Because of its simplicity, this thesis uses the asphericity Q to describe corneal shape. Most topographers do not reveal the exact algorithms used to determine corneal asphericity. However, the Medmont E300 used to capture the data presented throughout this thesis allows raw sagittal height data at specific radial distances to be extracted, and from analysis of these data asphericity Q can be derived.

1.3.3.2.1 Baker's equation

Using apical curvature (R_o) and shape factor (p), Baker (1943) derived an elegant equation to generate conic sections. This equation is as follows:

$$y^2 = 2R_o x - px^2$$

or the equation can be rewritten as

$$y^2 = 2R_o x - (Q+1)x^2$$

In the equation, x is the sagittal height (mm) over a specified chord length and y is the semi-chord length (radial distance in mm). However this equation is not convenient to calculate Q from raw corneal topographic data as it requires a prior knowledge of R_o.

1.3.3.2.2 Douthwaite's method

Douthwaite (1995,1996) developed a graphical method to determine the shape factor of ellipsoidal test surfaces. In this method topographic data were captured from ellipsoidal test surfaces using a Placido disc-based corneal topographer (EyeSys corneal analysis system,

EyeSys Laboratories, TZ, USA). The raw topographic radial distance data from the surface's apex to the periphery squared and the corresponding axial radii of curvatures squared for a given meridian were plotted in a graph. The linear equation ($y' = c + mx'$) derived from the best-fit line between these two squared continuous variables can be used to derive the shape factor p and apical curvature R_o. For this purpose Douthwaite used Bennett's original equation:

$$R_a = \sqrt{R_o^2 + (1 - p) \cdot y^2}$$

where R_a is axial radius of curvature and the remaining constants are the same as described above in Baker's equation. By squaring both sides, the equation could be rewritten as:

$$R_a^2 = R_o^2 + (1 - p) \cdot y^2$$

This rewritten equation is similar to the familiar linear equation for the straight line ($y' = c + mx'$) described before, in which the expressions R_a^2, $R_o^2, 1 - p$ and y^2 of the rewritten equation correspond to variable y', constant c, slope m and variable x' in the linear equation of the straight line respectively. Therefore from the regression equation derived from the graph plotted between squared radial distance and axial radius of curvature, the apical radius (R_o) can be calculated as the square root of the constant R_o^2. The slope ($1-p$) of the regression line can be used to determine the shape factor p by subtracting its value from unity. This method was initially used to determine the shape factor p for test surfaces and its use was later extended to normal human corneas (Douthwaite et al. 1999).

To illustrate this method, corneal raw data from a randomly chosen healthy volunteer's eye derived from the Medmont E300 corneal topographer is used. The radial distances of rings 1 to 28 and corresponding axial radii of curvatures of the nasal and temporal hemi-meridians are plotted and a straight line using the least squares method is fitted in . The linear equation, coefficient of determination (r^2) and the statistical significance of the fit are shown in the plot.

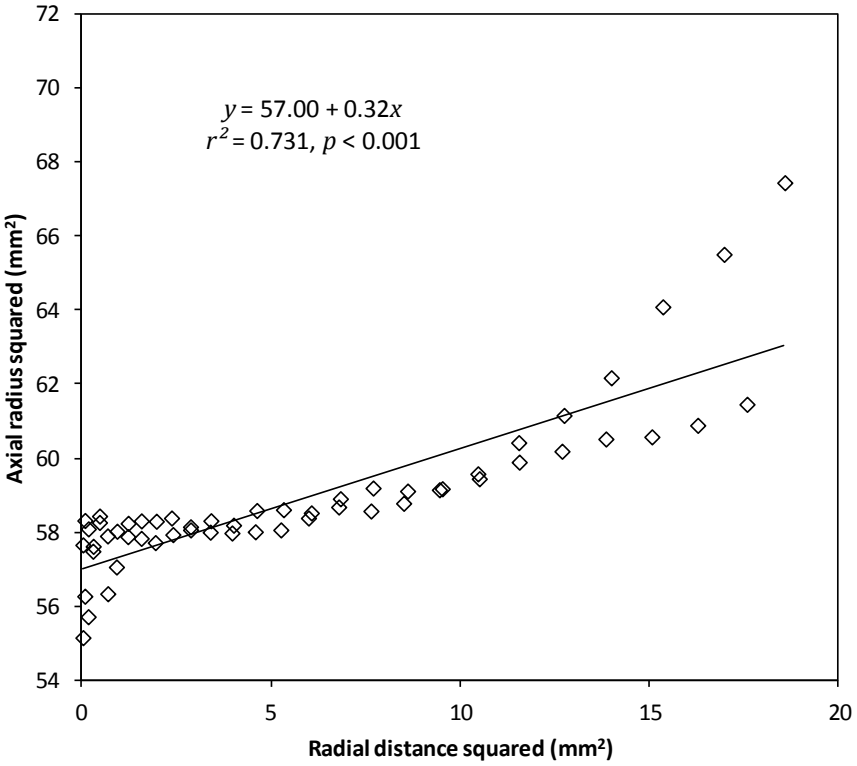

Figure 1-3. Douthwaite's method of calculating the shape factor. The scatter plot shows the relationship between the radial distance from the vertex normal (along the videokeratoscopic axis) squared to the axial radius of curvature squared of the horizontal corneal meridian of a subject. The corneal raw data from rings 1 to 28 are used for this plot. A significant positive correlation is shown. From the linear regression equation, the apical curvature (R_o) can be determined as $\sqrt{57.00} = 7.55$ mm and shape factor p = 1– 0.32 = 0.68.

There are certain limitations with this method. The graphical method to determine the shape factor p was accurate for surfaces whose shape factors ranged between 0.8 and 1.0 only (Douthwaite 1995). Further it can be noted from Figure 1-3 that the squared axial radius of curvature values near the vertex are spread wide apart from the best-fit line; this certainly should have a bearing on the calculation of both R_o and p. However, using the EyeSys corneal topographer, Douthwaite demonstrated that the values of R_o and p are similar whether or not one considered the data from the central rings (Douthwaite et al. 1999). Despite these limitations this method has been employed in several studies (Douthwaite et al. 1999, Hough and Edwards 1999, Cheung et al. 2000, Douthwaite 2003, Davis et al. 2005).

1.3.3.3 Corneal shape descriptor determined from the corneal topographer

Section 1.3.3.1 explained three mathematical descriptors of corneal shape which are interrelated (e, p and Q). Present day topographers provide all three or only some of these descriptors. In the latter situation the user may need to convert the given notation to the appropriate notation required. Most corneal topographers display corneal asphericity Q along the principal corneal meridians (steep and flat corneal meridians) along with the colour coded maps. The Medmont E300 corneal topographer, which is used in all studies of this thesis, gives the user the option to obtain corneal asphericity Q at each corneal full meridian as a function of the meridian angle and the chord diameter. However, the device does not provide the asphericity of hemi-meridians which is one of the important aspects required to assess corneal asymmetry. Moreover, the exact algorithms used to determine mathematical corneal descriptors in different topographers are proprietary and therefore not disclosed. Some approaches to determining corneal asphericity were discussed in Section 1.3.3.2.

1.3.4 Regional corneal shape in normal corneas

A number of previous studies have described corneal shape using a single corneal shape index, reporting the asphericity values for the whole cornea (Kiely et al. 1982, Guillon et al. 1986, Budak et al. 1999, Nieto-Bona et al. 2009), or meridionally (Kiely et al. 1984) or by hemi-meridian (Mandell and St Helen 1971, Sheridan and Douthwaite 1989, Zhang et al. 2011).

Kiely et al. (1982) determined asphericity values for a chord diameter of 3 mm in Caucasian subjects with a wide age range (16 to 80 years) using a photokeratoscope. Using the corneal radius values determined from the reflected image and ring position a best fitted rotationally symmetric conicoid function was fitted to calculate a global Q and a non-rotationally symmetric conicoid was fitted to derive meridional Q values. The mean global

Q was −0.26 ± 0.18 and the meridional Q values ranged between −1.44 and 1.28. This large variation of meridional Q suggests that the corneal shape in different meridians can vary to include prolate ellipse, oblate ellipse and hyperbola.

In another study Kiely et al. (1984) determined Q in 4 meridians for a chord diameter of 3 mm (horizontal, superior temporal-inferior nasal, vertical and superior nasal-inferior temporal meridians) of Caucasian young adults using the same method described previously (Kiely et al. 1982). The meridional Qs determined in the study were: horizontal meridian = −0.20 ± 0.15, superior temporal – inferior nasal meridian = −0.20 ± 0.20, vertical meridian = −0.20 ± 0.22 and superior nasal-inferior temporal meridian = −0.25 ± 0.21. This suggested that there is little variation in asphericity when only four meridians are considered. Lam and Douthwaite (1996) calculated corneal shape factor (p) in horizontal and vertical meridians in young Chinese adults using Douthwaite's method to show no difference between the two meridians or between right and left eyes.

Mandell and St Helen (1971) described the variation in hemi-meridional corneal shape using eccentricity e to show that nasal and superior corneal hemi-meridians flattened at a greater rate than temporal and inferior corneal hemi-meridians respectively. The rings reflected on the cornea projected by the photokeratoscope were used for the determination of e value. However due to the obstruction from ocular adnexa the capture of rings in the nasal and superior regions was restricted. In this manner the number of reflected rings used for the calculation varied between the hemi-meridians which essentially means that the e value was determined over a variable chord diameter.

Sheridan and Douthwaite (1989) assessed asphericity of hemi-meridians for a 3 mm chord diameter in terms of shape factor p and showed that the nasal cornea flattened at a faster rate than the temporal cornea. Recently Zhang et al. (2011) also showed a similar trend, where corneal asphericity (for a 6 mm chord diameter) in the nasal and superior hemi-meridians was more prolate than the temporal and inferior hemi-meridians respectively.

No previous study has investigated whether this regional variation has any impact on OK lens centration. Moreover, to understand the effect of corneal shape on OK lens decentration, corneal shape in terms of regions or sectors rather than meridians is likely to be more useful, because when an OK lens is worn, the lens is likely to rest over a region of the cornea rather than on a single meridian.

1.3.5 Toricity

Optical surfaces can be divided into two types rotationally: a) spherical surfaces and b) toroidal surfaces. Coaxial spherical refracting or reflecting surfaces possess symmetry about the optical axis (Rabbetts 2007). In simple terms, the curvature of a spherical surface remains uniform in all meridians circumferentially. A toroidal surface, on the other hand, possesses a low order of symmetry. It has minimum curvature along one meridian and maximum curvature along the other meridian, the minimum and maximum curvature meridians are mutually perpendicular to each other, and the curvature varies gradually between the two meridians (Rabbetts 2007).

1.3.5.1 Principal corneal meridians in corneal topography

Even in the case where the corneal surface is considered to be spherical, some degree of toricity is still generally present even though this may be clinically insignificant. The cornea also has steep and flat meridians which can be measured by a keratometer. But when using a corneal topographer the curvatures of the principal meridians are measured from an area matching to conventional keratometry which is approximately a 3 mm annular zone from the centre of the cornea. For this reason the values of the principal meridians derived from the corneal topographer are called 'simulated keratometry' values or simply indicated with the acronym 'Sim K' (Wilson and Klyce 1991). The magnitude of corneal toricity is then determined from the difference of curvatures at the principal meridians similar to the way this is carried out during conventional keratometry.

1.3.5.2 Corneal toricity or astigmatism

Corneal toricity is a condition where the cornea possesses toricity on its surface. Generally the term corneal astigmatism is interchangeably used to refer to corneal toricity, so it is important to make a distinction between these two terms. Corneal toricity exemplifies the physical shape of the corneal surface. It can easily be measured by keratometer or advanced corneal topographers. It can be calculated as the difference between maximum and minimum radii of curvature in millimetres (mm) or in dioptres. Corneal astigmatism, on the other hand, refers to the optical representation of the corneal toricity in total ocular astigmatism as determined by clinical refraction techniques. Once corneal toricity is measured by keratometer and expressed as the difference between maximum and minimum curvature in mm or in dioptres, corneal astigmatism can be derived. For example if the keratometry reading is 44.00 @ 90 / 42.00 @ 180, corneal toricity = 2.00 DC and corneal astigmatism is calculated as −2.00 axis 180 (Grosvenor 1994). While corneal astigmatism derived in this manner is clinically

used, it must be kept in mind that if one is interested to determine retinal image forming properties contributed by corneal sphere and astigmatism, more complex formulae will be required (Maloney et al. 1993) and for this purpose the corneal shape information overlying the pupillary area is needed.

The aim of this current thesis is to investigate corneal shape factors that influence OK lens decentration. For this reason the term corneal toricity is more appropriate than corneal astigmatism. For the purposes of brevity and consistency, the term corneal astigmatism, when used in previous papers, will be referred to as corneal toricity (unless a vision aspect is involved) in this thesis.

1.3.5.3 Corneal toricity and its contribution to refractive astigmatism

Refractive astigmatism is influenced by a combination of corneal and lenticular astigmatism, with corneal astigmatism derived from corneal toricity being identified as the major contributor to refractive astigmatism in infants and young children (Howland and Sayles 1985, Dobson et al. 1999, Shankar and Bobier 2004). In 1890, Javal formulated an equation to demonstrate that a linear relationship exists between the amount of corneal toricity derived from the keratometer and the refractive astigmatism:

Refractive astigmatism = ω (corneal toricity) + k

where $\omega \approx 1.25$ and $k \approx 0.50$ D against-the-rule. However, this formula has been simplified subsequently by Grosvenor et al. (1988) by replacing the constant ω with unity. It must be emphasised that Javal's rule assumes a constant refractive contribution from lenticular astigmatism (Elliott et al. 1994). Although the modified Javal's rule was close to true values for refractive astigmatism, the formula's validity in determining the values for an individual has been questioned (Dobson et al. 1999).

1.3.5.4 Classification of corneal toricity

One of the early overnight studies investigating the efficacy of OK lenses (Mountford and Pesudovs 2002) proposed that individuals with central corneal toricity that extended to the limbus were poor candidates for spherical OK. This proposal was entirely based on the clinical impressions of the authors and no scientific base of evidence was presented in support of this argument. But it is worth noting that an earlier study demonstrated an association between peripheral corneal toricity and the success of soft toric contact lens fitting (Reddy et al. 2000), indicating that higher and irregular toricity towards the periphery of the cornea may be one factor that adversely influences the performance of soft toric contact lens.

Therefore a more detailed classification of corneal toricity based on the orientation and extent of corneal toricity is required.

1.3.5.4.1 Orientation

Based on the orientation of the meridian of the maximum or minimum curvature, corneal toricity can be divided into with-the-rule (WTR), against-the-rule (ATR) or oblique toricities (Borish 1975). Based on the range in which the steeper corneal meridian may lie the classification can be described as follows:

With-the-rule corneal toricity: The curvature of greatest power lies nearest the vertical meridian, falling within the area of the 60^{th} and 120^{th} meridian (90 ± 30 degrees).

Against-the-rule corneal toricity: The curvature of greatest power lies nearest the horizontal meridian, falling between the 30^{th} and 150^{th} meridian (180 ± 30 degrees).

Oblique toricity: The meridian of greatest curvature lies between the 30^{th} to 60^{th} or the 120^{th} to 150^{th} meridian.

1.3.5.4.2 Extent

Early devices allowed clinicians or researchers to assess corneal curvature only in the central region, but the technological advance of videokeratoscopy now allows the assessment of corneal curvature not only in the central region but also towards the peripheral region of the cornea. Early corneal topographers could provide basic information about peripheral shape, but they were not able to provide information about corneal toricity in the peripheral regions. Reddy et al. (2000) classified corneal toricity based on its magnitude and location in central and peripheral regions. The five types of magnitude and extent of corneal toricity described by Reddy et al. were:

Type I (Spherical cornea): Central and peripheral corneal toricity ≤ 0.75 DC.

Type II (Central toricity): Central toricity > 0.75 DC and also 0.75 DC more than the peripheral corneal toricity.

Type III (Limbus-to-limbus equal toricity): Central toricity within 0.75 DC of peripheral corneal toricity.

Type IV (Limbus-to-limbus greater peripheral toricity): Peripheral toricity more than central toricity, the difference being ≥ 1.00 DC.

Type V (Limbus-to-limbus irregular peripheral toricity): Irregular peripheral toricity, with opposing hemi-meridians varying by > 3.00 DC.

Based on this classification, Reddy et al. (2000) showed that the performance of soft toric contact lenses is unpredictable in eyes with types IV and V detailed above. In this thesis a slightly modified version of this classification is provided to relate the extent of baseline corneal toricity to OK lens treatment zone decentration (see Section 5.2.3).

1.3.6 Influence of external factors on corneal shape

Uniformity of corneal shape is also influenced by age, ethnicity, eyelid shape and eyelid pressure, and eyelid position when carrying out near tasks.

1.3.6.1 Age

Considerable scientific evidence exists to show that the corneal shape is influenced by age. Gordon and Donzis (1985) used keratometry readings in a sample ranging between newborns to 35 years of age to show that corneas tend to be steeper in younger age groups than older age groups. Asbell (1990) also showed a steady flattening in keratometry values as a function of age in children whose age ranged from newborn to 90 months. Age is also an important factor that influences the magnitude and orientation of corneal toricity. Infant eyes are shown to exhibit significant astigmatism which is mostly corneal in origin (Howland and Sayles 1985, Friling et al. 2004, Isenberg et al. 2004). In addition some large sample studies have shown a high prevalence of with-the-rule corneal toricity during younger ages and a gradual shift towards against-the-rule corneal toricity with advancing age (Anstice 1971, Baldwin and Mills 1981, Hayashi et al. 1995), which was primarily due to steepening of the horizontal corneal meridian (Baldwin and Mills 1981).

1.3.6.2 Ethnicity

Lam and Loran (1991) compared various ocular parameters of Chinese and Caucasian young adults. Using the photo-electronic keratoscope to determine corneal topography the authors measured central corneal curvature and shape factor p. The study showed that Chinese eyes had steeper corneal curvature and a higher value of shape factor than Caucasian eyes, indicating a more gradual rate of corneal flattening (less prolate or more oblate) from the apex towards the periphery in Chinese eyes.

Cheung et al. (2000) used the TMS-1 (Tomey, MA) corneal topographer to analyse apical corneal curvature and shape factor p in Hong Kong Chinese young adults. The authors further compared their outcomes to the values reported by previous investigators who

investigated Caucasians (Kiely et al. 1984, Lam and Loran 1991) and Chinese subjects (Lam and Loran 1991, Lam and Douthwaite 1996). Their analysis showed no significant difference in corneal parameters between their Hong Kong Chinese cohort and the Chinese or Caucasian cohorts of other studies.

In a cross-sectional study involving a large sample of children, Twelker et al. (2009) compared ocular components of five different ethnicities including African American, Asian, Hispanic, Native American and Caucasian ('Whites' is the term used in the publication). Corneal power in the vertical and horizontal meridians, which was measured using an auto-keratometer, showed significant differences between ethnicities. Native Americans exhibited greater corneal toricity and Caucasians showed least corneal toricity, while the remaining three groups had no significant differences in the amount of corneal toricity.

1.3.6.3 Eyelid pressure, position and shape

Grosvenor (1978) speculated that a band-like pressure from the tarsal plate of the upper lid along the horizontal meridian during blinking might cause with-the-rule corneal toricity during early childhood, and with advancing age this exerted pressure from the tarsal plate is reduced to reveal a more spherical corneal shape. Wilson et al. (1982) measured corneal toricity using a keratometer with lids in the normal position (opposing the eyeball) and also when retracted using an eyelid speculum. The authors found that lifting of the eyelids using the speculum caused a decrease in with-the-rule corneal toricity. By analysing corneal power change in the vertical and horizontal meridians, the authors concluded that the reduction of less with-the-rule corneal toricity was not because of flattening of the vertical meridian but because of steepening of the horizontal meridian. Wilson et al. assumed that by lifting the eyelids, the cornea was liberated from the influence of eyelid pressure, thereby manifesting the inherent corneal toricity.

Eyelid tension was assessed in 100 patients by Vihlen and Wilson (1983). The mean eyelid tension measured was 3.22 g/mm (range 1.16 – 6.78 g/mm). No correlation was found between eyelid tension and corneal toricity. The method employed in assessing the eyelid tension could be questioned however, because of this unexpected outcome. The eyelid tension was assessed while it was pulled away from the eye surface so essentially this process was measuring the tension of the eyelid separate from, rather than when resting against, the globe.

The influence of eyelid position on the astigmatism of 50 young healthy eyes was investigated by Grey and Yap (1986). Refractive error was measured using an autorefractor with the normal palpebral aperture and when the aperture was deliberately narrowed and widened. There was no change in the spherical refractive error in all eyelid positions, but a significant increase in the cylindrical error (approximately 2.00 DC) was noted when the palpebral aperture was narrowed, indirectly demonstrating the effect of eyelid pressure on corneal curvature.

Lieberman and Grierson (2000) investigated central corneal shape in four eyes using a Computer Aided Design (CAD) surface modelling technique, to reveal changes to corneal shape when the eyelids were retracted from the cornea. Ehrmann et al. (2001) assessed the eyelid tension in a small number of Asians and Caucasians to reveal no significant difference between these groups. No direct relationship was established between eyelid tension and corneal shape by Ehrmann et al. However caution is indicated when generalising the results of these two studies because the results are based on measurements from only a few subjects.

Shaw et al. (2010) investigated the pressure of the upper eyelid in a static situation (no active blinking) in 11 young adults using a piezoresistive pressure sensor attached to a rigid contact lens placed under the central upper eyelid for approximately 12 seconds. From the investigation of different hypothesised models, the results of the experiment revealed that the upper eyelid exerted a mean pressure of 8.00 ± 3.40 mm Hg. The main aim of the study was to investigate the pressure of the eyelid but not its effect on the cornea.

The influence of eyelid shape (morphometry) on corneal shape of healthy subjects was first investigated by Read et al. (2007a). Some interesting relationships were found between the features of eyelid morphometry and corneal shape variables. The horizontal palpebral fissure width showed a positive correlation with corneal spherical equivalent power, and the angles of the eyelids were positively associated with the angles of corneal cylinder, indicating that slanting of the eyelid influences the orientation of corneal toricity. The lower eyelid was also shown to have interesting associations with corneal shape. Flatter lower eyelid shape was shown to be positively correlated with with-the-rule corneal toricity. These outcomes provide indirect evidence to support the previous assumptions that eyelid pressure influences corneal shape.

1.3.6.4 Visual tasks

Abundant past literature is available investigating the effects of the continuous presence of eyelids on corneal shape. Most of the previous authors have related monocular or binocular diplopia or blur to the corneal shape changes that occurred after a continuous visual task (Carney et al. 1981, Ford et al. 1997, Golnik and Eggenberger 2001).

Near tasks for a duration of as little as 15 minutes have been shown to have an influence on corneal shape. Carney et al. (1981) gave a 15-minute monocular microscope viewing task to 9 subjects, and corneal shape was assessed using a photokeratoscope in the opposite eye. Subjective responses about secondary images and their angular separation were recorded. Five out of 9 subjects reported monocular polyopia (viewing more than two images). A prediction of angular separation of images were made by ray tracing from the corneal shape information obtained from the photokeratosope images. There were significant positive correlations between the subjective and objective prediction of the angular separation of the secondary images, which suggested that the polyopia was induced by the distortions observed on the cornea.

In another controlled study, Ford et al. (1997) compared ocular measurements in six patients who presented with near vision disturbances in both eyes and also 28 healthy controls who had no visual symptoms. Both groups were given a 30 minute reading task. Ocular measurements included videokeratoscopy (TMS 1), examination of red reflex by performing direct ophthalmoscopy or retinoscopy, interpalpebral fissure width in primary and reading positions, and photographic documentation of the red reflex using a hand-held fundus camera (Kowa RC-2, Tokyo, Japan). The results showed significant differences in corneal shape parameters between symptomatic patients and the control group. Those subjects who developed a horizontal band on the red reflex also had subjective complaints of diplopia. The interpalpebral fissure width was significantly smaller in the symptomatic patient group than in the control group in both primary position and during reading. This study concluded that the position of the eyelid can cause corneal distortions in some individuals.

Golnik and Eggenberger (2001) evaluated corneal topography in 3 patients with symptoms of monocular blur or diplopia alongside 9 control asymptomatic subjects. All subjects were given a near reading task in downward gaze. Corneal topography was captured using Placido disc-based corneal topographers (EyeSys or TMS1). From the corneal topography subtractive maps it was found that the distortions in the cornea were the consequence of continous reading, as they disappeared after subjects assumed a normal primary gaze.

In another reading task study, Buehren et al. (2003) investigated corneal shape after 1 hour of reading to reveal wave-like distortions of corneal topography, which was assessed using the Keratron videokeratoscope. The study suggested evidence of eyelid effects on the cornea. Further, the corneal topography showed induction of 0.37 D spherical error and 0.41 DC of cylindrical error with change in cylindrical axis of up to 30 degrees when compared to the pre-reading corneal status. Later, Collins et al. (2006) demonstrated that the changes in corneal topography differed according to the kind of near visual task that was being performed. Shaw et al. (2008) continued this work to evaluate corneal refractive changes after 15 minutes of near tasks (reading and steady near fixation) at 20 degrees and 40 degrees of down gaze. Eyelid morphometry features were also collected to assess associations with the corneal changes measured after performing the near tasks. Corneal spherical equivalent power did not show significant change at 20 degrees downward gaze but showed significant change at 40 degrees downward gaze. The corneal vertical component of astigmatism (J_{180}) exhibited significant change for both near tasks at both angles of downward gaze. The corneal oblique component of astigmatism (J_{45}) revealed changes during steady fixation at the 20 degrees downward gaze angle and reading at 40 degrees downward gaze angle. During 40 degree near tasks, the downward and upward eyelid slants were correlated with negative and positive J_{45} changes respectively. This study emphasised that significant corneal changes could be observed with downward gaze near tasks, and that these are further related to the eyelid morphometry observed in these downward gazes.

1.3.7 Representing changes to corneal toricity

Corneal toricity possesses not only magnitude but also a direction. Considering the example quoted in Section 1.3.5.2, if the keratometry or Sim K reading in dioptres is 44.00 @ 90 / 42.00 @ 180, the magnitude of corneal toricity is 2.00 DC which means that by negating the spherical component of 42.00 D from the cornea an excess of 2.00 D power along the 90 degree meridian will remain. One cannot merely consider the magnitude of toricity and ignore the direction component when analysing corneal changes during OK. However, considering these values as scalar components does not allow for meaningful statistical analysis. Vector analysis methods have been proposed for such analyses, which will allow changes in corneal toricity to be analysed in a meaningful manner taking into account both magnitude and direction of corneal toricity.

1.3.7.1 Corneal power representation using Thibos's vector coordinates

Thibos et al. (1997) suggested the application of Fourier series in rectangular form to represent the conventional sphero-cylindrical format (sphere / cylinder at axis) of an optical lens. The decomposition of the conventional form thus leads to one spherical lens and two cross cylinders, one of whose axes is located at 0/180 degrees and the other at 45/135 degrees. The formulae used to derive these vector components are:

$$M = S + C/2$$

$$J_{180} = -(C/2)\cos 2\theta$$

$$J_{45} = -(C/2)\sin 2\theta$$

where S is the sphere, C is the magnitude of astigmatism and θ is the angle of astigmatism. M represents the spherical equivalent power, J_{180} represents the vertical astigmatism component and J_{45} represents the oblique astigmatism component. This method allows the description of changes in corneal power over time in spherical, vertical and oblique components of corneal power independently. A limitation in denoting the corneal power using Thibos's vector components is that the J_{180} and J_{45} components do not directly state the direction of corneal toricity and therefore cannot be used to denote change in the corneal toricity direction before and after OK lens wear or surgical procedures.

1.3.7.2 Other forms of vector analysis used to describe corneal toricity changes

Mountford and Pesudovs (2002) used two other forms of vector analysis to demonstrate changes in corneal toricity during OK. Both these methods use the powers and their angles along the principal corneal meridians before and after lens wear. The methods used by Mountford and Pesudovs (2002) to analyse corneal toricity changes after OK were:

- Bailey and Carney vector analysis
- Alpins vector analysis

1.3.7.2.1 Bailey-Carney vector analysis

Bailey and Carney (1970) devised a method to analyse astigmatic changes induced by contact lenses using vector analysis. In this graphical method, lens-to-cornea relationships before and after lens wear are established and plotted on a graph. These two points on the graph are called modes of fit. The vector joining the co-ordinates of these two modes of fit represents the change in corneal shape due to lens wear.

Figure 1-4 describes the method of plotting the vector to denote change in magnitude of corneal toricity. Four possible outcomes can be detected from this graphical method (Mountford and Pesudovs 2002):

1. If the vector derived from the pre-fit mode to post-fit mode lies parallel to the sphericity locus then there is no change in the amount of corneal toricity.

2. If the vector moves away from the sphericity locus, then it indicates an increase in with-the-rule corneal toricity or decrease in against-the-rule corneal toricity.

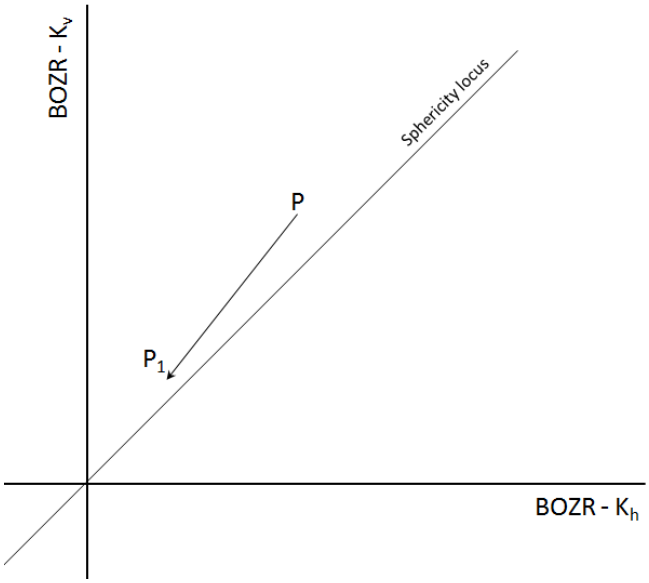

Figure 1-4. Representation of Bailey-Carney change in corneal toricity using the graphical vector method. The difference between the back optic zone radius of curvature (BOZR) of the lens (mm) and the radius of curvature (mm) of the cornea along the horizontal corneal meridian (K_h) is denoted on the horizontal axis of the graph and similarly the difference between the BOZR of the lens and the curvature along the vertical corneal meridian (K_v) is denoted on the vertical axis. The straight line passing through the origin of the graph and making an angle of 45 degrees with horizontal and vertical axes is called the 'sphericity locus'. The vector joining the pre-fit mode (P) and post-fit mode (P_1) represents the magnitude and direction of change in toricity after wearing a lens with the given BOZR. If the corneal meridians show no change in toricity then the mode of fit vector will lie parallel to the 'sphericity locus'. Figure adapted from Bailey and Carney (1970).

3. If the vector direction just intersects the sphericity locus, it indicates total abolition of corneal toricity and therefore the cornea assumes a spherical surface.

4. If the vector moves towards but does not intersect the sphericity locus it indicates reduction in corneal toricity but the cornea fails to attain complete sphericity.

There are some limitations to the Bailey-Carney method of vector analysis of corneal toricity changes. It is difficult to visualise this graphical method and is hard to determine the

change in corneal toricity in a clinical setting. It is apparent from the description that the method does not take the angles of radius of curvature of the cornea along horizontal (K_h) and vertical (K_v) meridians into account, thus failing to analyse the change in the angle of corneal toricity after contact lens wear. Although some information of change in the orientation of astigmatism (such as with-the-rule to against-the-rule) is inferred from this method, it is not the same as calculating actual change in the angle of corneal toricity.

1.3.7.2.2 Alpins vector analysis

Alpins (1993) applied vector analysis using rectangular coordinates to determine changes in corneal toricity after refractive surgery. Given the similarity in targeted refractive outcomes between refractive surgery and OK, the Alpins method can also be used to evaluate such changes during OK (Mountford and Pesudovs 2002).

The Alpins method takes into consideration the magnitude of corneal toricity and steeper corneal meridian angle before and after the surgical procedure, as well as the targeted reduction in ametropia. The polar notation (e.g. 2.00 @ 20) of these corneal meridional powers is converted to rectangular coordinates from which the correction achieved and residual or induced toricity can be determined. Further, it is possible to calculate index of success of the surgical procedure and also angle of error. This method is superior to the Bailey-Carney method because the analysis takes the angle of toricity into account. For consistency with the published work, the Alpins published terminology of using 'astigmatism' rather than 'toricity', which has been adopted throughout this thesis, has been retained.

Figure 1-5 shows the vector diagram plotting the X, Y coordinates calculated for each vector. The length of the vector from the origin denotes the magnitude of toricity and the angle from the positive x-axis indicates twice the angle of the steeper corneal meridian for each vector. Figure 1-5 also shows the vector magnitudes between the locations of preoperative toricity (preOp) and toricity that was targeted and achieved. The magnitude of the vector between the preOp and target is called the target-induced astigmatism (TIA) and the magnitude of the vector between preOp and achieved is called the surgically-induced astigmatism (SIA). Finally the magnitude of the vector between the target and achieved locations is called the 'difference vector' (DV), which is the amount of dioptric correction still required to reach the targeted correction of toricity.

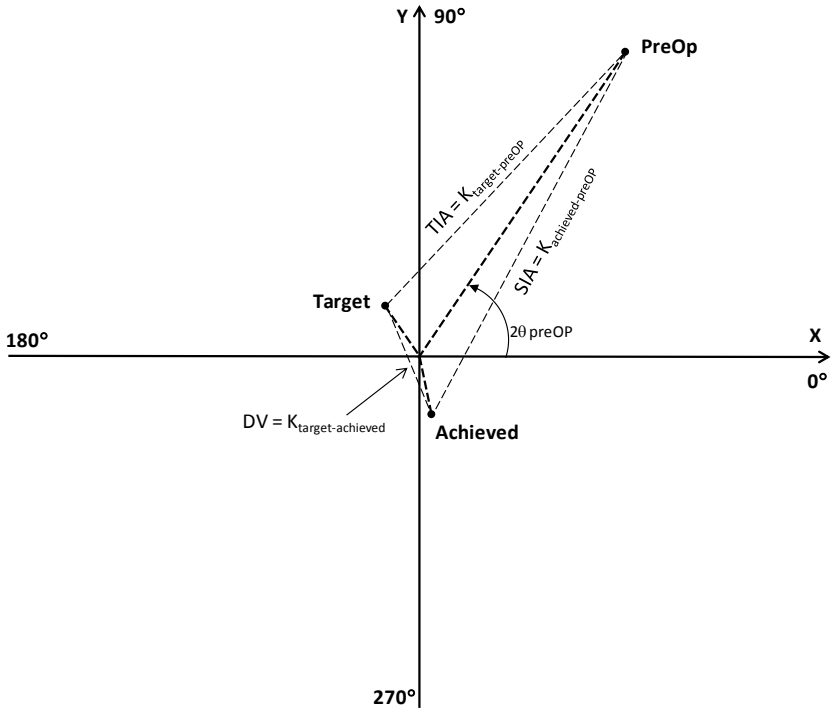

Figure 1-5. The double angle vector diagram to illustrate Alpins vector analysis. TIA = Target induced astigmatism, SIA = Surgically induced astigmatism and DV = difference vector. Figure adapted from Alpins (1993).

Alpins further calculated various useful indices from these vector analyses including magnitude of error, angle of error, coefficient of adjustment and index of success. The descriptions for these indices are as follows:

The magnitude of error is calculated as the difference between SIA and TIA in dioptres. The magnitude of error is positive if there is an over-correction and negative if there is an under-correction due to surgery (or OK treatment).

The angle of error is calculated from the double angle values as:

$$\theta_{error} = (\theta_{achieved - preOp} - \theta_{target - preOp})/2$$

A positive angle of error indicates that the correction of the angle due to the procedure is biased towards a counter clockwise direction and vice versa for a negative angle of error (Figure 1-6).

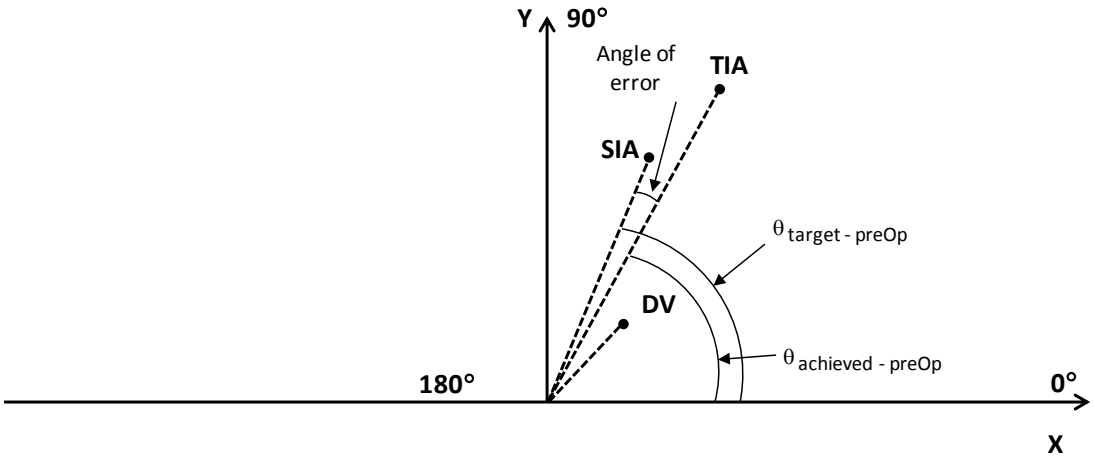

Figure 1-6. A single angle vector (180 degree format) diagram illustrating angle of vector determined from Alpins vector analysis. SIA: Surgically-induced astigmatism, TIA: Target-induced astigmatism and DV: difference vector.

The coefficient of adjustment is determined as the ratio between magnitudes of TIA and SIA vectors. If the coefficient of adjustment is greater than 1, then this indicates an undercorrection of the magnitude of toricity, while less than 1 indicates overcorrection.

The index of success is the ratio between the magnitude of DV and TIA, the value of which indicates the success of surgery (or OK treatment) which can easily be transformed into a percentage. The index of success can lie between 0 and 1, where 0 indicates that the complete magnitude of toricity that the treatment was targeted to correct has been achieved, 1 indicates that no treatment effect has been achieved, and a value lying between 0 and 1 indicates that partial correction was achieved. For example if the index of success is 0.28, the percentage of correction can be determined as 1−0.28 = 0.72 × 100 = 72 % of the targeted change to astigmatism was achieved.

The major limitation of both Bailey-Carney and Alpins vector analyses of corneal toricity change is that they are relatively unfamiliar to general optometry clinicians. Moreover, both of these methods consider that the corneal toricity is regular in that the steep and flat corneal meridians lie perpendicular to each other. But after refractive surgery and OK, the cornea may exhibit some irregularity in shape which means that the steep and flat corneal

meridians may no longer be perpendicular to each other. For this reason these methods are unlikely to adequately or appropriately describe changes in corneal shape and toricity in OK.

1.3.7.3 Analysis of corneal regular and irregular corneal astigmatism using Fourier analysis

Fourier analysis overcomes the limitations of the vector analysis methods of describing corneal toricity by decomposing corneal shape data into corneal regular, irregular and higher order irregularities (Hjortdal et al. 1995, Raasch 1995). Its attraction comes from the fact that each of these components can be independently analysed. The corneal power data determined from the reflected Placido disc image are treated using Fourier analysis to fit with trigonometric components which can be written using the formula (Keller et al. 1998):

$$f(\ ) = \sum_{n=1}^{N} [c_n \cos\ n(\omega + \alpha_n)]$$

where is the angular frequency, α_1 …. α_n is the phase shift angle, ½ a_0 gives the spherical equivalent power of the cornea and coefficients c_1 …. c_n describe various corneal irregularities including c_1 (asymmetry component), c_2 (regular astigmatism component), c_3 (irregular astigmatism component) and $c_{4....n}$ which measure higher order irregularity components. However the limitation remains that this analysis is not very user-friendly for an average practitioner to infer corneal shape changes.

1.4 SPHERICAL RIGID CONVENTIONAL AND ORTHOKERATOLOGY CONTACT LENS FITTING TECHNIQUES

To understand how OK lenses can influence corneal shape a familiarity with OK fitting techniques is required. However, the understanding is easier if the fitting process is explained by first describing the basics of fitting techniques for conventional spherical rigid contact lenses.

1.4.1 Spherical rigid gas permeable contact lens fitting techniques

The general approach in conventional spherical rigid gas permeable (Sph-RGP) contact lens fitting is to align the lens as closely as possible with the corneal surface to evenly distribute the weight of the lens. In general this requires the contact lens back optic zone radius (BOZR) or base curve to be fitted in alignment with the flatter meridian of the cornea in an approach termed the ‘on-K’ fitting method. The peripheral lens curves are then made

progressively flatter than the BOZR to allow continued alignment with the cornea which, as shown in Figure 1-1, is known to flatten towards the periphery. By carefully calculating the rate of change in peripheral lens curvature, an alignment fit can be maintained with the flat corneal meridian.

In the presence of corneal toricity a misalignment between the spherical back surface of the lens and the toric cornea is inevitable and becomes problematic once toricity exceeds 1.00 or 1.50 DC. The misalignment is due to the steeper corneal meridian being steeper than the back surface curvature of the lens, causing lens edge lift in the periphery that increases with greater amounts of corneal toricity. This leads to lens instability and possible decentration. In these cases, the 'one-third' rule or some other similar rule that steepens the lens base curve is used to improve lens fitting. Different authors have identified different rules of thumb with slight variations in their indications. One method is to calculate the base curve of the Sph-RGP lens to be steeper than the flatter corneal meridian by one-third of the difference in the corneal curvatures between the two principal meridians. Some authors have suggested this method should be used if the magnitude of corneal toricity ranges between 1.00 and 2.00 DC (Phillips 1997, Bennett and Sorbara 2009) while others have suggested the use of this approach if the magnitude is between 2.12 to 2.87 DC (Bennett and Sorbara 2009). Other suggested methods are to reduce lens radius of curvature (in mm) along the flatter corneal meridian by 0.50 mm for every 0.50 DC of toricity above 2.00 DC of corneal toricity (Guillon 1994). The underlying aim of these rules is to control the excessive edge lift along the steeper corneal meridian that would otherwise occur if the lens was fitted in alignment with the flatter corneal meridian, and to promote lens centration.

1.4.2 Orthokeratology lens fitting techniques

Modern OK lenses are fitted using a flat central BOZR and steeper peripheral curves (reverse geometry) designed to stabilise the peripheral lens fit and improve lens centration. These lenses are typically fitted to eyes with < 1.50 DC of corneal toricity (Walline et al. 2004). Although not previously investigated, fitting OK lenses on corneas with > 1.50 DC toricity is believed to cause lens decentration beyond acceptable limits. In this section, fitting techniques that are used to fit spherical OK lenses on eyes with < 1.50 DC corneal toricity will be described.

The fitting techniques can be broadly classified into:

- Base curve-based fitting technique
- Sag fitting technique

1.4.2.1 Base curve-based fitting technique

The base curve or back optic zone radius (BOZR)-based fitting technique is based on the theory that the OK lens is fitted with a base curve flatter than the flattest corneal curvature by an amount that is equal to the magnitude of myopia targeted for reduction. With this technique alterations of the BOZR bring about the desired myopic reduction by moulding the central cornea. Simultaneously, the manipulation of one or more peripheral curves attains an optimal lens centration.

Base curve-based fitting is dependent on the so-called Jessen factor (1962), which involves fitting a rigid contact lens with a base curve flatter in dioptres by an amount equivalent to the desired myopic reduction (absolute refractive error value, T, in dioptres). Therefore the formula for choosing the BOZR (in dioptres) of the initial OK lens is:

$$BOZR = K_f - T$$

where K_f (in dioptres) is the corneal curvature along the flatter corneal meridian. Many present-day OK lens manufacturers use this technique to define the required base curve in order to reduce myopia using the OK procedure (Dreim Lens, Taiwan; Paragon CRT, USA; Fargo, USA; Emerald, USA; eLens, China) (Mountford 2004a, Chan et al. 2008b). However, one problem with this method is that it is difficult to determine the peripheral reverse curves required to stabilise the flat fitting lens on a given cornea. Mountford (2004a) commented that the introduction of the reverse curve made the fitting procedure difficult and this is further complicated as the overall lens diameter is varied, leading to inconsistencies in OK fitting outcomes with early reverse geometry lenses.

Fitting an OK lens where the BOZR is chosen in accordance with the Jessen factor may lead to optimal reduction of myopia in the morning immediately after lens removal, but Mountford (1998) showed that the amount of myopic correction in the morning after lens removal tended to gradually regress during the day, eventually causing blurring of vision by the end of the day. To overcome this issue a further flattening factor loosely called the compression factor (CF) of 0.50 to 0.75 D in addition to the Jessen factor has been suggested

to compensate for day time regression. Thus the modified formula for choosing the appropriate base curve becomes:

$$BOZR = K_f - T - CF$$

Rah et al. (2002) and Chan et al. (2008b) showed a positive association between lens flatness (K_f − BOZR) and the amount of myopic reduction achieved after one year and 2 weeks of overnight OK lens wear respectively. Both studies gave regression equations to estimate the myopic reduction based on K_f – BOZR. Hypothetical data can be created by fixing the K_f value to 44.00 D and the target myopic reduction between 1 and 6.50 D. Using the regression equations from these two studies, the hypothetical data are plotted in Figure 1-7. It is apparent from the plot that, as the flatness of the fit is increased, greater myopic reduction is achieved. Since the K_f value is fixed, the K_f – BOZR should purely reflect myopia targeted for correction. Therefore in other words, as the target myopia increased the proportion of myopic correction achieved after OK lens wear was less. This suggests that although greater flattening of OK lenses resulted in greater reduction in myopia, the relationship is not 1:1, and the discrepancy is larger in eyes with greater amounts of myopia.

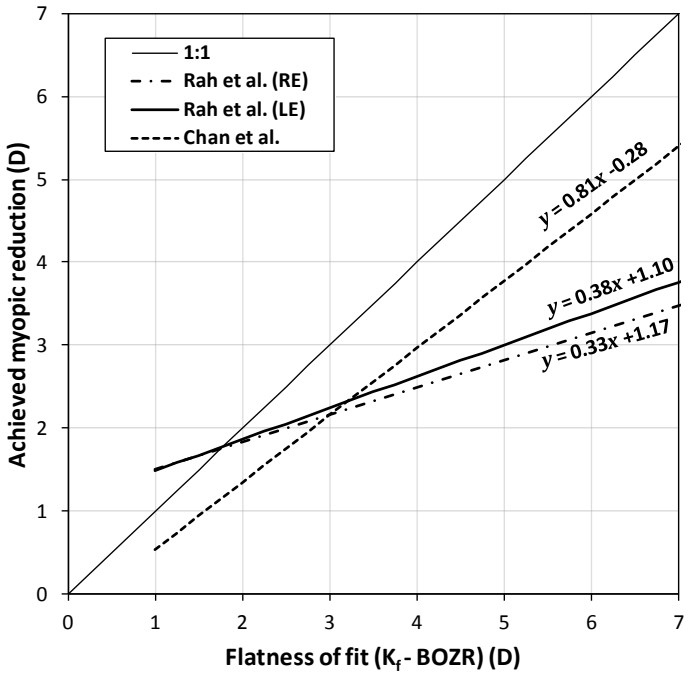

Figure 1-7. Association between the flatness of fit (Kf – BOZR) and achieved myopic correction after overnight wear of orthokeratology lenses from regression equations presented by Rah et al. (2002) and Chan et al. (2008b).

Caution is indicated when interpreting these analyses, because the results of both studies are affected by methodological limitations. The Rah et al. study combined the results from two different lens designs (the Fargo 6, GP Specialists, Phoenix, AZ and Paragon CRT, Paragon Vision Sciences, Mesa, AZ) which use different fitting techniques. The initial BOZR for the Fargo 6 lenses was selected using the formula BOZR (D) = Kf – 4 (the lens BOZR is 4 D flatter than the flatter corneal meridian), meaning there is no involvement of either targeted myopia or compression factor in determining the BOZR. On the other hand fitting Paragon CRT lenses the BOZR was determined using the formula BOZR (D) = Kf – T – 0.50, which involved the target myopia (T) and a compression factor of 0.50 D. Other limitations of the study were that more than one investigator fitted lenses as the study was conducted at multiple centres. The authors also admitted that there was only minimal training of these investigators with regards to lens fitting. Further, there was a large drop out of participants from the study. All these factors would have affected the regression equation determined from this study.

When it comes to the study conducted by Chan et al. (2008b), the authors evaluated the validity of the Jessen factor in addition to the compression factor during overnight OK, however, the compression factor used in this case was 0.75D (BOZR = K_f – T – 0.75). With this formula Chan et al. derived a linear regression equation whose slope was greater than that of Rah et al., indicating a better relationship between the flatness of fit and the amount of myopic reduction achieved but still showing that the relationship is not 1:1. The authors therefore suggested a slight modification in the fitting formula based on their regression equation. If an over-correction of 0.75 D is immediately after lens removal, the BOZR must be flattened by a factor of 1.23 times the target myopic reduction (T) plus 1.27 D. Therefore the revised formula to determine the BOZR (in dioptres) becomes:

$$BOZR = K_f – (1.23 \times T) – 1.27$$

For example, if 2.00 D myopic reduction is targeted, the lens base curve should be 3.73 D flatter than the flat corneal meridian [BOZR = K_f – (1.23 × 2) – 1.27 *or* BOZR = K_f − 3.73 D]. However the authors have suggested caution in using this new modified formula as their results were based on a retrospective analysis. A controlled prospective study is needed to further validate this modification in the formula. It must also be noted that the formula may hold correct only in their population of Asian eyes from which it was derived.

The major drawback with the base curve-based fitting technique is that the BOZR of the lens is determined only on the basis of the central corneal curvature and disregards the

peripheral corneal curvature. It is known that normal corneal curvature tends to vary from the centre towards the periphery and the rate of change shows individual variation (Kiely et al. 1982). Bibby (1979a, b) described the problems that may arise when designing conventional rigid contact lenses based on only the central corneal curvature, and also highlighted the need to take the peripheral corneal shape into account when designing the lens periphery. This generated the idea of sag-based fitting of conventional rigid contact lenses, which has since been adopted in fitting OK lenses.

1.4.2.2 Sag-based fitting technique

To overcome the fitting difficulties of the base curve-based fitting technique in OK, Mountford (2004a) proposed a sag-based fitting technique, where the sagittal (sag) depth of the OK lens with a reverse geometry design is calculated to match the corneal sag height over a common chord plus an allowance for tear layer thickness (TLT) at the corneal apex. The common chord is chosen to coincide with the intended peripheral bearing points of the lens (Figure 1-8).

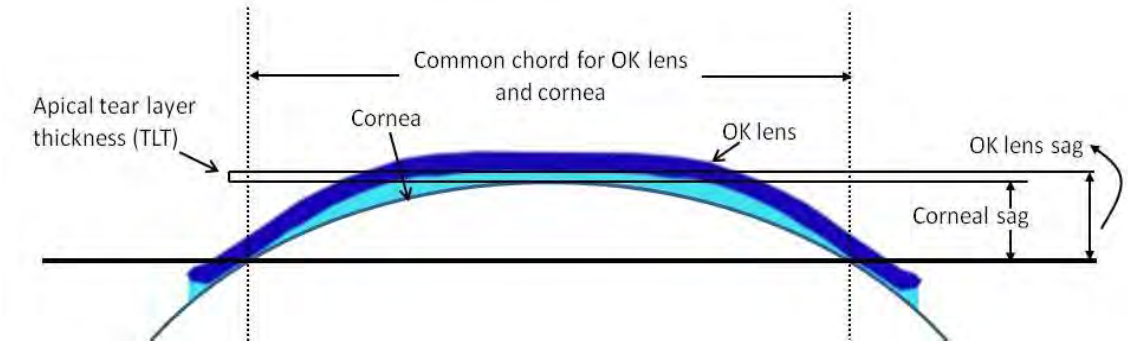

Figure 1-8. An illustration of the sag-based fitting technique.

Mountford (2004a) reviewed the hydraulic forces generated under conventional rigid contact lenses described by previous authors (Bibby 1979b, Guillon et al. 1983, Atkinson 1984, 1985). The review revealed that hydraulic forces help to maintain good lens centration by opposing eyelid forces. Based on this theory, he suggested that hydraulic forces generated under the OK lens could determine the dynamics of the OK lens fitting relationship to the cornea required to induce the refractive effect, as opposed to a direct moulding effect induced by the lens base curve. In order to generate adequate fluid forces under the OK lens the importance of maintaining an appropriate tear layer thickness (TLT) at the corneal apex was also proposed. Whereas the TLT at the apex should be approximately 20 μm during conventional rigid contact lens fitting, Mountford suggested that a maximum of 10 μm would

be needed during OK lens fitting in order to induce central corneal flattening. The TLT at the apex can be reduced towards a minimum of zero which means contact with the corneal surface. However this is not encouraged as it may induce corneal epithelial damage.

Corneal sag height (x) can be determined by rewriting Baker's equation as follows:

$$x = \frac{\left[R_o - \sqrt{R_o^2 - y^2 \cdot (Q+1)}\right]}{Q+1}$$

where R_o is apical corneal radius in mm, Q is the corneal asphericity of the flatter corneal meridian over a specified semi-chord length (y) in mm. The incorporation of Q over a specified chord length (which is usually greater than 4 mm) into this calculation indicates that the determination of the OK lens back surface design is dependent on corneal shape beyond the central zone.

To determine the sag height of the OK lens, the sag formula is applied for BOZR and each peripheral curve of the lens up to the specified chord length. The addition of all of these individual sag heights gives the overall sag height of the OK lens. The calculation of lens sag is based on the number of curves on the lens back surface. If the lens is designed to be a tricurve then the same formula described above can be used to determine the sag height at each peripheral curve separately and then added together. The formula then becomes:

Total lens sag = (sag of BOZR at BOZD) + (sag of BPR_1 at BPD_1 – sag of BPR_1 at BOZD) + (sag of BPR_2 at TD – sag BPR_2 at BPD_1) + TLT

where BOZD is the back optic zone diameter, BPR_1 and BPD_1 are radius of curvature and width of the first peripheral curve respectively, BPR_2 and TD are radius of curvature of the second peripheral curve and total diameter of the lens respectively, and TLT is the tear layer thickness. Thus an accurate lens fit is established by selecting a lens that has a sag height which matches the corneal sag height plus an allowance for TLT.

Mountford (1997a) employed the sag-based fitting technique when fitting Contex OK series lenses (Sherman Oaks, California) to demonstrate a high positive correlation between change in refraction after overnight OK lens wear and change in mean keratometry (r = 0.88, p < 0.001) and also apical corneal curvature (r = 0.95, p < 0.001). Mountford (1997a) subsequently compared the outcomes from fitting these lenses by following the company guidelines of fitting the initial lens 1.50 D flatter than the flattest corneal meridian, and also following the sag-based fitting technique. This revealed the superior performance of the sag-

based fitting method which reduced the apical curvature by approximately 0.50 D more than when the manufacturer's recommendation was followed. BE OK lenses (Capricornia Contact Lens, Australia) are fitted using the sag-based fitting technique.

1.4.3 Orthokeratology fitting methods

Sag-based fitting is reliant on accurate corneal topography data, which leaves a margin of possible error. Furthermore, there are external factors such as the eyelid which can influence the lens fitting relationship on the eye. A number of different fitting approaches have been developed to overcome these limitations, and in some cases to allow lens fitting based on corneal keratometry values in place of accurate corneal topography data. These fitting techniques largely fall into the following categories:

- Empirical fitting
- Trial lens or diagnostic fitting
- Inventory-based fitting

1.4.3.1 Empirical fitting

The empirical fitting method is the simplest approach to take. The practitioner takes all the required ocular measurements which include refraction, eye dimensions such as horizontal visible iris diameter, and corneal measurements such as keratometry or corneal topography. These details are then either forwarded to the lens manufacturer for fabricating the lens, or entered into a computer program provided by the manufacturer to determine the lens parameters that are subsequently sent directly to the manufacturer. The manufacturer then delivers the final contact lens to the practitioner. The lens is expected to perform well in terms of fitting and also provide appropriate vision on its initial application.

A major advantage of the empirical fitting approach is that it can reduce the number of patient visits that are required, but there are also many limitations with this method. The patient would not have an experience (if a neophyte) of how the lens will feel on the eye until the ordered lens is dispensed. The lens may need to be re-ordered with altered parameters if the empirically ordered lens does not fit correctly, losing the main benefit of the empirical fitting method. Furthermore, in some systems, control of the lens fit is governed entirely by the laboratory, meaning that the practitioner has little control over the lens fitting process. The NightMove® OK lens manufactured by Gelflex Laboratories (Perth, Australia) adopts the empirical method.

1.4.3.2 Trial lens or diagnostic fitting

Trial lens or diagnostic lens fitting relies on corneal topography data to allow determination of the initial lens parameters in order to select a lens from a diagnostic set of lenses held by the practitioner. Diagnostic sets typically hold approximately 20 lenses designed to cover a range of different sag heights, and are not designated to correct the full refractive error. This gives the practitioner an opportunity to try different lenses until the fit is satisfactorily stabilised, to give confidence in ordering the final lens specification from the laboratory. Overnight trials are generally conducted until a satisfactory topographic outcome is achieved. Then, based on performance of the final best-fitting trial lens, a lens is ordered to match the diagnostic lens fitting characteristics and provide the desired refractive change. Although multiple trials may be required, the practitioner gains confidence about the performance of the lens fit before having to commit to a final lens order. However, the major limitation is that this process can be time-consuming, particularly in the case of OK which requires overnight wear of lenses to determine clinical outcomes. This means that the patient may be required to wear various trial OK lenses on several nights to allow the practitioner to decide about the lens parameters that give a clinically acceptable topographic pattern. Moreover, to wear off any effect of previous lens wear a washout period between overnight trials may also be necessary. This can become tedious for the patient and practitioner if multiple visits eventuate. The BE lens design uses a trial lens fitting approach.

1.4.3.3 Inventory-based fitting

This method is a slightly enhanced version of the trial lens method in that the practitioner now holds a bank of lenses with combinations of different sag heights and different targeted refractive corrections. The general aim is for the set to completely cover a typical range of sag heights and refractive corrections. Although the fitting process is essentially the same as for trial lens fitting, the lens can also be targeted to provide the refractive change required. This means that the final lens can often be dispensed directly from the inventory on the same day to the patient, avoiding any delay that may occur due to ordering and receiving the final lens from the manufacturer. Any changes to the lens that are required can also be sourced directly from the inventory set. However, the major disadvantage is that the practitioner must own a large inventory of contact lenses, which needs to contain in the region of 120 lenses, making this an expensive upfront investment for the practitioner to make. Paragon CRT (Paragon Vision Sciences, USA) employs an inventory-based OK lens fitting process.

1.4.3.4 Comparing the performance of different fitting methods

Only a few studies have compared the outcomes of different OK fitting methods. Tahhan et al. (2003a) compared the performance of four different types of OK lens design by following the fitting protocols recommended by the manufacturers. Fitting of two lens designs (DreimLens, FL, and Contex D Series, CA) required following an empirical method of fitting and the other two lens designs (Rinehart Reeves, FL, and BE, Ultravision Capricornia, Australia) required following a trial lens fitting method. The authors reported no difference in clinical performance with regards to the reduction of myopia between the OK lens designs. The rate of refitting after dispensing the lenses was shown to be minimal for both types of fitting approaches, and no refitting was needed with BE OK lens, leading the authors to attribute this success to the trial lens-based fitting method employed with these lenses. Another study (Maldonado-Codina et al. 2005) compared the OK lens manufactured by No.7 Contact Lens Laboratories (UK), fitted using an empirical method, and BE OK lenses supplied by NKL Contactlenzen (the Netherlands) fitted using the trial lens method. In terms of reduction of myopia and first lens fit success the BE OK lenses were shown to perform better than the No.7 contact lenses.

1.5 CORNEAL TOPOGRAPHIC MAPS IN ORTHOKERATOLOGY LENS FITTING

In order to understand the effects of OK lenses on corneal shape, it is necessary to become familiar with various corneal topographic maps that are displayed by a typical corneal topographer. Each topographic map display has its own advantages and disadvantages when reviewing corneal shape either before or after OK. This section provides an overview of these aspects with special attention to OK.

1.5.1 Determination of local curvature of an optical surface/cornea

Before describing details about various corneal topographic maps, a brief review on different ways of describing local curvatures of an optical surface will be presented. As described before (Section 1.3.5.1), an optical surface shape can be described using the principal curvatures along steep and flat meridians which are orthogonal to each other. In a similar manner, curvature at any given point on the surface can also be described by two principal sections, one in a radial direction and the other perpendicular to this section. The former is called the ‘tangential curvature’ and the latter is called as ‘sagittal curvature’.

1.5.1.1 Tangential curvature

Tangential curvature (also called instantaneous radius of curvature, meridional radius of curvature or true radius of curvature) describes curvature measured at a point on a radially symmetrical optical surface which includes the normal to the surface. Tangential curvature is orientated in the direction of the meridional (or radial) plane which passes through the optical axis (Menchaca and Malacara 1984, Lu and Smith 1990) (Figure 1-9).

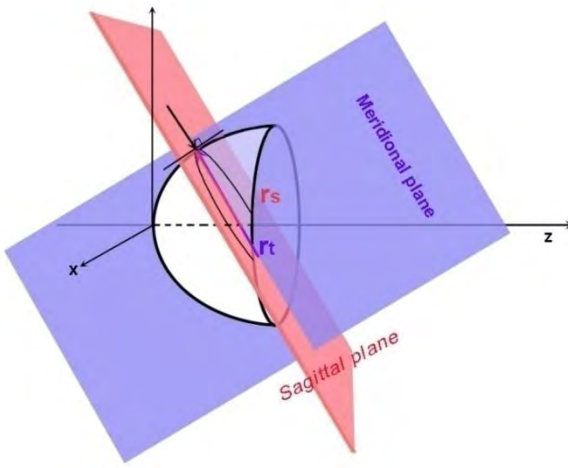

Figure 1-9. A diagrammatic illustration of tangential (r_t) and sagittal curvatures (r_s) of an optical surface. The x and z axes are the horizontal and anterio-posterior axes of the surface respectively. Adapted from Menchaca and Malacara (1984) and Lu and Smith (1990).

1.5.1.2 Axial curvature

Axial curvature is defined as the reciprocal of the distance measured between a point on the optical surface and a point on the optical axis, along the normal of the surface, in the meridional plane (Klein and Mandell 1995b, a, Klein 1997) (Figure 1-9). The term axial curvature is used interchangeably with the term sagittal curvature (El Hage and Leach 1999), however this only holds true when the sagittal curvature is described along the meridional plane which is coincident with the optical axis.

Because the Medmont E300 corneal topographer measures radii of curvatures along the meridional plane the terms 'tangential' and 'axial' are used, and the same terminology is used in this thesis.

It must be kept in mind that these definitions only hold true if the cornea is assumed to be rotationally symmetric, but in general the normal cornea is not rotationally symmetric. Further, when determining the corneal local radii of curvature using videokeratoscopes, it is also assumed that the instrument's central axis (videokeratoscopic axis) is aligned with the line of sight. However in reality these rarely align giving rise to errors in the exact measurement of these curvatures. In general, the higher the misalignment between the two axes the greater the errors in the measurement of radius of curvature (Mandell et al. 1995). This issue will be discussed further in Section 1.8.3.

1.5.2 Axial curvature maps

These corneal maps are derived from the axial radius of curvature determined by the topographer. Axial radius of curvature can be converted into dioptric notation (P_a) using the formula:

$$P_a = \frac{n' - n}{r_a}$$

where n' and n are the refractive indices of the cornea (the corneal refractive index is generally considered to be 1.3375) and air vaccum (1.000) and r_a is the corneal axial radius of curvature in metres. The Medmont E300 corneal topographer allows the user to export the raw corneal data at each meridian location over a fixed radial distance. For this reason it is possible to determine corneal curvature at every meridional plane, thus determining the axial curvature rather than sagittal curvature.

The advantage of axial curvature maps is that the instrument can easily be calibrated using spherical test surfaces with good repeatability (Roberts 1994a). Further, these maps are useful to understand the optical effects of changed corneal shape due to OK. The major limitation in using axial curvature maps is that the measurement of the radius of curvature is biased to the optic axis and therefore fails to represent the true corneal shape. The error in the measurement of axial corneal curvature increases as the distance from the corneal centre to the peripheral corneal point being measured increases. Figure 1-10a gives an example of an axial power map displayed by the Medmont E300 corneal topographer.

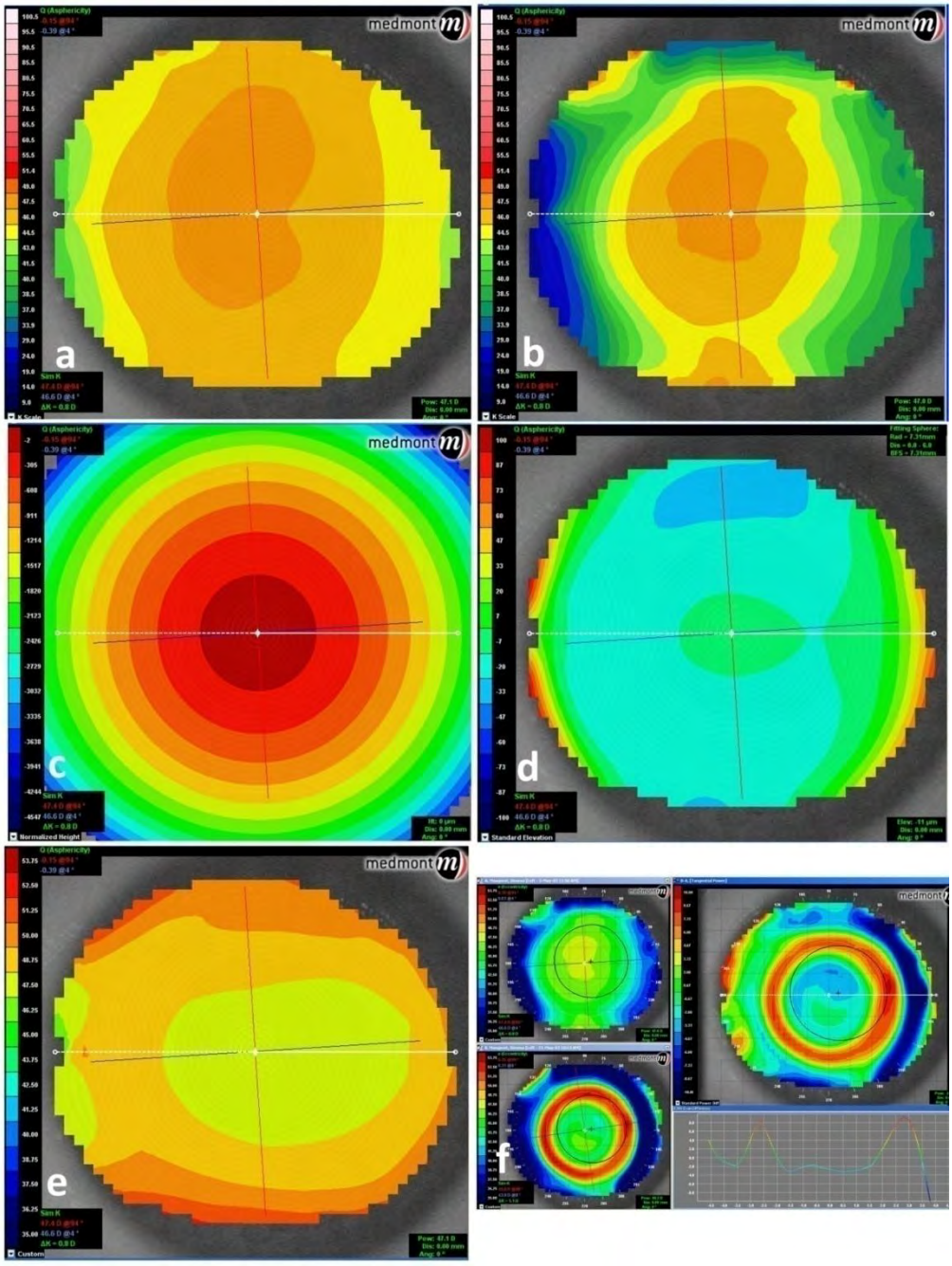

Figure 1-10. Examples of various maps displayed by the Medmont E300 corneal topographer from the same subject: (a) axial power map, (b) tangential power map, (c) corneal height map, (d) corneal elevation map, (e) corneal refractive power map and (f) tangential power difference map. In figure f, the left side top and bottom figures represent corneal tangential power maps before and after OK wear and the difference between these two maps is displayed in the same figure on the right side.

1.5.3 Tangential curvature maps

These corneal maps are derived from the tangential radius of curvature determined by the topographer. Tangential radius of curvature can be converted into dioptric notation (P_t) using the formula:

$$P_t = \frac{n' - n}{r_t}$$

where n' and n are the refractive indices of the cornea (1.3375) and air vaccum (1.000) respectively and r_t is the corneal tangential radius of curvature in metres. The major advantage is that tangential curvature is not optical axis biased as is axial radius of curvature. These maps are best to represent true corneal shape and are very sensitive to detect localised fluctuations in shape. Therefore these maps are very practical in detecting and monitoring irregular corneal shapes especially in conditions such as keratoconus, post-refractive surgery and after OK (El Hage and Leach 1999). An example of a tangential power map from the Medmont E300 corneal topographer is given in Figure 1-10b.

Although the terms 'axial curvature' map and 'tangential curvature' map actually represent curvature in dioptric units, the Medmont E300 uses these terms when displaying maps with radius of curvature in mm. The terms 'axial power' map and 'tangential power' map are instead used when displaying curvature in dioptric units.

1.5.4 Height maps

These maps display sagittal distances from a plane aligned to the corneal apex to various locations on the corneal surface distributed at specific distances from the point of intersection of the plane to the videokeratoscopic axis. In the Medmont E300 corneal topographer the height maps are displayed in microns. These maps have minimal importance either at baseline or after overnight OK wear. A pre-OK corneal height map appears almost the same as a post-OK corneal height map, and the change that is induced because of OK is not discernable on the topography display because the major component of corneal shape change is spherical. However, corneal height maps can be used as difference maps as will be explained in following sections. An example of a corneal height map from the Medmont E300 corneal topographer is given in Figure 1-10c.

1.5.5 Elevation maps

Elevation maps are determined by elevations or depressions of the corneal surface with regards to a fixed reference surface. Corneal surface points lying above the reference surface are represented by positive values and below the reference surface are represented by negative values. This essentially removes the major component of corneal shape, hence allowing subtle variations to become apparent. The surface to which the cornea or test surface is referenced can be a spherical surface (Kiely et al. 1982, Salmon and Horner 1995, Auffarth et al. 2000, Iskander et al. 2002, Yoshida et al. 2003) or a biconic (Cano et al. 2004) surface. Whereas spherical surfaces are used for corneas with minimal amounts of corneal toricity, biconic surfaces are used with higher amounts of corneal toricity. The curvature of the spherical reference surface can be steeper or flatter than the original test surface (Salmon and Horner 1995). The centre of the reference surface is fixed at the corneal vertex aligning with the videokeratoscopic axis. Typically, corneal or test surface height data is referenced to a best-fit spherical surface. Best-fit is meant in the sense that the curvature of the reference sphere is manipulated to result in a minimal fit error when positioned with respect to the corneal vertex along the videokeratoscopic axis. The fit error determines how close is the best-fit surface to the actual corneal surface or test surface. The value of fit errors can changed based on the chord diameter of the surface being analysed. Some corneal topographers (such as the Medmont E300) allow the user to fix the curvature of the reference sphere instead of using a best-fit sphere, giving more control to the user. An example of a corneal elevation map from the Medmont E300 corneal topographer is given in Figure 1-10d.

1.5.6 Refractive power maps

These maps represent the true refractive power of the corneal surface and are therefore determined from ray tracing based on Snell's law using the angles of incidence and refraction. During OK, these maps are useful in estimating the refractive change achieved after OK wear and also to show the exact diameter of the treatment zone. The Medmont E300 corneal topographer, besides displaying the corneal refractive power map, allows the user to export raw corneal height and radial distance data to further determine corneal refractive power (P_R) at specific corneal points using the formula:

$$P_R = \frac{n'}{z + \frac{x}{\tan(\theta_i - \theta_t)}}$$

where n' is the keratometric refractive index (1.3375), z is the sagittal height (mm), x is the radial distance (mm) from the videokeratoscopic centre, θ_i is the incident ray angle and θ_t is

the refracted ray angle. An example of a corneal refractive power map from the Medmont E300 corneal topographer is given in Figure 1-10e. However it needs to be kept in mind that these refractive power maps are not aligned to the pupil centre, so do not necessarily reflect the refractive effect of the corneal surface on ocular refraction.

1.5.7 Difference maps

Difference maps are the maps produced by subtracting pairs of axial, tangential, height or refractive power maps. During OK, the pair of maps typically includes one recorded before OK treatment and the other after OK treatment. The computer subtracts one map from the other to display a difference map, which allows the examiner to evaluate the changes that have occurred to the corneal shape because of OK lens wear. An example of a corneal refractive power difference map from the Medmont E300 corneal topographer is given in Figure 1-10f. Difference maps play an important role in understanding the treatment zone centration, treatment zone diameter and refractive change following OK lens wear because they allow immediate identification of changes to corneal curvature or height. Characteristics of these topography difference map patterns during OK trial fitting guide the OK practitioner to alter OK lens parameters to successfully attain the desired central corneal flattening and para-central steepening.

The colour coding of the maps provides important cues to understand corneal shape (Smolek et al. 2002a). Colours are divided into as cooler and warmer colours. Cooler colours including green, violet and blue represent flatter areas of the cornea and warmer colours including red, yellow and orange denote steeper areas of the cornea. An ideal topographic difference map after OK should present a central blue or violet area indicating corneal flattening and a surrounding para-central annular red ring indicating steepening of the cornea. There are a number of different topographic difference map patterns that may be produced after OK wear. These patterns indicate specific behaviour of the OK lens during overnight wear particularly with respect to centration. The lens fitting practitioner needs to understand these patterns in order to take necessary steps to optimise lens fitting.

1.5.8 Orthokeratology post-fitting evaluation

The research reported in this thesis mainly uses BE spherical OK lenses. For that reason an overview of fitting evaluation of these lenses is provided in this section. Some authors have used the same terminology to describe post-fitting outcomes during OK fitting using other lens designs (Chui and Cho 2003, Chan et al. 2009, Villa-Collar et al. 2009, Lorente-Velázquez et al. 2011, Cho et al. 2012).

As indicated in Section 1.4.3.2, BE OK lenses are fitted using a trial lens-based fitting method. The first trial lens is selected based on calculations performed by the BE software program (BE Enterprises Studio). The corneal topography information supplied to the software program includes apical corneal curvature (R_o) in dioptres, corneal sag height in mm along the flatter corneal meridian measured at a fixed chord diameter of 9.35 mm or, if eccentricity-based fitting is chosen, eccentricity (e) along the flatter corneal meridian is instead provided. Other information required by the software includes target refractive correction in dioptres, regression factor and horizontal visible iris diameter in mm. The lenses that are determined by the software are then trialled on an overnight basis until an optimal lens fitting is achieved. The lens fitting is indirectly judged based on the appearance of the corneal topography difference maps.

The physical centration of OK lenses on eye after eye opening following overnight wear is not necessarily the true representation of lens centration during sleep. An alternative way of judging the lens position during sleep is to evaluate the treatment zone centration using subtractive topography difference maps captured after the removal of the OK lens in the morning after eye opening. Mountford (2002) provided a detailed view on topographic evaluation following OK lens wear. He classified post-OK topographic patterns that can be used to understand lens centration and also provided tips on how to overcome problems associated with inappropriate topographic patterns in subsequent lens fittings.

To evaluate the topographic patterns before and after OK wear, one should use difference maps provided by the topographer. Axial, tangential and refractive curvature difference maps are generally examined when assessing OK-induced changes to corneal curvature. Although all are describing the same information, the axial and refractive maps tend to give a better representation of refractive change while the tangential maps give a better representation of localised areas of change, particularly around the edge of the treatment zone, which is useful for assessing centration of the treatment effect. The types of corneal

topography patterns that are typically observed on difference maps following overnight wear are broadly classified by Mountford (2002) as follows:

1.5.8.1 Bull's eye pattern

A bull's eye pattern represents the ideal topographic outcome after myopic OK lens wear. This pattern is characterised by a central blue area indicating flattening which is surrounded by an annular para-central red area indicating steepening (Figure 1-11a). The central flattening is the result of compression from the flat central base curve of the OK lens and the para-central steepening is due to steepening under the reverse curve of the OK lens in the mid-periphery. The extreme periphery exhibits little or no change. For optimal visual outcomes the central flattened zone should completely encompass the pupillary zone.

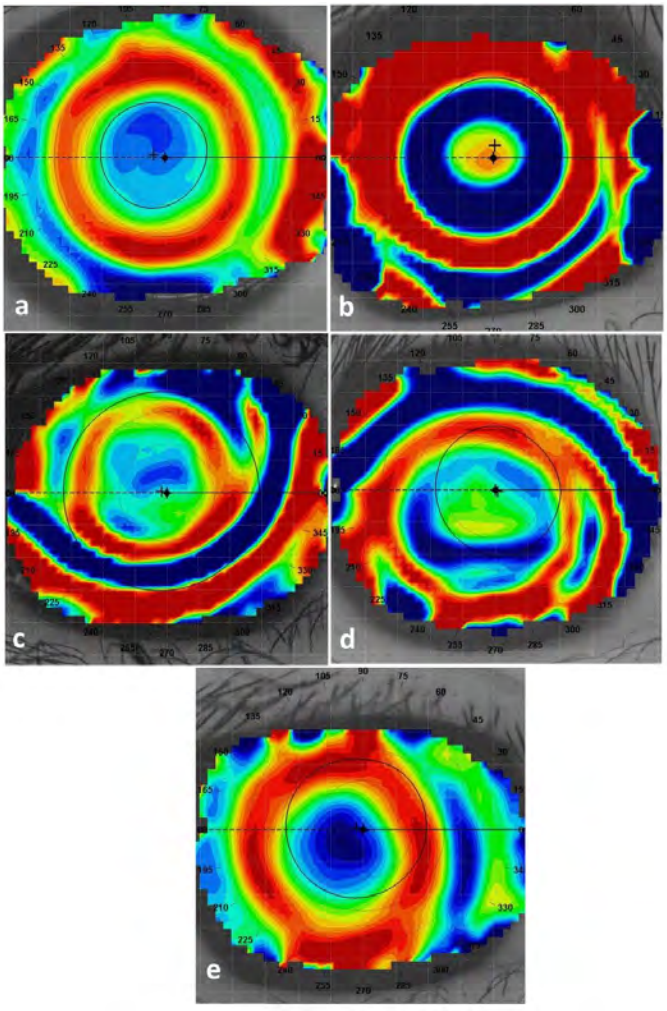

Figure 1-11. Tangential power difference maps (post-OK – pre-OK topography) showing various patterns, (a) bull's eye pattern, (b) central island pattern, (c) smiley-face pattern, (d) frowny-face pattern and (e) lateral decentration. The blue and violet zones in each map represent corneal flattening and red, orange, and yellow zones represent corneal steepening. Green zones represent no change in curvature.

1.5.8.2 Central island

The central island pattern is characterised by the appearance of a small 1 to 3 mm zone of steepening in the middle of the blue central flattening zone (Figure 1-11b). Central island patterns are caused by an over-estimation of corneal sagittal height or an underestimation of corneal eccentricity leading to calculation of an overly large lens sag height. Lenses with deeper lens sag create excessive apical clearance, resulting in a loss of central lens compression which shows as a small area of apical steepening. Resolution generally requires the lens sag to be reduced and the overnight trial repeated. However if there is only a slight indication of a central island, in some cases this will resolve after a few further nights of lens wear without changing the lens specifications. A decision whether to continue overnight wear in these situations is largely based on practitioner experience. Sagittal height of lenses can be decreased by flattening the reverse curve and/or alignment curves.

1.5.8.3 Smiley-face pattern

The smiley-face pattern (Figure 1-11c) is the characteristic feature of superiorly decentred OK lenses during overnight wear and is generally an indication of underestimation of corneal sagittal height or eccentricity leading to the trial lens having inadequate sag depth. The remedy for superior decentration is fitting the next trial lens with slightly deeper lens sag, which could be determined by recalculating the lens sag height with a lower eccentricity value and steepening the reverse and/or alignment curves.

1.5.8.4 Frowny-face pattern

The frowny-face pattern (Figure 1-11d) indicates inferior decentration of OK lenses during overnight wear. This pattern appears only where the alignment curve is too tight, and therefore the next trial lens should be fitted with a flatter alignment curve.

1.5.8.5 Lateral decentration

A lateral decentration pattern (Figure 1-11e) is evident with smaller OK lenses or in cases where the cornea exhibits significant nasal versus temporal shape asymmetry with the nasal cornea flattening more rapidly towards the periphery than the temporal cornea. Fitting larger diameter lenses usually solves the problem of lateral decentration.

The classification of the patterns described above by Mountford is purely based on his extensive OK fitting experience and there is no scientific corroboration. The OK trial lens parameters are modified and overnight trials are performed until a bull's eye topographic pattern is achieved. The bull's eye topographic pattern does not ensure full correction of the

refractive error, but ensures optimal lens fitting. The information of residual refractive error after the overnight trial in which a bull's eye pattern is achieved, the trial OK lens parameters and the desired TLT are used to determine the final OK lens parameters to achieve the desired refractive effect.

1.6 CORNEAL TOPOGRAPHIC PARAMETERS AND THEIR CHANGES DURING SPHERICAL ORTHOKERATOLOGY

Section 1.3.3 described how corneal shape is determined using various shape descriptors. This section is aimed at describing the details of those various corneal parameters, and will review the past literature on how OK lenses influence these parameters after overnight lens wear.

1.6.1 Changes to corneal rate of flattening

As far as importance of corneal shape during overnight OK is concerned, Mountford (1997b) demonstrated a positive relationship between changes in apical corneal curvature (R_o) and eccentricity (e). The apparent change in eccentricity of the cornea from prolate before OK treatment to spherical (e = 0) after treatment led him to propose that the cornea tends to assume a spherical shape as a result of OK lens wear. However, the author himself raised concerns about the validity of the eccentricity values provided by the videokeratoscope used in his study (EyeSys 2000). Whether the algorithm used by the corneal topographer for determining the eccentricity was capable of defining oblate corneal shape was not known. As indicated in Section 1.3.3.1.1, eccentricity is an inappropriate index to describe an oblate corneal shape. This may explain why Mountford was able to demonstrate corneal shape change only to a sphere after OK treatment, and failed to find any oblate change due to the topographer erroneously indicating an eccentricity of zero for oblate surfaces. Despite this important limitation, some later studies have still analysed corneal shape changes after OK using eccentricity as the corneal shape index (Tahhan et al. 2003a, Stillitano et al. 2007).

Other corneal shape descriptors which have been analysed to demonstrate change in corneal shape include shape factor p (Lui and Edwards 2000), e^2 (Nichols et al. 2000), and Q (Chan et al. 2008a). Lui and Edwards (2000) used shape factor p to analyse corneal hemi-meridional shape change after overnight OK, but the authors concluded that their values were invalid because the ellipse model is not the best representative of corneal shape after OK. Nichols et al. (2000) showed a significant decrease in e^2 values over time after 60 days of overnight OK, confirming Mountford's observations that the cornea assumes a less prolate

corneal shape after OK. Chan et al. (2008a) showed that the normal corneal shape indicated by a negative Q (prolate shape) changes to a positive Q (oblate shape) as a result of OK lens wear.

Although corneal shape indicators have been used in previous studies to indicate changes during OK, these are potentially flawed because the cornea does not assume an elliptical shape after OK. This is further complicated when decentration of the OK lens induces corneal distortion. Another potential limitation is that one single number for the shape index may be inadequate to describe overall corneal shape because corneal shape in a given eye varies meridionally (Kiely et al. 1984) and hemi-meridionally (Mandell and St Helen 1971, Sheridan and Douthwaite 1989, Zhang et al. 2011). It should also be remembered that the value of the shape index varies depending on the chord diameter over which it is calculated and therefore it is difficult to compare the shape indices presented in different previous studies. However, these shape indicators do retain some value for determining corneal shape at baseline to understand its implications on OK lens dynamics such as lens centration.

1.6.2 Changes in the principal meridians and corneal toricity from orthokeratology

1.6.2.1 Changes in the principal corneal meridians during orthokeratology

Several authors have reported on changes in power along the principal corneal meridians during OK, however in all cases these changes were investigated as an additional aim rather than as the main purpose of their research. Outcomes from these studies with regards to changes along the principal corneal meridians are summarised in Table 1-2.

Except for the long-term wear analysis by Zhong et al. (2009) all studies have shown similar changes from OK in both principal corneal meridians, and none have performed statistical analyses to investigate differences in effect between the principal meridians.

Author (year)	Sample size	OK lens used	Device used	Final study visit	Baseline steep K / flat K	Post-wear steep K / flat K	Change	Statistical significance
					Mean ± SD (dioptres)			
Rah et al (2002)	60 (31 completed)	Paragon CRT	Keratometer	3 months	44.40 ± 1.44/ 43.71 ± 1.38†	43.01 ± 1.58/ 42.06 ± 1.34†	Not provided	Not provided
Soni et al (2003)	10	Contex OK B and D series	Orbscan	3 months	44.24 / 43.50	Not provided	Not provided	Both meridians $p \leq 0.01$
Sridharan and Swarbrick (2003)	9	BE	Medmont E300	8 hours	Not provided	Not provided	−0.92 ± 0.53 / −0.90 ± 0.63	Both meridians $p < 0.001$
Cho et al (2005)	43 (35 completed)	Lenses made in Boston XO or HDS 100 material (design not mentioned)	Keratometer	24 months	Not provided	Not provided	−1.35 ± 0.86 / −1.51 ± 0.72	Both meridians $p < 0.001$
Sorbara et al (2005)	30 (23 completed)	Paragon CRT	Autorefractor/keratometer	28 days	43.94 ± 1.36δ	41.61 ± 1.36δ	Not provided	$p < 0.01$
Stillitano et al (2007)	14 (26 eyes)	BE	Medmont E300	8 nights	44.17 ± 1.11/ 43.01 ± 1.21	42.28 ±1.08/ 41.44 ± 1.18	Not provided	Both meridians $p = 0.001$
Chan et al (2008a)	73	DriemLens and eLens	Medmont E300	6 months	44.79 ± 1.65/ 43.38 ± 1.52	43.14 ± 1.67/ 41.61 ± 1.55	Not provided	Both meridians $p < 0.001$
Zhong et al (2009)	30 (60 eyes)	Lenses made in Boston XO (Macro Vision, China)	Orbscan II	1 night	43.80 ± 1.80 / 42.80 ± 1.70	43.00 ± 1.70 / 41.80 ± 1.60	Not provided	Both meridians $p < 0.001$
	26 (51 eyes)			5 years	Not provided	43.40 ± 2.00 / 41.50 ± 1.70	Not provided	steep K: $p = 0.334$ flat K: $p = 0.006$

Table 1-2. Changes in corneal power along principal corneal meridians from previous studies. The sign '†' indicates that the data quoted are from the right eye and the sign 'δ' indicates that the data quoted are from the flatter corneal meridian K.

1.6.2.2 Changes in corneal toricity during spherical orthokeratology

Corneal toricity is the major contributor to refractive astigmatism (see Section 1.3.5.3). Therefore any reduction in corneal toricity induced by OK should manifest as overall change in refractive astigmatism. Only a few studies have investigated changes in corneal toricity due to orthokeratology, but there is considerable literature available on assessing changes in refractive components of astigmatism (see Section 1.7). Table 1-3 summarises the outcomes from previous studies with regards to changes in corneal toricity. From the table it is evident that the results from previous studies are mixed. Mountford and Pesudovs (2002) demonstrated about 50% reduction in the amount of corneal toricity, when measured around the zone equivalent to an area where a conventional keratometer takes measurements. Sorbara et al. (2005) instead showed a slight but significant increase in corneal toricity after one single night wear of spherical OK lenses. The remaining studies showed no significant change after spherical OK. An important aspect to note from these studies is that all have focussed on assessing changes in corneas with minimal amounts of corneal toricity (2.00 DC or less), with no studies published on the effect of spherical OK lenses on corneas with moderate or high amounts of toricity.

1.6.2.3 Changes in corneal vector powers during spherical orthokeratology

To date there is only one study (Mountford and Pesudovs 2002) that investigated corneal toricity changes using vector analysis methods other than Thibos's vector method. Mountford and Pesudovs analysed corneal toricity changes in 23 subjects using both Bailey-Carney and Alpins methods. Using the Bailey-Carney method of vector analysis the authors reported 50% reduction from initial corneal toricity. With Alpins method, a 50% reduction in initial corneal toricity was also noted.

1.6.2.4 Corneal astigmatic changes using Fourier analysis in orthokeratology

Hiraoka et al. (2004b) adopted Fourier analysis in analysing astigmatic changes using corneal topographic raw data. In their study, participants with moderate myopia and astigmatism < 1.00 DC were enrolled. The refractive astigmatism at baseline was −0.22 ± 0.33 DC and after 3 to 5 months (mean = 4.06 ± 0.81 months) it was −0.14 ± 0.34 DC. Whether this change was statistically significant is not stated. Using Fourier analysis, the study demonstrated significant increase in corneal regular astigmatism from 0.53 ± 0.23 DC at baseline to 0.63 ± 0.40 DC after treatment (p = 0.021), and the asymmetry component increased from 0.35 ± 0.22 D to 0.64 ± 0.40 D after treatment (p < 0.001). No significant change was observed in corneal higher order irregularities (p = 0.217).

Author (year)	Sample size	OK lens used	Device used	Follow-up period	Baseline corneal toricity or magnitude of vector components	Post-wear corneal toricity or magnitude of vector components	Change	Statistical significance
					Mean ± SD (dioptre cylinder)			
Mountford and Pesudovs (2002)	16	BE	Eyesys 2000	≈ 2 months	Range: 0.75 – 2.00	Not provided	50% reduction (for 1.50 mm half-chord length)	Significant
Sridharan and Swarbrick (2003)	9	BE	Medmont E300	8 hours	0.56 ± 0.24	Not provided	−0.01 ± 0.36	Not significant
Sorbara et al (2005)	30 (23 completed)	Paragon CRT	Autorefractor/keratometer	28 days	0.64 ± 0.47	Not provided	Not provided	1 night: (0.78 ± 0.39 D, $p < 0.01$) After 28 nights: not significant
Cheung et al (2009)	30	DriemLens	Medmont E300	At least 6 months	J_{180} = 0.80 J_{45} = −0.06	J_{180} = 0.83 J_{45} = −0.03	0.04 ± 0.37 0.03 ± 0.43	Both vector components not significant

Table 1-3. Changes in corneal toricity or corneal vector components after spherical orthokeratology, from previous studies.

1.7 SPHERICAL ORTHOKERATOLOGY AND ITS EFFECT ON REFRACTIVE ASTIGMATISM

Section 1.6.2 summarised the previous studies that investigated OK-induced changes in corneal toricity or regular and irregular corneal astigmatism using different approaches. However it is incomplete to discuss changes in corneal toricity without describing the effect on refractive astigmatism, because the final aim of OK is to provide best possible vision correction to patients. It is logical to state that any OK-induced changes to corneal topography will influence final ocular refractive measurements. Therefore it is important to know the effect of spherical OK lenses on refractive astigmatism. This section presents a review of previous literature that investigated changes in refractive astigmatism during spherical OK.

Studies which investigated the performance of spherical OK lenses have shown either a reduction (Fan et al. 1999), or no change (Tahhan et al. 2003a, Cheung and Cho 2004, Hiraoka et al. 2004a, Walline et al. 2004) in refractive astigmatism from baseline. The primary aim of these studies was to investigate the efficacy of overnight OK on reduction of myopia and other clinical outcomes such as change in visual acuity, contrast sensitivity or higher order-aberrations, and not to investigate changes in refractive astigmatism specifically. For this reason many of these studies did not provide details about astigmatism such as baseline refractive astigmatism or change in astigmatism after OK. A summary of the studies, their methodology and outcomes in terms of changes in refractive astigmatism is presented in Table 1-4.

Author (year)	Sample size	Selection criteria (refractive astigmatism in dioptres)	OK lens used	Follow-up period (months)	Baseline refractive astigmatism or magnitude of vector components	Post-wear astigmatism or magnitude of vector components	Change	Results and comments
					Mean ± SD (dioptres)			
Fan et al (1999)	54	0 to −3.25	Dynalens and Sightform lens	6	Not provided	Not provided	Not provided	After 6 months, 2/3rd of astigmatism reduced in eyes with < 3.00 DC of refractive astigmatism
Tahhan et al (2003a)	46	≤ 1.50	Rinehart Reeves, Contex, DreimLens, BE	1	RE: −0.37 ± 0.34 LE: −0.36 ± 0.31	Not provided	Not provided	No significant change
Walline et al (2004)	23	Axis 180 ± 20˚ ≤ 2.00 Other axes ≤ 1.00	Paragon CRT	6	Not provided	Not provided	Not provided	No significant change in Thibos's vector components
Cheung and Cho (2004)	30	Not available	Not available	12-36	−0.61 ± 0.45	−0.59 ± 0.63	Not provided	No significant change
Hiraoka et al (2004a)	31	Not available	Emerald	3	−0.22 ± 0.33	−0.14 ± 0.34	Not provided	No significant change
Cheung et al (2007)	31	≤ 2.50	Not available	3-36	J_{180} = 0.19 ± 0.27† J_{45} = −0.06 ± 0.14†	J_{180} = 0.18 ± 0.33† J_{45} = −0.03 ± 0.25†	Not provided	Statistical significance of change not provided
Chan et al (2008a)	27	0 to 4.25	Dreimlens and eLens	6	Not provided	Not provided	Not provided	No significant change
Cheung et al (2009)	30	0.75 to 2.25	Dreimlens	at least 6	J_{180} = 0.50 ± 0.29 J_{45} = 0.00 ± 0.14	J_{180} = 0.19 ± 0.34 J_{45} = 0.08 ± 0.11	J_{180} = −0.31 ± 0.35 J_{45} = 0.09 ± 0.16	Significant reduction in J_{180} and slight increase in J_{45}

Table 1-4. Changes in refractive astigmatism or refractive vector components after spherical orthokeratology, from previous studies. The sign '†' indicates that the data quoted are from the group categorised as 'worse eye'.

From inspection of the table it is apparent that spherical OK has been prescribed to patients with varying ranges of astigmatism (as high as 4.25 DC). Studies in which participants with higher amounts of astigmatism (> 2.50 DC) were enrolled (Fan et al. 1999, Chan et al. 2008a) have suffered serious limitations. Fan et al. (1999) enrolled subjects with highly astigmatic eyes to wear OK lenses on a daily rather than overnight schedule, therefore giving no information on how overnight OK lens wear would change astigmatism in these eyes. Chan et al. (2008a) enrolled participants with a wide range of astigmatism (0 to −4.25 DC), but data from only 27 participants from the original 108 participants were used to analyse changes in refractive astigmatism because only in these participants was the data collected at all visits. The analysis revealed no significant change in astigmatism in this smaller cohort. Whether these data consisted of eyes with severe astigmatism was not stated in their report. An important finding from this study was that analysis of the whole data set revealed a positive correlation between the residual refractive cylinder after OK and the pre-treatment cylinder (r = 0.44, p < 0.001), which suggests that the residual astigmatism after spherical OK was greater in eyes that had higher amounts of astigmatism at baseline. This indicates that spherical OK lens wear may provide only limited reduction in refractive astigmatism.

Many of these studies have not investigated changes in astigmatism in relation to decentration of the OK lenses, although one study (Tahhan et al. 2003a) reported that a better centration of lenses could have possibly led to minimal or no induction of astigmatism, but this was not corroborated with statistical analysis.

It is difficult to compare the results of these studies due to differences in study methodologies. For example, some studies enrolled participants with a wide range of refractive astigmatism and some of them with a modest range. Similarly, the age range of the participants, lens designs used, and selection criteria would limit any comparisons between the outcomes of these studies.

In summary, the results of previous studies investigating the effect of spherical OK lenses on changes in refractive astigmatism are fundamentally limited due to the use of methodologies which were not aimed at correcting refractive astigmatism. Thus controlled studies are required to specifically investigate changes in astigmatism using spherical OK.

1.8 TREATMENT ZONE EVALUATION DURING ORTHOKERATOLOGY

During overnight OK for myopia correction, the OK lens reshapes the cornea by inducing central flattening and para-central steepening. The central flattened zone reduces the converging power of the cornea resulting in the correction of myopic refractive error. In previous studies the central flattened zone as observed on axial or tangential power maps has been defined as the treatment zone (TZ) (Owens et al. 2004, Hiraoka et al. 2009). Others have considered both the central flattened zone and surrounding para-central steepened zone as equally important components of the TZ (Lu et al. 2007b) on the basis that, depending on pupil diameter, the para-central steepened zone may interfere with paraxial vision. The ideal OK outcome is to induce central flattening across the whole pupillary area. However, if there is decentration of the TZ or if the pupil diameter is greater than the area of central flattening, para-central steepening may fall in the pupillary area, resulting in a poor visual outcome due to induction of unwanted ocular aberrations (Berntsen et al. 2005, Hiraoka et al. 2005, Hiraoka et al. 2008). Therefore the two important parameters with respect to the TZ are its diameter and centration relative to the pupil.

1.8.1 Treatment zone diameter

Previous studies that used reverse geometry contact lens designs for OK defined the TZ diameter as the horizontal distance between the two zero change locations denoting the junction of the flattened zone with the para-central steepening zone on a difference map (Sridharan and Swarbrick 2003, Tahhan et al. 2003a, Owens et al. 2004, Lu et al. 2007b). Mountford (2004b) believed that the TZ diameter that is determined using axial and tangential curvature difference maps tends to over- and under-estimation respectively due to the averaging nature of the algorithms used in determining the corneal curvatures, and alternatively suggested the use of refractive power maps for an accurate measurement of TZ diameter. However, to date no study has evaluated the scientific basis of this suggestion. In this thesis corneal refractive power maps have been used to determine TZ because these maps closely relate to vision as the determination of corneal power is based on ray tracing using Snell's law. The values of TZ diameters measured in various previous studies are summarised in Table 1-5.

Author (year)	Measurement visit	Method used to determine TZ	TZ diameter (mm)	Method of assessment of decentration	Magnitude of decentration (mm) (polar decentration values, unless x and y values are given for Cartesian coordinate system)	Direction of decentration Number of eyes (%)
Sridharan and Swarbrick (2003)	8 hours	Locating zero power change on difference power map (type of map not mentioned)	5.59 ± 0.83	Not assessed	-	-
Tahhan et al (2003a)	1 week	Locating zero curvature change on axial curvature difference maps	5.30 ± 1.10 (BE lenses)	Centre of the entrance pupil to geometric centre of TZ	x = −0.30 ± 0.40 y = −0.10 ± 0.40 (BE lenses)	Not available
Owens et al (2004)	4 weeks	Locating zero power change on axial curvature maps	3.32 ± 1.08 (vertical measurement)	Corneal apex to the position (centre?) of the flattened zone	x = −0.50 ± 0.40 y = 0.10 ± 0.30	Not available
Yang et al (2005)	1 month	Change in corneal power value within 1 dioptre	Not assessed	Distance from pupillary centre to intersection of lines drawn from farthest four edges of TZ	0.57 ± 0.41	Nasal 19 (14.4%) Superior 7 (5.3%) Temporal 81 (61.4%) Inferior 25 (18.9%)
Lu et al (2007a)	1 night	Central flattened zone from tangential maps	Not assessed	Centre of topography map to centre of TZ	0.50 ± 0.25 (Menicon Z) 0.54 ± 0.29 (Equalens II)	Not available
Lu et al (2007b)	4 weeks	Locating zero curvature change on tangential curvature difference maps	3.61 ± 0.07	Centre of topography map to centre of TZ	x = −0.66 ± 0.38 (Right eyes) x = −0.67 ± 0.43 (Left eyes)	Not available
Hiraoka et al (2009)	3 months	Sixteen points plotted along an equi-refractive power line surrounding the central flattened area of tangential curvature maps	Not assessed	Distance from pupillary centre to the centre of best-fit ellipse fitted to 16 points marked	0.81 ± 0.51	Temporal (74%) Inferior (74%)

Table 1-5. Methodologies used and results obtained in previous studies for determining treatment zone (TZ) diameter, and magnitude and direction of decentration.

1.8.2 Treatment zone centration

As discussed earlier in Section 1.5.8, Mountford (2002) described various TZ decentration patterns based on the evaluation of corneal topography difference maps after OK. However, the subjective classification of TZ parameters from the topographic difference maps has major limitations. Subjective assessment of TZ decentration patterns requires good clinical experience, and this kind of assessment does not provide any quantification of the TZ centration.

While most authors (Tahhan et al. 2003a, Owens et al. 2004, Lu et al. 2007b) have used topography difference maps to manually measure the distance from the corneal vertex to the centre of the flattened area from the computer screen display, their exact methodology was not described. Others have developed more sophisticated methods of determining TZ centration. Yang et al. (2005) used a transparency over the computer screen to mark the outline of the central flattened area. Using the coloured scale on the corneal topography map, a one dioptre change in the keratometric value from the corneal apex was considered as the edge of the flattened zone. Yang et al. also proposed a method for defining the centre of the TZ as the intersection between lines drawn between the four farthest edge points. However, this method suffers some limitations. Firstly, the dioptric value had to be selected from a specific colour assigned by the topographer, which often covers a range rather than a fixed dioptric value. Secondly, a one dioptre value difference in the keratometric value does not necessarily mark the edge of the TZ. This kind of estimation is limited by the examiners' ability to detect a proper edge of the TZ and several estimations may be required to determine the final TZ measurement. As a result the measurement becomes tedious, time consuming and inaccurate.

Hiraoka et al. (2009) improved on the method reported by Yang et al. (2005) by plotting 16 points on the display monitor that had the same refractive power value on the post-OK wear tangential curvature maps. The centre of the best-fit ellipse fitted to the 16 TZ defining points was regarded as the centre of the TZ; however it is not clear from their description what dioptric power was actually used to demarcate the TZ edge. Moreover, this method also involved manual identification of the TZ edge, giving rise to the same limitations as the previous method. Table 1-5 provides a summary of TZ decentration values from various previous studies.

The studies evaluating the direction of TZ decentration revealed a tendency for the OK lens to decentre towards the temporal and/or inferior regions (Tahhan et al. 2003a, Yang et al. 2005, Hiraoka et al. 2009). Although not investigated specifically, some authors have speculated that nasal versus temporal corneal asymmetry, where the temporal cornea is steeper than the nasal cornea, is a possible reason for temporal decentration (Yang et al. 2005, Hiraoka et al. 2009). No logical reason has been either speculated or established for the tendency towards inferior lens decentration.

1.8.3 Reference axis and points

Different ocular reference axes can be used to describe the optical characteristics of the eye, each of which forms different intersections with the corneal surface. It is important to understand these axes, reference points and the relationships between them, because this forms a basis for choosing a particular reference point from which the centre of the TZ is determined. This section gives an overview on various ocular axes and corneal reference points, and also other reference points which are independent of ocular axes.

1.8.3.1 Videokeratoscopic axis and vertex normal

The videokeratoscopic axis or keratometric axis is the optical axis of an instrument that is aligned perpendicular to the cornea to determine corneal shape. This axis intersects the centre of measured corneal curvature (Mandell 1994, Mandell et al. 1995, Mandell 1996) (Figure 1-12). The corneal reference point through which the keratometric or videokeratoscope axis passes is called vertex normal (VN) or corneal vertex. Topographic maps displayed by corneal topographers are centred on the VN. It is important that the term VN is not confused with the term corneal apex as these two are different entities. Mandell suggested using the term videokeratoscopic axis (VK axis) point as an alternative. However, in the literature the terms VN (Coorpender et al. 1999, Read et al. 2006) and corneal vertex (Mattioli and Tripoli 1997) are commonly used to refer to this reference point.

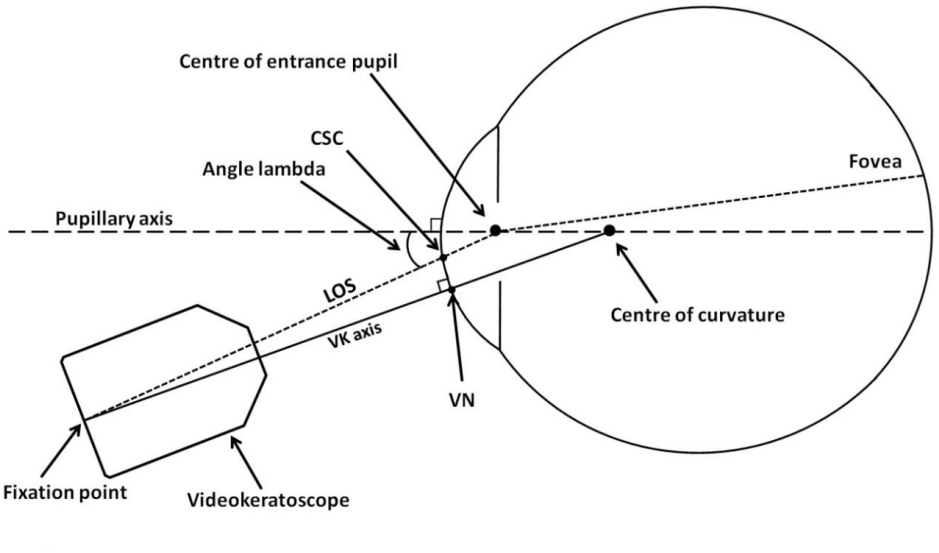

Figure 1-12. An illustration to describe relative orientation of different reference axes and points. CSC: corneal sighting centre, LOS: line of sight, VK axis: videokeratoscopic axis, VN: vertex normal. Figure adapted from Mandell (1994).

1.8.3.2 Visual axis

The visual axis is defined as the line joining the fixation point and the fovea of the eye through the nodal point (or points) of the eye (Emsley 1953, Mandell 1994). In reality, it is not possible to locate the nodal points of the eye in a clinical situation, thus the use of visual axis is particularly limited to theoretical constructions of the model eye and to establish object and image relationships.

1.8.3.3 Entrance pupil

The entrance pupil is the image of the original pupil formed due to the optical system in front of it, which include tear film, cornea and aqueous humour.

1.8.3.4 Pupillary axis

The pupillary axis (PA) is defined as the line normal to the cornea and passing through the centre of the entrance pupil and centre of curvature of the cornea (Uozato and Guyton 1987, Mandell et al. 1995) (Figure 1-12). This axis serves as an anatomical and optical reference axis (Mandell et al. 1995). The corneal position through which the pupillary axis passes can be located by determining the centre of the entrance pupil.

1.8.3.5 Line of sight and corneal sighting centre

The line of sight (LOS) is defined by the chief ray joining the point of fixation, centre of the entrance pupil and the fovea (Loper 1959, Uozato and Guyton 1987, Applegate and Howland 1995, Mandell et al. 1995) (Figure 1-12). The corneal reference point through which

the LOS passes is called the corneal sighting centre (CSC) (Mandell 1994). The LOS is considered important for describing ocular refractive characteristics as this represents the centre of the bundle of light rays emerging from the fixation point and entering the eye. Applegate and Howland (1995) stated that the CSC is the ideal reference point for three reasons. Firstly, light rays from the fixation point and surrounding neighbouring points on an object can be traced through the CSC and centre of the entrance pupil to construct retinal image characteristics. Secondly, the CSC can easily be defined with reference to other anatomical reference axes. Finally, the CSC is useful to transform the raw corneal or ocular refractive data to a more useful form for evaluating the visual performance of the eye.

The VK axis from corneal topography measurement and the LOS are not aligned because the former intersects the centre of curvature of the cornea and the latter passes through the centre of the entrance pupil, meaning that the VN representing the VK axis and CSC representing the LOS are not coincident at the corneal plane.

Measuring angle lambda is the optimal way to locate the CSC. Angle lambda is the angle between the PA and the LOS. Angle lambda can be determined accurately in a clinical set-up and usually requires customised apparatus (Loper 1959, Mandell 1995). However the image of the pupil as recorded by the corneal topographer can be used indirectly to locate the line of sight, and then it is a simple process of using the centre of the entrance pupil image as the CSC. Others have shown that this is an accurate representation (Mandell 1995).

1.8.3.6 Optical axis of the eye

The optical axis of the eye is defined as the axis that joins all the centres of curvatures of the optical elements of the eye. However, although the misalignments are generally very minimal, in reality the centres of curvatures of all the optical elements of the eye do not lie on a common axis (Charman 1991). Furthermore, even if an empirical optical axis is determined by ignoring the minimal misalignments between the optical elements, the axis does not intersect the retina at the foveal region but intersects a point slightly towards the periphery, which averages 1.50 mm nasal and 0.50 mm superior to the fovea (Emsley 1953). Because of this misalignment with the fovea, the optical axis is not particularly useful as a reference axis to define the optical characteristics of the eye.

1.8.3.7 Corneal apex

The corneal apex is the point on the corneal surface that defines the maximum corneal curvature or shortest radius of curvature (Mandell et al. 1995) as measured on a tangential curvature map (Chan et al. 1995, Mandell 1996). If there is a small zone of constant maximum curvature then the centroid of the zone should be considered as the corneal apex (Mandell et al. 1995, Mandell 1996). This reference point is particularly useful when describing corneal shape, for example to describe corneal symmetry. Further, it has been shown that corneal apex position is likely to have an influence on rigid contact lens centration.

Mandell and St Helen (1969) assessed corneal apex position in a sample of seven participants by performing keratometry at various pre-defined locations while advising the participants to rotate their eyes to different gaze positions. No specific trend was observed in the position of the corneal apex relative to the line of sight (CSC). Because of this variation the displacement of the corneal apex from the corneal VN needs to be measured in each individual.

By using a photoelectronic keratoscope (PEK), Tomlinson and Schwartz (1979) measured the displacement of the corneal apex from the visual axis to show that the corneal apex was mostly located on the temporal side of the visual axis with no bias in vertical position. However as mentioned earlier in this section, it is not possible to locate the nodal points of the eye in a clinical situation. Therefore it is likely that Tomlinson and Schwartz were instead referring to the VN defined by the centre of the PEK image rather than the visual axis.

Mandell et al. (1995) assessed the position of the corneal apex with reference to the VN using the EyeSys model II videokeratoscope. This method also required the participant to rotate their eye to align the corneal apex to the optical axis of the videokeratoscope. The investigators achieved this by first capturing corneal topography in the regular alignment method. From the tangential curvature topographic map thus obtained, the point of steepest corneal curvature along the steeper corneal meridian was located. The position of this point denoted the distance and angle by which the participant should rotate their eye. After 2 to 5 repetitions, the location of the corneal apex was determined relative to the VN. The mean distance from the VN to the corneal apex was 0.62 ± 0.23 mm, and in 15 out of 20 eyes was located below the VN. The study also determined the difference in corneal toricity between the two reference positions to be only 0.05 ± 0.31 DC, which is clinically negligible.

1.8.3.8 Corneal geometric centre

As the name implies, this is the geometric centroid of the cornea. The location of the geometric centre can be determined by locating the intersection of the largest and smallest diameters of the cornea (Soper et al. 1962). As a reference point, the geometric centre of the cornea has the advantage that it can act as the true anatomical reference point with the benefit that its location is not altered after corneal reshaping procedures such as OK or corneal refractive surgery as it is dependent on the corneal diameters. The position of rigid and soft contact lenses is usually described with reference to the corneal geometric centre. Although the geometric centre is often used in relation to other corneal reference points, it provides no direct benefit in describing corneal shape or its refractive properties (Mandell et al. 1995).

1.8.4 Which is the ideal reference point?

The advantage of using a topographic map with its default centre (VN) as the reference point is that no data reduction procedures are required (transforming raw corneal data to more useable data centred to a desired reference point). Further, these maps are routinely used by OK clinicians in judging the outcomes of OK with respect to TZ decentration. However, the disadvantage of using this point as the reference point is that the TZ decentration determined after OK treatment may actually be an artefact, and not the true TZ decentration that is relevant in terms of visual outcomes, due to the misalignment of the VK axis and line of sight.

Although the corneal apex is important in describing contact lens centration on the eye, it is not suitable for describing TZ centration during OK, primarily because the central corneal flattening induced by overnight OK shifts the apex (or steepest corneal) position to a more peripheral location associated with the induced para-central steepening. Hence it is not valid to use the corneal apex as a reference point when considering OK.

The corneal geometric centre is basically used as an anatomical reference point and remains consistent in the sense that its position is not affected during corneal reshaping procedures such as OK. However this reference point is not aligned to the corneal sighting centre which is more important if one desires to know the optical effects of TZ decentration on vision after OK.

Among the various reference points described, the CSC is often considered as the preferred reference point for describing ocular refractive properties as it represents the location through which the chief ray of light from the fixation point passes. To accurately

determine the TZ decentration and to eliminate any artefacts arising from misalignments, pre-OK and the post-OK topographic maps should be centred to the CSC and subtractive maps can then be used to determine TZ centration. Pupil offsets provided by the topographer can be used to align the CSC as the centre of the topographic map, and in this thesis this analysis was conducted post-hoc to confirm conclusions reached based on the analysis using the VN as the primary reference centre.

1.9 TORIC ORTHOKERATOLOGY: AN OVERVIEW

By clinical convention, spherical OK is generally not suitable for eyes with moderate to high amounts of astigmatism (> 1.50 DC) (Caroline 2001). Although lens decentration has been anecdotally believed to be the primary reason for this limitation, from a thorough review of the literature presented in the previous sections it is apparent that there are no published studies that have specifically investigated the effect of spherical OK lens wear on corneas with higher amounts of corneal toricity, particularly in relation to decentration of OK lenses. However, clinical experience of failures to accomplish appropriate outcomes on moderate and highly toric corneas has encouraged lens manufacturers to develop advanced OK lens designs to control decentration on corneas with moderate to high amounts of toricity.

Despite no scientific evidence relating to OK lens decentration on corneas with moderate to high amounts of toricity, reports on toric OK lens designs either claiming to control decentration (Caroline and Andre 2009) or presenting evidence of reductions of moderate to high amounts of astigmatism (Chan et al. 2009, Caroline and Andre 2009, Chan et al. 2009, Baertschi and Wyss 2010,Chen and Cho 2012) have recently been published. This section summarises these recent publications and also gives an overview on current toric OK lens designs.

1.9.1 Currently available toric OK lens designs

Toric OK lenses can be broadly classified into two designs, which are both back surface toric designs.

1.9.1.1 Toric periphery OK lens designs

Toric periphery OK lens designs have a spherical central back optic zone with toroidal peripheral curves. Peripheral curves include the reverse curve and peripheral alignment curve. One or both of these peripheral curves are designed to be toric. The claimed advantage of this type of design is good centration as a result of maintaining good alignment in the periphery of

the toric cornea and avoiding excessive meridional edge lift along the steeper meridian which may result when fitting standard spherical back surface OK lens designs.

1.9.1.2 Full toric OK lens designs

A full toric OK lens design has a toroidal central back optic zone with toroidal peripheral curves. The advantage of full toric designs may be that the toricity in the periphery limits the decentration and the toricity in the central region exerts differential pressure on the central cornea to achieve an altered central corneal toricity that results in partial or complete correction of refractive astigmatism.

The majority of toric OK lenses currently available are designed with a spherical central curve and toric periphery, with only two manufacturers offering full toric designs. Table 1-6 provides a summary of currently available toric OK lenses from different lens manufacturers.

Lens	Manufacturer	Lens design		Nominal material Dk	Fitting method
		Back optic zone	Periphery		
Paragon CRT, Dual axis™	Paragon CRT, Arizona, USA	Spherical	Toric	Paragon HDS, Dk: 100	Trial fitting
FOKX	FALCO, Switzerland	Spherical	Toric	Boston XO, Dk: 100	Empirical fitting
Menicon Z- Night toric	Menicon, Japan	Spherical	Toric	Menicon Z, Dk: 163	Empirical fitting
Dream Lite TRX®	Procornea, The Netherlands	Spherical	Toric	Boston XO, Dk: 100	Empirical fitting
AstigMove®	Gelflex, Australia	Spherical/ Toric	Toric	Boston XO, Dk: 100	Empirical fitting
Precilens	Precilens, France	Toric	Toric	Boston XO, Dk: 100	Empirical fitting
Custom design	BE Capricornia, Australia	Spherical/ Toric	Toric	Boston XO, Dk: 100 or Boston XO2 Dk: 141	Trial fitting

Table 1-6. Currently available toric orthokeratology lenses.

1.9.2 Efficacy of currently available toric orthokeratology lens designs

Case reports on correcting moderate to high amounts of astigmatism using toric OK lenses have been published in recent years (Caroline and Andre 2009, Chan et al. 2009, Baertschi and Wyss 2010, Chen and Cho 2012). The outcomes of these case reports are summarised in Table 1-7. Results from controlled studies with larger sample sizes evaluating the performance of toric OK lenses have also been published (Chen et al. 2012, Pauné et al. 2012).

Caroline and Andre (2009) illustrated improvement in centration of OK lenses with the Paragon CRT dual axis lens design on a moderately toric cornea. This lens is designed with a spherical central zone and a dual return zone depth system. A single uniform landing zone angle is designed at the extreme periphery of the lens to align with the peripheral corneal shape. However, the authors stated that the landing zone angle can also be made in dual axis design if required. The return zone is designed to be shallow along one axis to align with the flatter corneal meridian, and deeper in the perpendicular axis to align with the steeper corneal meridian. The idea is that the disparity between the principal axes of the return zones will promote lens centration on the toric cornea. The lens can also be manufactured with differing landing zone angles to further improve centration. However, the authors neither calculated the amount of decentration nor presented the changed refractive status of the patient after wear of this toric OK lens.

Chan et al. (2009) presented a single case report describing the performance of the Menicon Z night toric lens. The report demonstrated a reduction of refractive cylinder by 87.5% in the right eye and 67.4% in the left eye. Baertschi and Wyss (2010) also presented a single case correcting 87% of total initial refractive astigmatism of 3.75 DC with a toric periphery OK lens design. Most recently Chen and Cho (2012) presented two cases of highly myopic astigmatic cases fitted with toric periphery OK lens designs. A base curve-based fitting technique (see Section 1.4.2.1) was followed to choose the initial BOZR of the lens with a compression factor of 0.50 D. If the initial lens achieved the complete refractive correction (≤ 0.50 D of myopia) within 2 to 4 weeks after commencing overnight lens wear, the authors continued lens wear. If the targeted reduction was not reduced (> 0.50 D of myopia), then another lens was trialled with a new BOZR based on the residual refractive error using the base curve-based fitting technique with a compression factor of 0.50 D. The two cases were followed up for a period of one year during which corneal topography was captured using the

Author (year)	Age in years	Eye	Lens design	Follow-up duration	Initial refractive error	Final refractive error	Comments
Caroline and Andre (2009)	25	Both	Paragon CRT Dual axis design	single overnight ?	2.87 DC corneal toricity	Not given	Good centration of OK lens demonstrated in RE
Chan et al (2009)	13	RE	Menicon Z night toric	15 months	−4.25 / −1.50 × 165	Plano / −0.50 × 170	-
		LE			−4.25 / −2.50 × 180	−0.50 / −0.75 × 180	-
Baertschi and Wyss (2009)	22	RE	FOKX	2 months	−4.25 /−3.75 × 8	Plano / −0.50 × 8	-
Chen and Cho (2012)	9	RE	Menicon Z night toric	12 months	−6.00 /−2.25 × 6	−3.50 / −1.50 × 180	Authors deliberately attempted to fit toric OK for high myopia
		LE			−5.50 / −3.00 × 180	−2.75 / −1.75 × 175	
	10	RE	Menicon Z night toric	12 months	−8.50 /−2.25 × 180	−2.25 / −0.50 × 170	
		LE			−8.75 /−2.50 × 180	−3.25 / −0.25 × 165	

Table 1-7. Outcomes of astigmatism correction after toric orthokeratology (OK) lens wear in previous case reports.

Medmont E300 corneal topographer. In the first case, after one year of overnight toric OK lens wear, the authors reported approximately 37.5% and 40% reduction in refractive astigmatism in the right and left eyes respectively. Interestingly the corneal toricity showed no change in the right eye but the left eye revealed a reduction of 21% in corneal toricity.

In the second case, at the end of the treatment period, the refractive astigmatism was reduced by 71% and 87.5% in the right and left eyes respectively. The corresponding reduction in corneal toricity was 15% and 25% in the right and left eyes respectively. Both subjects demonstrated good lens centration in both eyes, presenting with bull's eye topographic patterns after OK lens wear during the aftercare visits. However, neither the lens nor the TZ decentration was quantified in the report.

Chen et al. (2012) were the first to publish on the efficacy of toric OK lenses with a large sample study. Using the Menicon Z night toric OK lenses (NKL, Contactlenzen BV, Emmen, the Netherlands) the study demonstrated a reduction of refractive astigmatism and corneal toricity in 43 subjects after one month of OK lens wear. The lens has a spherical central optic zone with toric peripheral curves. The baseline refractive astigmatism was with-the-rule in all cases and ranged between 1.25 and 3.50 DC. The authors reported an average of 79% reduction of refractive astigmatism and 44% reduction in corneal toricity at the end of the treatment. It is worth noting that the fitting success was 95% with the first trial lens and only two subjects needed refitting due to centration problems.

Pauné et al. (2012) presented a retrospective analysis of 32 patients with > 1.25 DC refractive astigmatism. All patients were fitted with Precilens (Precilens, Creteil, France), a full toric OK lens design (toric back optic zone with toric reverse and alignment curves). The mean duration of lens wear was not specified, however patients fitted with OK between January 2008 and December 2010 were considered for the study The authors demonstrated a significant decrease in corneal toricity from 2.40 ± 1.27 DC at baseline to 1.30 ± 0.69 DC after OK wear (p < 0.001) and also reduced refractive astigmatism from −2.18 ± 1.36 DC at baseline to −0.38 ± 0.41 DC after OK wear (p < 0.001). Although significant reduction was noted in refractive J_{180} (0.68 ± 0.95 D to 0.11 ± 0.20 D after OK wear, p < 0.001), no significant change was noted in refractive J_{45} (0.08 ± 0.54 D to 0.01 ± 0.15 D after OK wear, p = 0.557). The investigators followed a careful fitting procedure where the fit was assessed after 20 minutes of closed eye wear and dispensed for overnight wear only if good lens centration was seen on fluorescein fit assessment. However, neither lens decentration nor TZ decentration was

quantified. The major limitation of this study was that the examiner was not masked and both lens fitting assessments and measurements were performed by the same investigator.

These initial studies describing performance of toric OK lenses provide a reasonable insight on how much refractive correction might be achieved with these lens designs, but some authors have warned of significant individual variations (Chen and Cho 2012) in the treatment outcomes, thus revealing a potential area for further research. Further, none of these studies quantified decentration of the OK lenses, which is a crucial step in understanding the failures of toric OK lenses in some cases.

1.10 RATIONALE FOR RESEARCH

Traditional OK lenses used during the day primarily failed in achieving good centration, resulting in induced astigmatism. Attempts to improve centration by fitting these lenses with a slightly steeper back optic zone improved centration but the concept was not widely adopted. Advances in both contact lens materials and lens manufacturing led to the introduction of reverse geometry lens designs which could be worn overnight, which was a huge leap forward leading to the inception of modern OK. The reverse geometry design, which features a zone of steeper curvature towards the lens periphery relative to the centre of the lens, has greatly improved centration when fitting lenses on eyes with relatively spherical corneas.

Although much of current research provides evidence that a small amount of OK lens decentration is present on minimally toric corneas, predominantly towards the temporal and/or inferior regions of the cornea, no reason has been established for this disposition (see Section 1.8.2). One suggestion to explain the decentration of lenses is baseline corneal asymmetry, particularly the temporal cornea being steeper than the nasal cornea. But to date no reports are available investigating the baseline corneal asymmetry in relation to decentration of OK lenses. This suggests a need to understand the importance of baseline normal corneal asymmetry.

Normal corneal shape has been identified to be asymmetric when investigated in terms of hemi-meridians with much of the previous research showing that the nasal and superior cornea flatten at a greater rate than the temporal and inferior cornea respectively (see Section 1.3.4). However it must be remembered that OK lens dynamics are better explained by the corneal shape in sectors than hemi-meridians because it is rational to state that the lens rests over a wider area of the cornea than on a single hemi-meridian during lens wear. Because of the lack of past literature pertaining to sectorial corneal shape, there is also a

need to investigate corneal shape more thoroughly at sectorial level. During such investigation the influence of various external factors (Section 1.3.6) cannot be ignored, particularly ethnicity and eyelid morphometry. Ethnicity is particularly relevant during OK because most OK lens users are in East Asia rather than in non-East Asian countries (Swarbrick 2006). From our general observation it is also known that the eyelid shape characteristics of Asians are different from non-East Asians. It is possible that eyelids of East Asians may have a different impact on corneal shape to non-East Asian eyelids. No previous research has investigated the association between eyelid morphometry and corneal shape taking ethnicity into account.

Previous research on spherical OK is primarily confined to fitting OK lenses on eyes with minimal amounts of corneal toricity, with anecdotal reports stating that fitting OK lenses on eyes with higher amounts of corneal toricity leads to greater OK lens decentration. However no scientific evidence has been presented to date to support this claim. This indicates the need to scientifically investigate the magnitude and direction of OK lens decentration during spherical OK lens wear on eyes with moderately toric corneas.

During the era of traditional OK, fitting non-reverse geometry rigid lenses with steeper BOZR showed promising results with respect to lens decentration in eyes with minimally toric corneas (Nolan 1972, Coon 1984). However the concept was not widely adopted at that time. When fitting conventional spherical rigid gas permeable contact lenses on eyes with moderately toric corneas, the lens BOZR is made steeper in an attempt to limit the edge lift and control decentration of the lenses (see Section 1.4.1). As far as reverse geometry lens fitting is concerned, no such modification to steepen the lens fit either by steepening the base curve or by deepening the lens sag has been proposed to control lens decentration. This warrants further investigation.

Various baseline corneal parameters may influence the magnitude and direction of OK lens centration during overnight wear, leading to a decentred TZ upon removal of the OK lens. These baseline corneal parameters include apical corneal curvature, magnitude (minimal or moderate) and direction of corneal toricity (with-the-rule, against-the-rule and oblique) and the extent of corneal toricity (central versus limbus-to-limbus). No previous study has investigated OK lens decentration in relation to these parameters. The knowledge of spherical OK lens dynamics influenced by these corneal parameters will be useful to justify the need for more complex lens designs such as toric OK lenses.

Current toric OK lenses have been shown to cause a significant reduction in refractive astigmatism, however individual variations are still present (see Section 1.9.2). These reports on evaluating the efficacy of toric OK lenses did not analyse OK lens or TZ decentration in relation to magnitude of baseline corneal toricity or other baseline corneal parameters. This knowledge will allow current OK practitioners to fit, modify and evaluate toric OK lenses in a scientific manner and also will be helpful to establish a possible reason for individual variations in the outcomes of toric OK lens fitting on moderately toric corneas.

The aim of the research presented in this thesis is to improve our current understanding of lens decentration during overnight wear of spherical OK lenses in eyes with minimal and moderate amounts of corneal toricity. This will help identify possible strategies to improve spherical OK lens centration as well as establishing scientifically based upper limits of corneal toricity that can be successfully fit with these lens designs. This research will also investigate whether toric OK lenses offer any improvement over spherical OK lens designs in terms of TZ decentration.

1.11 THESIS STRUCTURE

The major purpose of this thesis is to establish relationships between OK lens decentration and baseline corneal topography in minimally toric corneas (≤ 1.50 DC) and moderately toric corneas (1.50 to 3.50 DC). Since this requires a thorough understanding of corneal shape at sectorial level, Chapter 2 is aimed at investigating normal corneal shape in different sectors in terms of corneal asphericity. Because ethnicity and eyelid morphometry may influence corneal shape an additional aim of Chapter 2 is to investigate differences in eyelid morphometry between East Asians and non-East Asians and evaluate its influence on sectorial corneal shape.

As there is no previously reported accurate method to determine TZ decentration, Chapter 3 is aimed at establishing an objective digital method to determine TZ decentration using retrospective data. This chapter is also aimed at investigating relationships between TZ decentration and baseline corneal shape parameters such as sectorial corneal asphericity and other topographic parameters in eyes with ≤ 1.50 DC, after one night and 2 weeks of OK lens wear.

The main aim of OK is to induce uniform central corneal flattening over the pupillary area and a para-central annular steepening surrounding the flattened area. However, the decentration of OK lenses during lens wear may not create this effect leading to non-uniform

corneal shape changes. Therefore in Chapter 4, using the same retrospective cohort as in Chapter 3, a detailed investigation of changes due to OK lens wear in sectorial corneal shape and corneal refractive power will be performed after one night and 2 weeks of lens wear.

To date no literature has presented the effect of spherical OK lens on TZ decentration on eyes with moderately toric corneas (1.50 to 3.50 DC). Therefore Chapter 5 is aimed at investigating TZ decentration characteristics in moderately toric corneas after a single overnight use of spherical OK lenses fitted using an empirical method. These TZ decentration characteristics found in eyes with moderately toric corneas will be compared with the results found after a single overnight use of spherical OK lenses on eyes with minimally toric corneas, which are also fitted using the same fitting method. To make this comparison, retrospective data from Chapter 3 where spherical OK lens were fitted in minimally toric corneas will be used. Furthermore, the effects of modifying the fitting technique in a similar fashion to the 'one-third' rule used in conventional RGP fitting on toric corneas will be evaluated. Other secondary aims of this chapter include investigating the effect of spherical overnight OK lens wear for a single night on corneal topographic features such as apical corneal curvature, corneal vector components (M, J_0, J_{45}) and corneal toricity.

Chapter 6 reports exploratory research to understand TZ decentration with empirically fitted peripheral toric OK lens designs on moderately toric corneas after one and seven nights of OK lens wear. Finally in Chapter 7, an overall summary and conclusion of all studies reported in Chapters 2 to 6 will be provided. In the same chapter possible models for OK lens decentration with respect to various observations made from the series of studies will be given.

CHAPTER 2 SECTORIAL CORNEAL TOPOGRAPHY DIFFERENCES IN RELATION TO ETHNICITY AND EYELID MORPHOMETRY

2.1 INTRODUCTION

Corneal profile may play a role in the centration of orthokeratology (OK) lenses. Therefore an understanding of normal corneal topography in terms of asphericity (Q) is important.

A range of asphericity Q values (−0.15 to −0.48) have been reported for the normal cornea (Mandell and St Helen 1971, Kiely et al. 1982, Guillon et al. 1986, Sheridan and Douthwaite 1989, Eghbali et al. 1995). These values were often confounded by ethnicity, chord length of the measurement, corneal meridian and also the type of device used in assessing the corneal topography. In addition, these studies have described asphericity in a single meridian or hemi-meridian. The dynamics of contact lenses on the cornea are likely to be governed by regional corneal shape. Yang et al. (2005) and Hiraoka et al. (2009), who investigated decentration of the treatment zone induced by overnight OK lenses, speculated that nasal versus temporal corneal asymmetry at baseline may play a role in determining the direction of lens decentration. However, no previous study has investigated normal corneal shape asymmetry and its relation to OK lens dynamics.

From Section 1.3.6, it is also known that the corneal topography is influenced by various external factors such as age, ethnicity, eyelid position, eyelid morphometry, eyelid pressure and time of the day. Read et al. (2007a) extensively researched the influence of eyelid morphometry on normal corneal shape. However, their work did not investigate its relation to regional corneal shape. Furthermore the sample was comprised predominantly of Caucasian subjects.

The main aim of the study reported in this chapter is to establish normative trends in sectorial corneal shape by investigating sectorial corneal asphericity. Additional aims include investigating differences in corneal shape between East Asians (EAs) and non-East Asians (non-EAs), because it is evident from our general observation, and also from previous research (Kunjur et al. 2006), that these ethnic groups present contrasting shapes of eyelid. A further investigation was performed relating eyelid morphometry with corneal shape.

2.2 MATERIALS AND METHODS

2.2.1 Study design

Participants were recruited via advertising posters displayed within the University of New South Wales (UNSW). Participants were scheduled for a morning visit (before noon) where the study measurements were taken within 2.49 ± 1.02 hours after waking by a single examiner (VM). Study measurements included objective refraction, habitual vision correction, anterior eye photographs and corneal topography, in sequence. Data from two eyes were obtained from each participant to allow compensation for any head tilt in the image capture process. Only the right eye data were analysed for the reason that right and left palpebral fissure measurements (Lam et al. 1995) and corneal topography (Dingeldein and Klyce 1989, Smolek et al. 2002b) demonstrate a high degree of mirror symmetry.

2.2.2 Participants

Thirty two EAs (age range 18 – 37 years; 13 males, 19 females; 20 myopic, four emmetropic, eight hyperopic) and thirty two non-EAs (age range 18 – 30 years; 10 males, 22 females; 13 myopic, 14 emmetropic, five hyperopic) were enrolled in the study. Participants were predominantly optometry students and staff of the School of Optometry and Vision Science, UNSW. The study protocol obtained approval from the institutional Human Research Ethics Advisory Panel (Approval No. HREA 090031) and participants were treated in accordance with the tenets of the Declaration of Helsinki. An informed written consent was also obtained from the participants prior to their enrolment. Only participants having < 1.50 DC corneal toricity, < 6.00 D of myopia, good ocular health and free from any systemic disease that may interfere with eyelid morphometry, were enrolled. Soft contact lens wearers who mostly were occasional contact lens users were advised to discontinue using lenses for at least 48 hours prior to the measurements. Short-term soft contact lens wear has been shown to have minimal and clinically negligible impact on corneal topographic parameters (Sanaty and Temel 1996). A conservative period of 48 hours without lens wear was chosen to avoid the potential of short term changes to corneal topography from soft lens insertion and removal. Rigid contact lens wearers were not included.

2.2.3 Measurements

2.2.3.1 Refraction

Central non-cycloplegic objective refraction was obtained using the Shin-Nippon NVision K5001 autorefractor (Tokyo, Japan). The optimum value (the most reliable of multiple

measurements obtained from the device) from 5 consecutive measurements of refraction was taken as the final value as recommended by the manufacturer.

2.2.3.2 Visual acuity

High contrast visual acuity was measured using a LogMAR chart displayed on a computer monitor at 6m (Test Chart 2000 Pro, Thomson Software, London, England), while wearing habitual spectacle correction.

2.2.3.3 Slit lamp biomicroscopy

A routine slit lamp biomicroscopy examination was performed to detect any gross corneal abnormalities such as superficial punctate keratitis or scars that could interfere with capture of corneal topography.

2.2.3.4 Corneal topography

Four corneal topography maps (Medmont E300, Medmont Pty Ltd, Melbourne, VIC) were captured from each eye. All topography measurements were taken in the morning and participants were advised to refrain from prolonged near work prior to the topography recording session to avoid possible eyelid influence on corneal shape from prolonged down gaze (Buehren et al. 2003). Care was taken to avoid lashes obstructing the mire image. Topography images were captured only when the participant steadily held the blink. Participants were advised to blink immediately before capturing the image to avoid any dry areas forming on the corneal surface that may distort the mire image. To maximise corneal exposure during topography capture, participants were advised to open their eyes as widely as possible during the measurement procedure. In eyes with small palpebral fissure height, the examiner (VM) held the upper eyelid and also occasionally participants were instructed to draw down the lower eyelid. The Medmont topographer assigns a score between 0 to 100 based on centration, focus and movement. Although a score over 75 is considered as good according to the instrument's user manual, only images with scores above 95 were accepted for analysis. Captured images were reviewed before analysis, and maps with artefacts and distorted mires were eliminated. In this manner a cluster of 4 maps from each of 40 participants, a cluster of 3 maps from 19 participants and a cluster of 2 maps from 5 participants were available for analysis.

2.2.3.5 Eye photographs

External eye photographs were captured in high-resolution (4288 X 2848 pixels) using a Nikon D5000 12 megapixel digital SLR camera (Nikon Corp., Japan) fitted with a 18-55 mm

zoom lens set to 50 mm focal length. All photographs were taken in the same examination room under the same lighting conditions. The camera was mounted on a tripod at a distance of 50 cm from the participant's eye, and set in manual mode with a shutter speed of 0.01 secs at ISO 100. The camera's built in flash, whose intensity in the manual mode has been rated to have a guide number of 13, was used in all photographs. The flash was set to fire on front curtain flash sync so that the image was captured before any effects from the flash induced a blink reflex. A chin and forehead rest was used to keep the participant's head stable while capturing the eye photographs and to ensure inter-subject consistency.

Figure 2-1 illustrates the setup used for capturing eye photographs. A millimetre ruler was placed on the side bar of the head-chin rest and included in all the photographs that were captured for calibration purposes. The camera height was maintained at the same level as the participant's eye to avoid any parallax error and this was ensured by placing a right angled stand next to the camera. An image of both eyes was captured at the same time, while the participant was instructed to assume a natural relaxing position and to view into the camera's lens aperture. In order to avoid camera movements a Nikon ML-13 control was used to remotely release the shutter.

Figure 2-1. Set-up used for capturing eye photographs. a. view from behind the camera and b. view from above the camera and participant chin rest. Permission granted by participant for reproduction of this figure.

2.2.4 Determining the hemi-meridional corneal asphericity

2.2.4.1 Corneal topography raw data and its interpolation

The Medmont E300 topographer enables the user to export the raw topography data in ASCII format. These files include radial distance, sagittal height, axial curvature, tangential curvature and slope files. Each of these files consisted of matrices of size up to 300 × 32. Each row represents corneal hemi-meridional data centred to vertex normal (along the VK axis) and separated by 1.2 degree intervals. The radial distance data and the corresponding sagittal height data of all participants from the topographer were imported into a custom MATLAB (The MathWorks, Inc. Version 7.12) program. Since the sagittal height along each hemi-meridian was determined at uneven spacing of radial distance locations by the topographer, the data were interpolated to a fixed spacing of 0.15 mm distance. The interpolation step involved the use of Delaunay triangulation of the scattered data points which were interpolated in a linear manner.

2.2.4.2 Corneal raw data extrapolation

The interpolated sagittal height data of the available maps from each participant were then averaged. The topographer assigns a zero value for missing data. While in most cases topography data was available beyond 5 mm along horizontal hemi-meridians the data along the vertical meridians were generally restricted by the ocular adnexa. Each hemi-meridional data set was assessed and where data were not available within a 4 mm radius from the corneal vertex, a 4^{th} order polynomial was fitted based on the least squares method of fitting curves to extrapolate data for the missing locations. This method of extrapolating corneal data towards the corneal periphery was shown to be efficient giving rise to minimal fit errors. A root mean square error (RMSE) value determined an average fit error that described the amount by which the best fit 4^{th} order polynomial curve departed from the original hemi-meridional data set, with lower RMSE values representing a better polynomial fit. The RMSE value of extrapolated corneal data typically ranges between 2 – 5 µm if the extrapolation is restricted to a radius of 4 mm from the reference centre (Iskander et al. 2007).

The hemi-meridional data alone is not enough to fit the best-fit conic section. In order to complete one end of the conic section, each of the hemi-meridional data set was mirrored to give a conic section with a total chord diameter of 8 mm. A best-fit conic section was then fitted to this data using Taubin's generalised eigenvector fit (Taubin 1991) (Figure 2-2).This method approximates the data by using either an ellipse or a hyperbola, whichever best fits to the data. As described in Section 1.3.3.1, corneal shape is best described using conic sections.

Kiely (1982) demonstrated that the Q values of corneal hemi-meridians ranged between -1.44 to 1.28, indicating that corneal shape is best represented by a range of conic sections including oblate ellipse (Q > 0), prolate ellipse (Q < 0 & > -1) and hyperbola (Q < -1). The coefficients of the general form of conic equation were determined from the equation:

$$Ax^2 + Bxy + Cy^2 + Dx + Fy + G = 0$$

in which A, B, C, D, F and G are the coefficients of the equation and x and y are the radial distance data and their corresponding sagittal height data respectively. Based on the value of the determinant calculated from the coefficient values the type of best-fit conic was determined from which the Q value could be calculated for each hemi-meridian (Appendix A.1).

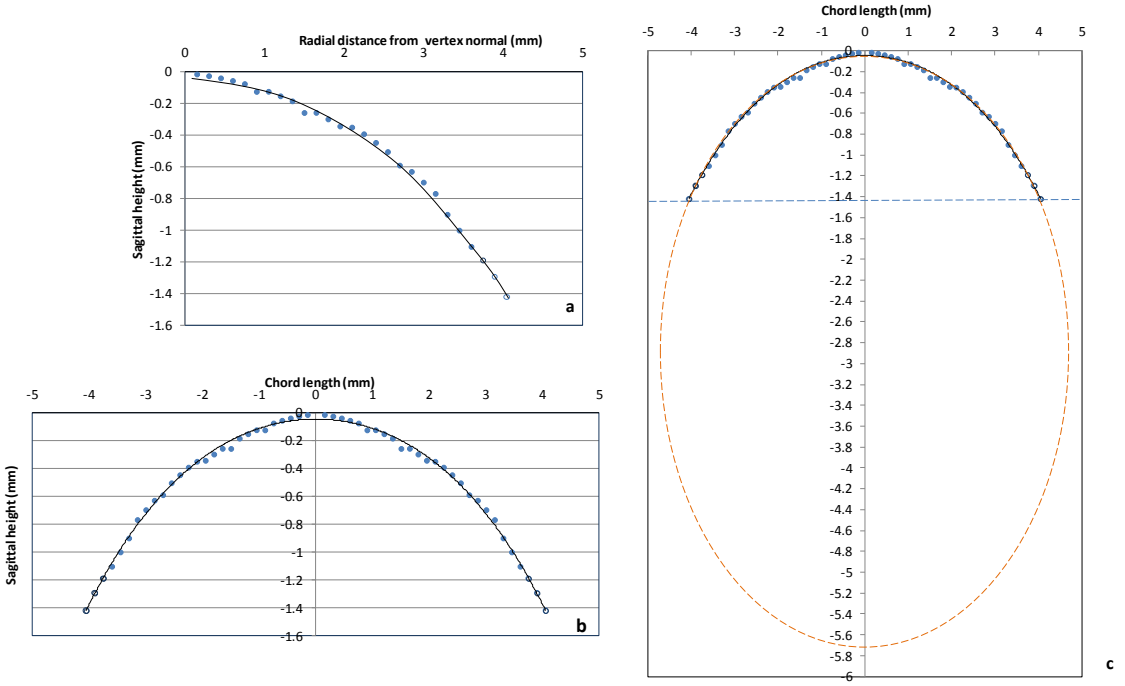

Figure 2-2. Method used to extrapolate radial data and to calculate a best-fit conic curve. a. The height data plotted as a function of radial distance for a single hemi-meridian. The solid circles represent the uniformly spaced data points interpolated from the true data as derived from the topographer and the empty circles represent the uniformly spaced data points extrapolated using a fourth order polynomial. The origin denotes the vertex normal. b. Mirroring the data about the vertex normal in order to enable sufficient data to fit a conic section. c. Fitting a best-fit conic section to the data points. In the current figure, a best-fit ellipse is shown as an example. The asphericity (Q) value was calculated from the parameters of the conic section as described in Appendix A.1.

2.2.5 Validity of Q value determination

To validate the MATLAB algorithm used to determine hemi-meridional asphericity Q described in Section 2.2.4, sagittal height data for a range of elliptical and hyperbolic sections at various chord lengths were determined using ellipse and hyperbolic equations. The general ellipse equation (see Appendix A.1) with its foci on y-axis can be rewritten to determine y (sagittal height in mm) for a desired x (radial distance in mm) as:

$$y = \sqrt{\frac{a^2(b^2 - x^2)}{b^2}}$$

Similarly, the equation for a hyperbola (see Appendix A.1) can be rewritten to determine y for a desired x as:

$$y = \sqrt{\frac{a^2(b^2 + x^2)}{b^2}}$$

In both equations a and b are major and minor axes respectively. Arbitrary values of a and b were used such that the Q values for hyperbolas and ellipses would range between −1.45 and 1.25. The asphericity Q for an ellipse can be determined from the major and minor axes from the equation:

$$Q = \frac{b^2}{a^2} - 1$$

and for a hyperbola from the equation:

$$Q = -\left(1 + \frac{b^2}{a^2}\right)$$

This range of test Q values was chosen to represent the range of hemi-meridional Q values observed in normal eyes (Kiely et al. 1982). The apical curvature for all conic sections was set to 7.60 mm.

Figure 2-3 shows a perfect linear relationship (coefficient of determination $r^2 = 1.00$) between test Q values and the Q values determined by the MATLAB algorithm suggesting that the Q values determined by the MATLAB algorithm were identical to the test Q values.

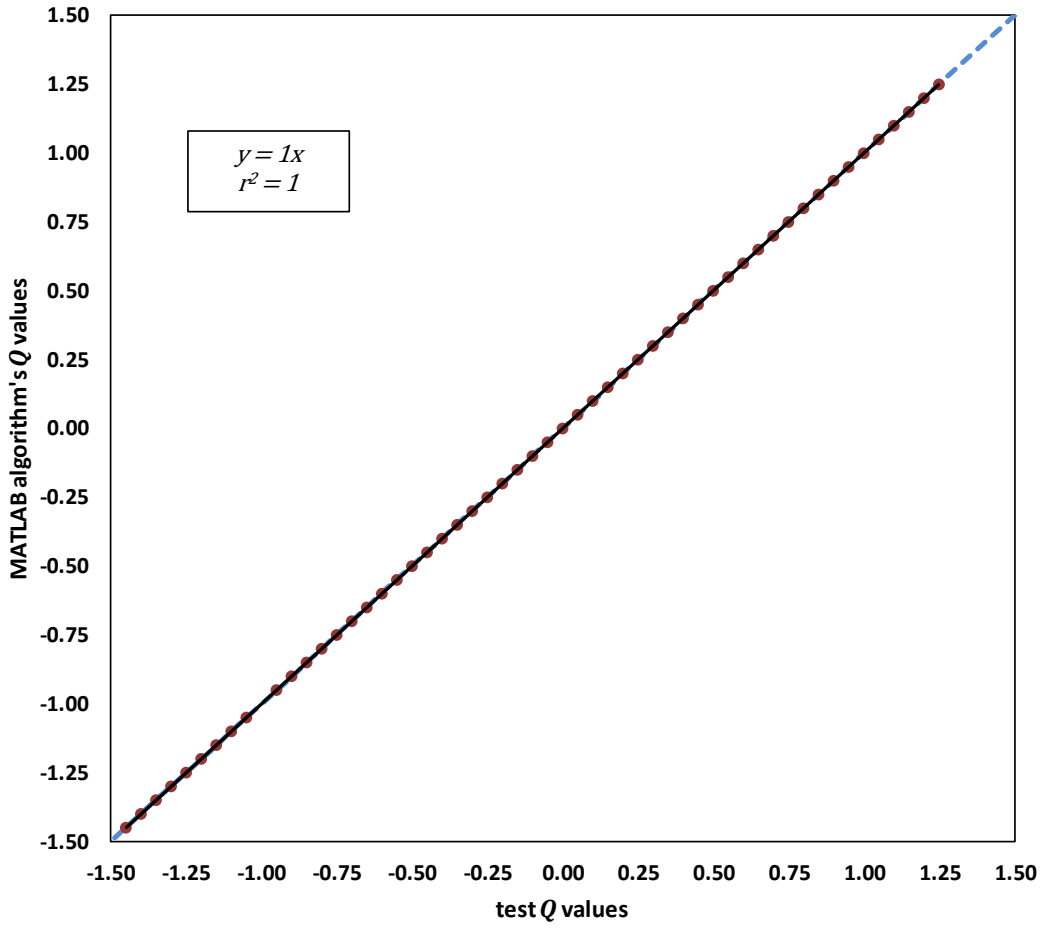

Figure 2-3. The relationship between test Q values determined from arbitrary major and minor axes of either hyperbola or ellipse and those determined using the MATLAB algorithm. The solid dark line represents the relationship between test and the MATLAB derived Q values which is perfectly aligned to the discontinuous 1:1 blue line showing a perfect relationship.

2.2.6 Corneal sectors

The calculated hemi-meridional Q values were averaged at each angle location for all participants within each ethnic group and in total (for all participants regardless of ethnicity). For each set of grouped data, the averaged 300 hemi-meridional Q values were divided into 60 degree sectors (each consisting of 50 averaged hemi-meridional values) starting from the zero degree hemi-meridian representing the horizontal nasal hemi-meridian of the cornea and east direction on a normal compass orientation (Figure 2-4). The 50 Q values within each sector were then averaged to give 6 mean asphericity values, one for each of the six sectors. These sectors include supero-nasal (0 to 60 degrees), superior (61-120 degrees), supero-temporal (121-180 degrees), infero-temporal (181-240 degrees), inferior (241-300 degrees) and infero-nasal (300-360 degrees) sectors. To provide nasal versus temporal corneal symmetry the two nasal (supero-nasal and infero-nasal) and two temporal (supero-temporal and infero-temporal) sectors were also combined and compared.

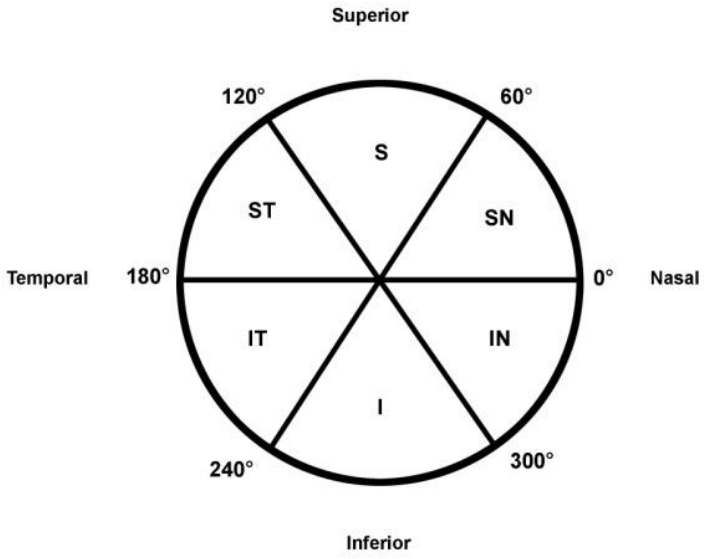

Figure 2-4. Distribution of corneal sectors about the vertex normal (video-keratoscopic axis). SN = supero-nasal, S = superior, ST = supero-temporal, IT = infero-temporal, I = inferior and IN = infero-nasal.

2.2.7 Eyelid morphometry features

Eyelid morphometry features were determined by using i-Metrics software (Courtesy: Dr. Robert Iskander, Institute of Biomedical Engineering and Instrumentation, Wroclaw University of Technology, Wroclaw, Poland) (Figure 2-5). The software allows a digital image to be imported and enables the user to manually mark outlines of morphological features of the anterior eye. Before performing any measurements using i-Metrics, all the digital photographs consisting of two eyes were corrected for any head tilt present during the photograph capture. This correction was performed in the i-Metrics program by a line joining inner canthi of both eyes to determine the degree of misalignment between two eyes, which was considered as head tilt, and rotating the photos accordingly. Photographs were then cropped for single right eyes of size 1200 × 800 pixels.

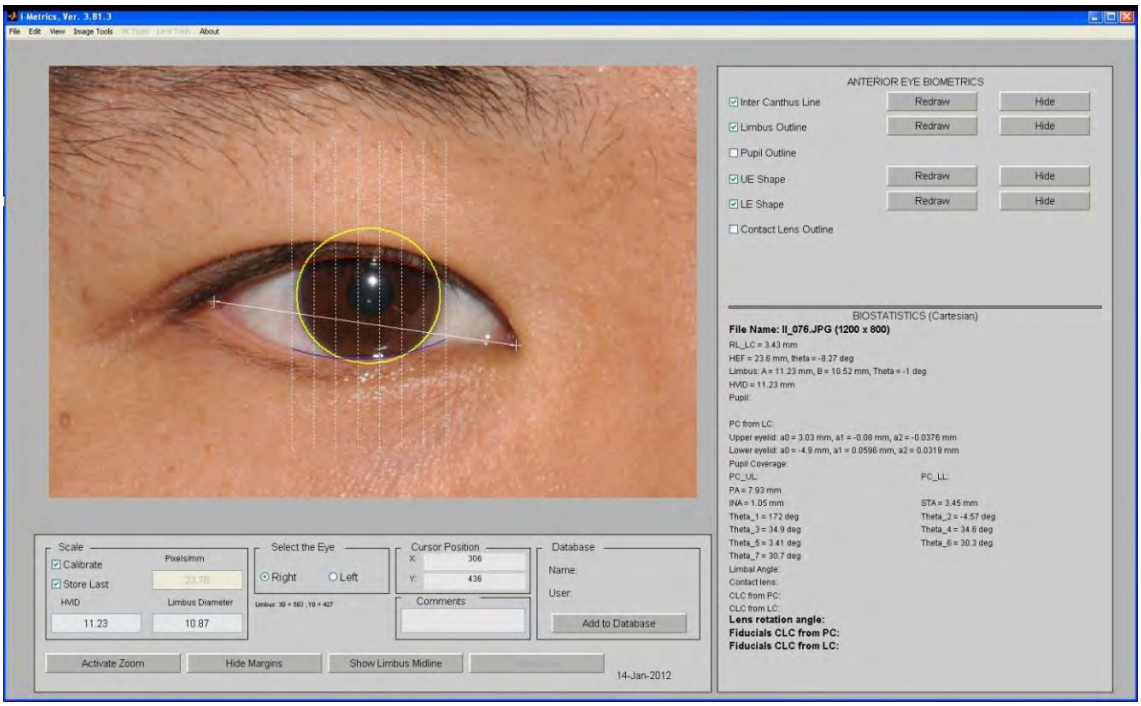

Figure 2-5. A screen shot of the i-Metrics graphic user interface showing the processed digital photograph of a right eye. (i-Metrics software courtesy: Dr. Robert Iskander, Institute of Biomedical Engineering and Instrumentation, Wroclaw University of Technology, Wroclaw, Poland).

These single eye photographs corrected for the head tilt were then analysed using i-Metrics software. To allow analysis the user identified 16 points along the limbus and 8 points along each eyelid margin. Finally, a straight line was drawn joining the nasal and temporal canthi. The software then determined various anterior eye biometrics based on the points chosen on the photograph overlying on a co-ordinate geometric plane. Although the software also enables the user to mark the pupil size and centration, the main interest was to

investigate the eyelid morphometry features and their influence on corneal shape, and therefore pupil parameters were not assessed. Various anterior eyelid morphometry features chosen in the current study are illustrated in Figure 2-6 and described in Table 2-1.

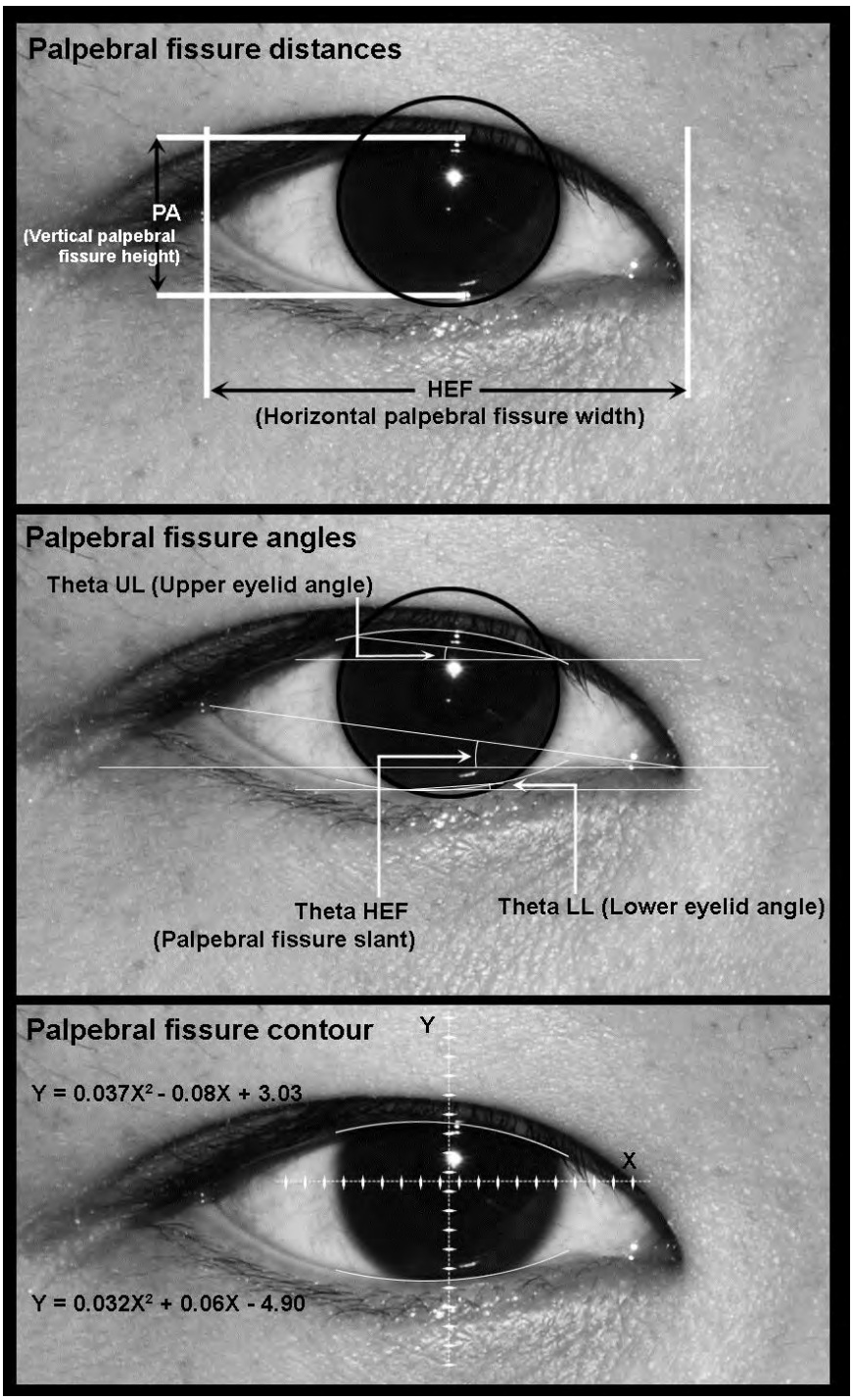

Figure 2-6. A diagrammatic description of the palpebral fissure measurements on a typical digital photograph. Adapted from Read et al. (2006).

Abbreviation used in i-Metrics software	Terminology used in the current study	Description
Palpebral fissure distances (mm)		
PA	Vertical palpebral fissure height	The vertical distance between the upper and lower lid as measured through the centre of the ellipse defined by the limbus.
HEF	Horizontal palpebral fissure width	The horizontal distance between the nasal and temporal canthi.
Palpebral fissure angles (degrees)		
Theta HEF	Palpebral fissure slant	The angle between the temporal and nasal canthus (a positive angle indicates the nasal canthus is vertically higher than the temporal canthus).
Theta UL	Upper eyelid angle	The angle made between the line joining the two points where the upper lid intersects the limbus and the horizontal (a positive angle indicates that the nasal portion of the central upper eyelid is vertically higher than the temporal portion of the central upper eyelid).
Theta LL	Lower eyelid angle	The angle made between the line joining the two points where the lower lid intersects the limbus and the horizontal (a positive angle indicates the nasal portion of the central lower eyelid is vertically higher than the temporal portion of the central lower eyelid).
Palpebral fissure contour		
A second order polynomial ($Y = a2 \cdot x^2 + a1 \cdot x + a0$) was fit to the points marked on both eyelid margins. Each coefficient represents an eyelid parameter as described below.		
a0	Eyelid position (polynomial term C)	Position of the eyelid in mm from the centre of the ellipse fitted to 16 points selected along the limbus. A high positive value for the upper eyelid and a high negative value for the lower eyelid respectively indicate a greater distance of the eyelid position from the limbus centre.
a1	Eyelid slope (polynomial term B)	Slope of the eyelid (no units). A positive angle (both for upper and lower eyelids) indicates the nasal end of the eyelid is vertically higher than the temporal end.
a2	Eyelid curvature (polynomial term A)	Curvature of the eyelid in mm^{-1}. A higher negative value for the upper eyelid and a higher positive value for the lower eyelid indicate a more curved eyelid.

Table 2-1. Descriptions used for various eyelid morphometry feature measurements obtained using i-Metrics software. Table adapted from Read et al. (2006).

2.2.8 Repeatability of i-Metrics

Each anterior eye photograph was analysed twice on two different days using i-Metrics by the same observer. The photograph sequence was randomised at both occasions. The average of the values from the two measurements was used for analysis. Since the eyelid features were manually marked by the examiner, the agreement between two measurements on the same photograph was assessed. A linear regression analysis was performed to compare the results of the two repeated eyelid morphometry measurements obtained. The mean coefficient of determination (r^2) for all the eyelid morphometry measurements was 0.95 ± 0.05, and the mean slope was 0.94 ± 0.05, indicating that the two measurements performed by the single observer on different days were closely correlated. An example of agreement between two measurements for palpebral fissure slant is illustrated in Figure 2-7 and Figure 2-8. The regression analysis plots and the Bland-Altman agreement plots for the remaining measurements of eyelid variables are given in Appendix A.2.

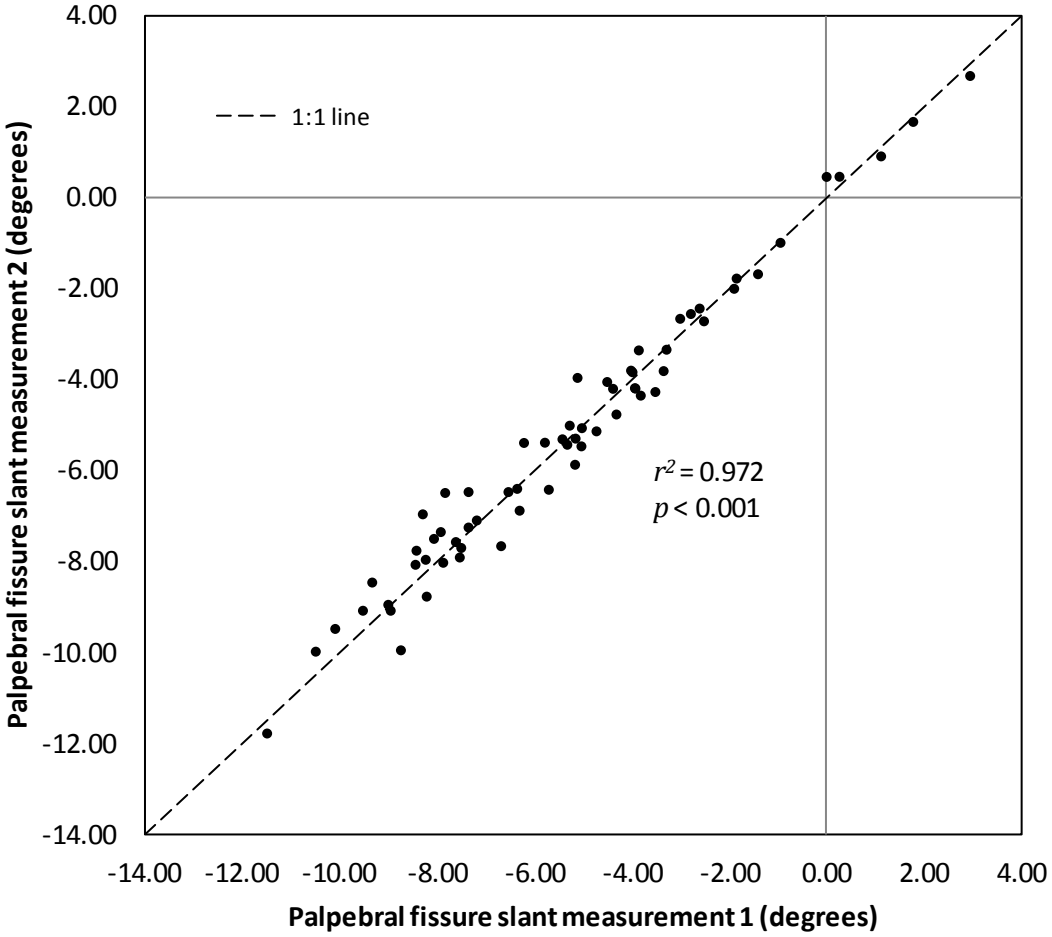

Figure 2-7. An example showing good agreement between two measurements of palpebral fissure slant on eye photographs (r^2 = 0.972). The measurements points lying close to the 1:1 line indicate a good agreement between the two measurements.

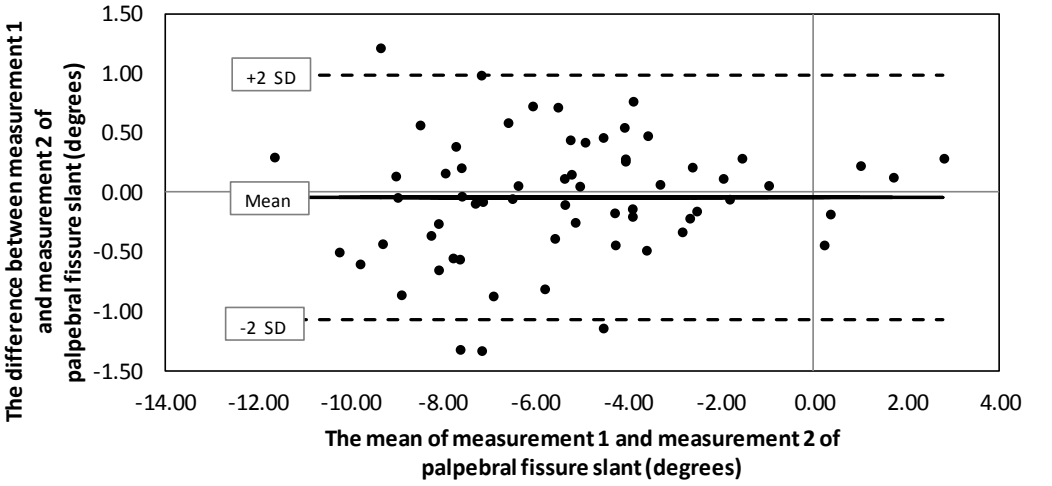

Figure 2-8. Bland-Altman plot showing good agreement between two measurements of palpebral fissure slant. Dashed lines represent limits of agreements (mean difference ± 2 × standard deviation of difference).

2.2.9 Statistical analysis

All the statistical analyses were performed using IBM SPSS version 20, (SPSS Inc, Chicago, IL, USA). Mixed analysis of variance was used to compare sectorial Q values within and also between the two ethnic groups. The mixed analysis of variance tests for mean differences between two or more independent groups, in which at least one between-subjects variable and one within-subjects variable is present. The sectorial Q values are the within-subjects variable and the ethnicity has two independent groups as East Asian and non-East Asians. As in any analysis of variance, the mixed analysis of variance is also based on the assumption that variances in each sector are similar which is called sphericity assumption. Mauchly's test was used to test for this assumption. If the test showed any violation of the assumption of asphericity, the Greenhouse-Geisser correction was used. Shapiro-Wilk's test, which compares whether the distribution of a given variable is the same between two groups was performed to test the parametric distribution of the data sets. Independent sample t-tests were used to analyse differences in baseline refractive parameters, corneal parameters, and corresponding sectorial Q and eyelid morphometry characteristics between the two ethnic groups. If the data sets are not normally distributed then the Mann-Whitney U test, a non-parametric test to compare two groups was used. Multivariate analysis of variance (MANOVA) was performed to relate each eyelid morphometry feature to corneal parameters by combining the data of both groups. MANOVA allows detecting any interactions present between one independent variable and several dependent variables, and it also allows investigation of differences between groups in the way the independent and dependent variables interact. If any significant interaction was found between the variables, a bivariate Pearson's or Spearman's correlation, based on the data normality, was used to investigate the relationships between eyelid morphometry features and corneal variables. Both Pearson's and Spearman's correlation tests the relationship between two continuous variables. Spearman's correlation test is a non-parametric equivalent of Pearson's correlation test. A perfect positive linear correlation will have an r value of 1 and similarly a perfect negative linear correlation will have an r value of -1. A p-value less than 0.05 was used to denote statistical significance.

2.3 RESULTS

2.3.1 Baseline variables

There was no statistically significant difference in refractive power M, J_{180}, J_{45} and corneal M, J_{180} and J_{45} between the two ethnic groups (Table 2-2). Note: For the calculation of refractive and corneal parameters, the vertex normal was used as the reference centre in all the studies reported in this thesis.

Variable	East Asians	Non-East Asians	p - value
Age (years)	22.66 ± 3.76	24.13 ± 3.41	0.106
Refractive M (D)	−2.01 ± 2.19	−1.08 ± 2.09	0.086
Refractive J_{180} (D)	−0.07 ± 0.27	−0.02 ± 0.23	0.491
Refractive J_{45} (D)	0.07 ± 0.14	0.10 ± 0.16	0.459
Corneal M (D)	43.44 ± 1.26	43.48 ± 1.72	0.906
Corneal J_{180} (D)	−0.33 ± 0.26	−0.27 ± 0.25	0.356
Corneal J_{45} (D)	0.16 ± 0.21	0.07 ± 0.18	0.074

Table 2-2. Age, refractive and corneal biometric data (mean ± SD) of East Asians and non-East Asians. D = Dioptres.

2.3.2 Hemi-meridional corneal asphericity (Q) variation

Of a total 227 corneal topography data files from 64 participants, the mean minimum radial distance from the vertex normal up to which the data were complete without missing data points was 4.07 ± 0.25 mm (range: 3.15 to 4.50 mm). The hemi-meridional data were extrapolated only if the obtained data from each data set extended less than 4 mm. Sixty eight maps required extrapolation beyond 3.90 mm, in which the average percentage of hemi-meridians that needed extrapolation was 14% (ranging between 1 and 45%). In one topographic map, 5% of the hemi-meridional height data required extrapolation beyond 3.15 mm.

The mean RMSE value, considering topographic data from all the participants in the current study, was 0.80 ± 1.34 μm. This low RMSE value indicates that the polynomial method used for extrapolation was efficient, and suggests that the values extrapolated would be very close to the original data if measured.

Figure 2-9 gives a visual representation of variation in the mean hemi-meridional Q values from all participants through 360 degrees of the cornea. It can be seen that as the angle of the hemi-meridian increased in counter-clock wise direction from the zero degree (nasal) hemi-meridian, the Q values tend to become less negative and the change in trend was more rapid in the superior sector. The Q values tend to become more negative gradually in supero-temporal, infero-temporal, inferior and infero-nasal sectors. The wider standard error bars of the mean in the superior sector suggest an increased variation of the asphericity in this region of the cornea, probably caused by interaction of the upper eyelid.

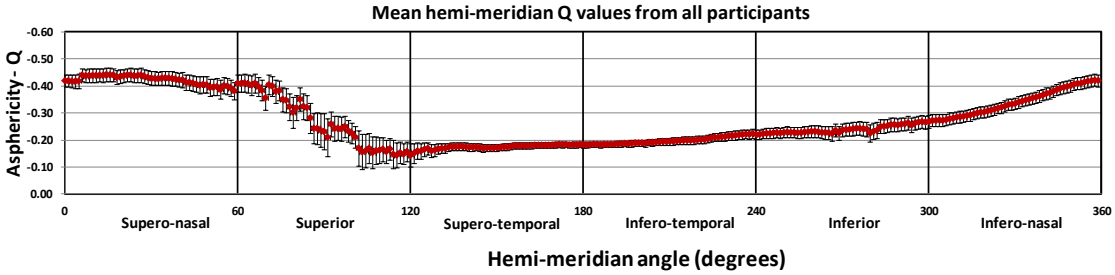

Figure 2-9. The variation in the mean hemi-meridional asphericity (Q) across the cornea along each measured hemi-meridian. The origin on the horizontal axis represents the nasal hemi-meridian. The horizontal axis was further divided into 6 sectors of 60 degrees each. A higher negative value indicates greater prolate asphericity. The error bars represent 95% standard error of the mean.

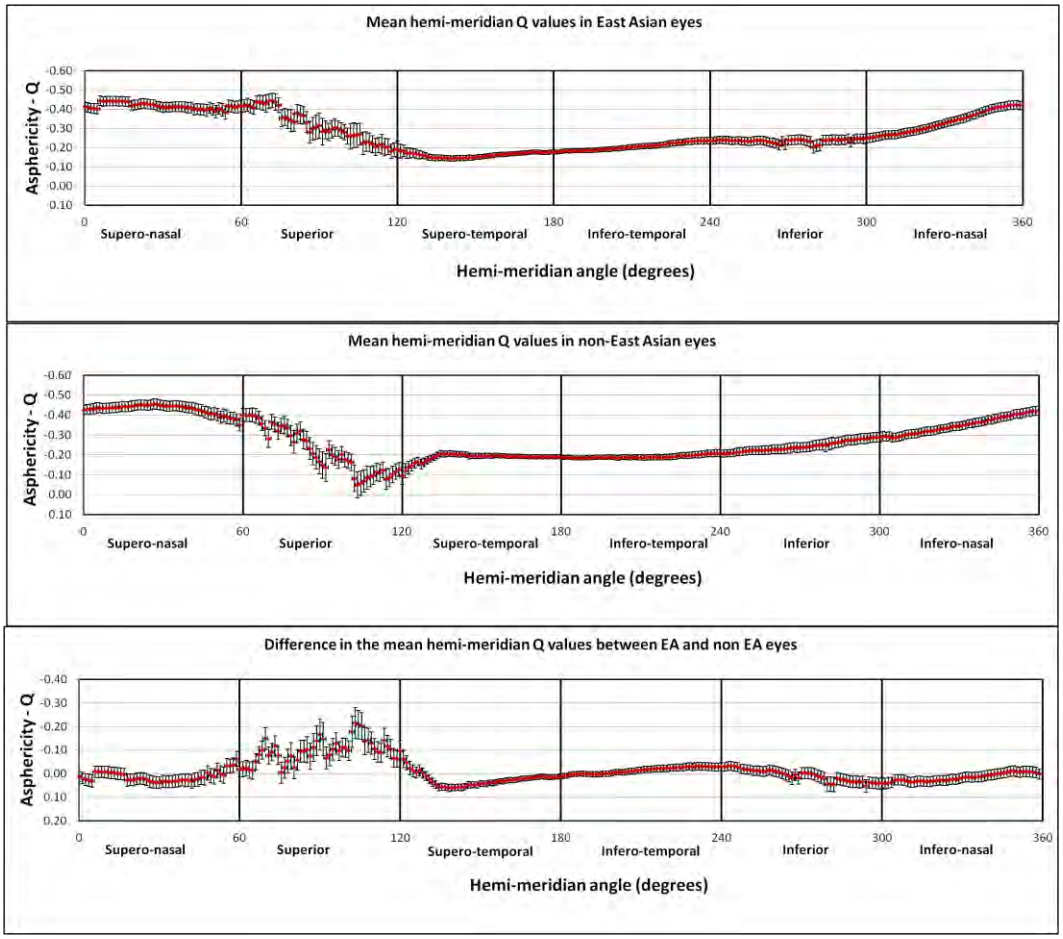

Figure 2-10. The variation in the mean hemi-meridional asphericity (Q) across the cornea along each measured hemi-meridian in East Asian eyes (top), non-East Asian eyes (middle), and the difference between the two ethnic groups (bottom). The East Asian eyes tend to have higher negative Q values in the superior sector indicating a more prolate shaped cornea in those eyes than non-East Asian eyes in this sector. The error bars indicate 95% standard error of the mean.

Figure 2-10 presents the trend in the Q value variation across the cornea in EA and non-EA groups and the difference between the two groups. It can be seen that there was a sudden decrease in the Q values in the superior sector in both ethnic groups indicating an abrupt change towards less prolate corneal shape in this region. Furthermore, the sudden variation in the superior sector was sharper in non-EA eyes.

2.3.3 Sectorial corneal asphericity

Table 2-3 presents the sectorial variation of the asphericity for the complete data set and in both ethnicities separately. Considering the combined data from both ethnicities, there was a significant variation in the sectorial corneal asphericity (Mixed-ANOVA: $F_{(1.16,\ 114.13)}$ = 327.210, p < 0.001). The variation was also different between the two ethnicities (Mixed-ANOVA: $F_{(1.16,\ 114.13)}$ = 18.771, p < 0.001). From the combined data, the supero-nasal sector was most prolate followed by infero-nasal, superior, inferior, infero-temporal and supero-temporal sectors. A paired t-test between nasal sectors (averaging the hemi-meridional Q values of supero-nasal and infero-nasal sectors) and the temporal sectors (averaging the hemi-meridional Q values of supero-temporal and infero-temporal sectors) revealed a statistically significant difference (−0.20 ± 0.06, p < 0.001), indicating a significant nasal versus temporal corneal asymmetry. There was no significant difference in the asphericity between superior and inferior corneal sectors (−0.03 ± 0.12, p = 0.088).

Similar to the variation observed when the entire data set was considered, the EA eyes also showed the supero-nasal sector was most prolate followed by infero-nasal, superior, inferior, infero-temporal and supero-temporal sectors. The overall mean Q of the nasal sectors in EA eyes was −0.37 ± 0.06, and in the temporal sectors was −0.18 ± 0.03. The difference in the mean asphericity between the nasal and temporal sectors was statistically significant (−0.19 ± 0.07, p < 0.001). There was also a significant difference in the mean asphericity between superior and inferior corneal sectors (−0.08 ± 0.08, p < 0.001).

	Corneal sectors					
	Supero-nasal	**Superior**	**Supero-temporal**	**Infero-temporal**	**Inferior**	**Infero-nasal**
Combined data	−0.42 ± 0.02	−0.27 ± 0.11	−0.17 ± 0.02	−0.20 ± 0.01	−0.24 ± 0.02	−0.34 ± 0.05
EA group	−0.42 ± 0.02	−0.32 ± 0.08	−0.16 ± 0.01	−0.20 ± 0.02	−0.23 ± 0.01	−0.33 ± 0.06
Non-EA group	−0.43 ± 0.02	−0.22 ± 0.11	−0.19 ± 0.02	−0.19 ± 0.01	−0.24 ± 0.02	−0.35 ± 0.04

Table 2-3. Corneal asphericity (mean ± SD) at each corneal sector for the combined data set and separately for East Asian (EA) and non-East Asian (Non-EA) eyes.

The trend in hemi-meridian Q value variation was slightly different in non-EA eyes, where the supero-nasal sector was most prolate followed by infero-nasal, inferior, superior, infero-temporal and supero-temporal sectors. The overall mean of the nasal sectors in non-EA eyes was −0.39 ± 0.05, and in the temporal sectors was −0.19 ± 0.02. The difference in the mean asphericity between the nasal and temporal sectors was statistically significant (−0.20 ± 0.05, p < 0.001). There was no significant difference between superior and inferior corneal sectors (0.02 ± 0.14, p > 0.999).

Several sectors showed a significant difference in the mean asphericity between EA and non-EA eyes (EA minus non-EA). The greatest difference was observed in the superior sector (−0.10 ± 0.05, p < 0.001), followed by supero-temporal (0.03 ± 0.03, p < 0.001), infero-temporal (−0.01 ± 0.01, p < 0.001) and supero-nasal (0.01 ± 0.02, p = 0.002) sectors. No significant difference was observed between inferior (0.01 ± 0.02, p = 0.053) and infero-nasal (0.02 ± 0.02, p = 0.108) sectors between ethnic groups.

2.3.4 Eyelid morphometry variables

Most of the eyelid morphometry features showed significant differences between the two ethnic groups. The horizontal palpebral fissure width (HPFW) was smaller, vertical palpebral fissure height was shorter, and palpebral fissure slant was larger in EA than non-EA eyes (all p < 0.05, independent Student t-tests). The upper eyelid was positioned lower, sloped more and curved less in the EA than non-EA eyes (all p < 0.05, independent Student t-tests). The lower lid sloped less and tilted less in EA than non-EA eyes (both p < 0.05, independent Student t-tests) (Table 2-4).

Eyelid feature	East Asians	Non-East Asians	Difference	Significance (Independent Student t-test)
Horizontal palpebral fissure width (mm)	26.35 ± 1.50	27.75 ± 1.90	−1.40	$p = 0.002$*
Vertical palpebral fissure height (mm)	8.97 ± 0.94	9.98 ± 1.14	−1.00	$p < 0.001$*
Palpebral fissure slant (degrees)	−6.65 ± 2.88	−4.35 ± 2.75	−2.30	$p = 0.002$*
Upper eyelid position (mm) (Polynomial term C)	3.16 ± 0.77	3.92 ±0.67	−0.77	$p < 0.001$*
Upper eyelid slope (Polynomial term B)	−0.06 ± 0.05	−0.03 ± 0.05	−0.03	$p = 0.049$*
Upper eyelid curvature (Polynomial term A)	−0.03 ± 0.01	−0.04 ± 0.01	0.01	$p = 0.001$*
Upper eyelid angle (degrees)	−4.23 ± 3.05	−2.95 ± 3.27	−1.27	$p = 0.113$
Lower eyelid position (mm) (Polynomial term C)	−5.85 ± 0.58	−6.09 ± 0.73	0.24	$p = 0.147$
Lower eyelid slope (Polynomial term B)	0.02 ± 0.06	0.05 ± 0.05	−0.03	$p = 0.023$*
Lower eyelid curvature (Polynomial term A)	0.02 ± 0.01	0.02 ± 0.01	0.00	$p = 0.995$
Lower eyelid angle (degrees)	1.57 ± 3.14	3.53 ± 3.19	−1.96	$p = 0.016$*

Table 2-4. Eyelid morphometry measurements (mean ± SD) and their difference between East and non-East Asians (East Asian minus non-East Asian). Any p-value flagged with an asterisk indicates statistically significant difference between the two groups.

2.3.5 Interaction between eyelid morphometry and corneal parameters

2.3.5.1 Eyelid morphometry feature interaction with corneal vector components

Considering all the corneal vector components (M, J_{180}, J_{45}) significant interactions were found between horizontal palpebral fissure width (HPFW) and the corneal vector components (MANOVA: F = 3.573, p = 0.019). However, the interaction was not different between the ethnic groups (F = 2.256, p = 0.091). Upon performing individual correlations, HPFW was significantly correlated with corneal spherical equivalent power M (r = −0.369, p = 0.003, Figure 2-11), which suggests that eyes which have larger HPFW tend to have flatter corneas. Further, HPFW did not show any association with corneal J_{180} (r = 0.009, p = 0.947) or J_{45} (r = −0.198, p = 0.116).

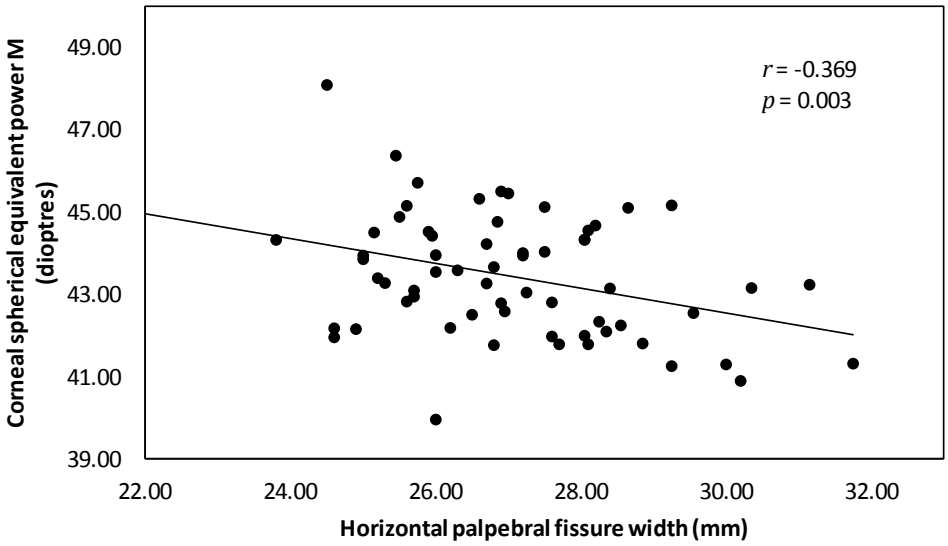

Figure 2-11. The relationship between horizontal palpebral fissure width (HPFW) in all participants measured using i-Metrics software and corneal spherical equivalent power M, determined from corneal topography. Note that the cornea tends to become flatter with increasing HPFW.

Upper eyelid curvature also significantly interacted with corneal vector components (MANOVA: F = 7.657, p < 0.001) and the association was significantly different between the two ethnic groups (MANOVA: F = 5.029, p = 0.004). In the entire study population there was a significant correlation between upper eyelid curvature and corneal spherical equivalent power M (r = −0.377, p = 0.002). From individual correlations, EA upper lid curvature did not show correlation with corneal spherical equivalent power M (r = 0.093, p = 0.611, Figure 2-12), but non-EA eyes showed significant correlation (r = 0.691, p < 0.001) which indicates that eyes with more curved upper eyelids tend to have steeper corneas in non-EA eyes but not in EA eyes. Further, individual associations did not reveal significant correlation between upper eyelid curvature and corneal J_{180} (r = 0.133, p = 0.296) and corneal J_{45} (r = −0.042, p = 0.744) in the entire study population.

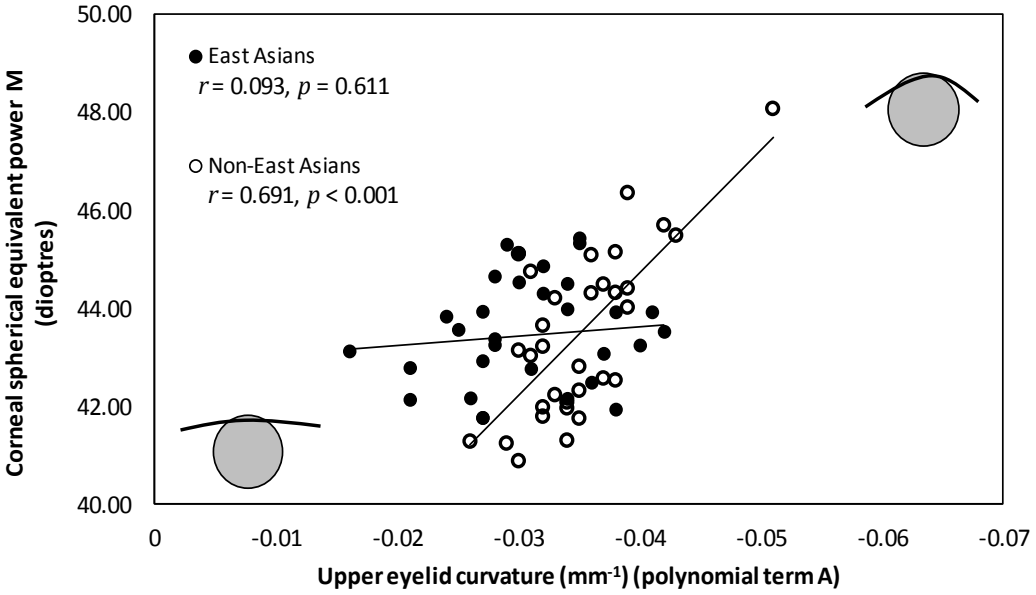

Figure 2-12. The relationship between the upper eyelid curvature and corneal spherical equivalent power. Steeper upper eyelids are associated with steeper corneas. A difference between the East and non-East Asian eyes in the relationship can be noted.

Lower eyelid slope showed significant interaction with the corneal vector components (MANOVA: F = 2.776, p = 0.049), however the association was not significantly different between the ethnic groups (MANOVA: F = 0.883, p = 0.455). Individual associations revealed significant correlation of lower eyelid slope with corneal J_{45} (r = 0.262, p = 0.037, Figure 2-13) but no correlation was found with corneal J_{180} (r = 0.223, p = 0.076) or corneal spherical equivalent power M (r = 0.112, p = 0.376). A positive corneal J_{45} indicates relatively steeper curvature along the 135 degree meridian of the cornea and vice versa for a negative corneal J_{45}. From Figure 2-13 it is apparent that a positive eyelid slope is associated with an increase in corneal oblique astigmatism, with steeper corneal curvature along 45 degrees, and a negative eyelid slope is associated with an increase in corneal oblique astigmatism with steeper corneal curvature along the 135 degree meridian.

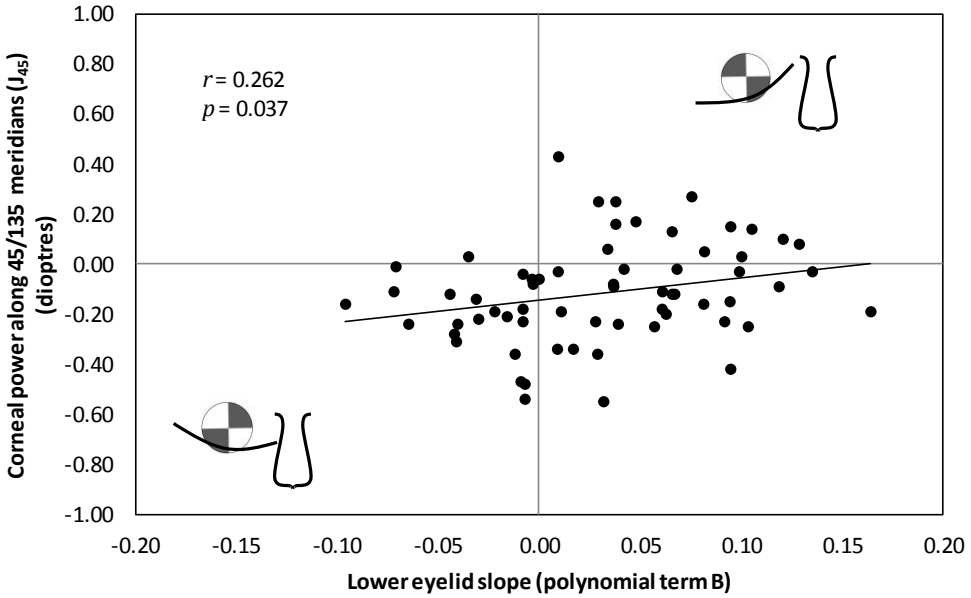

Figure 2-13. The relationship between the lower eyelid slope and corneal power along 45/135 meridians. The steeper corneal meridians are indicated in shaded areas in the insets. Note that a negative eyelid slope is associated with a steeper cornea along the 45 degree meridian and similarly a positive eyelid slope is associated with a steeper cornea along the 135 degree meridian of the cornea.

2.3.5.2 Eyelid morphometry feature interaction with sectorial corneal asphericity

Table 2-5 enumerates the associations between eyelid morphometry features and mean sectorial asphericity. For this MANOVA, the horizontal palpebral fissure width (HPFW), vertical palpebral fissure height, and palpebral fissure slant were considered as independent variables while the mean corneal asphericity of all the corneal sectors were considered as covariates. In order to avoid any coincidental correlations between the eyelid and unrelated corneal parameters, when the MANOVA was performed with upper eyelid measurements as the independent variables only superior corneal sectors were considered as covariates, and when the lower eyelid measurements were considered as independent variables only the inferior corneal sectors were considered as covariates.

Independent variable	Covariates	F, p-value
Horizontal palpebral fissure width (mm)	SN,S,ST,IT,I,IN	F = 0.630, p = 0.706
Vertical palpebral fissure height (mm)	SN,S,ST,IT,I,IN	F = 2.642, p = 0.025*
Palpebral fissure slant (degrees)	SN,S,ST,IT,I,IN	F = 0.515, p = 0.795
Upper eyelid position (mm) (Polynomial term C)	SN,S,ST	F = 0.615, p = 0.608
Upper eyelid slope (Polynomial term B)	SN,S,ST	F = 0.354, p = 0.786
Upper eyelid curvature (mm^{-1}) (Polynomial term A)	SN,S,ST	F = 0.647, p = 0.588
Upper eyelid angle (degrees)	SN,S,ST	F = 0.366, p = 0.778
Lower eyelid position (mm) (Polynomial term C)	IT,I,IN	F = 1.052, p = 0.377
Lower eyelid slope (Polynomial term B)	IT,I,IN	F = 2.091, p = 0.111
Lower eyelid curvature (mm^{-1}) (Polynomial term A)	IT,I,IN	F = 2.880, p = 0.044*
Lower eyelid angle (degrees)	IT,I,IN	F = 2.037, p = 0.119

Table 2-5. Interaction between eyelid morphometry features and the sectorial corneal asphericity using multivariate analysis of variance. SN = supero-nasal sector, S = superior sector, ST = supero-temporal sector, IT = infero-temporal sector, I = Inferior sector, IN = infero-nasal sector. Any *p*-value flagged with an asterisk sign indicates statistically significant interaction between each eyelid feature as an independent variable and the group of selected dependent corneal parameters.

From the interactions, although vertical palpebral fissure height showed significant interaction with mean asphericity Q values of all the corneal sectors, it failed to show any significant interaction with mean asphericity of any individual corneal sector. None of the upper eyelid morphometry features showed an interaction with the mean sectorial asphericity Q values. Among the lower eyelid features, only the lower eyelid curvature showed interaction with inferior corneal sectorial Q values.

The lower eyelid curvature showed significant interaction with the mean sectorial Q values (MANOVA: F = 2.880, p = 0.044), and there was no significant difference in the association between the ethnic groups (MANOVA: F = 1.310, p = 0.280). Individual associations revealed that the lower eyelid curvature correlated negatively with infero-nasal (r = −0.351, p = 0.004, Figure 2-14) and infero-temporal (r = −0.250, p = 0.047, Figure 2-15) sectorial mean Q values.

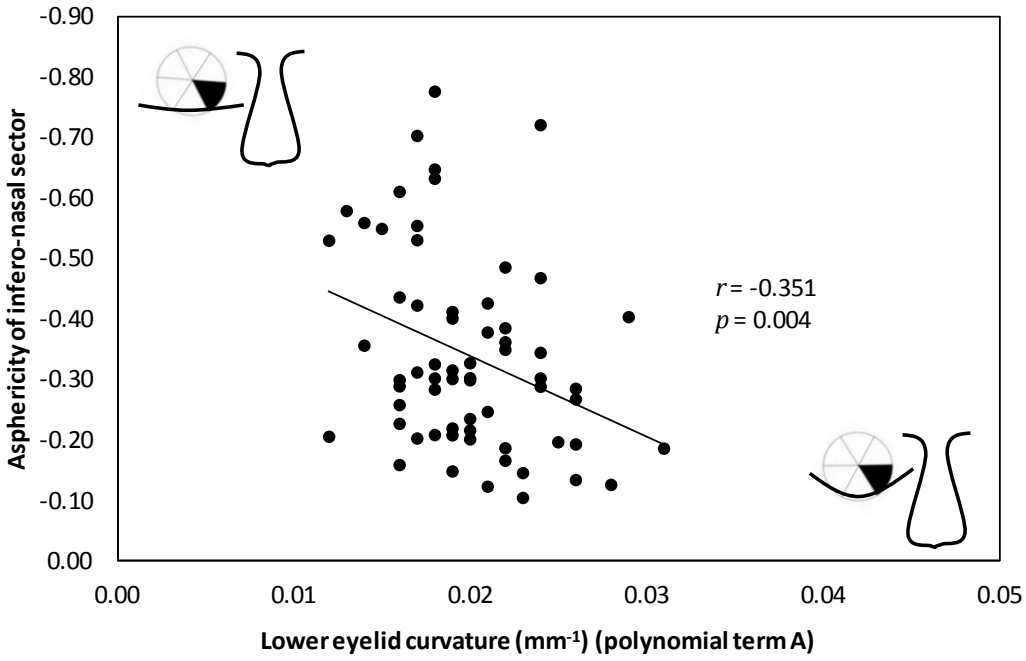

Figure 2-14. Relationship between the lower eyelid curvature and asphericity of the infero-nasal sector of the cornea in all participants.

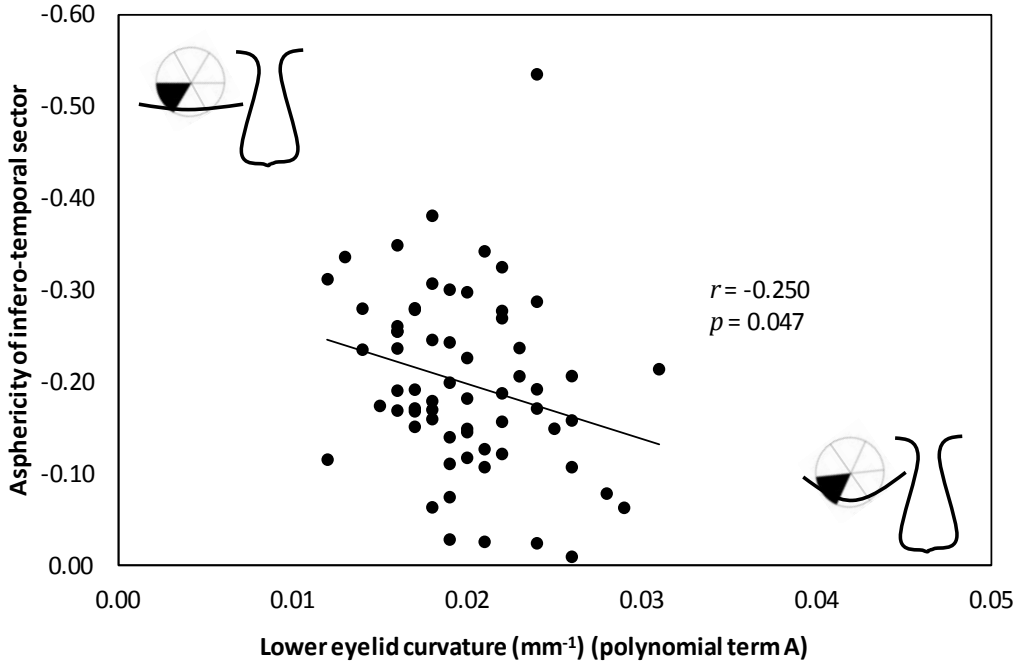

Figure 2-15. Relationship between the lower eyelid curvature and asphericity of the infero-temporal sector of the cornea in all participants.

2.4 DISCUSSION

This study has shown that for eyes with up to 1.50 dioptres of corneal toricity, the corneal shape is not uniform when investigated in terms of asphericity in different corneal sectors. Furthermore, differences in the corneal shape were observed between EA and non-EA eyes. Certain eyelid morphometry features showed significant associations with corneal parameters and, except for upper eyelid curvature, none of the eyelid morphometry features showed a difference in association between EA and non-EA eyes.

A better understanding of corneal shape variation can be obtained from the visual inspection of corneal asphericity variation along each hemi-meridional angle location. Whereas a gradual increase in asphericity was observed through the inferior meridians from temporal to nasal, the variation across the superior meridians was abrupt, with a sharp transition occurring in the superior (60 - 120°) region. Although the overall trend in the variation appeared to be the same when the data from both groups were combined, as well as when separated into different ethnicities, the sectorial analysis revealed significant differences in mean asphericity Q values between the two ethnic groups.

Considering the sectorial analysis from combining the data of both ethnicities, there was a statistically significant difference in corneal asphericity between nasal and temporal sectors revealing nasal-temporal corneal asymmetry, which indicates that the nasal cornea tends to flatten at a greater rate towards the periphery than the temporal cornea. This observation was found even after separating the data with respect to ethnicity. Similarly, there was no statistically significant difference overall in corneal asphericity between superior and inferior sectors. However, when each ethnic group was analysed separately EA eyes showed significant differences between the mean asphericity of the superior and inferior corneal sectors, revealing that the superior cornea was more prolate than the inferior cornea, although this difference was not significant in non–EA eyes. The asymmetry in eyes with limited corneal toricity may influence the dynamics of a contact lens over the cornea, particularly the centration of contact lenses. For example, Yang et al. 2005 and Hiraoka et al. (2009) quoted nasal and temporal corneal asymmetry as a possible reason for the temporal decentration of the treatment zone during overnight OK, despite failing to show any significant relationship between corneal asymmetry and lens decentration. Further, it could also be speculated that OK lenses may not only decentre temporally but also inferiorly in EA eyes due to the vertical corneal asymmetry observed in these eyes.

Others have investigated corneal shape only in certain full meridians (Kiely et al. 1984, Guillon et al. 1986) or hemi-meridians (Mandell and St Helen 1971, Sheridan and Douthwaite 1989, Zhang et al. 2011). These studies fail to give a complete picture of corneal shape as their investigation was limited to full meridians or hemi-meridians at specific angles. The current study gives a much broader view of corneal shape as it has investigated corneal shape in sectors encompassing the entire cornea over the central 8 mm zone. This detailed investigation is important to further understand contact lens dynamics over the cornea.

It makes most sense to compare the current study results to previous studies that investigated hemi-meridional corneal shape in order to describe corneal asymmetry. The results of the current study are in agreement with the outcomes of these previous studies. Mandell and St Helen (1971) described variation in hemi-meridional corneal eccentricity (e) using the corneal apex as the reference centre, with the nasal and superior corneal hemi-meridians flattening at a greater rate than the temporal and inferior cornea respectively. Sheridan and Douthwaite (1989) assessed asphericity in terms of shape factor p (Q+1) in nasal and temporal hemi-meridians by grouping participants according to refractive error to show that the nasal cornea flattened at a greater rate than the temporal cornea with respect to

geometric centre. In a more recent study of Chinese participants Zhang et al. (2011) also showed a similar trend, where the corneal asphericity in the nasal and superior hemi-meridians was more prolate than the temporal and inferior hemi-meridians respectively.

Eyelid morphometry features showed significant distinction between the two ethnicities, and are in agreement with most previous studies. The horizontal palpebral fissure width (HPFW), vertical palpebral fissure height, and upper eyelid slant are in close agreement with previous studies in similar ethnic groups (Park et al. 1990, Park et al. 2008, Kunjur et al. 2006, Price et al. 2009, Patil et al. 2011). When considering the interaction of eyelid morphometry with corneal topography, only horizontal eyelid fissure width, upper eyelid curvature, lower eyelid slope and lower eyelid curvature showed significant interaction with corneal parameters. Except for the upper eyelid curvature none of these exhibited a difference in association between the two ethnic groups.

The HPFW correlated significantly with corneal spherical equivalent power, with increasing palpebral fissure width associated with greater corneal flattening. This finding of the current study was also observed by Read et al. (2007a), who speculated that the harmony maintained between growth of anterior eye structures during development may yield such a similarity that individuals with larger horizontal palpebral fissure width are also likely to have larger corneas, and consequently flatter corneal curvature. This speculation was also supported by Denis et al. (1995) who investigated relationships between several orbito-facial measurements in foetuses to reveal positive associations between growth of the ocular structures including inter-canthal distance, horizontal palpebral fissure length and the body including the face.

In the present study, upper eyelid curvature also correlated significantly with corneal spherical equivalent power, with steepening upper eyelid curvature associated with greater corneal steepening. This finding was not found in any previous research. A possible reason for this association may lie in the previous explanation on synonymous ocular and body growth (Denis et al. 1995), whereby eyes with steeper eyelid curvatures generally tend to have steeper corneas. Although Denis et al. did not investigate eyelid curvature and corneal curvature, such inferences may be drawn from the relationships they present. However further studies studying synonymous ocular and body growth are needed to confirm this new theory.

Lower eyelid slope showed significant correlation with corneal J_{45}, which means that a positive eyelid slope was associated with greater corneal power along the 135 degree corneal

meridian and vice versa. This may be because a positively sloped lower eyelid is in close apposition with the 135 degree corneal meridian in the inferior region and a negatively sloped lower eyelid is in close apposition with the 45 degree corneal meridian. This is an important finding because pressure induced by the upper eyelid alone was previously thought to influence the corneal shape (Grosvenor 1978), but more recently it has been suggested that features of the lower eyelid are also likely to contribute to influence the shape of the cornea (Read et al. 2007a, Shaw et al. 2009). The outcomes from this current study provide evidence to support this hypothesis.

Lower eyelid curvature correlated well with the mean Q values of infero-nasal and infero-temporal sectors, which indicates that a steeper lower eyelid curvature was associated with less prolate corneal asphericity in these sectors. While this association could be coincidental, Read et al. (2007a) have shown that the influence of lower eyelid curvature over the corneal astigmatic component (J_{180}) cannot be ignored, emphasising that the lower eyelid curvature is likely to have some influence over the corneal shape. It may be that the curved lower eyelid is in close proximity with the cornea giving rise to greater pressure over these corneal locations leading to a less prolate corneal shape. No previous study thoroughly investigated the influence of lower eyelid pressure on the corneal shape leading to a potential area for further research which might give some clues on the relationship between lower eyelid curvature and variation in the corneal shape.

A key finding from the distribution of the mean hemi-meridional Q values at the corresponding angle locations is that there was a rapid change in the corneal asphericity in the superior region of the cornea. This was the case for data from all participants and also when data from each ethnic group were considered separately. The region exhibited a sharp variation from being more prolate to less prolate. It is reasonable to assume that the presence of the upper eyelid on the superior cornea would contribute to this effect, but none of the upper eyelid parameters demonstrated an association with asphericity in the superior corneal sector. Although this analysis suggests that upper eyelid morphometry features alone may not influence superior corneal shape, we did not measure upper eyelid pressure, which could have been a co-variant.

Pressure from the upper eyelid has been shown to influence corneal astigmatism (Grosvenor 1978, Wilson et al. 1982), and induce anterior corneal shape distortions during various near activities (Buehren et al. 2003, Collins et al. 2006, Shaw et al. 2008, 2009). Corneal epithelial changes due to pressure exerted from the upper eyelid were quoted as a possible

mechanism for these distortions. Although most of these previous studies have investigated corneal shape changes during near activities where the upper eyelid is positioned close to the pupil, a similar interaction could be true during primary gaze as was considered in the current study. Investigating a direct association between the upper eyelid pressure in primary gaze and corneal asphericity change in this region may yield positive correlations.

It should also be considered that the position of the upper eyelid may indirectly account for the presence of eyelid pressure. However, Shaw et al. (2009) suggested that there may be individual variations in the extent of eyelid pressure as well as biomechanical properties of the cornea, therefore the presence of the eyelid alone may not explain the variation in asphericity in this region. Based on these previous studies, if one concludes that the corneal shape change in the superior region is a consequence of upper eyelid pressure, the retention of variation in corneal shape across the superior region despite the eyelids being retracted during topography capture in the current study needs further explanation. A previous study investigating the recovery of corneal shape after overnight OK has shown that the cornea responds to the OK lens rapidly but takes a longer time to regain its original shape (Wu et al. 2009). This observation may appropriately explain the retention of altered corneal shape even after the elimination of eyelid pressure by manual retraction during topography capture.

A possible limitation of the current study is that the corneal asphericity was limited to the central corneal zone with a diameter of 8 mm. The remaining nearly 2 to 2.5 mm corneal annular zone was not considered in the shape determination, potentially losing any interaction that may otherwise have been detected if that zone was included in the study. Present Placido-based topography systems limit their ability to capture the corneal surface approximately to a diameter of 9 mm horizontally and 7.5 mm vertically. By developing a software algorithm that allowed one to combine central and peripheral cornea, Franklin et al. (2006) were successful in representing an average of 11.3 mm of the cornea horizontally and 10.3 mm vertically. However, the procedure was tedious and computationally intensive. The current study did not deviate from its main aim which was to investigate any shape differences within the cornea and also between ethnic groups. The purpose to investigate the interaction of eyelids with corneal shape was secondary and therefore an attempt to capture a larger corneal area was not made.

Another possible shortcoming of this study is that corneal topography was centred to vertex normal (along the VK axis). When investigating corneal shape, the corneal apex

denoting shortest radius of curvature on tangential curvature maps is an ideal reference centre (Mandell et al. 1995). In their study, Mandell et al. (1995) showed that the distance between the corneal apex and the vertex normal averaged 0.62 ± 0.23 mm. Since the asphericity Q value was derived by mirroring the hemi-meridional corneal data centred to the vertex normal, the greater the distance between the apex and the vertex normal the greater would be the discrepancy in the determined hemi-meridional Q value.

2.5 CONCLUSIONS

This study provided an overview of corneal shape in terms of its sectorial variation in asphericity, specifically showing a sudden variation in the asphericity in the superior corneal region in all participants and also when the subject group was separated by ethnicity. There was a significant nasal versus temporal corneal asymmetry irrespective of ethnicity. In EA eyes, asymmetry was also noticed in the vertical sectors. Whether the decentration of OK lenses towards a temporal direction during OK as noticed in previous studies is because of this corneal asymmetry will be investigated in the following chapter. It also appears that the decentration may be slightly different between EAs and non-EAs considering the differences found in the sectorial corneal shape and also in eyelid shape.

CHAPTER 3 BASELINE CORNEAL SHAPE AND ITS EFFECT ON TREATMENT ZONE CENTRATION DURING SPHERICAL ORTHOKERATOLOGY

3.1 INTRODUCTION

In chapter 2, significant sectorial variations in corneal shape were found in eyes with less than 1.50 DC of corneal toricity. Specifically, the study revealed that the temporal cornea tends to be less prolate than the nasal cornea. This asymmetry in corneal shape may contribute to lens decentration during orthokeratology (OK). This may further be supported from findings of previous studies which reported temporal decentration of OK lenses leading to temporal treatment zone (TZ) decentration in myopic OK (Yang et al. 2005, Hiraoka et al. 2009) as well as hyperopic OK (Gifford and Swarbrick 2008). The authors have cited nasal versus temporal corneal asymmetry prior to lens wear as a possible cause for driving OK lenses towards a temporal direction. However, these studies have not investigated the relationship between the baseline corneal shape and subsequent lens decentration.

During overnight OK for myopia, the OK lens reshapes the cornea by inducing central flattening and para-central steepening. The central flattened zone reduces the converging power of the eye resulting in the correction of myopic refractive error. In previous studies the central flattened zone as observed on axial or tangential power maps has been defined as the treatment zone (Owens et al. 2004, Hiraoka et al. 2009), while others have considered both the central flattened zone and surrounding para-central steepened zone as equally important components of the TZ (Lu et al. 2007b). This could be because, depending on pupil diameter, the para-central steepened zone may interfere with paraxial vision. The ideal OK outcome is to induce central flattening across the whole pupillary area. However, decentration of the TZ, or pupil diameter being greater than the area of central flattening, could lead to the para-central steepening falling in the pupillary area resulting in poor visual outcomes due to induction of unwanted ocular aberrations (Berntsen et al. 2005, Hiraoka et al. 2005, Hiraoka et al. 2008). Furthermore, it has been recently speculated that OK-induced para-central corneal steepening may instead be beneficial in influencing off-axis refraction, which has been implicated as a method for controlling the progression of myopia (Kakita et al. 2011, Kang and Swarbrick 2011).

Previous studies have used different methods to determine TZ diameter and centration. A review of these methods and their limitations is given in Section 1.8 and presented in Table 1-5. In summary, it can be concluded from these studies that most of these methods displayed corneal topography difference maps on the computer monitor from which the TZ diameter or centration was identified. Among these methods, Hiraoka et al. (2009) used a sensible method, where 16 points of equi-refractive power (the exact power was not defined) were identified on the post-OK wear tangential curvature maps. The centre of the best-fit ellipse fitted to the 16 TZ edge points was regarded as the centre of the TZ, but the manual identification of the edge points may have given rise to error in determining the TZ decentration.

The purpose of this study was to establish a method to precisely determine TZ parameters and to analyse the effect of baseline corneal shape on these parameters over a 2 week period of overnight myopic OK lens wear.

3.2 MATERIALS AND METHODS

3.2.1 Original study design

The study data were obtained retrospectively from two previously conducted studies.

- Study 1: A total of 11 participants (age range 20 to 39 years; 6 females and 5 males) were fitted with OK lenses in both eyes with two different materials, randomly assigned to each eye. The clinical response to OK treatment in one eye fitted with Boston EO (nominal Dk = 58 ISO units) material was compared with the response in the opposite eye wearing Boston XO (nominal Dk = 100 ISO units; Polymer Technology Corporation, Wilmington, MA). The study outcomes are reported elsewhere (Lum and Swarbrick 2011).
- Study 2: A total of 10 participants (age range 23 to 40 years, 6 females and 4 males) were fitted with OK lenses in both eyes with two different materials randomly assigned to each eye. The clinical response to OK treatment in one eye fitted with Boston XO2 (nominal Dk = 141 ISO units; Polymer Technology Corporation) material was compared with the response in the opposite eye wearing Boston XO (unpublished data).

Both studies followed an identical lens wearing and study measurement protocol. Approval from the UNSW Human Research Ethics Advisory (HREA) panel had been received for both studies (Approval Nos Study 1: 06171 and Study 2: 11032) and the conduct of the studies

followed the tenets of the Declaration of Helsinki. Informed written consent was obtained from all subjects before study enrolment. A screening visit was conducted prior to enrolment to ensure subjects had good ocular health, with less than −4.50 D of myopia associated with corneal toricity ≤ 1.50 DC.

3.2.1.1 Contact lenses

All subjects were assigned to wear BE OK lenses (Capricornia Contact Lens, Queensland, Australia) manufactured in Boston XO material (Bausch & Lomb Boston, Wilmington, MA, USA; nominal central thickness 0.22 mm resulting in nominal Dk/t values of 46 ISO units) in one eye chosen at random on an overnight schedule for two weeks. The same lens design was fitted to the fellow eye but manufactured in different materials. The total lens diameter of the lenses was 11 mm and the optic zone diameter was 6 mm. BE lens fitting software was used to determine the trial lenses to be fitted, with overnight lens wearing trials conducted until an acceptable fitting was established.

Study lenses were dispensed with full instructions on insertion and removal. Boston Advance Cleaner, Boston Advance Conditioning Solution and Bausch & Lomb Sensitive Eyes Saline Solution (Bausch & Lomb Australia, Sydney, Australia) were issued for lens care. Subjects were instructed to insert the lenses prior to sleep, and remove them on waking after approximately 8 hours of sleep unless attending a scheduled study visit in which case they were asked to attend while still wearing the lenses. At morning study visits the lenses were removed by the research optometrist.

3.2.1.2 Study measurements

Study measurements were taken in the morning and again 7 hours after the morning visits.

Refraction: Non-cycloplegic objective and subjective refractions were performed.

Corneal topography: The Medmont E300 corneal topographer (Medmont Studio 4 software version 4.14.1.1, Medmont International Pty Ltd, Victoria, Australia) was used to obtain topographic data.

Ocular health: Clinical slit lamp biomicroscopy was used to monitor corneal health and integrity at each measurement session. Corneal integrity was assessed with topical application of sodium fluorescein dye.

Corneal thickness: The Holden-Payor optical pachometer was used to measure the central corneal thickness.

3.2.2 Present study analysis

From the combined data set 21 adult myopes with no prior experience of rigid lens wear were enrolled (age range 18 to 40 years; 12 females and 9 males). The data retrieved from Boston XO lens wearing eyes from both studies were combined and regarded as a single data set for this retrospective analysis. Measurement data were retrieved from baseline, after one overnight (day 1, morning visit), and after 14 days overnight (day 14, morning visit) OK lens wear, within 1.20 ± 1.48 hours after lens removal in the morning. Only study 1 data on the clinical outcomes of lens materials have been previously published (Lum and Swarbrick 2011). The current analysis related to treatment zone centration has not been previously published from either of the above-mentioned studies.

3.2.2.1 Study variables retrieved from the original study data

Refraction: The subjective refraction values collected were converted to power vectors refractive M, refractive J_{180} and refractive J_{45} using formulae derived by Thibos et al. (1997) where refractive M is the mean spherical equivalent error, J_{180} is the horizontal/vertical astigmatic component and J_{45} is the oblique astigmatic component.

Corneal topography: The raw data from the Medmont E300 corneal topographer (Medmont Studio 4 software version 4.14.1.1, Medmont International Pty Ltd, Victoria, Australia) were exported and further analysed using customised MATLAB programs. Corneal topography variables such as apical corneal curvature (R_o), steep K, flat K and their angles were also retrieved from the topographer. These variables were also converted into the vector forms to give corneal M, corneal J_{180} and corneal J_{45}.

3.2.2.2 Sectorial corneal asphericity (Q) determination

The method described in Section 2.2.4 for calculating the mean asphericity (Q) in six pre-defined corneal sectors was used for this analysis. From the visual analysis of the raw topographic data obtained in studies 1 and 2 it was apparent that for some maps the interference from the upper eyelid and lashes had restricted the range of accurate data capture in the superior quadrant. In the analysis described in Chapter 2, the sagittal height values were extrapolated to 4 mm semi-chord length (8 mm chord diameter) and a 4^{th} order polynomial was used to determine hemi-meridional Q values. Using the same method to extrapolate corneal topography height data in the current data set led to an increased mean fit

error of 14 μm. Therefore, it was decided to only extrapolate topography data to a smaller hemi-meridional radius to 3 mm (6 mm chord diameter), which minimised the highest mean fit error to a more acceptable limit of 2.1 μm.

3.2.2.3 Determination of treatment zone parameters

A MATLAB (The MathWorks, Inc. Version 7.12) algorithm was developed to subtract baseline refractive power values at each hemi-meridian from post-lens wearing values (Appendix B). Refractive power was calculated using the following formula described by Klein (1992):

$$P_R = \frac{n'}{z + \frac{x}{\tan(\theta_i - \theta_t)}}$$

where n' is the keratometric refractive index (1.3375), z is the sagittal height extracted from the Medmont E300 elevation data, x is the radial distance from the vertex normal, θ_i is the incident angle and θ_t is the refracted angle. The measurement values along each hemi-meridian of the difference map data were then assessed from the corneal vertex towards the periphery to determine the edge of the TZ, where the smallest positive value (ideally zero) was considered as the edge of the TZ for that hemi-meridian. A best-fit ellipse was fitted to all TZ edge points, with the centre of the ellipse denoting the TZ centre (Figure 3-1). The decentration of the TZ centre from the vertex normal was calculated from simple trigonometric formulae. Further the horizontal TZ diameter was defined as the distance between two ends of the ellipse measured horizontally.

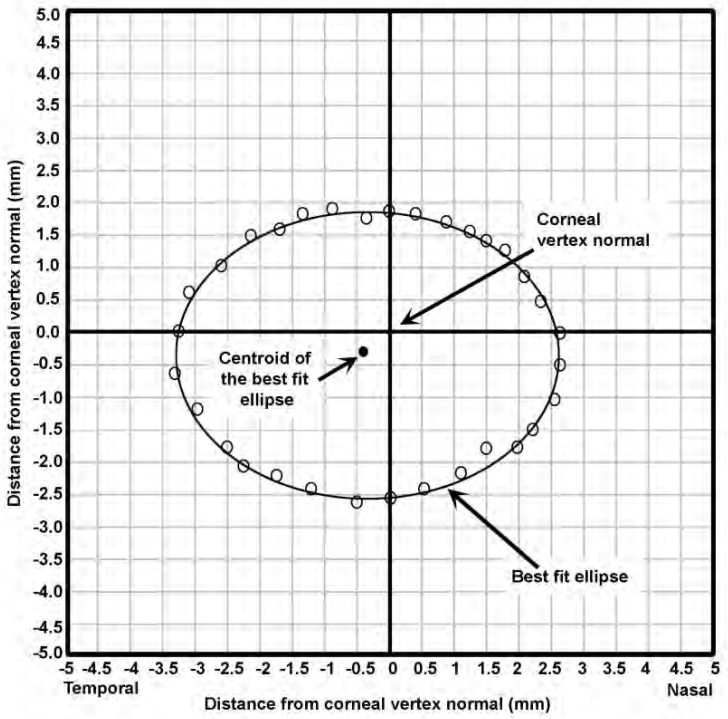

Figure 3-1. A diagrammatic illustration of determining treatment zone (TZ) decentration. The empty circles represent locations closest to zero refractive power change after OK lens wear. The best-fit ellipse and its centroid with respect to vertex normal are shown.

To determine the direction of TZ decentration, the Cartesian co-ordinates (x, y) of the decentration were transformed to polar format (angle of orientation, radial distance magnitude). The angle of orientation was represented in one full rotation (0 to 360 degrees) beginning from the positive x-axis leading in a counter-clockwise direction. Further, the angles of TZ orientation were categorised into sectors using the same method as was used to represent mean sectoral asphericity whose orientation was represented by the median angle. For example, if the TZ angle is 50 degrees then this will fall into the category of supero-nasal sector (range 0 to 60 degrees) represented by a median angle of 30 degrees.

3.2.3 Statistical analysis

All statistical analyses were performed using IBM SPSS version 20 (SPSS Inc, Chicago, IL, USA). To aid analysis, the left eye corneal topographic data were reversed along the vertical axis such that the analyses were made considering all eyes as right eyes. Repeated measures analysis of variance (RM-ANOVA) with protected post-hoc t-tests with Bonferroni correction was used to determine changes in the corneal and refractive parameters over time. RM-ANOVA was used when subjects from a random sample were measured under a number of different test conditions over different time points. RM-ANOVA suffers the same limitations

as any ANOVA. Mauchly's test was used to test for asphericity, and if the test showed any violation of the assumption of asphericity, the Greenhouse-Geisser correction was used. The reasons for performing these tests have been described in Section 2.2.9. Bonferroni correction is an adjustment made for the p-value when several comparisons are made simultaneously in a given data set.

The variation in sectorial asphericity (Q) at baseline and TZ parameters over time were analysed using a random intercept model of linear mixed model analysis. The test was called mixed model analysis because it incorporated both fixed and random effects giving rise to the mixed model design. An effect in a scientific study would be considered as fixed if all possible treatment exposures were present in the study. In contrast an effect would be referred to as random if the investigator chooses all possible exposures at random in the study. The Q value or amount of TZ decentration was set as a dependent variable and sector location or day of visit as fixed factors respectively. The Intercept that was derived from the relationship between variables was regarded as a random effect in this model. To investigate the nasal versus temporal corneal asymmetry, the mean of all hemi-meridional Q values of the two nasal sectors (supero-nasal and infero-nasal sectors combined) was compared with the mean of all hemi-meridional Q values of the two temporal sectors (supero-temporal and infero-temporal sectors combined) by independent sample t-test.

Shapiro-Wilk's test was used to check the normality of the baseline refractive, corneal and TZ parameters. Pearson's correlations or Spearman's rank correlations were used according to the normality of data to relate baseline corneal shape parameters with the TZ parameters. To investigate the relationship between baseline sectorial corneal asphericity and TZ parameters, each corneal sector was denoted by the median of angle range over which the sector was spread. For example the supero-nasal sector (0 - 60 degrees) was denoted by angle 30 and the superior sector (61 - 120) was denoted by angle 90. The remaining sectors were designated in the same manner. The median angle of the sector to which the TZ was decentred was correlated with the median angles of least and most prolate corneal sectors using Spearman's rank correlation. Discussion regarding most of these statistical tests was provided in Section 2.2.9. A critical p-value of 0.05 was used to represent statistical significance.

Relationships were established between baseline corneal shape and TZ decentration parameters. The baseline parameters included were corneal R_o; corneal M, J_{180} and J_{45}; steep and flat K; and least and most prolate corneal sectors. The TZ parameters included from the

post-treatment visits were the horizontal TZ diameter and the amount and direction of TZ decentration.

3.3 RESULTS

Table 3-1 gives the descriptive data of refractive and corneal variables at baseline, day 1 and day 14 visits. There was a significant change in refractive M over time (F = 186.583 $_{(2, 40)}$, p < 0.001). There was a significant reduction in refractive M from baseline to day 1 (−1.52 ± 0.51 D, p < 0.001) and further reduction by day 14 (−2.70 ± 0.66 D, p < 0.001). There was no statistically significant change in the refractive J_{180} or refractive J_{45} over time (both p > 0.05).

Variable (dioptres)	Baseline	Day 1	Day 14	RM-ANOVA (F, p-value)
Refractive variables				
Refractive M	−2.63 ± 0.99	−1.11 ± 0.93	0.07 ± 0.48	F = 186.583, p < 0.001
Refractive J_{180}	−0.10 ± 0.19	−0.11 ± 0.20	−0.09 ± 0.20	F = 0.180, p = 0.836
Refractive J_{45}	0.01 ± 0.15	−0.01 ± 0.15	0.02 ± 0.13	F = 0.709, p = 0.498
Corneal variables				
Corneal M	44.81 ± 1.30	42.92 ± 1.23	42.12 ± 1.27	F = 156.922, p < 0.001
Corneal J_{180}	−0.28 ± 0.34	−0.29 ± 0.42	−0.28 ± 0.28	F = 0.019, p = 0.981
Corneal J_{45}	0.01 ± 0.21	0.09 ± 0.23	−0.04 ± 0.22	F = 3.695, p = 0.034
steep K	44.25 ± 1.37	43.39 ± 1.30	42.50 ± 1.38	F = 125.658, p < 0.001
flat K	43.37 ± 1.31	42.46 ± 1.24	41.73 ± 1.20	F = 123.779, p < 0.001
Corneal toricity	0.88 ± 0.38	0.93 ± 0.63	0.77 ± 0.47	F = 0.537, p = 0.257

Table 3-1. Mean ± SD of corneal and refractive variables at baseline, day 1 and day 14 visits. The degrees of freedom for all F values were 2 and 40.

The targeted refractive correction was set as the baseline refractive M, and the achieved correction at each post treatment visit was determined by subtracting post-wear refractive M from baseline refractive M. There was no correlation between the targeted and achieved correction at day 1 (r = 0.377, p = 0.092), but a significant positive correlation was reached at day 14 (r = 0.912, p < 0.001, Figure 3-2) suggesting that targeted refractive correction was achieved by day 14.

There was a significant change in corneal M over time (F = 132.545 $_{(2, 40)}$, p < 0.001). There was a significant reduction in corneal M from baseline to day 1 (1.16 ± 0.63 D, p < 0.001) and further reduction by day 14 (2.34 ± 0.63 D, p < 0.001). There was no statistically significant change in the corneal J_{180} (F = 0.019 $_{(2, 40)}$, p = 0.981) but corneal J_{45} showed significant change over time (F = 3.695 $_{(2, 40)}$, p = 0.034).

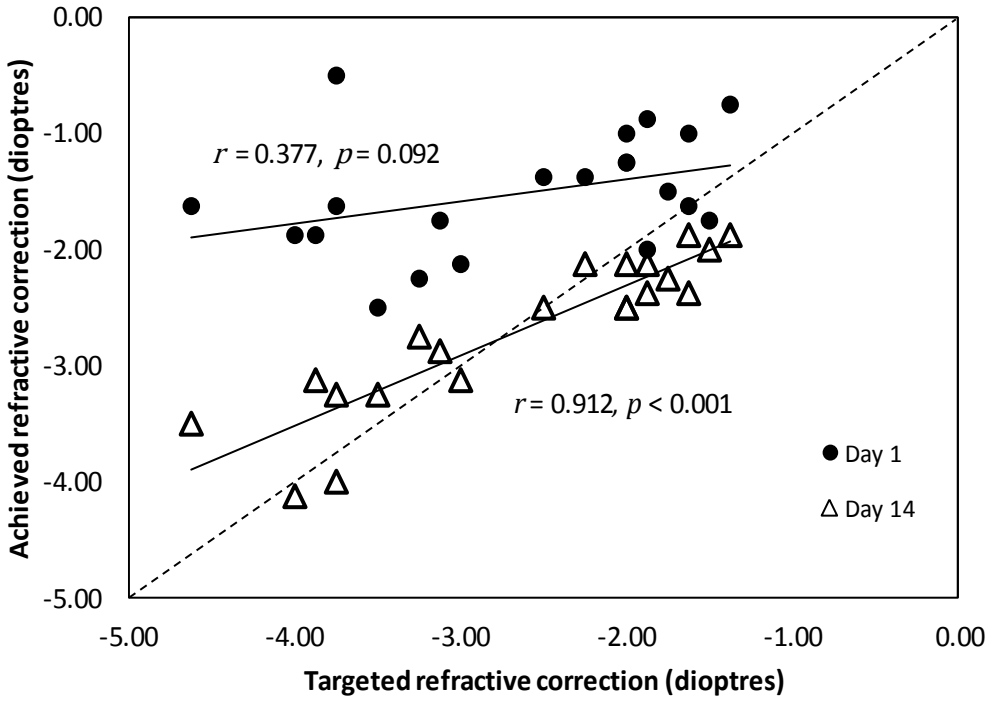

Figure 3-2. Relationship between targeted refractive correction and correction achieved at day 1 and day 14. The dotted line represents the 1:1 line.

Both steep K (F = 125.658 $_{(2, 40)}$, p < 0.001) and flat K (F = 123.779 $_{(2, 40)}$, p < 0.001) showed a significant change over time. steep K showed significant flattening from baseline to day 1 (0.86 ± 0.42 D, p < 0.001), with further flattening at day 14 (1.75 ± 0.60 D, p < 0.001). There was significant flattening in flat K from baseline at day 1 (0.91 ± 0.44 D, p < 0.001), with further flattening at day 14 (1.64 ± 0.52 D, p < 0.001).

3.3.1 Sectorial corneal asphericity at baseline

Asphericity Q values for each sector are presented in Figure 3-2. The mean corneal asphericity Q values at baseline were significantly different between the sectors (F = 247.356, p < 0.001). The inferior sector was least prolate (−0.10 ± 0.01) and the supero-nasal sector was most prolate (−0.24 ± 0.02). The mean asphericity of the nasal cornea (supero-nasal and infero-nasal sectors combined) was −0.19 ± 0.05 and the mean asphericity of the temporal cornea (supero-temporal and infero-temporal sectors combined) was −0.13 ± 0.01. The difference between the nasal and temporal cornea was statistically significant (−0.07 ± 0.04, p < 0.001), revealing that the nasal cornea flattened towards the periphery at a greater rate than the temporal cornea. A significant difference in the mean corneal asphericity was also noted between superior and inferior corneal sectors (−0.09 ± 0.16, p < 0.001), indicating that the superior corneal sector flattened at a greater rate than the inferior sector.

	Supero-nasal	Superior	Supero-temporal	Infero-temporal	Inferior	Infero-nasal
Baseline sectorial corneal asphericity (Q)	−0.24 ± 0.01	−0.19 ± 0.03	−0.14 ± 0.01	−0.12 ± 0.01	−0.10 ± 0.01	−0.15 ± 0.03

Table 3-2. Mean ± SD of the asphericity Q values in different sectors at baseline.

3.3.2 Treatment zone variables

3.3.2.1 Treatment zone diameter

A significant change in the horizontal TZ diameter was noted over time ($F = 1787.023_{(2, 19)}$, p < 0.001). Mean horizontal TZ diameter measured 4.62 ± 0.48 mm after a single overnight lens wear and increased by 0.62 ± 0.55 mm to 5.24 ± 0.45 mm after 14 nights of lens wear (p < 0.001) (Table 3-3).

	Horizontal TZ diameter (mm)	Polar decentration (mm)	X decentration (mm)	Y decentration (mm)
Day 1	4.62 ± 0.48 (3.67 to 5.41)	0.44 ± 0.25 (0.06 to 0.90)	−0.35 ± 0.27 (0.08 to −0.75)	0.01 ± 0.25 (0.36 to −0.55)
Day 14	5.24 ± 0.45 (4.38 to 5.96)	0.62 ± 0.27 (0.10 to 1.16)	−0.41 ± 0.37 (0.35 to −1.06)	−0.12 ± 0.38 (0.41 to −1.11)
p - value	p < 0.001*	p < 0.001*	p < 0.001 *	p = 0.141

Table 3-3. Mean ± SD and range of the treatment zone (TZ) parameters at day 1 and day 14. The polar decentration magnitude, its angle and X and Y decentration magnitude are relative to vertex normal. Statistically significant difference in the TZ parameter over time is indicated by '*'.

3.3.2.2 Treatment zone decentration

The mean polar decentration of the TZ centre from the corneal vertex normal was significantly different over time (F = 61.802$_{(2,\ 40),}$ p < 0.001). Mean TZ decentration was 0.44 ± 0.25 mm after a single overnight lens wear and increased by 0.18 ± 0.27 mm to 0.62 ± 0.27 mm after 14 nights of lens wear (p < 0.001). The TZ decentration directions of all 21 eyes at day 1 and day 14 are summarised in Table 3-4 and presented in Figure 3-3.

Sector of treatment zone decentration	**Day 1**	**Day 14**
	Number of eyes (%)	
Supero-nasal	1 (5%)	0 (0%)
Superior	3 (14%)	3 (14%)
Supero-temporal	8 (38%)	4 (19%)
Infero-temporal	8 (38%)	10 (48%)
Inferior	1 (5%)	3 (14%)
Infero-nasal	0 (0%)	1 (5%)

Table 3-4. Direction of treatment zone decentration at day 1 and day 14 visits, presented as number of eyes (percentage).

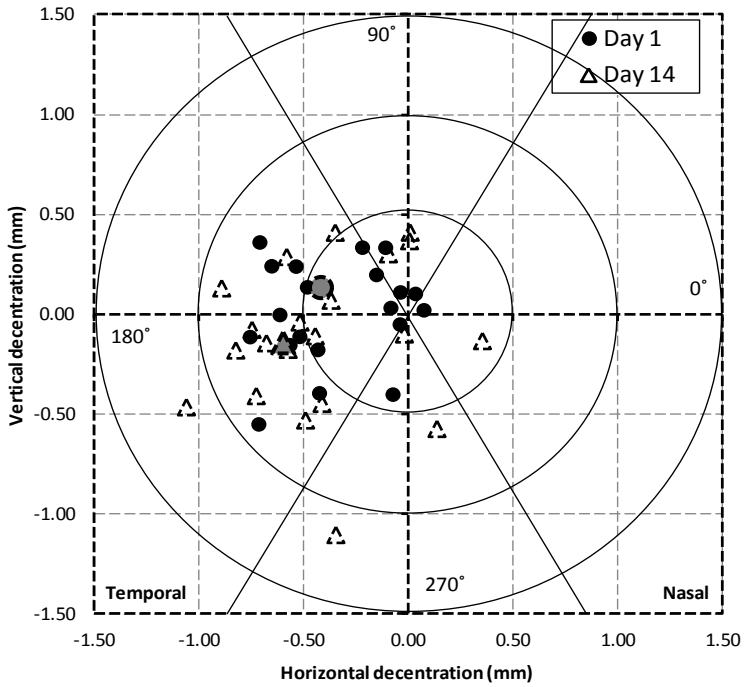

Figure 3-3. Decentration of treatment zone (TZ) from the vertex normal in 21 eyes at two post-wear visits. The larger grey circle and triangle represent the mean amount and direction of TZ decentration at day 1 and day 14 respectively.

The distribution of number of eyes and percentage showing TZ decentration direction towards a specific sector is given in Table 3-4. From the table it is evident that at day 1, vertically most eyes (57%, confidence interval CI = 36% to 78%) exhibited superior decentration, and horizontally 76% (CI = 58% to 94%) of eyes exhibited temporal decentration. By day 14, both vertically and horizontally most eyes (67%, CI = 46% to 87%) exhibited inferior decentration and temporal decentration.

3.3.3 Correlation between baseline corneal parameters and TZ parameters

3.3.3.1 Corneal parameters and TZ parameter correlations

Among corneal parameters (excluding sectorial corneal asphericity), only the angle of the steep K meridian revealed significant correlation to TZ parameters at day 1. The remaining baseline corneal parameters showed no significant correlations with TZ parameters at either post-wear visit (Table 3-5).

	Day 1		Day 14	
Baseline corneal parameters	Treatment zone magnitude (mm)			
	r	p-value	r	p-value
Corneal R_o (D)	−0.266	0.252	−0.152	0.512
Corneal M (D)	−0.167	0.470	−0.070	0.764
Corneal J_{180} (D)	−0.221	0.337	0.027	0.909
Corneal J_{45} (D)	0.084	0.781	−0.360	0.109
Corneal toricity (DC)	−0.303	0.190	0.144	0.533
steep K (D)	−0.327	0.149	−0.109	0.639
flat K (D)	−0.240	0.295	−0.153	0.509
	Treatment zone decentration direction (polar angle in degrees)			
steep K angle (degrees)	−0.435	0.049*	−0.424	0.056
flat K angle (degrees)	0.075	0.748	0.414	0.058
	Treatment zone diameter (mm)			
Corneal M (D)	−0.082	0.724	−0.298	0.189
Corneal R_o (D)	−0.067	0.772	−0.280	0.219

Table 3-5. Relationships between baseline corneal parameters and treatment zone amount, direction and diameter at day 1 and day 14 visits. A statistically significant correlation ($p < 0.05$) is indicated by '*'.

3.3.3.2 Sectorial corneal asphericity and TZ parameter correlations

Table 3-6 presents participant-wise least and most prolate corneal sectors at baseline and the sector to which the TZ was decentred at day 1. There was a significant negative correlation between the angles of the most prolate corneal sector and the angles of the sector to which the TZ was decentred at day 1 (r = −0.478, p = 0.028), but not at day 14 (r = −0.309, p = 0.172), indicating that the direction of TZ decentration was away from the direction of the most prolate corneal sector at day 1. Furthermore, at day 1 there was no significant correlation between the angles of least prolate corneal sector and the angles of the sector to which the TZ was decentred (r = 0.035, p = 0.882); however there was a moderately positive and statistically significant correlation (r = 0.498, p = 0.022) at day 14.

.

Participant number	Least prolate corneal sector at baseline	Sector median angle (degrees)	Most prolate corneal sector at baseline	Sector median angle (degrees)	Sector of treatment zone decentration at day 1	Sector median angle (degrees)	Sector of treatment zone decentration at day 14	Sector median angle (degrees)
1	IN	330	IT	210	S	90	S	90
2	I	270	IN	330	S	90	IT	210
3	IT	210	IN	330	IT	210	IT	210
4	IN	330	ST	150	I	270	I	270
5	I	270	S	90	ST	150	IT	210
6	ST	150	SN	30	ST	150	IT	210
7	IT	210	I	270	ST	150	ST	150
8	ST	150	IN	330	ST	150	ST	150
9	I	270	S	90	IT	210	IT	210
10	ST	150	IN	330	ST	150	S	90
11	IT	210	SN	30	IT	210	IT	210
12	IT	210	SN	30	IT	210	IT	210
13	IT	210	SN	30	ST	150	IT	210
14	I	270	SN	30	IT	210	IT	210
15	I	270	SN	30	IT	210	ST	150
16	I	270	SN	30	IT	210	IT	210
17	I	270	SN	30	IT	210	I	270
18	IT	210	S	90	ST	150	ST	150
19	S	90	IT	210	ST	150	S	90
20	I	270	ST	150	SN	30	IN	330
21	IN	330	IT	210	S	90	I	270

Table 3-6. Participant-wise corneal least and most prolate corneal sectors at baseline and the sector to which the treatment zone decentred at day 1. SN = supero-nasal, S = superior, ST = supero-temporal, IT = infero-temporal, I = inferior and IN = infero-nasal.

3.3.3.3 Refractive correction and TZ parameter correlations

There was no significant correlation between the amount of achieved correction and the amount of TZ decentration at day 1 (r = 0.166, p = 0.473), but there was a significant negative correlation at day 14 (r = −0.446, p = 0.043) indicating either that greater correction was achieved in eyes that exhibited less TZ decentration, or that lenses fitted to achieve greater correction tended to decentre less (Figure 3-4).

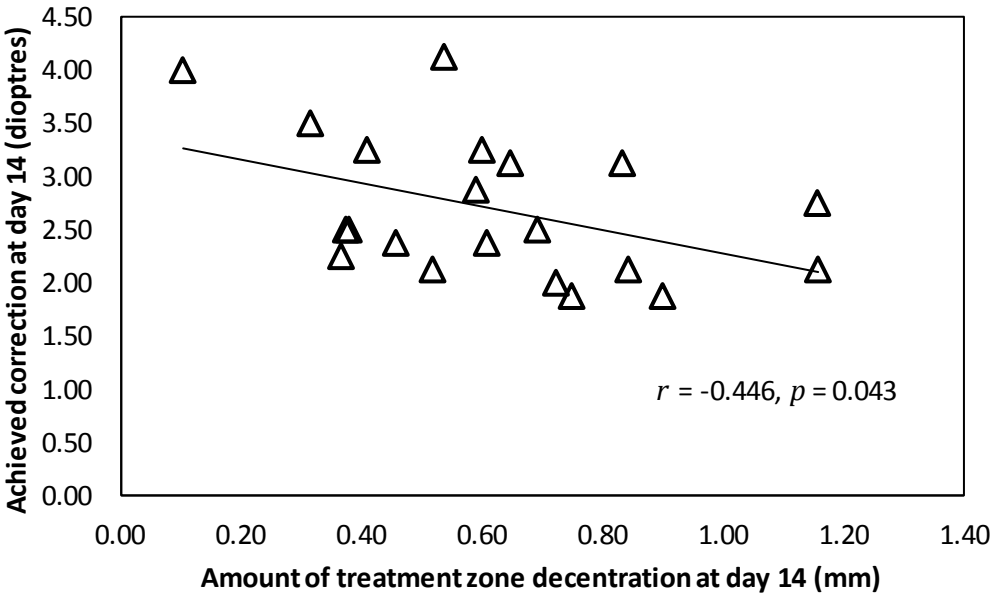

Figure 3-4. Relationship between amount of treatment zone (TZ) decentration and achieved correction at day 14. Note that as the amount of TZ decentration increased the achieved correction was reduced.

3.4 DISCUSSION

In this study a new method to determine TZ parameters was established. This method is superior to methods described in previous studies (Yang et al. 2005, Hiraoka et al. 2009) in a number of ways. Whereas these previous methods mostly relied on manual identification of the edge of the TZ from coloured topography maps on computer screens this new method used raw data extracted from the corneal topographer. Manual identification involved choosing only a few selected points over the coloured topography map, whereas in contrast the current method used the entire raw data set to identify the TZ border along every corneal hemi-meridian from the reference centre. This computerised method allows for more efficient objective identification of TZ parameters, making it especially useful for accurately and reliably analysing multiple topography maps from multiple visits after OK treatment.

The other important aim of the study was to identify baseline corneal parameters that could possibly influence OK lens decentration resulting in a decentred TZ. Therefore, in the current study corneal asymmetry was assessed first and later this was related to TZ decentration direction. Sectorial corneal shape at baseline showed significant horizontal and vertical corneal asymmetry. Overall, the nasal and superior cornea became flatter at a faster rate than the temporal and inferior cornea respectively, which is in agreement with findings reported in Chapter 2.

When sectorial corneal shape was related to TZ direction important relationships were observed. A significant negative association between the direction of the most prolate corneal sector and the direction of TZ decentration at day 1 implies that OK lenses displace away from the most prolate corneal region where the cornea tends to become flatter at a faster rate. By day 14, a significant positive correlation was instead observed between the TZ direction and the direction of the least prolate corneal sector measured at baseline. However, this relationship has less causational validity because the decentration of the OK lenses at this treatment visit is likely to be highly dependent on the corneal shape that was already altered due to OK lens wear. The intention of the next chapter is to investigate regional tangential curvature by sectors which may identify post-OK corneal factors that control decentration of lenses during longer periods of OK lens wear.

A crucial finding from this study is that by the end of the study period, eyes that demonstrated less TZ decentration achieved greater correction possibly because greater central corneal flattening was achieved with a centred lens. Conversely, eyes which exhibited greater TZ decentration resulted in corneal flattening away from the central cornea giving less central refractive correction. This emphasises the need for good TZ centration during OK. On the other hand an alternative but less likely interpretation of this relationship is that lenses that achieved greater central corneal flattening retained better centration.

The amount of TZ decentration reported in this study is in agreement with previous reports on TZ decentration (Tahhan et al. 2003a, Owens et al. 2004, Yang et al. 2005, Lu et al. 2007a, b, Hiraoka et al. 2009). The current analysis reveals that the amount of TZ decentration increased significantly over time. However, Yang et al. (2005) found no significant change over time when assessing this parameter, although the method they employed for identifying the TZ centre could have affected their decentration measurements.

In the current study the TZ diameter was 4.62 ± 0.48 mm at day 1 and 5.24 ± 0.45 mm at day 14 and these values, which are based on corneal refractive power difference maps, were comparatively smaller than values reported Tahhan et al. (2003a), and larger than the values reported by Lu et al. (2007b). The dimension of TZ diameter measurements depends on the type of map on which this analysis is based (Mountford 2004b). The TZ diameter values determined based on corneal refractive power difference maps would be larger than those determined using tangential curvature difference maps and smaller than those reported using axial curvature difference maps (Section 1.8.1). Tahhan et al. (2003a), who used axial power difference maps, reported TZ diameter to be 5.50 ± 0.60 mm and 5.70 ± 0.70 mm at 1 day and 1 month after BE OK overnight lens wear respectively. Lu et al. (2007b), who used tangential curvature difference maps, reported TZ diameter (central flattened zone) to be 3.41 ± 0.09 mm and 3.61 ± 0.07 mm at day 1 and day 28 after overnight use of Paragon CRT lenses.

With regards to direction of decentration based on the classification used in this study, horizontally, temporal decentration was found in 76% of the eyes at day 1 and 67% at day 14. Vertically, superior decentration was found in 57% of the eyes and the remaining 43% of the eyes showed inferior decentration at day 1, whereas, at day 14 the majority of eyes (67%) exhibited inferior decentration. The same tendency was also noted in previous studies (Yang et al. 2005, Hiraoka et al. 2009). Yang speculated that the temporal cornea being steeper than the nasal cornea was a possible cause for temporal decentration of OK lenses. However, neither Yang nor Hiraoka specifically related corneal shape to the direction of TZ decentration.

A possible shortcoming of the method developed to demarcate the TZ in the current study is the reliance on detecting a zero or positive value of corneal refractive power change after the treatment. There were instances, particularly after a single overnight wear, where there was no change in power towards zero or positive value in certain hemi-meridians resulting in all negative values. This difficulty was also encountered by Owens et al. (2004) after a single overnight wear of OK lenses. In the current study this problem of identification was partly overcome by fitting an ellipse to all points of most positive values, meaning that the TZ decentration values determined should only be minimally affected.

It should be pointed out that the Q values determined in this study are less prolate than those reported in Chapter 2. A major difference in the analyses between the two studies was that Q was measured over a 6 mm chord diameter in the current analysis rather than 8 mm due to increased fit errors when calculated over the larger chord. The Q value tends to be more prolate (more negative) with larger chord diameter (Read et al. 2006,

Gonzalez-Meijome et al. 2007), which adequately explains why Q values were less negative in the current study.

The current study only considers the influence of baseline corneal parameters on TZ decentration. Other factors such as eyelid pressure and the position of the eyes during sleep are also likely to affect the decentration of lenses during overnight wear. Therefore, correlations presented between baseline corneal parameters and TZ parameters in the current study must be considered with caution because correlation does not necessarily imply causation. Only limited research has been published on the effects of eyelids during OK. Tahhan et al. (2003b) revealed no significant role of eyelid force during OK lens centration, but their study measured eyelid tension during the open eye condition and not in a closed eye situation, which is not analogous to sleeping in OK lenses.

A further limitation of this study is that only central corneal shape parameters were related to TZ decentration parameters and peripheral corneal shape was not taken into consideration. Peripheral corneal shape may also play a role in OK lens decentration because the alignment curve of the lens rests on the cornea towards the periphery. Read et al. (2006) investigated corneal asphericity (in eyes having refractive astigmatism up to −2.75 DC astigmatism) in the steep and flat corneal meridians over 6, 8 and 9 mm diameter chords to reveal large variation in asphericity between the principal meridians in the central zones (6 and 8 mm diameter) but less variation in the periphery (9 mm diameter). Therefore it is reasonable to suggest that the peripheral corneal shape may contribute only minimally to lens decentration in eyes having minimal corneal toricity.

3.5 CONCLUSIONS

This study established a new method to determine TZ centration, which is intended to be used in the following studies reported in this thesis. This study also revealed that OK lenses tend to displace away from the most prolate corneal region as a first response after a single overnight wear and further decentration during the subsequent wearing period may depend on the altered corneal shape induced by OK itself. The following chapter is aimed at exploring sectorial corneal shape variations as a consequence to OK wear in the same sample as the present study, to establish possible causes for TZ decentration during lens-wearing periods beyond one night of wear.

CHAPTER 4 SECTORIAL CORNEAL CHANGES DURING SPHERICAL ORTHOKERATOLOGY

4.1 INTRODUCTION

The target of orthokeratology (OK) is to create a uniform flattening of the central cornea with a simultaneous annular steepening of the para-central cornea. However it has been demonstrated in Chapter 2 that corneal shape is not uniform over different sectors in eyes with minimal corneal toricity. This raises the question whether rotationally symmetrical OK lenses will cause uniform post wear changes across the sectors, or instead whether the cornea will mould towards a more symmetrical shape to match the OK lens profile.

Further, in Chapter 3 it was shown that OK lenses have a tendency to displace away from the more prolate corneal region after a single night of lens wear. The non-uniform corneal shape at baseline in addition to the decentration of lenses may result in non-uniform corneal reshaping in the centre and also in the periphery after OK treatment. Previous studies on OK have confined their investigation of corneal shape to central changes and only specific meridians, predominantly either steep versus flat meridians (Stillitano et al. 2007, Zhong et al. 2009) or horizontal versus vertical meridians (Sridharan and Swarbrick 2003). Few studies have reported on para-central corneal curvature changes (Lu et al. 2007b, Zhong et al. 2009).

The purpose of this study is to investigate sectorial corneal shape changes after OK treatment at day 1 and at day 14 visits in the same study participants as in Chapter 3. Furthermore, changes to corneal curvature and power within each sector between measurement visits were analysed in addition to differences between sectors at each post lens wear visit.

4.2 MATERIALS AND METHODS

4.2.1 Original study methodology

The study data were retrieved from the same retrospective data set as described in Chapter 3. The original study methodology details are provided in Section 3.2.1.

4.2.2 Present study analysis

Corneal topography data at baseline, day 1 and day 14 obtained from the Medmont E300 topographer (Medmont Studio 4 software version 4.14.1.1, Medmont International Pty Ltd, Victoria, Australia) were used for sectorial corneal analysis. Corneal tangential

curvature and corneal refractive power were calculated in the central circular zone (CCZ) and the para-central annular zone (PAZ) as described below. Each zone was further sub-divided into sectors, also described below.

4.2.2.1 Corneal sectors and development of program algorithm

To analyse the cornea sectorially in the two different zones, a customised algorithm (Appendix C) was used to read the raw Medmont E300 files (Section 2.2.4.1). A further algorithm divided corneal topography data into a CCZ of 5 mm diameter and a PAZ ranging between 5 and 8 mm diameter. The zone beyond 8 mm was excluded from the analysis due to it often being obscured by the ocular adnexa. Each zone was further divided into nasal, superior, temporal and inferior sectors each encompassing 90 degrees (Figure 4-1). Because only one topographic map was available per participant, there were some images where the para-central corneal information was partially lost. To prevent inclusion of potentially erroneous data a cut-off rule was applied to exclude any sector where the number of captured points was less than 70%. To aid analysis, left eye corneal data were reversed along the vertical axis such that the analyses were made considering all eyes as right eyes.

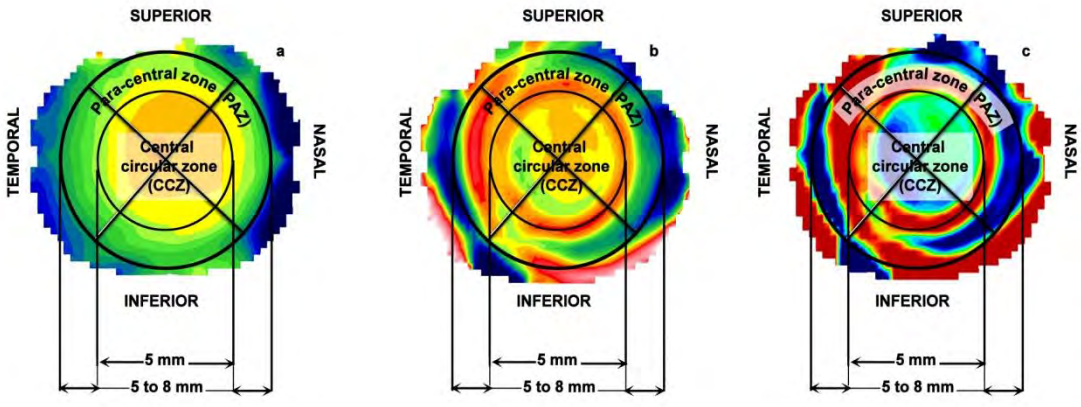

Figure 4-1. Corneal topography (tangential curvature) maps at (a) baseline, (b), at lens removal after one overnight wear of OK and (c) the difference. In each map red indicates steeper areas and blue indicates flatter areas.

Tangential curvature was converted from mm to dioptres using the keratometric refractive index of 1.3375. Refractive power was calculated using the formula described by Klein and Mandell (1995a) (Section 1.5.6).

4.2.3 Statistical analysis

A random intercept linear mixed-model analysis was performed with corneal curvature or power as dependent variables while the sector location and time were treated as fixed factors (see Section 3.2.3). Post hoc pair-wise comparisons, with Bonferroni correction subsumed within the linear mixed model, were used to determine significance of corneal curvature/power changes in a given zone over time. Post hoc Student paired t-tests with Bonferroni correction were also used to compare effects in each sector between visits. A critical p-value of 0.05 was used to represent statistical significance.

4.3 RESULTS

The mean age of 21 participants who were enrolled into the original prospective studies was 29 ± 6 years (12 females and 9 males).

4.3.1 Baseline variables

The descriptive data of refractive and corneal variables at baseline, day 1 and day 14 were presented in Table 3-2. Baseline tangential curvature and refractive powers in the various zones and sectors are summarised in Table 4-1.

	Nasal	Superior	Temporal	Inferior	p-value
Tangential curvature					
Central circular zone	43.26 ± 1.29	43.56 ± 1.49	43.48 ± 1.25	43.78 ± 1.32	< 0.001
Para-central annular zone	39.72 ± 1.94	40.58 ± 1.53	41.38 ± 1.33	41.28 ± 1.71	< 0.001
Refractive power					
Central circular zone	43.96 ± 1.33	44.29 ± 1.49	44.08 ± 1.33	44.37 ± 1.40	< 0.001
Para-central annular zone	44.78 ± 1.56	45.08 ± 1.64	45.37 ± 1.44	45.38 ± 1.39	< 0.001

Table 4-1. Corneal tangential curvature and refractive power in dioptres (mean ± SD) in nasal, superior, temporal and inferior sectors of the central circular zone and para-central annular zone at baseline. The p-value represents the statistical significance of variation present between the sectors in each specified zone from the linear mixed model analysis.

At baseline the corneal tangential curvature was significantly different between sectors in the CCZ ($F = 7.685_{(3, 60.00)}$, $p < 0.001$). The inferior sector showed steepest curvature followed by superior, temporal and nasal sectors (Table 4-1). Pair-wise comparisons from the mixed model revealed no significant corneal asymmetry between horizontal (temporal -nasal = 0.23 ± 0.40 D, $p = 0.304$) or vertical sectors (inferior – superior = 0.22 ± 0.58 D, $p = 0.310$).

At baseline the corneal tangential curvature was significantly different between sectors in the PAZ (F = 11.871$_{(3,\ 58.00)}$, p < 0.001). The temporal sector showed steepest curvature followed by inferior, superior and nasal sectors (Table 4-1). Pair-wise comparisons from the mixed model revealed a significant corneal asymmetry between horizontal sectors (1.66 ± 1.71 D, p < 0.001) but not between vertical sectors (0.70 ± 1.50 D, p = 0.625).

At baseline the corneal refractive power was significantly different between sectors in the CCZ (F = 7.513$_{(3,\ 60.00)}$, p < 0.001). The inferior sector showed greatest refractive power followed by superior, temporal and nasal sectors consistent with corneal tangential curvature variation (Table 4-1). Pair-wise comparisons from the mixed model revealed no significant asymmetry in the refractive power between horizontal (0.12 ± 0.34 D, p > 0.999) or vertical sectors (0.08 ± 0.45 D, p > 0.999).

At baseline the corneal refractive power was significantly different between sectors in the PAZ (F = 11.303$_{(3,\ 56.03)}$, p < 0.001). The inferior sector showed greatest refractive power followed by temporal, superior and nasal sectors (Table 4-1). Pair-wise comparisons from the mixed model revealed significant asymmetry in the refractive power between horizontal (0.59 ± 0.66 D, p < 0.001) sectors but not between the vertical sectors (0.30 ± 0.67 D, p = 0.221).

4.3.2 OK-induced changes to corneal tangential curvature

4.3.2.1 Central Circular Zone (CCZ)

The corneal tangential curvature was significantly different between sectors at day 1 (F = 10.662$_{(3,\ 60.00)}$, p < 0.001) and day 14 (F = 8.004$_{(3,\ 60.00)}$, p < 0.001) indicating that the corneal shape was not uniform in the CCZ after OK treatment at both post wearing visits. At day 1, the temporal sector showed flattest curvature followed by nasal, superior, and inferior sectors (Figure 4-2a). Pair-wise comparisons revealed a significant horizontal mirror asymmetry (−0.45 ± 0.66 D, p = 0.041) but not vertically (0.36 ± 0.75 D, p = 0.310). At day 14, the temporal sector continued to show the flattest curvature followed by superior, inferior and nasal sectors (Figure 4-2a). Pair-wise comparisons revealed a significant horizontal mirror asymmetry (−1.11 ± 1.02 D, p < 0.001) but not vertically (0.06 ± 1.56 D, p > 0.999).

Changes in the tangential curvature over time in the CCZ are presented in Figure 4-2b. Considering data from all visits (baseline, day 1 and day 14) there was a significant difference in the tangential curvature between CCZ sectors (F = 17.455$_{(3,\ 220.00)}$, p < 0.001). Significant change was also noted in the overall tangential curvature over time (F = 22.068$_{(2,\ 220.00)}$,

$p < 0.001$). However the change in curvature was not uniform across the sectors ($F = 5.172_{(6, 220.00)}$, $p < 0.001$). The overall tangential curvature flattened significantly by day 1 (−0.21 ± 0.56 D, $p = 0.047$) and showed further flattening by day 14 (−0.58 ± 0.88 D, $p < 0.001$). The difference in flattening between day 1 and day 14 was statistically significant (−0.37 ± 0.67 D, $p < 0.001$).

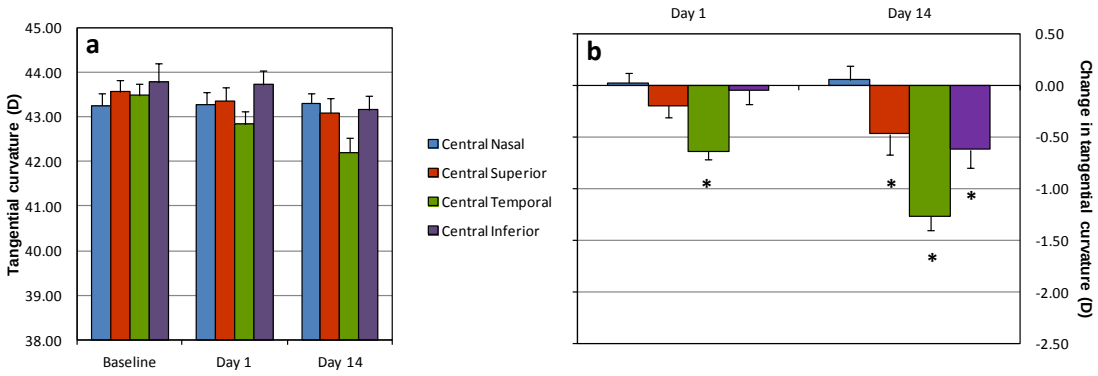

Figure 4-2. Corneal tangential curvature (dioptres) (a) at all visits and (b) curvature change from baseline at day 1 and day 14 in each sector of the central circular zone (CCZ). Error bars represent the standard error of the mean and '*' indicates a statistically significant change from baseline.

The temporal sector flattened by day 1 (−0.64 ± 0.37 D, $p < 0.001$), with further flattening by day 14 (−1.27 ± 0.62 D, $p < 0.001$). The central superior and inferior sectors, which revealed no significant change in curvature from baseline to day 1 (superior: −0.19 ± 0.55 D, $p = 0.121$, inferior: −0.05 ± 0.62 D, $p = 0.730$), showed significant flattening by day 14 (superior: −0.46 ± 0.91 D, $p = 0.028$, inferior: −0.62 ± 0.83 D, $p = 0.003$). There was no significant change in the central nasal sector at day 1 (0.03 ± 0.42 D, $p = 0.784$) or at day 14 (0.05 ± 0.62 D, $p = 0.893$).

4.3.2.2 Para-central Annular Zone (PAZ)

The corneal tangential curvature was significantly different between sectors at day 1 ($F = 17.311_{(3, 52.27)}$, $p < 0.001$) and day 14 ($F = 14.143_{(3, 54.98)}$, $p < 0.001$) indicating that the corneal shape was not uniform in the PAZ after OK treatment at both post wearing visits. At day 1, the temporal sector showed steepest curvature followed by inferior, superior, and nasal sectors (Figure 4-3a). This trend in curvature variation continued to present at day 14 (Figure 4-3a). Pair-wise comparisons revealed a significant horizontal mirror asymmetry at day 1 (3.04 ± 2.34 D, $p < 0.001$) and also at day 14 (3.73 ± 3.00 D, $p < 0.001$) but no significant vertical asymmetry was noted either at day 1 (0.36 ± 1.87 D, $p > 0.999$) or at day 14 (1.20 ± 3.28 D, $p = 0.515$).

Changes in tangential curvature over time in the PAZ are presented in Figure 4-3b. Considering data from all visits there was a significant difference in tangential curvature between PAZ sectors ($F = 34.238_{(3, 204.51)}$, $p < 0.001$). Significant change was noted in the overall tangential curvature with time ($F = 15.334_{(2, 204.10)}$, $p < 0.001$). However the change was not uniform over the sectors ($F = 2.157_{(6, 204.05)}$, $p = 0.049$). The overall curvature showed no significant change at day 1 (−0.14 ± 1.79 D, $p > 0.999$) but showed significant steepening at day 14 (1.21 ± 1.57 D, $p < 0.001$). The steepening between day 1 and day 14 was statistically significant (1.35 ± 2.18 D, $p < 0.001$).

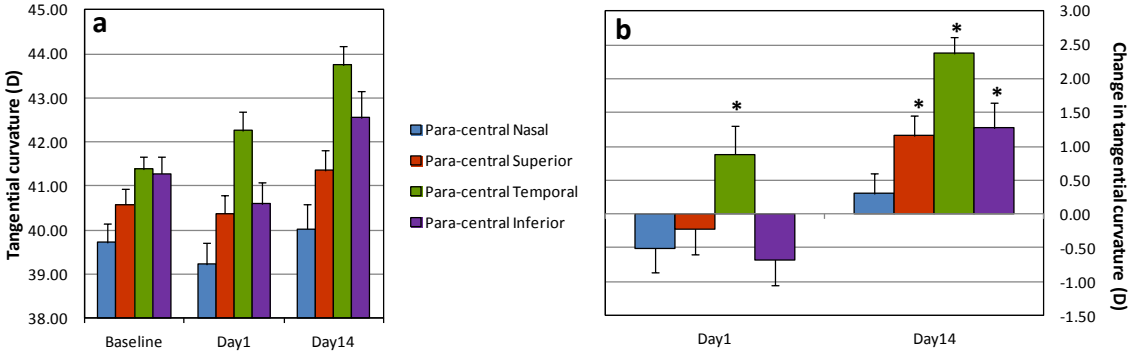

Figure 4-3. Corneal tangential curvature (dioptres) (a) at all visits and (b) curvature change from baseline at day 1 and day 14 in each sector of the para-central annular zone (PAZ). Error bars represent the standard error of the mean and '*' indicates a statistically significant change from baseline.

The temporal sector steepened by day 1 (0.89 ± 1.89 D, $p = 0.044$), with further steepening by day 14 (2.37 ± 1.09 D, $p < 0.001$). The para-central superior and inferior sectors, which revealed non-significant change at day 1 (superior: -0.22 ± 1.59 D, $p = 0.420$, inferior: −0.68 ± 1.74 D, $p = 0.088$), showed significant steepening by day 14 (superior: 1.16 ± 1.50 D, $p = 0.027$, inferior: 1.27 ± 1.66 D, $p = 0.002$). There was no significant change in the para-central nasal sector at day 1 (−0.50 ± 1.68 D, $p = 0.187$) or at day 14 (0.30 ± 1.36 D, $p = 0.326$).

4.3.3 OK-induced changes to corneal refractive power

4.3.3.1 Central Circular Zone (CCZ)

The corneal refractive power was significantly different between sectors at day 1 ($F = 6.828_{(3, 60)}$, $p < 0.001$) and day 14 ($F = 16.289_{(3, 60)}$, $p < 0.001$) indicating that the corneal refractive power was not uniform in the CCZ after OK treatment at both post wearing visits. At day 1, the temporal sector showed lowest refractive power followed by nasal, superior, and inferior sectors (Figure 4-4a). Pair-wise comparisons revealed no significant mirror asymmetry

either horizontally (0.32 ± 0.58 D, p = 0.099) or vertically (−0.26 ± 0.71 D, p > 0.999). At day 14, the temporal sector continued to show the lowest refractive power followed by superior, nasal and inferior sectors (Figure 4-4a). Pair-wise comparisons revealed a significant horizontal mirror asymmetry (−0.61 ± 0.47 D, p < 0.001) but not vertically (0.28 ± 0.64 D, p = 0.113).

Changes in refractive power over time in the CCZ are presented in Figure 4-4b. Considering data from all visits there was a significant difference in corneal refractive power between CCZ sectors ($F = 18.756_{(3, 220)}$, p < 0.001). Significant reduction was noted in the overall corneal refractive power over time ($F = 393.747_{(2, 220)}$, p < 0.001). However, the reduction in power was not uniform over all sectors ($F = 3.115_{(6, 220)}$, p = 0.006). The overall corneal refractive power in the CCZ showed significant reduction by day 1 (−0.89 ± 0.44 D, p < 0.001) and showed further reduction by day 14 (−1.78 ± 0.61 D, p < 0.001). The difference in reduction between day 1 and day 14 was also statistically significant (−0.89 ± 0.53 D, p < 0.001).

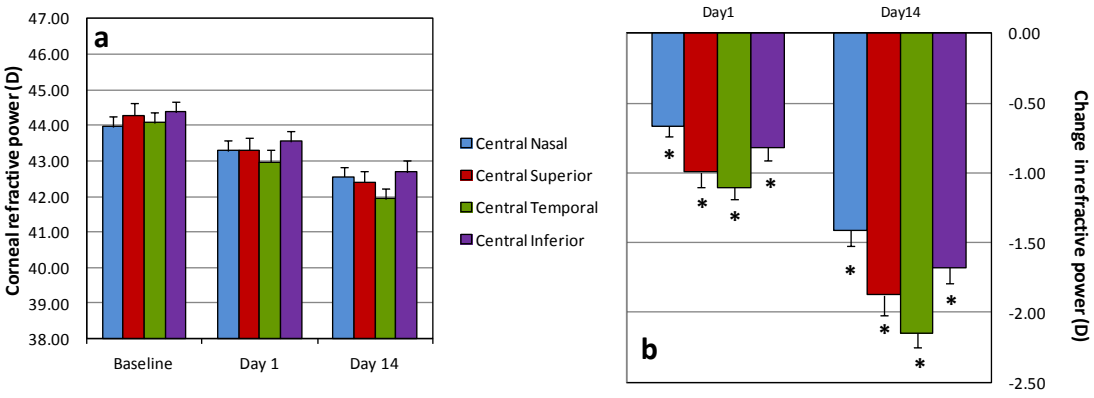

Figure 4-4. Corneal refractive power (dioptres) (a) at all visits and (b) power change from baseline at day 1 and day 14 in each sector of the central circular zone (CCZ). Error bars represent the standard error of the mean and '*' indicates a statistically significant change from baseline.

The central temporal sector showed the greatest reduction in refractive power (day 1: −1.10 ± 0.39 D, p < 0.001; day 14: −2.14 ± 0.49 D, p < 0.001), followed by central superior (day 1: −0.99 ± 0.49 D, p < 0.001; day 14: −1.87 ± 0.65 D, p < 0.001), central inferior (day 1: −0.81 ± 0.46 D, p < 0.001; day 14: −1.68 ± 0.51 D, p < 0.001) and central nasal sectors (day 1: −0.66 ± 0.32 D, p < 0.001; day 14: −1.41 ± 0.55 D, p < 0.001).

4.3.3.2 Para-central Annular Zone (PAZ)

The corneal refractive power was significantly different between sectors at day 1 ($F = 13.330_{(3,\ 52.056)}$, $p < 0.001$) and day 14 ($F = 7.291_{(3,\ 54.059)}$, $p < 0.001$) indicating that the corneal refractive power is not uniform in the PAZ after OK treatment at both post wearing visits. At day 1, the inferior sector showed highest refractive power followed by temporal, superior and nasal sectors (Figure 4-5a). Pair-wise comparisons revealed a significant horizontal mirror asymmetry (0.40 ± 0.50 D, $p = 0.003$) but not vertically (0.34 ± 0.62 D, $p > 0.999$). At day 14, the inferior sector continued to show highest refractive power followed by nasal, temporal and superior sectors (Figure 4-5a). Pair-wise comparisons revealed no significant mirror asymmetry either horizontally (−0.14 ± 0.43 D, $p > 0.999$) or vertically (0.62 ± 0.70 D, $p = 0.127$).

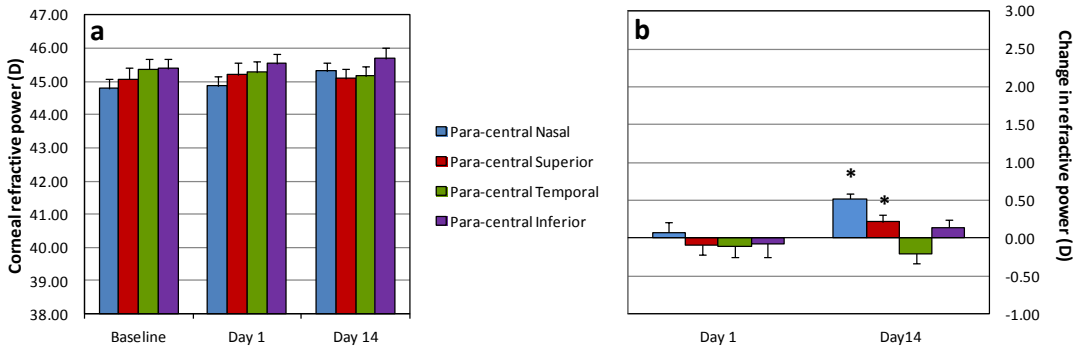

Figure 4-5. Corneal refractive power (dioptres) (a) at all visits and (b) power change from baseline at day 1 and day 14 in each sector of the para-central annular zone (PAZ). Error bars represent the standard error of the mean and '*' indicates a statistically significant change from baseline.

Changes in the refractive power over time in the PAZ are presented in Figure 4-5b. Considering data from all visits there was a significant difference in corneal refractive power between PAZ sectors ($F = 19.683_{(3,\ 204.05)}$, $p < 0.001$). Linear mixed model analysis showed significant change in the overall corneal refractive power over time ($F = 3.103_{(2,\ 204.01)}$, $p = 0.047$), however post-hoc tests showed no significant change at day 1 (−0.04 ± 0.63 D, $p > 0.999$) or day 14 (0.15 ± 0.51 D, $p = 0.205$). The change in the refractive power was not uniform over the sectors ($F = 2.361_{(6,\ 204.01)}$, $p = 0.032$).

At day 1 none of the para-central sectors showed a significant change in corneal refractive power. However, at day 14 a significant increase in refractive power was noted in nasal (0.52 ± 0.31 D, $p < 0.001$) and superior sectors (0.21 ± 0.33 D, $p = 0.024$).

4.4 DISCUSSION

A uniform flattening of the central cornea and steepening of the para-central cornea is a desirable response to OK treatment. In the current study overall flattening of the central cornea and steepening of the para-central zone were observed, which is consistent with results shown by previous authors (Mountford 1997b, Lu et al. 2007a, Queiros et al. 2010b). However, this study demonstrated that OK leads to sectorial differences in curvature in the central and para-central cornea. Previous studies have reported meridional changes of the central and para-central cornea (Mountford 1997b, Lu et al. 2007a, Queiros et al. 2010b). However, except for Queiros et al. (2010a), none of these studies provide useful quantitative information related to regional corneal changes. Either they have provided graphical information with no quantification of the curvature/power (Mountford 1997b), or they have averaged powers of corresponding hemi-meridians to offer overall information on the para-central area (Lu et al. 2007b).

In the CCZ, a significant corneal flattening was noted by day 1, which is in agreement with previous studies (Nichols et al. 2000, Soni et al. 2003, Owens et al. 2004, Sorbara et al. 2005). When changes in the horizontal sectors of the CCZ are considered, the temporal sector responded to OK earlier than the other sectors. This sector also flattened the most when compared to other sectors, by −0.64 ± 0.37 D after 1 night and −1.27 ± 0.62 D after 14 nights of wear. The nasal sector did not change significantly from baseline. This trend in flattening is in agreement with Queiros et al. (2010a) who assessed tangential curvature changes across the horizontal corneal meridian to reveal greater flattening temporally (−2.13 ± 1.40 D) than nasally (−0.56 ± 1.44 D) when measured 1 mm from the videokeratoscopic centre after three months of overnight Paragon CRT lens wear.

In the PAZ, a significant overall change in the tangential curvature was found over time but this change was not uniform over the sectors. Between the horizontal sectors of this zone only the temporal sector showed significant steepening with no significant change in the nasal sector. Queiros et al. (2010a) performed a similar analysis after three months of OK lens wear to reveal the opposite profile of less steepening in the temporal cornea 2 mm (+0.40 ± 1.36 D) and 3 mm (+1.89 ± 1.82 D) mm from the videokeratoscopic centre than in the corresponding nasal cornea (2 mm: +2.01 ± 1.29 D; 3 mm: +2.38 ± 1.90 D). Both studies referenced the corneal topography to the videokeratoscopic centre. However the duration of lens wear was different, with measurements conducted after three months of lens wear compared to two weeks in the current study. This suggests that para-central corneal curvature may continue to

alter with longer periods of lens wear. An alternative explanation could be differences in the lens design (Paragon CRT versus BE) between the two studies.

The differential change in the corneal curvature over time across the sectors of CCZ and PAZ revealed in this study suggests that spherical OK lenses do not provide the same effect within each individual sector. Furthermore, there was non-uniformity of corneal shape at each measurement interval. If the primary mechanism of OK lenses is moulding, the cornea should have become more uniform over time, consistent with the rotationally symmetrical back surface shape of the OK lens. A possible explanation for the non-uniform end result in corneal shape is that there is insufficient malleability of corneal epithelium to achieve the OK lens moulding effect. An alternative and perhaps more likely explanation is that the lens decentration itself caused the differential effect across the sectors during post lens wear visits, masking any uniformity that may be present had the lenses centred well.

When considering only the horizontal sectors, the temporal CCZ showed significant flattening after a single night of lens wear, while at the same time the adjacent temporal PAZ showed significant steepening. However, there was no significant change to corneal curvature in either the CCZ or PAZ in the nasal sector. The temporal lens decentration reported in Chapter 3 offers a possible explanation for this horizontal asymmetry between the temporal and nasal sectors. Whereas temporal lens decentration would cause the annulus of para-central steepening to fall entirely within the temporal side of the PAZ, by shifting temporally in line with lens decentration, part of the annulus of para-central steepening would now fall within the nasal side of the CCZ (Figure 4-6). This would lead to the nasal CCZ sector containing part of the central flattened zone as well as the annulus of para-central steepening, which when averaged could cancel each other out to give the appearance of no change, while the temporal CCZ would instead only contain flattening and temporal PAZ only steepening.

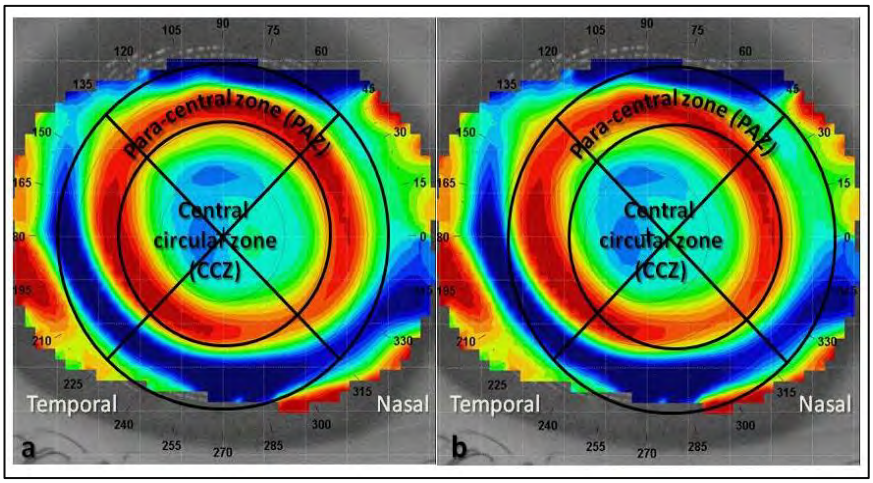

Figure 4-6. An example from one of the study participants' corneal tangential curvature difference map to demonstrate the effect of temporal treatment zone (TZ) decentration. Red indicates steepening, blue flattening, and green no change. a) A well centred TZ with respect to the videokeratoscopic axis. b) The same map as a, except that the analysis sectors have been shifted nasally to simulate temporal TZ decentration. In b, note that within the nasal quadrant the annulus of para-central steepened area falls partly into the CCZ while in the PAZ there is relatively little change. Within the temporal quadrant the annulus of para-central steepening instead falls completely within the PAZ.

In the vertical sectors, both the superior and inferior sectors showed significant flattening in the CCZ, and steepening in the PAZ after 14 nights of lens wear. Furthermore, at no point during the treatment period was significant vertical asymmetry present, indicating no difference in curvature between the superior and inferior sectors. Although the analysis reported in Chapter 3 revealed inferior TZ decentration in a majority of eyes (14 out of 21), the magnitude of decentration was small and failed to reach statistical significance (-0.12 ± 0.38 mm, $p = 0.141$). The same explanation given for horizontal asymmetry, when applied to a vertically centred lens, would lead to central corneal flattening and para-central steepening changes falling within the CCZ and PAZ respectively, and consequently greater likelihood of vertical mirror symmetry.

Using the same study data set, it was shown in Chapter 3 that OK lenses decentred away from the most prolate corneal region after a single overnight wear. However inability to describe corneal shape during lens wearing periods with conic sections meant that it was not possible to relate TZ decentration to the altered corneal shape. Dividing corneal shape into sectors in the current analysis overcomes these limitations to allow more accurate insight into the influence of corneal shape at day 1 on subsequent TZ decentration by day 14. The horizontal asymmetry in the PAZ described above, with the temporal sector significantly steeper than the nasal sector, became more pronounced with longer periods of lens wear. From clinical experience of fitting rigid lenses on post-refractive surgery corneas, it is generally

known that contact lenses tend to decentre towards a relatively steeper area of the cornea (Cutler 2001). If the same applies during OK lens wear, temporal steepening after the first night of lens wear would cause the lenses on subsequent wear to decentre in a temporal direction, offering an explanation for the increase in temporal TZ decentration that was observed at day 14.

This analysis has revealed sectorial differences in OK-induced changes in the refractive power of CCZ at both treatment visits and also in the PAZ at the day 14 visit. This is an important observation because it has been demonstrated that peripheral retinal image formation is an influential factor in regulating the development of refractive error (Smith et al. 2005), and it has been suggested that OK-induced steepening of para-central corneal curvature could create a beneficial myopic shift in peripheral refraction image shells (Charman et al. 2006, Walline et al. 2009). OK-induced changes to peripheral refraction profiles along the horizontal meridian have since been demonstrated (Charman et al. 2006, Queiros et al. 2010a, Kang and Swarbrick 2011, Kang and Swarbrick 2012). Some of these studies have revealed markedly asymmetrical profiles (Charman et al. 2006, Kang and Swarbrick 2011, Kang and Swarbrick 2012) that could be explained by the asymmetry in post-OK lens wear corneal shape identified in the current study. OK-induced decrease in corneal refractive power in the temporal CCZ and increased corneal refractive power in the nasal PAZ is consistent with the hyperopic shift in the central temporal visual field and myopic shift towards the extreme nasal visual field reported by Kang and Swarbrick (2012).

No previous studies have investigated peripheral refraction profiles in the vertical meridian during OK. This study has revealed asymmetry to corneal refractive power in the horizontal sectors but not in the vertical sectors. The symmetry of outcomes of corneal refractive power change only in one meridian offers a possible explanation for the differences in effect of OK on myopia control that have been observed between individuals (Cho et al. 2005, Walline et al. 2009). If OK lenses do not induce sufficient PAZ change across all meridians to provide a myopic shift in peripheral image there may not be sufficient summation of effect to overcome the influence from the macula. These observations may raise sufficient concern of differences in refraction change between corneal sectors to warrant further investigation of peripheral refraction profiles in more than the horizontal meridian alone.

The retrospective nature of the study is a major limitation of this study, and in particular this meant that only a single topography map was available from each eye for each study visit. Previous studies have cautioned about the use of peripheral corneal topographic

data as it is less repeatable than central data. It has been recommended to average the numerical data obtained from a number of repeated topographic maps to enhance repeatability (Zadnik et al. 1995).

The results of the current study cannot be generalised to populations with different ocular characteristics such as children, high myopes, against-the-rule/oblique corneal toricity or the elderly. For example eighty percent of the current study participants had with-the-rule corneal toricity, and the outcomes may be different in eyes with against-the-rule and oblique corneal toricity. Similarly, older adults who wear OK lenses may exhibit differences in lens decentration and therefore a different sectorial corneal change after OK, not only due to relatively flaccid eyelids (Vihlen and Wilson 1983) but also because of a shift in the corneal toricity towards against-the-rule (Read et al. 2007b). Furthermore, in Chapter 2 it was shown that the corneal shape variation may be different between East Asians and non-East Asians, implying that ethnicity could also affect sectorial corneal changes during OK.

4.5 CONCLUSION

The current study evaluated two weeks of overnight OK lens wear in minimally toric corneas wear to demonstrate non-uniform changes to curvature in the central and para-central regions of the cornea. Possible relationships between post OK lens wear corneal shape and subsequent lens centration were explored to explain the tendency towards temporal TZ decentration that was reported in Chapter 3. The asymmetry between the nasal and temporal PAZ sectors that was identified may influence the potential of OK lenses for use in myopia control. Further studies are warranted to determine if OK induces the same pattern of corneal change over longer periods of lens wear.

CHAPTER 5 EVALUATING THE PERFORMANCE OF SPHERICAL ORTHOKERATOLOGY LENSES ON TORIC CORNEAS

5.1 INTRODUCTION

Most of the previous research in orthokeratology (OK) has concentrated on correcting moderate myopia with low degrees of astigmatism using spherical OK lenses (Swarbrick 2006, Cheung et al. 2009). A possible reason that spherical OK lens fitting is usually restricted to eyes with minimal amounts of corneal toricity (≤ 1.50 DC) is based on anecdotal reports that greater degrees of corneal toricity lead to excessive lens decentration. However, other than a single case study (Caroline and Andre 2009), there are no previously reported studies to justify this lens fitting limitation. Caroline and Andre (2009) illustrated excessive lens decentration during spherical OK fitting on an eye with 2.87 DC of corneal toricity, although magnitude of decentration was not quantified. The inability of spherical OK lenses to centre well on moderately toric corneas should not be ruled out without a detailed investigation. Even if lens decentration was found to be a limiting factor, greater understanding of treatment zone (TZ) characteristics would be beneficial towards developing ways to improve centration using advanced OK lens designs.

Although there are design and fitting related differences between conventional spherical rigid gas permeable contact lenses (Sph-RGP) and OK contact lenses, techniques known to improve Sph-RGP lens fitting on moderately toric corneas may provide similar benefits for OK lenses when fitted to corneas of moderate toricity. Sph-RGP lenses are typically fitted to align their back optic zone radius with the flatter corneal meridian, however in the presence of > 1.50 DC of corneal toricity the 'one-third' rule is typically applied to improve the lens fit and centration on the cornea. This general rule of thumb involves calculating the base curve of the Sph-RGP lens to be steeper than the flatter corneal meridian by one third the difference in the corneal curvatures between the two principal meridians (Grosvenor 1994, Phillips 1997, Bennett and Sorbara 2009). The aim is to control the excessive edge lift that would otherwise occur along the steeper corneal meridian were the lens to be fit in alignment with the flatter corneal meridian.

During the era of traditional OK, some authors described a similar technique using a programmed application of Sph-RGP lenses to provide an OK effect to correct myopia in the presence of moderate corneal toricity (Nolan 1972, Coon 1984, Potts 1997). The initial lens was fitted slightly steeper based on the 'one-third' rule and the lens back optic zone radius was then progressively flattened at subsequent after care visits until the OK effect was achieved. There are no current published reports describing modification of modern spherical reverse geometry OK lens fitting techniques to improve fitting outcomes in moderately toric corneas.

The primary purpose of this study was to investigate the magnitude of TZ decentration after a single overnight wear of spherical OK lenses when fitted to eyes with 1.50 to 3.50 DC of corneal toricity, and to make comparisons with outcomes for eyes with ≤ 1.50 DC corneal toricity reported in Chapter 3. An additional aim was to assess whether the spherical OK lens fit could be modified to improve TZ decentration in eyes with moderately toric corneas. One eye was fitted using the conventional OK fitting approach to align with the flattest corneal meridian, while in the fellow eye a similar method to the Sph-RGP 'one-third' rule was applied, with the lens instead fitted with a deeper sagittal height equivalent to the corneal flat meridian plus one-third the difference in sagittal height between the steep and flat meridians.

5.2 MATERIALS AND METHODS

5.2.1 Study design

The study data were obtained from one prospectively conducted study and two previously conducted studies. In the prospective study, participants with a moderate amount of corneal toricity (1.50 to 3.50 DC) were enrolled. The retrospectively analysed data were retrieved from the two studies described in Section 3.2.1, in which the participants had minimal amounts of corneal toricity (≤ 1.50 DC).

5.2.1.1 Prospective data, Group-1 (Eyes with corneal toricity 1.50 to 3.50 DC)

Participants were recruited via advertising posters within the University of New South Wales (UNSW), Sydney, Australia. A baseline visit was conducted to enrol participants with moderate amounts of corneal toricity in at least one eye. Study measurements including refraction, corneal topography and slit lamp biomicroscopic examination were conducted at baseline and after a single overnight wear in the morning after lens removal and again 7 hours after the morning visit. The purpose of the afternoon visit was to ensure the regression of lens wearing effects that has been shown to occur in myopic OK in eyes with ≤ 1.50D of corneal toricity.

5.2.1.1.1 Participants

Twelve participants aged between 19 and 45 were enrolled in this prospective study. Participants wearing soft contact lenses were advised to discontinue using lenses for at least 48 hours prior to taking study measurements. Conventional rigid contact lens wearers were not included. The study obtained approval from the UNSW Human Research Ethics Advisory Panel (Approval No. HREA 11019) and participants were treated in accordance with the tenets of the Declaration of Helsinki. Informed written consent was also obtained from the participants prior to enrolment.

5.2.1.1.2 Lens design

BE spherical OK trial lenses (Capricornia Contact Lens, Australia) manufactured in Boston XO material (Dk 100 ISO/Fatt; Bausch & Lomb Boston, Wilmington, MA) by Capricornia Contact Lens were used in this study. The total lens diameter was 11 mm and the back optic zone diameter was 6 mm.

5.2.1.1.3 Lens fitting protocol

Participants with corneal toricity between 1.50 and 3.50 DC in both eyes were fitted with OK lenses in both eyes. One eye was fitted using a 'conventional fitting method' and the other eye was fitted using an 'adjusted fitting method'. The assignment of method of fitting was randomised between the eyes and a computer generated randomisation list was used for this purpose. In participants where corneal toricity ranging between 1.50 and 3.50 DC was present in only one eye, the eligible eye was fitted with each fitting method sequentially on two different occasions. The sequence of fitting method was randomised. A washout period of at least 2 weeks was given between the fitting methods to give an adequate period of time for the cornea to recover its shape. In all cases the investigators were masked from the eye allocation, or order of lens fitting. All participants in Group-1 wore lenses overnight for a minimum of 8 hours and study measurements were taken after lens removal in the morning. The two fitting methods employed were as follows:

Conventional fitting method for moderately toric corneas (Group-1a):

This is an empirical fitting approach where the spherical OK lens parameters were determined by the lens manufacturer's software program (BE Enterprises Studio, Version 2.4). The corneal topography information required by the software program included apical corneal curvature (R_o) and corneal sagittal height at the flatter corneal meridian (sag_{fl}) measured at a 9.35 mm chord diameter (Figure 5-1). Other parameters entered into the software program

were target refractive correction and horizontal visible iris diameter. The purpose of the study was to investigate the influence of baseline magnitude of corneal toricity on the magnitude of TZ decentration and not to correct the original refractive errors. For this reason the actual refractive error of the participants was disregarded and for all eyes the target refractive correction was set to −2.00 D. The lens sag height for the conventional fitting method was determined as:

$$\text{Conventional OK lens sag} = \text{corneal sag}_{fl}$$

Adjusted fitting method for moderately toric corneas (Group-1b)

The same empirical methodology described above for conventional fitting was applied except that the corneal sag height entered into the computer software was adjusted to apply a similar effect to the 'one-third' rule typically used when fitting Sph-RGP lenses on moderately toric corneas. The corneal sag height data were adjusted to be equivalent to the corneal flat meridian plus one-third of the difference in sag height between the flat (sag_{fl}) and steep (sag_{st}) meridians. In this manner the calculated trial lens would have a sag height deeper than the conventional fit by one-third the sag height difference between the flat and steep meridians (Figure 5-1). The lens sag height for the adjusted fitting method was determined as:

$$\text{Adjusted OK lens sag} = \text{corneal sag}_{fl} + ([\text{corneal sag}_{st} - \text{corneal sag}_{fl}]/3)$$

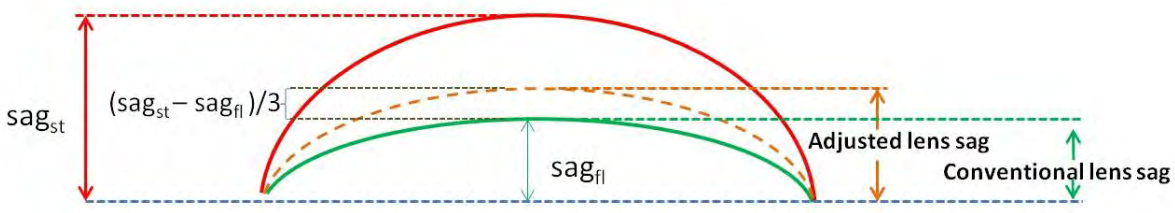

Figure 5-1. A diagrammatic illustration of determining orthokeratology (OK) lens sagittal (sag) height for fitting lenses using conventional and adjusted methods. The lens sag height for the conventional fitting method is determined based on sag height of the flat corneal meridian (sag_{fl}) and the lens sag height for the adjusted fitting method is determined based on the one-third rule i.e. adding one-third of the difference between sag height of the steep corneal meridian (sag_{st}) and sag_{fl} to sag_{fl}.

5.2.1.2 Retrospective data, Group-2 (Eyes with corneal toricity ≤ 1.50 DC)

These sets of data were derived from the same participant data described in Chapter 3, to serve as a control for Group-1a described above. However, to allow greater consistency in method of analysis between the prospective and retrospective data, instead of using the retrospective data already analysed and presented in Chapter 3, data gained from the initial empirically-defined lens fitting process were analysed instead. In this case baseline measurements were captured before dispensing the first pair of empirical OK lenses to both eyes. Lens fitting followed the same schedule as described for Group-1a in Section 5.2.1.1.3 based on corneal topography data. The lenses were then worn for a single night and study measurements were repeated in the morning after lens removal. As described in Section 3.2.1, the lens materials used in each eye were different during the subsequent two week lens wearing period. Only the data from those eyes eventually fitted with Boston XO material were analysed in this study. A flow diagram describing subject grouping is given in Figure 5-2.

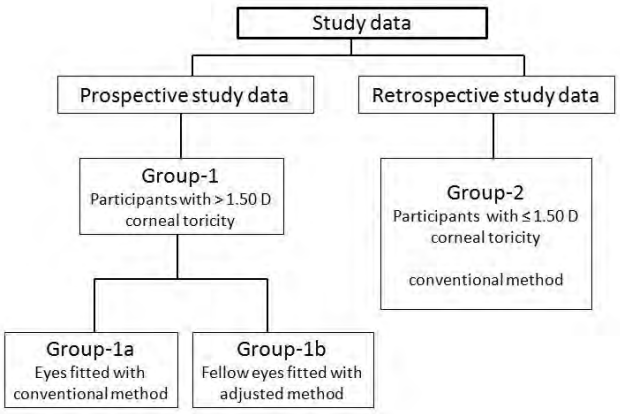

Figure 5-2. Grouping of the study data.

5.2.2 Corneal topography

In the prospective study and the two retrospective studies, the Medmont E300 corneal topographer (Medmont Studio 4 software version 4.14.1.1, Medmont International Pty, Ltd, Victoria, Australia) was used to capture corneal topography at baseline and during all scheduled treatment visits. The same procedure as described in Section 2.2.3.4 was followed in capturing the corneal topography and also reviewing the topography maps. For Group-1, a total of eight topographic maps were captured from each eligible eye. Topographic maps with artefacts and distorted mires were eliminated. In this manner a range of 4 to 7 maps

(mode = 6) were available at baseline and 4 to 8 (mode = 6) maps were available after one night wear of OK lenses were available for each participant. In Group-2 only one topographic map was available for each participant before and after the overnight lens wear of OK lenses.

5.2.3 Classification of corneal toricity

Corneal toricity can be confined to the central region only or can be extended up to the periphery close to the limbus. Section 1.3.5.4.2 gave an overview on classification of corneal toricity based on the extent in a previous study (Reddy et al. 2000). Extent of corneal toricity is likely to affect OK lens decentration (Caroline and Andre 2009). In order to relate extent of corneal toricity with the amount of TZ decentration, corneal toricity was determined in the central and peripheral corneal regions.

5.2.3.1 Central corneal toricity

In Chapter 3, corneal toricity was defined as the difference in corneal curvature (in dioptres) between the principal meridians. The curvature along the principal corneal meridians was defined by keratometry values which in this case were not measured directly using a keratometer, but instead determined from corneal topography data over an annular zone extending between 3 and 4 mm diameter (Section 1.3.5.1). These simulated keratometry (Sim K) values chiefly represents central corneal toricity and were used to denote corneal toricity in previous chapters. In this current study the same Sim K measurements were used to describe central corneal toricity, meaning that the terminology ‘central corneal toricity’ used here is synonymous with ‘corneal toricity’ used previously.

5.2.3.2 *Peripheral corneal toricity*

All eyes with moderately toric corneas were also tested for the presence of peripheral toricity. The corneal toricity along the principal corneal meridians was determined towards the periphery by calculating the sagittal radius of corneal curvature (R_s in mm) over an 8 mm chord diameter (4 mm hemi-chord length) using the following equation (Rabbetts and Edward 2007):

$$R_s = \sqrt{{R_o}^2 + (1-p) \cdot y^2}$$

where R_o is the apical curvature (in mm), p is the shape factor determined as 1–e^2, both R_o and e are derived from the topographer along both steep and flat corneal meridians and y is the hemi-chord length fixed at 4 mm. The sagittal corneal curvature (R_s) was then used to determine tangential corneal curvature (R_t in mm) along the principal corneal meridians using the formula (Salmon and Horner 1995, Rabbetts and Edward 2007):

$$R_t = R_s^3 / R_o^2$$

After converting R_t to dioptres, the peripheral toricity was determined by calculating the dioptric difference in R_t between the steep and flat meridians (Figure 5-3). The tangential radius of curvature was preferred over the axial radius of curvature for determining peripheral corneal toricity because tangential curvature represents true corneal shape (Section 1.5.1.1).

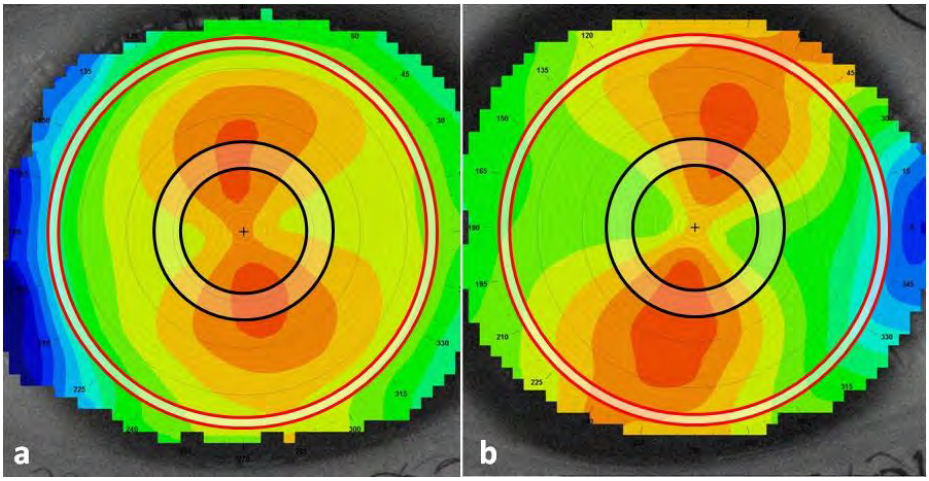

Figure 5-3. Baseline corneal axial power maps showing (a) central corneal toricity and (b) extension of corneal toricity towards the periphery. The black and red rings represent approximate zones from which the toricity in central (3-4 mm) and peripheral (8 mm) corneal regions respectively are determined. Note the extension of the steep corneal meridian (coloured red) towards the periphery in figure b.

5.2.3.3 Classification of corneal toricity into types

Based on the amount of corneal toricity in the central and peripheral corneal regions, corneal toricity was divided into 4 types as shown in Table 5-1.

Type		Central toricity (DC)	Peripheral toricity (DC)
Type-1	Relatively spherical cornea	≤ 1.50	≤ 1.00
Type-2	Central toricity only	1.50 to 3.50	≤ 1.00
Type-3	Limbus-to-limbus toricity	1.50 to 3.50	> 1.00
Type-4	Peripheral toricity only	≤ 1.50	> 1.00

Table 5-1. Classification of corneal toricity based on the magnitude of corneal toricity in the central and peripheral regions.

5.2.4 Treatment zone decentration determination

The MATLAB program described in Section 3.2.2.3 was used for determining the TZ decentration in this study. Although the algorithm functioned correctly when used on OK TZ outcomes in mildly toric corneas investigated in Chapter 3, it was unable to accurately identify the TZ margins for moderately toric corneas. In an attempt to rectify this, the MATLAB algorithm was customised to identify only a zero (or the most positive) change in refractive power along hemi-meridians. Despite this alteration, however, there remained some cases where the TZ decentration was excessive enough to cause both edges of the TZ to fall within the same hemi-meridian (Figure 5-4). In this instance the first positive values close to the centre of the map were falsely identified as the edge of the TZ leading to errors in TZ centration values based on the best-fit ellipse, and giving rise to underestimated values of TZ decentration.

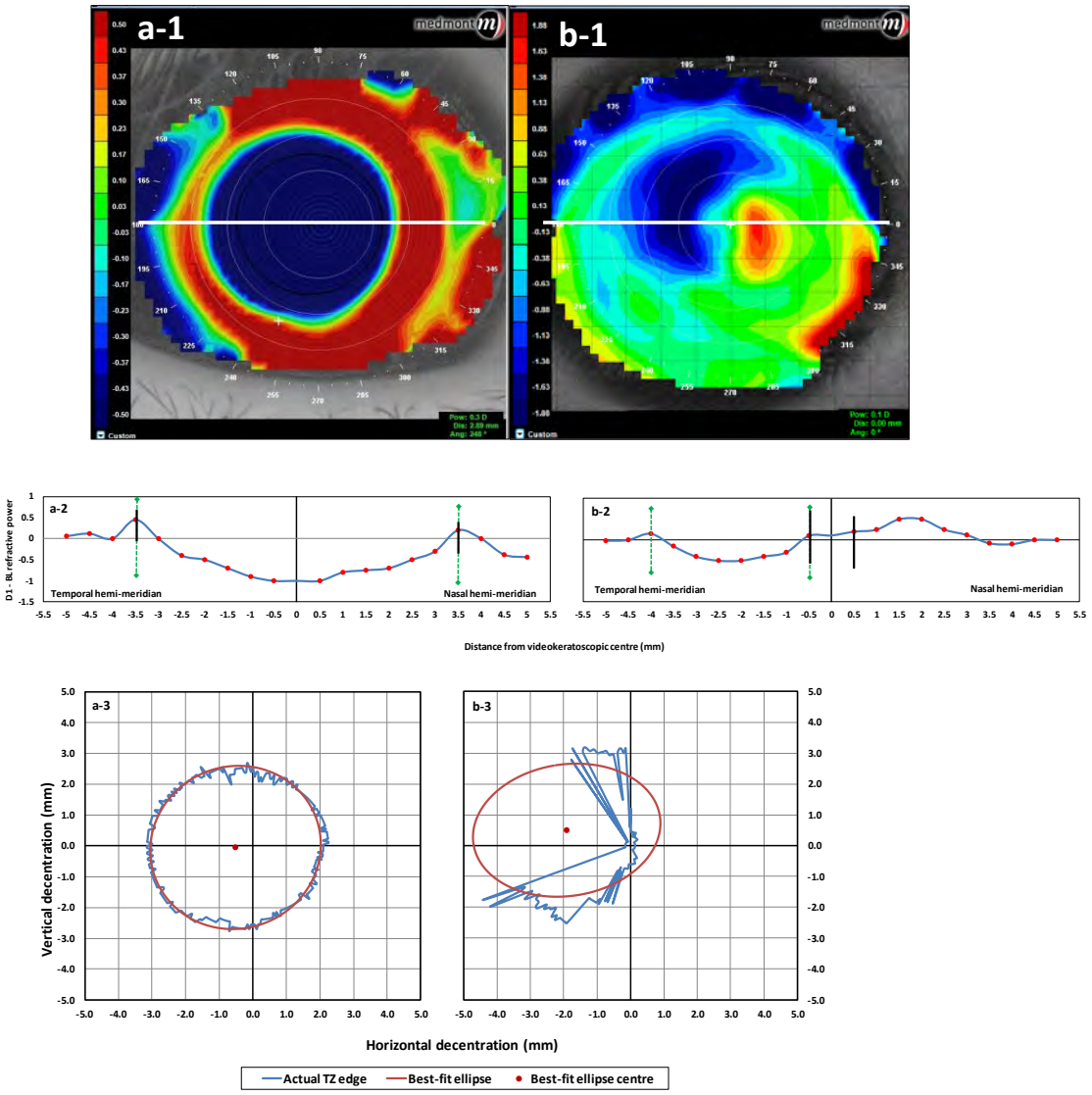

Figure 5-4. An example to show the inapplicability of the MATLAB algorithm in detecting the exact edge of the treatment zone (TZ) in moderately toric corneas. In the top figure, a-1 and b-1 represent right eye corneal refractive power difference maps; a-1 shows a slightly temporally centred TZ in a minimally toric cornea and a-2 shows a significant supero-temporal TZ decentration in a moderately toric cornea. In the middle figure, a-2 and b-2, the corneal profile of the difference map along the full horizontal meridian as depicted by the horizontal white line in top figures a-1 and b-1 is shown. Further, the vertical uninterrupted line marks the edge of the TZ as determined by the algorithm and the vertical dashed line with the diamond edges marks the actual TZ edge. Figure a-3 and b-3 represent the TZ decentration edge along each hemi-meridian as determined by the MATLAB algorithm. In both cases the best-fit ellipse is also shown. Note that in a-3, for all hemi-meridians the edge is detected accurately and the best-fit ellipse closely matches the actual TZ centration shown in a1, whereas in b-3 for several hemi-meridians on the temporal side the algorithm failed to accurately detect the edge resulting in an inappropriate fitting of the best-fit ellipse.

Once it was recognised that the MATLAB algorithm was unable to define the TZ in these moderately toric corneas, a modification of the manual method previously described by Yang et al. (2005) and Hiraoka et al. (2009) was instead adopted. A cartesian and polar grid was printed on to a transparency sheet (Figure 5-5). The cartesian gridlines were marked for every 0.50 mm, and the polar grid had its radial spokes at 20 degree intervals passing through the origin. This transparency sheet was placed directly on the computer monitor to align over the displayed refractive difference map with the origin of the cartesian graph aligned with the videokeratoscopic centre of the topographic difference map. Further, the first positive or least negative value was identified over each spoke on the transparency. In this manner a total of 18 points were marked on the transparency. The cartesian coordinates of these data points were then used to fit a best-fit ellipse using the MATLAB program. The centre of the best-fit ellipse with reference to the videokeratoscopic centre was defined as the TZ decentration.

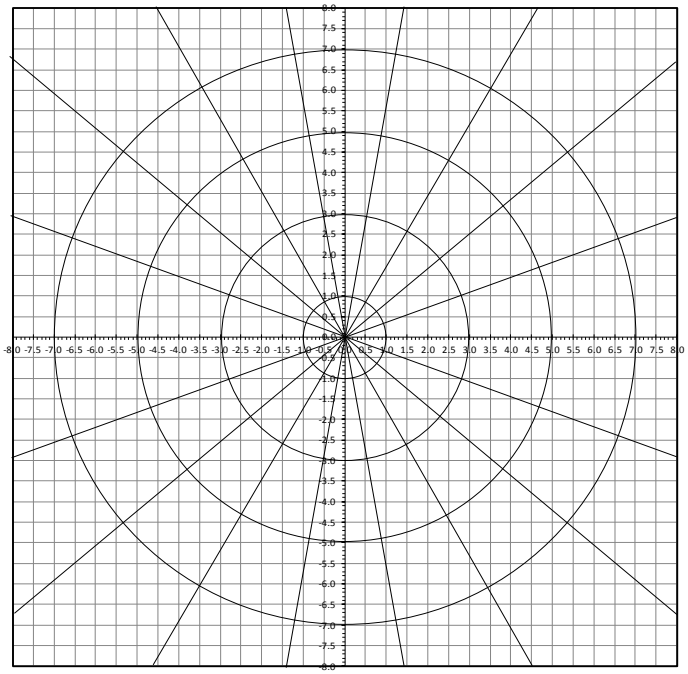

Figure 5-5. The cartesian and polar grid photo-copied on to a transparency to use over the computer screen in manually delineating the treatment zone (TZ) edge.

5.2.5 Sectorial corneal asphericity determination

The sectorial corneal asphericity for eyes in Group-1 was determined using the same procedure as described in Sections 2.2.4 and 2.2.5. The asphericity was determined over a 6 mm chord diameter. The sectorial Q values for eyes in Group-2 were already determined previously and reported in Section 3.3.1 and Table 3-2.

5.2.6 Statistical analysis

To aid analysis, the left eye corneal topographic data were reflected about the vertical axis such that the analyses were made considering all eyes as right eyes. The Shapiro-Wilk's test was used to check the normality of the age, baseline corneal and TZ parameters. A random intercept model of linear mixed model analysis was used to compare overall differences between baseline corneal variables of Group-1a, 1b and Group-2 (see Section 3.2.3 for the description on mixed model analysis). The change in each corneal variable from baseline to day 1 was tested using a paired sample t-test. The random intercept model of linear mixed model was also used to investigate differences in TZ decentration and also the change over time between Group-1a, 1b and Group-2. When performing the linear mixed model analysis the model was set to make comparisons between Group-1a and 1b and also between Group-1a and Group-2.

The variation in sectorial asphericity (Q) at baseline was analysed using the linear mixed model. Independent sample t-tests with Bonferroni correction were used to compare the differences in the corresponding sectorial Q values between Group-1a and Group-1b, and also between Group-1a and Group-2.

The age distribution in Group-1 did not meet normality criteria, therefore a Mann-Whitney test was used when comparing the age between Group-1 and Group-2. Pearson's correlations or Spearman's rank correlations were used according to the normality of data to relate baseline corneal shape parameters with the TZ parameters. To investigate the relationship between baseline sectorial corneal asphericity and TZ parameters, each corneal sector was denoted by the median of angle range over which the sector was spread in the same manner as described in Section 3.2.3. A critical p-value of 0.05 was used to represent statistical significance.

Relationships were established between baseline corneal shape and TZ parameters. The baseline parameters included were corneal R_o; corneal M, J_{180} and J_{45}; steep and flat K powers; and least and most prolate corneal sectors.

As described in Section 3.2.3, when relating principal corneal meridian angles to the TZ decentration angles, the corneal meridian angles more than 90 degrees and TZ decentration angles greater than 180 degrees were transposed for the angles to be symmetric around the horizontal axis.

5.3 RESULTS

The mean age of the 12 participants in the prospective study in which participants with moderately toric corneas enrolled was 26.17 ± 7.94 years (age range 19 to 45 years; 7 females and 5 males) and the mean age of the 21 participants in the retrospective study in which participants with minimally toric corneas enrolled was 29.27 ± 6.24 years (age range 20 to 40 years; 12 females and 9 males). The difference in age between the two groups was not statistically significant (p = 0.063).

In Group-1, the duration between lens removal after waking and the time at which the study measurements taken ranged between 1 - 85 minutes, with a mean duration of 20.50 ± 24.62 minutes. For one participant, measurements were taken 85 minutes after waking due to the presence of superficial punctate keratitis at lens removal, which delayed measurements until sufficiently resolved to allow accurate corneal topography capture. Two other participants preferred to sleep at their residence, which was located close to or within the UNSW campus. The duration between lens removal and the time at which the measurements were conducted for these participants was 40 and 43 minutes. In Group-2 the mean duration between lens removal in the morning and the study measurements was 96.62 ± 75.79 minutes.

5.3.1 Corneal variables

At baseline, in Group-1 all participants had with-the-rule (WTR) corneal toricity in the eligible eyes. In Group-2, of 21 participants 17 participants had WTR corneal toricity and the remaining 4 had against-the-rule (ATR) corneal toricity.

The linear mixed model analysis revealed significant differences in baseline central corneal toricity, peripheral corneal toricity and corneal J_{180} between Group-1a, 1b and Group-2. Other corneal parameters did not show significant differences (Table 5-2). Pair-wise comparisons revealed that there were significant differences in central corneal toricity ($p < 0.001$), peripheral corneal toricity (p = 0.018), and corneal J_{180} ($p < 0.001$) between Group-1a and Group-2 eyes (all $p < 0.001$). Further there was no significant difference between Group-1a and Group-1b (central toricity: p = 0.288, peripheral toricity: p = 0.651 and corneal J_{180}: p = 0.310). This analysis confirmed that participant eyes in the prospective study were correctly assigned into cohorts for conventional and adjusted fitting by corneal toricity and that eyes in Group-2 were an appropriate control for Group-1a eyes.

Variable (dioptres)	Group-1a	Group-1b	Group-2	Linear mixed model analysis ($F_{(df)}$, p-value)
	1.50 to 3.50DC corneal toricity		≤ 1.50 DC corneal toricity	
steep K	44.88 ± 1.53	44.76 ± 1.42	44.25 ± 1.42	F = 1.385 $_{(2,16.10)}$, p = 0.279
flat K	42.46 ± 1.54	42.49 ± 1.42	43.37 ± 1.31	F = 1.651 $_{(2,16.12)}$, p = 0.223
Central corneal toricity	2.42 ± 0.44	2.28 ± 0.51	0.88 ± 0.39	F = 51.826 $_{(2,24.04)}$, p < 0.001*
Peripheral corneal toricity	4.18 ± 1.66	3.80 ± 1.89	2.52 ± 1.56	F = 3.852 $_{(2,24.45)}$, p = 0.035*
Corneal M	43.67 ± 1.52	43.62 ± 1.40	43.77 ± 1.33	F = 0.159 $_{(2,16.00)}$, p = 0.854
Corneal J_{180}	−1.18 ± 0.21	−1.10 ± 0.24	−0.29 ± 0.33	F = 35.032 $_{(2,17.09)}$, p < 0.001*
Corneal J_{45}	0.06 ± 0.29	0.04 ± 0.30	0.01 ± 0.20	F = 0.145 $_{(2,42.00)}$, p = 0.866

Table 5-2. Mean ± SD of corneal variables at baseline in Group-1a, 1b and Group-2. The significance of difference between these three groups from the linear mixed model analysis is also shown; a statistically significant difference is indicated by *.

Combining data from Group-1a, 1b and Group-2, there was a significant positive correlation between baseline central and peripheral corneal toricity (r = 0.606, p < 0.001), indicating that eyes with greater amounts of central corneal toricity also had greater amounts of peripheral corneal toricity (Figure 5-6). According to the classification of central and peripheral corneal toricity the distribution of eyes to each specific type is given in Table 5-3.

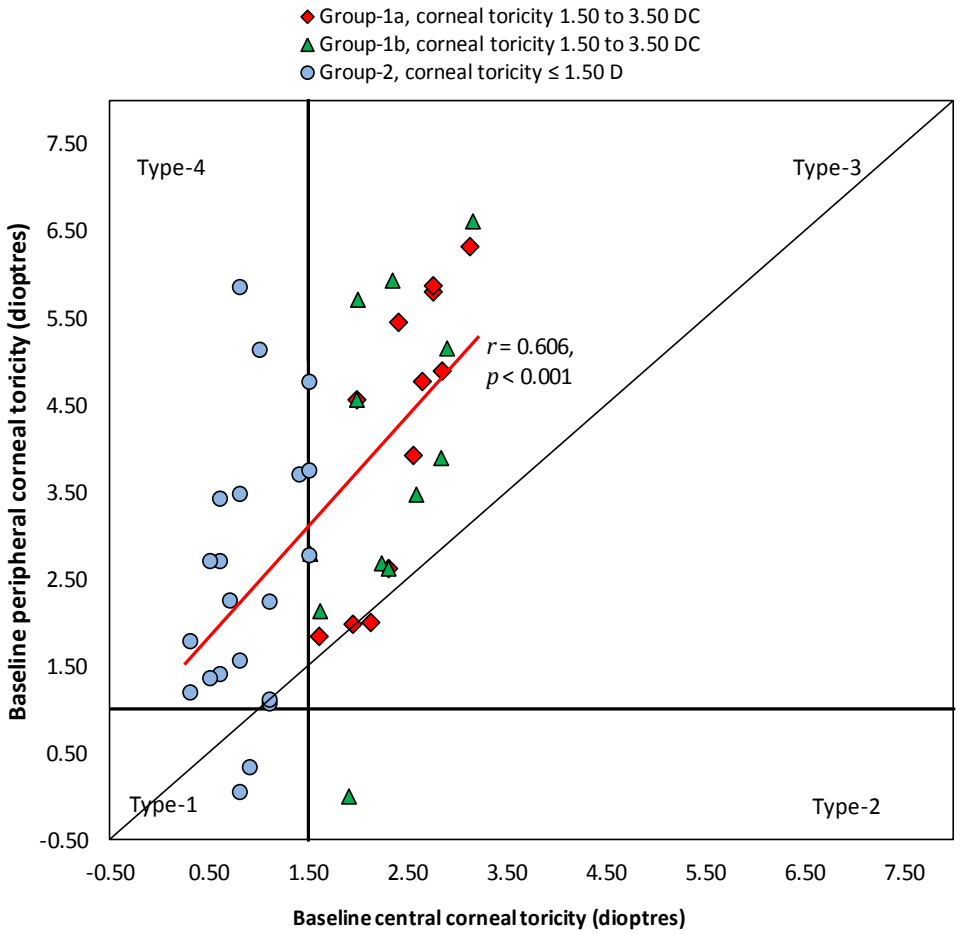

Figure 5-6. Relationship between central and peripheral corneal toricity. The graph is also divided into quadrants to show the distribution of eyes in each type of corneal toricity classified based on the magnitude of toricity in central and peripheral corneal regions. The red line indicates linear best fit and the black line indicates baseline central corneal toricity = baseline peripheral corneal toricity.

Type		Sim K (DC)	Peripheral toricity (DC)	No of eyes (%)	Study group
Type-1	Relatively spherical cornea	≤ 1.50	≤ 1.00	2 (5%)	Group-2
Type-2	Central toricity only	1.50 to 3.50	≤ 1.00	1 (2%)	Group-1
Type-3	Limbus-to-limbus toricity	1.50 to 3.50	> 1.00	21 (49%)	Group-1
Type-4	Peripheral toricity only	≤ 1.50	> 1.00	19 (44%)	Group-2

Table 5-3. Classification of corneal toricity based on the magnitude in the central and peripheral regions.

Table 5-4 summarises the change in corneal variables after a single overnight use of OK lenses in Group-1a, 1b and Group-2. The table also presents the overall significance of difference in change between the three groups from the linear mixed model analysis.

There was a significant flattening in steep and flat K from baseline in all groups. For steep K, linear mixed model analysis revealed a difference in change from baseline between the groups, however pair-wise comparisons revealed a significant difference only between Group-1a and Group-2 (p = 0.019), indicating that when the conventional fitting method was used, eyes with minimally toric corneas showed greater reduction in the steep K than eyes with moderately toric corneas. For flat K, linear mixed model analysis revealed no difference in change between Group-1a, 1b and Group-2. Student t-tests were performed between the change observed in the steep and flat K meridians in all groups to determine which of the two meridians showed greatest change. In Group-1a greater flattening was noted in the flat K than in the steep K (p = 0.002). In both Group-1b and Group-2 there was no significant difference in the change between the steep and flat K (p = 0.349 and p = 0.220 respectively).

Variable (dioptres)	Group-1a (1.50 to 3.50 DC corneal toricity)		Group-1b (1.50 to 3.50 DC corneal toricity)		Group-2 (≤ 1.50 DC corneal toricity)		
	Mean ± SD	Change from baseline (p-value)	Mean ± SD	Change from baseline (p-value)	Mean ± SD	Change from baseline (p-value)	Change between groups ($F_{(df)}$, p-value)
steep K	−0.23 ± 0.19	0.002*	−0.39 ± 0.36	0.003*	−0.68 ± 0.55	< 0.001*	F = 3.975 $_{(2, 22.75)}$, p = 0.033*
flat K	−0.54 ± 0.33	< 0.001*	−0.50 ± 0.41	0.002*	−0.77 ± 0.44	< 0.001*	F = 1.702 $_{(2, 26.99)}$, p = 0.201
Central corneal toricity	0.31 ± 0.26	0.002*	0.11 ± 0.38	0.349	0.09 ± 0.31	0.215	F = 1.927 $_{(2, 26.53)}$, p = 0.165
Corneal M	−0.38 ± 0.24	< 0.001*	−0.45 ± 0.34	0.001*	−1.09 ± 0.61	< 0.001*	F = 7.503 $_{(2, 16.32)}$, p = 0.005*
Corneal J_{180}	−0.12 ± 0.14	0.015*	−0.05 ± 0.19	0.339	−0.03 ± 0.18	0.522	F = 1.076 $_{(2, 23.46)}$, p = 0.357
Corneal J_{45}	−0.03 ± 0.33	0.781	−0.01 ± 0.20	0.890	−0.01 ± 0.44	0.957	F = 0.018 $_{(2, 28.91)}$, p = 0.983

Table 5-4. Mean ± SD of change from baseline in corneal variables after single overnight wear of OK lenses in Group-1a (conventional fitting, corneal toricity 1.50 to 3.50 DC), 1b (adjusted fitting, corneal toricity 1.50 to 3.50 DC) and Group-2 (conventional fitting, corneal toricity ≤ 1.50 DC). The overall significance of change between the groups is based on a linear mixed model analysis. The significance of change in each corneal variable from baseline is based on t-tests. Statistical significance is indicated by '*'.

Conventional fitting of spherical OK lenses in moderately toric corneas induced an increase in central corneal toricity from baseline. However despite this apparent difference in response between the fitting approaches, the linear mixed model analysis failed to indicate a significant difference in the change from baseline between Group-1a, 1b and Group-2.

Corneal M exhibited a significant decrease after a single overnight wear in all groups. Linear mixed analysis revealed a significant difference in change between Group-1a, 1b and Group-2. The change in corneal M in Group-1a was not significantly different from Group-1b (−0.07 D; CI = −0.25 D to 0.11 D; p = 0.427), but did show a significant difference from Group-2 (−0.71 D; CI = −1.09 D to −0.34 D; p = 0.001). This indicates that when the conventional fitting method is used in eyes with minimally toric corneas a greater reduction in corneal M was found than when the same method was used in eyes with moderately toric corneas.

Although t-tests revealed significant change in corneal J_{180} in Group-1a, the linear mixed model analysis did not show any significant difference in change between Group-1a, 1b, and Group-2. Corneal J_{45} did not show significant change in either Group-1a, 1b or Group-2.

5.3.2 Sectorial corneal asphericity at baseline

The baseline asphericity Q values for each sector in eyes of Group-1a, 1b and Group-2 are presented in Table 5-5. Group-2 data, although previously reported as sectorial Q values in Table 3-2, have been included here to allow a direct comparison with Group-1 data.

In all groups the supero-nasal sector was the most prolate at baseline. In Group-1a and 1b, the supero-temporal sector was least prolate, and in Group-2, the inferior sector was least prolate. Linear mixed model analysis revealed significant differences in the overall mean Q value between Group-1a, 1b and Group-2 ($F = 14.763_{(2, 59.74)}$, $p < 0.001$) and the differences between groups was dependent on sector location ($F = 74.083_{(10, 13451.01)}$, $p < 0.001$). Therefore differences in the corresponding sector Q values were evaluated. There were no differences between Group-1a and 1b in any sector (all $p > 0.05$). Between Group-1a and 2 there was a significant difference only in the supero-temporal sector (p = 0.016), with Group-2 eyes having greater asphericity in this sector when compared to Group-1a.

Baseline sectorial corneal asphericity (Q)	Supero-nasal	Superior	Supero-temporal	Infero-temporal	Inferior	Infero-nasal
Group-1a	−0.23 ± 0.04	−0.03 ± 0.05	−0.01 ± 0.03	−0.06 ± 0.02	−0.11 ± 0.01	−0.18 ± 0.06
Group-1b	−0.20 ± 0.04	0.01 ± 0.06	−0.01 ± 0.03	−0.06 ± 0.02	−0.08 ± 0.01	−0.16 ± 0.06
Group-2	−0.24 ± 0.01	−0.19 ± 0.03	−0.14 ± 0.01	−0.12 ± 0.01	−0.10 ± 0.01	−0.15 ± 0.03

Table 5-5. Mean ± SD of the asphericity Q values in different sectors at baseline in Group-1a (conventional fitting, corneal toricity 1.50 to 3.50 DC), 1b (adjusted fitting, corneal toricity 1.50 to 3.50 DC) and Group-2 (conventional fitting, corneal toricity ≤ 1.50 DC).

5.3.3 Treatment zone decentration

The mean and range of polar decentration of the TZ centre from the corneal vertex normal in Group-1a, 1b and Group-2 are given in Table 5-6. Linear mixed model analysis showed a statistically significant difference in the magnitude of TZ decentration between Group-1a, 1b and Group-2 (F = 5.479, p = 0.009). Pair-wise comparisons revealed no significant difference in the magnitude of TZ decentration between Group-1a and Group-1b (0.11 ± 0.39 mm, p = 0.655), indicating that there is no significant difference in the magnitude of TZ decentration between conventional and adjusted methods of fitting in moderately toric corneas. However Group-1a revealed a significantly greater magnitude of TZ decentration than Group-2 (0.48 mm, 95% CI: 0.14 to 0.83 mm, p = 0.004) than Group-2, indicating that conventional fitting of spherical OK lenses leads to a greater decentration in higher degrees of corneal toricity. Overall there was no significant difference between the three groups in either horizontal (X) or vertical decentration (Y) in isolation, possibly as a result of inadequate sample size, which was originally determined for polar decentration analysis.

Lens fitting method	Polar decentration (mm)	Range (mm)	X decentration (mm)	Y decentration (mm)
Group-1a	1.06 ± 0.57	0.19 - 1.84	−0.60 ± 0.66	−0.43 ± 0.73
Group-1b	0.95 ± 0.44	0.11 - 1.68	−0.65 ± 0.66	−0.36 ± 0.38
Group-2	0.57 ± 0.29†	0.21 - 1.27	−0.20 ± 0.40	−0.01 ± 0.48
p-value	0.009*		0.077	0.089

Table 5-6. Mean ± SD of treatment zone (TZ) parameters in Group-1a (conventional fitting, corneal toricity 1.50 to 3.50 DC), 1b (adjusted fitting, corneal toricity 1.50 to 3.50 DC) and Group-2 (conventional fitting, corneal toricity ≤ 1.50 DC). A statistically significant difference in TZ parameters between the groups as found by linear mixed model analysis is indicated by '*' and † indicates a significant difference from Group-1a.

The distribution of eyes and percentage showing TZ decentration direction towards a specific sector is given in Table 5-7. The individual TZ decentration directions for participants in Group-1a, 1b and Group-2 are presented in Figure 5-7. From the table and the figure it is evident that irrespective of amount of baseline corneal toricity and fitting methods used, most eyes exhibited temporal decentration. In eyes with moderate corneal toricity inferior decentration was also predominant.

Sector of treatment zone decentration	**Group-1a** ***n*** **= 12**	**Group-1b** ***n*** **= 12**	**Group-2** ***n*** **= 21**
Supero-nasal	0 (0%)	0 (0%)	1 (5%)
Superior	0 (0%)	0 (0%)	3 (14%)
Supero-temporal	4 (33%)	2 (17%)	8 (38%)
Infero-temporal	5 (42%)	7 (58%)	5 (24%)
Inferior	2 (17%)	2 (17%)	3 (14%)
Infero-nasal	1 (8%)	1 (8%)	1 (5%)

Table 5-7. Direction of treatment zone decentration in Group-1a (conventional fitting, corneal toricity 1.50 to 3.50 DC), 1b (adjusted fitting, corneal toricity 1.50 to 3.50 DC) and Group-2 (conventional fitting, corneal toricity ≤ 1.50 DC). Data presented as number of eyes (percentage).

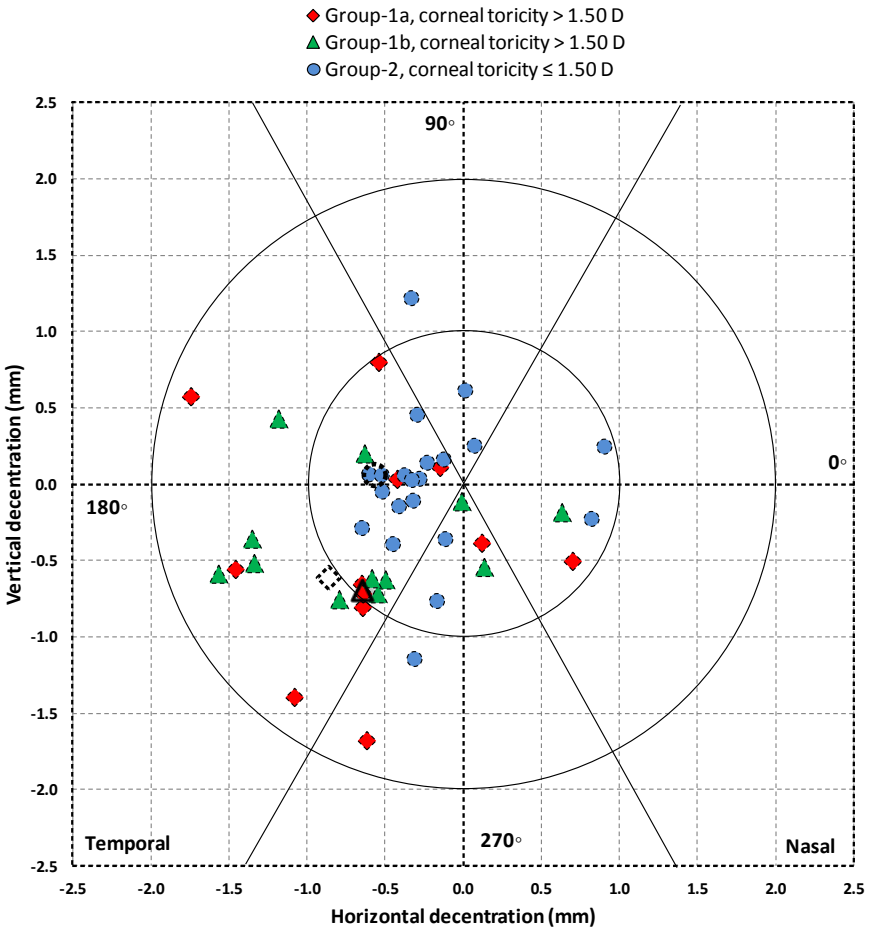

Figure 5-7. Decentration of the treatment zone from the vertex normal in Group-1a (conventional fitting, corneal toricity 1.50 to 3.50 DC), 1b (adjusted fitting, corneal toricity 1.50 to 3.50 DC) and Group-2 (conventional fitting, corneal toricity ≤ 1.50 DC). The large empty diamond, triangle and circle represent the mean amount and direction in Group-1a, 1b and Group-2 respectively.

5.3.3.1 Corneal parameters and TZ parameter correlations

Table 5-8. summarises associations observed between baseline corneal parameters and TZ decentration magnitude and direction. None of the baseline corneal parameters showed a correlation with the magnitude of TZ decentration in Group-1a, 1b and Group-2 in isolation, but significant correlations were observed when the conventional lens fit data from Group-1a and Group-2 were combined. Baseline corneal R_o, corneal M, corneal J_{180} and flat K showed a negative correlation with the magnitude of TZ decentration (Figure 5-8 a to d) and the magnitude of baseline central corneal toricity showed a positive correlation (Figure 5-8e). Among these corneal parameters, univariate analysis revealed corneal R_o to be the main variable influencing the TZ decentration ($F = 7.940$, $p = 0.009$). There was no significant correlation between the angles of principal corneal meridians (steep K and flat K) and polar angles of TZ decentration when the data were isolated or when the Group-1a and Group-2 data were combined.

Baseline corneal parameters	Group-1a n = 12		Group-1b n = 12		Group-2 n = 21		Group-1a and Group-2 combined n = 33	
	Treatment zone decentration magnitude (mm)							
	r	p-value	r	p-value	r	p-value	r	p-value
Corneal R_o (D)	−0.456	0.137	-0.394	0.206	−0.324	0.152	−0.419	0.015*
Corneal M (D)	−0.487	0.108	−0.425	0.169	−0.317	0.162	−0.406	0.019*
Corneal J_{180} (D)	−0.156	0.628	0.144	0.656	−0.003	0.989	−0.367	0.036*
Corneal J_{45} (D)	−0.378	0.226	0.451	0.141	0.286	0.208	0.049	0.786
Central corneal toricity (DC)	0.176	0.585	−0.015	0.962	0.014	0.952	0.346	0.048*
Peripheral corneal toricity (DC)	0.255	0.423	0.194	0.545	−0.060	0.797	0.154	0.392
steep K (D)	−0.457	0.135	−0.421	0.173	−0.334	0.140	−0.218	0.222
flat K (D)	−0.505	0.094	−0.415	0.180	−0.349	0.121	−0.444	0.010*
	TZ decentration direction (polar angle in degrees)							
steep K angle (degrees)	0.552	0.063	−0.028	0.931	−0.118	0.610	0.131	0.469
flat K angle (degrees)	−0.413	0.183	0.056	0.863	−0.118	0.610	−0.156	0.385
	Median angles of the sector to which the TZ was decentred							
Median angle of the most prolate corneal sector	−0.271	0.394	−0.024	0.941	−0.225	0.326	−0.209	0.244
Median angle of the least prolate corneal sector	0.309	0.329	−0.174	0.589	0.430	0.050*	0.238	0.182

Table 5-8. Relationships between baseline corneal parameters and treatment zone (TZ) magnitude and direction. A statistically significant correlation is indicated by '*'.

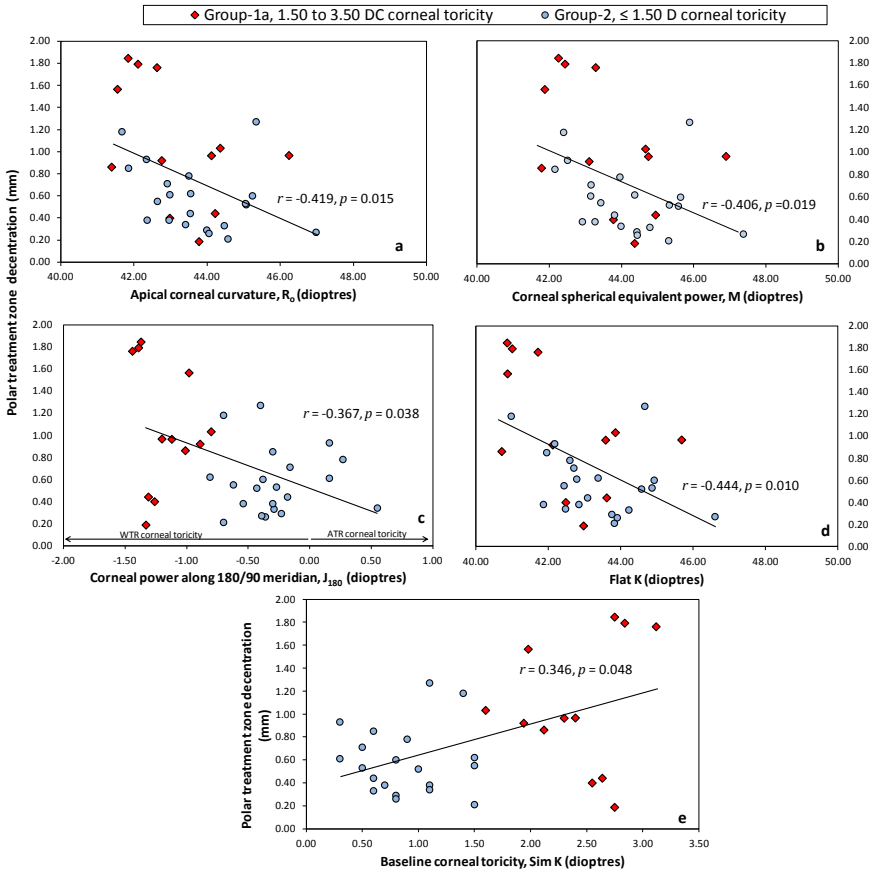

Figure 5-8. Relationship between baseline corneal parameters and treatment zone decentration from the combined data of Group-1a (conventional fitting, 1.50 to 3.50 D corneal toricity) and Group-2 (conventional fitting, ≤ 1.50 D corneal toricity). The baseline corneal parameters presented in the figure are: a. apical corneal curvature (R_o), b. corneal spherical equivalent power (M), c. corneal power along 180/90 meridian (J_{180}), d. power at flatter corneal meridian (flat K) and e. central corneal toricity from Sim K in dioptres. These data are plotted against the polar magnitude of treatment zone decentration. In figure c, WTR denotes with-the-rule and ATR denotes against-the-rule.

5.3.3.2 Sectorial corneal asphericity and TZ parameter correlations

In Group-2, a borderline significant positive correlation was observed between the median angles of least prolate corneal sector and the sectors to which the TZ were decentred (r = 0.431, p = 0.051), indicating an affinity of spherical OK lenses to decentre towards the least prolate corneal sectors when fitted using a conventional method of fitting. No correlations were observed between the median angles of the least/most prolate corneal sectors and the angles of the sectors to which the TZ was decentred either in Group-1a or Group-1b in isolation or even when Group-1a and Group-2 data were combined.

5.4 DISCUSSION

This study, which is the first to investigate the effects of spherical OK lenses in eyes corneal toricity above 1.50 DC, has demonstrated greater amounts of TZ decentration from conventionally fitted spherical OK lenses than when the same fitting technique is adopted in eyes with minimal corneal toricity. This finding can further be supported by the positive relationship revealed between the amount of baseline corneal toricity and the magnitude of TZ decentration, when the data from both minimal and moderately toric corneas were combined. In this way the current study adds scientific credibility to the clinical anecdote that higher amounts of corneal toricity lead to greater TZ decentration during spherical OK.

A likely reason for greater decentration of OK lenses in eyes with higher amounts of corneal toricity is reduced alignment of the lens back surface with the corneal surface of these eyes. Conventional fitting of OK lenses is typically based on matching the lens sag height with the corneal sag height along the flatter corneal meridian. This method of selecting the lens parameters should ideally lead to the closest alignment of lens back surface with the corneal surface in all meridians. However as the amount of corneal toricity increases, conventional fitting of OK lenses will lead to greater discrepancy in alignment between the lens and the corneal surface along the steeper corneal meridian. The unequal alignment of OK lens along the principal meridians will influence lens fit stability (Caroline and Andre 2009), increasing the likelihood of lens decentration, and consequent decentration of the TZ after overnight wear.

In an attempt to control OK lens decentration on moderately toric corneas an adjusted fitting method was employed in the current study which is analogous to the ‘one third’ fitting technique employed in fitting Sph-RGP lenses. The hypothesis was that by fitting a deeper lens (increased sag height) lens edge lift would be minimised towards the periphery on the steeper corneal meridian, thus increasing lens fit stability. However, this alternative method of fitting proved to have no benefit in terms of arresting the lens decentration, as no significant difference in the magnitude of TZ decentration was noted between the adjusted and conventional methods of fitting OK lenses.

A likely reason for poor success with the adjusted fitting method used in the current study could be that the lenses were made deeper only by one third of the difference between steep and flat meridians. Further deepening of the lens sag may be needed to achieve better centration. This raises the question, however, whether further deepening of lens sag may instead compromise overall myopic reduction. The OK procedure achieves myopic refractive error correction mainly by flattening of the central cornea and if the sag height were increased

it is possible that the central compressive effect provided by the lens would be reduced leading to loss of refractive effect.

Even though the adjusted fitting method did not achieve better lens decentration, some important observations could be made with respect to its influence on corneal parameters after overnight lens wear. Both fitting methods caused flattening of steep and flat K. However, whereas the conventional fitting method caused greater flattening to the flat K meridian than the steep K meridian, with the adjusted method there was no significant difference in flattening effect between the meridians. The unequal flattening between the principal meridians with conventional fitting on moderately toric corneas led to an increase in corneal toricity after a single overnight wear, which is consistent with a previous study (Hiraoka et al. 2004a). However, no significant change in toricity was noted in moderately toric corneas fitted with the adjusted fitting method.

A possible explanation for the increased central corneal toricity in moderately toric corneas fitted with conventional fitting is that the close lens alignment with the flatter corneal meridian will maximise the OK-induced compressive forces leading to flattening of flat K. In the steeper corneal meridian, however, greater lens standoff towards the periphery would limit compressive forces leading to less flattening effect along the steeper corneal meridian. In the adjusted fit the lens sag was increased. This would lead to less peripheral lens standoff along the steep meridian but at the same time, with lens sag now deeper than the corneal sag along the flatter meridian, the lens would be prevented from aligning closely with the corneal apex leading to loss of central compression. In adjusted fitting the reduced flattening effect to flat K despite changes that were also made to steep K indicated a more uniform rate of change (Figure 5-9). Given the uniformity of change it is reasonable to suggest that had wearing time been continued for longer then the adjusted fitting technique may have yielded more positive results.

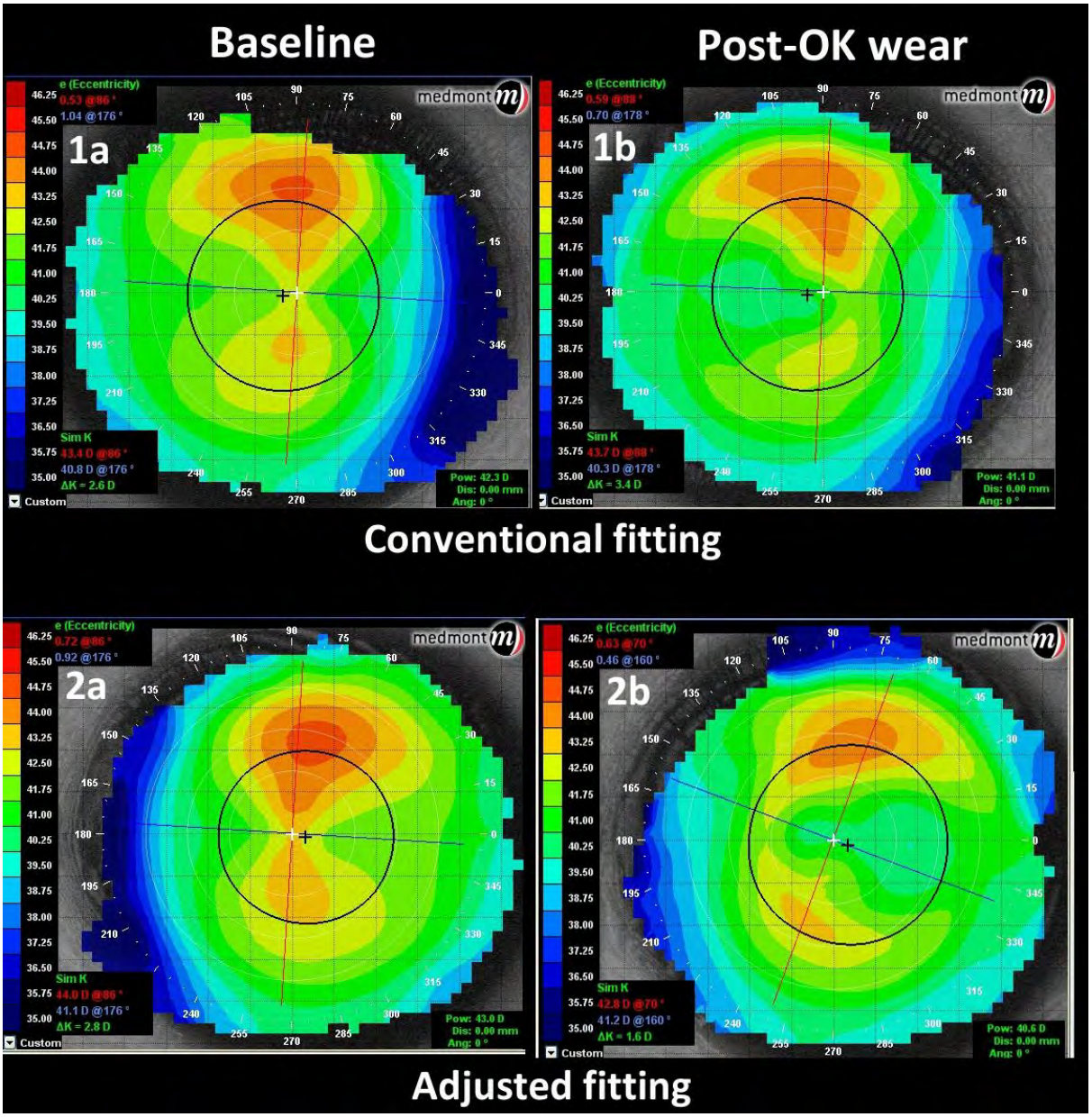

Figure 5-9. An example showing induction of central corneal toricity with the conventional fitting method and reduction of central corneal toricity with the adjusted fitting method, in a study participant of the current study. In the top figure, 1a and 1b represent axial power maps at baseline and after 1 night of OK lens wear respectively in the right eye fitted using the conventional fitting method. In the bottom figure, 2a and 2b are from same subject as the top figure but for the left eye fitted using the adjusted fitting method. Note the changes in Sim Ks given in the lower left hand box for each map. In the top figure, note the relative significant reduction in power along the flatter corneal meridian, resulting in the induction of corneal toricity after lens wear, whereas in the left eye (lower figure) there is a reduction in corneal power along steeper and flatter corneal meridians resulting in an overall reduction in corneal toricity.

When baseline corneal parameters within the individual groups were related to the magnitude of TZ decentration, no correlations were detected. However, some correlations were identified when the data of eyes with minimally toric corneas and moderately toric corneas fitted with the conventional method were combined. A possible reason to detect a relationship when the data were combined could be that the range of corneal toricity in each isolated group may be too narrow, but when combined the greater range of corneal toricity allowed significant relationships to become apparent.

Among the significant correlations with baseline corneal parameters, corneal R_o, corneal M, corneal J_{180} and flat K showed negative associations and central corneal toricity showed a positive association with the magnitude of TZ decentration. The negative associations of corneal R_o, corneal M and flat K indicate that the magnitude of TZ decentration tends to be less in eyes with steeper corneas. The negative association with corneal J_{180} (and the corresponding positive association with central corneal toricity) indicates that the TZ decentration is greater in eyes with high amounts of with-the-rule (WTR) corneal toricity and the decentration tends to be minimal as the WTR corneal toricity reduced. This finding is further emphasised by the positive correlation found between baseline central corneal toricity and the magnitude of decentration. But it cannot be concluded that the decentration will be minimal with ATR corneal toricity because in the data set from which the relationships were established there were only 4 out of 45 eyes with ATR corneal toricity. When considered as a whole these relationships imply that the TZ decentration is greater with higher amounts of central corneal toricity and also with flatter corneas. When a univariate analysis was performed corneal R_o was revealed to be the most highly influential parameter on the TZ decentration.

According to the corneal toricity classification used in the current study a majority of eyes (49%) had 'limbus-to-limbus' type of corneal toricity followed by 'peripheral corneal toricity' only (44%). When combined this means that more than 90% of eyes exhibited some form of peripheral corneal toricity that was greater than 1.00 DC. From Figure 5-6 it is apparent that almost all eyes with moderately toric corneas exhibited 'limbus-to-limbus' corneal toricity whereas the minimally toric corneas were clustered into 'relatively spherical' or 'peripheral toricity only' types. This high number of eyes with peripheral corneal toricity is similar to what was observed by Reddy et al. (2000) but high in comparison to that observed by Read et al. (2006). However, a direct comparison between these two studies is difficult

owing to the inconsistencies in determining the peripheral corneal toricity and also definitions used for each toricity type.

Mountford and Pesudovs (2002), based on their clinical experience, suggested that subjects having eyes with limbus-to-limbus corneal toricity make poor candidates for spherical OK lens wear due to poor on-eye lens stability with these lenses. Further, Caroline and Andre (2009) also speculated that the peripheral corneal toricity could be an important baseline corneal parameter that may play a role in lens decentration. Contrary to these speculations, the current study revealed no significant correlation between the magnitude of TZ decentration and baseline peripheral corneal toricity in individual groups or when eyes with minimally toric corneas and moderately toric corneas fitted with the conventional method were combined. Thus the current study outcomes based on the relationships between the central and peripheral corneal toricities imply that the central corneal toricity is more influential than the peripheral corneal toricity in decentring spherical OK lenses. Whether this peripheral corneal toricity provides any benefit in controlling decentration using lenses whose peripheral design is manufactured to match this region is worth investigating.

At baseline, corneas with moderate toricity showed significant variation in sectorial corneal asphericity. This finding is consistent with observations of corneal asphericity variation in minimally toric corneas in Chapters 2 and 3. Overall the nasal and superior cornea became flatter at a faster rate than the temporal and inferior cornea respectively. In Chapter 3 it was shown that the baseline regional corneal shape is influential on TZ decentration. In particular it was shown that in minimally toric corneas, the lenses decentred away from the most prolate corneal region as a primary response to OK lens wear. When the sectorial corneal shape was related to TZ direction in the current study, a positive correlation was again found when initial trial lenses were worn on minimally toric corneas. But no correlations were observed between the locations of least or most prolate corneal sectors and the TZ decentration in moderately toric corneas. A possible reason for this difference in response between eyes with minimal and moderate amounts of corneal toricity is that the magnitude of baseline corneal toricity in moderately toric corneas may have overwhelmed the regional variation of asphericity in determining the decentration of the lens.

With regards to direction of decentration in horizontal versus vertical directions, temporal decentration was found in 75% of eyes in both conventional and adjusted fitting methods in moderately toric corneas. In the same eyes, inferior decentration was found in 67% of eyes fitted with the conventional fitting method and 83% in the eyes fitted with the

adjusted fitting method. In eyes with minimal corneal toricity fitted with the conventional method, temporal decentration was still predominant (62%) horizontally, but superior decentration was instead more prevalent (57%) vertically. The TZ decentration patterns give some clue of the lens behaviour during eye closure and overnight wear. Generally a superior decentration is considered as a feature of flat fitting OK lenses whereas inferior decentration is typically associated with steep fitting OK lenses (Mountford 2004c, Hiraoka et al. 2009).

It must be emphasised here that the general conventions of lens cornea fitting relationships (Mountford 2004c, Hiraoka et al. 2009) may hold true only when fitting OK lenses in minimally toric corneas and these conventions may be violated when the lenses are fitted on highly toric corneas. Since the lens becomes too unstable on these eyes other external forces such as eyelid force may predominate in pushing lenses inferiorly during overnight wear causing inferior OK lens decentration. As far as the superior decentration in minimally toric corneas fitted using the conventional method is concerned, the initial trial lens chosen based on the flat K meridian more or less closely matches to the corneal curvature in all meridians and the eyelids have minimal influence, in which case the lens may be drawn superiorly due to superior positioning of the closed eye due to Bell's phenomenon (Wilkins and Brody 1969).

The current study investigated the effects of only the first empirical fitting stage of a diagnostic fitting method. It is general clinical practice to employ further lens trials in the case of a failed attempt of the empirical method. However the next step to improve centration in these eyes fitted with a conventional method is to trial with a slightly steeper base curve or deeper sag, which is essentially what was attempted using the adjusted fitting method. This approach showed no improvement with respect to centration of lenses on moderately toric corneas. It is reasonable to suggest that advanced lens designs such as toric OK lenses may align better with the toric corneal surface and reduce the magnitude of TZ decentration.

The MATLAB algorithm devised for detecting the TZ decentration parameters did not accurately detect the edge of the TZ when used after OK on moderately toric corneas. A non-uniform corneal flattening after one overnight wear rather than an error with the MATLAB code is the reason for this. Lenses were worn only for a single night which led to asymmetrical corneal flattening in these eyes. In other words some corneal meridians responded to OK better than other meridians. A more uniform flattening could have been possible had the lens wear continued for longer duration which could have made the detection of the TZ edge less problematic. However, we considered that it is ethically unacceptable to continue lens wear on

participants because of known deleterious effects on vision due to significant amounts of TZ decentration (Hiraoka et al. 2009).

Another shortcoming of this study is that the mean time interval between lens removal and time at which the study measurements were taken was different between Group-1 and Group-2 (approximately one hour). This difference could have possibly led to slight errors in estimation of TZ decentration in eyes in Group-2 due to regression of the OK effect.

5.5 CONCLUSION

When spherical OK lenses are fitted using a conventional method on moderately toric corneas, TZ decentration is found to increase compared to use of the same fitting technique on minimally toric corneas. Reduced alignment between the back surface of the OK lens and cornea in the presence of moderate toricity is the most likely reason for increase in TZ decentration. The current study shows that adjusting the lens fit by increasing the sag height by one-third of the difference between steep and flat meridian sag in an attempt to improve alignment did not lead to significant improvement in TZ decentration in moderately toric corneas after a single night of lens wear. Alternatively toric OK lenses, which theoretically conform better to the toric corneal surface, could lead to better lens centration and better clinical outcomes. The following chapter is aimed at investigating TZ decentration in eyes with moderate amounts of corneal toricity using toric OK lenses.

CHAPTER 6 TREATMENT ZONE DECENTRATION DURING TORIC ORTHOKERATOLOGY ON EYES WITH 1.50 TO 3.50 DC OF CORNEAL TORICITY

6.1 INTRODUCTION

In response to poor clinical outcomes from spherical orthokeratology (OK) lenses when fit to highly toric corneas a number of OK lens manufacturers have developed toric OK lens designs. In Chapter 5 it was shown that TZ decentration is positively associated with corneal toricity, with TZ decentration increasing with higher degrees of corneal toricity. An important factor influencing the increase in TZ decentration is the greater mismatch between the spherical back surface of the OK lens and the toroidal surface of the cornea, with greater amounts of corneal toricity leading to increasingly excessive edge lift along the steep meridian. The principle underlying toric OK lens designs is to create a toroidal back surface either in the peripheral bearing curves alone, or across the whole back surface of the lens, to provide greater conformity between the back surface of the lens and the cornea.

To date there has been little scientific research published on toric lens designs, however the case reports and large sample studies that have reported on the performance of toric OK lenses have shown promising results in reducing refractive astigmatism (Chan et al. 2009, Baertschi and Wyss 2010, Chen et al. 2012, Chen and Cho 2012). Although reduction in astigmatism has been reported, the current literature does not provide a detailed account on how these lenses perform relative to spherical OK lenses. Whether these advanced design lenses tend to improve TZ centration and achieve a better OK effect through improved lens to cornea alignment is not known.

The purpose of the current study is to investigate whether toric OK lenses improve TZ centration and refractive and corneal topography outcomes relative to spherical OK lenses in moderately toric corneas. A major difficulty that was faced was the limited availability of lens designs and the logistical problem of importing them from overseas. This difficulty was compounded by the low prevalence (10.8%) of higher amounts of astigmatism in the general population (Young et al. 2011). Consequently observations were limited to four participants.

6.2 MATERIALS AND METHODS

6.2.1 Study design

Participants with 1.50 to 3.50 DC of corneal toricity in both eyes were enrolled prospectively. OK lenses with toric periphery design were fitted empirically for overnight wear in both eyes. Study measurements were taken at baseline, and after the first (day 1) and seventh (day 7) nights of lens wear, in the morning within 1 hour of lens removal on waking. Changes from baseline to corneal topography, refraction and visual acuity were assessed. TZ decentration was measured and compared between spherical and toric OK lenses. Individual participant data were evaluated to identify the key influential characteristics of the toric OK lens-to-cornea fitting relationship on clinical outcomes. The study obtained approval from the UNSW Human Research Ethics Advisory Panel (Approval No. HREA 11065) and participants were treated in accordance with the tenets of the Declaration of Helsinki. Informed written consent was also obtained from the participants prior to enrolment.

6.2.1.1 Participants

Three participants were recruited from the earlier study described in Chapter 5, which investigated the effects of spherical OK lenses on moderately toric corneas (Group 2, 1.50 to 3.50 DC central corneal toricity). The participant data from the conventional fitting lens that was investigated in this earlier study provided the control data in this current study. A further participant with corneal toricity 1.50 to 3.50D was recruited from a response to advertising posters that had been displayed within the University of New South Wales (UNSW), Sydney, Australia. Because this participant had not been involved in the study described in Chapter 5 there was no spherical OK control data, so before proceeding to toric lens wear this participant was fitted with a spherical OK lens using a conventional method in one eye, selected by coin toss, for a single night of lens wear as described in Section 5.2.1.1.3. After a 3 week washout period of no lens wear the participant proceeded to toric OK lens fitting.

6.2.2 Contact lens design

The toric OK lens used in this study was the DreamLite TRX toric periphery reverse geometry lens design manufactured by Procornea, The Netherlands in Boston XO material (Dk 100 ISO/Fatt; Bausch & Lomb, Boston). The DreamLite TRX is available in total lens diameters of 10.10, 10.50, 10.90 and 11.30 mm with an optic zone diameter of 6 mm. The central base curve of the lens is spherical and the peripheral curves, which include the reverse curve and the alignment curves, are toroidal.

Although both eyes were fitted using a toric periphery OK lens design, only data from the eyes that were fitted with spherical OK lenses conventionally for one single night were chosen for analysis. The purpose of fitting the non-analysed eye with toric OK lens was to ensure good binocular vision for participants during the lens wearing period.

6.2.3 Contact lens fitting and dispensing

6.2.3.1 Lens fitting

The DreamLite TRZ toric OK lens design was fitted following the empirical method described by the manufacturer. The lens design parameters are based on corneal elevation data from a single corneal topography image, which in this case was captured using the Medmont E300. EyeLite proprietary contact lens fitting software (version 2012/3) provided by Procornea was used to determine the lens parameters based on the imported corneal topography elevation data. The software also required manual entry of unaided visual acuity, subjective refraction in conventional form (spherical, cylinder and axis), best corrected visual acuity, vertex distance (the distance from the back surface of the corrective lens to the corneal apex in mm) and horizontal visible iris diameter in mm. The full lens design parameters were then electronically transmitted to the manufacturing laboratory. The spherical back optic zone radius and the radii of curvatures of the peripheral curves were determined to provide 8 μm tear layer thickness at the corneal apex based on the sag-based fitting technique.

6.2.3.2 Lens dispensing

Participants were requested to return to the clinic once the lenses had been received. After checking ocular integrity using the slit lamp biomicroscope the lenses were inserted and the dynamic and static fit assessed using white light and blue light following instillation of sodium fluorescein dye. All participants were taught how to insert, remove and care for their lenses. Along with study lenses a lens case, Boston Advance Cleaner, Boston Advance Conditioning Solution and Bausch & Lomb Sensitive Eyes Saline Solution (Bausch & Lomb Australia, Sydney, Australia) were issued for lens care. Written instructions were also given on lens handling and care.

Participants were advised to insert study contact lenses before sleeping. The study protocol required participants to return to the clinic in the morning after the first night of lens wear while still wearing the lenses. However, when the first participant returned for their first overnight visit, it was apparent to the lead investigator (VM) that lens movement during open

eye wear was interfering with lens centration and creating a possible detrimental influence on TZ centration. To overcome this possible bias the study protocol was altered to request the participants to remove the lenses on waking and to attend for study visits as soon as feasibly possible after lens removal. The participant who had already attended for their first overnight wear study visit was asked to discontinue wear for one month to recover from any effects before restarting lens wear following the changed study protocol. The other participants were advised to follow this changed protocol and present to the clinic within one hour after eye opening without the lens in the eye.

6.2.4 Study measurements

Study measurements were taken in the following order.

6.2.4.1 Slit lamp biomicroscopy

Slit lamp biomicroscopy was performed at baseline and at all study visits to monitor eye health. The same procedure as described in Section 2.2.3.3 was followed.

6.2.4.2 Visual acuity

High contrast unaided and best corrected visual acuity were assessed and recorded using logarithm of minimum angle of resolution (Log MAR) notation. The same procedure as described in Section 2.2.3.2 was followed.

6.2.4.3 Objective and subjective refraction

For objective refraction, the same procedure as described in Section 2.2.3.1 was followed. Subjective refraction was performed using standard optometric procedures at all visits.

6.2.4.4 Corneal topography

The same procedure as described in Section 2.2.3.4 was followed. A total of eight topographic maps were captured from each eye. Topographic maps with artefacts and distorted mires were eliminated and the remaining maps were used for analysis.

6.2.4.5 Treatment zone variables

In eyes fitted with spherical OK lenses the treatment zone (TZ) variables including magnitude of decentration and its orientation were measured using the transparency grid method described in Section 5.2.4. The same TZ variables in addition to horizontal TZ diameter were measured in eyes fitted with toric OK lenses both at day 1 and day 7 using the MATLAB program described in Section 3.2.2.3.

6.2.5 Statistical analysis

Statistical analyses were performed when definitive trends in the mean group changes associated with minimal variation were observed. Student t-tests were performed between two groups and a p value < 0.05 denoted a statistically significant change between groups. The Student t-test is used when comparing the means of two groups and assumes that the data in each of the two groups follow normal distribution. To assess normality of each group the Shapiro-Wilk's test for normality was used (See Section 2.2.9). The Student t-test was performed only if the normality assumption was satisfied.

6.3 RESULTS

Four East Asians, with central corneal toricity between 1.50 and 3.50 DC were enrolled in this exploratory study. The mean age of the participants was 28.00 ± 11.46 years. The individual participant age, sex and the eye that was considered for the study analysis are given in Table 6-1. The mean duration between lens removal after waking and the time at which the study measurements were taken ranged between 40 – 120 minutes (day 1 = 77.30 ± 33.02 minutes and day 7 = 87.30 ± 30.08 minutes). The parameters of the DreamLite TRX toric periphery lenses dispensed to each participant are given in Table 6-2. The baseline corneal and refractive parameters are given in Table 6-3 and Table 6-4 respectively.

Participant No	Age (years)	Sex	Eye
P1	45	Male	Left
P2	23	Male	Right
P3	24	Female	Left
P4	20	Female	Right

Table 6-1. Individual participant's age, sex and study eye.

Participant No	Back optic zone radius	Radius of curvature of Reverse curve1/ Reverse curve2	Radius of curvature of Alignment curve1/ Alignment curve2
P1	8.85	7.60/6.90	8.10/7.75
P2	8.75	6.90/6.00	7.80/7.30
P3	8.50	6.85/6.50	7.55/7.35
P4	9.30	7.50/6.50	8.30/7.80

Table 6-2. The parameters of the DreamLite TRX toric periphery reverse geometry contact lenses dispensed to each participant. All measurements are in mm. The total diameter was 10.90 mm and the back vertex power was +0.75 dioptres in all cases.

Participant No	steep K	flat K	Central corneal toricity	Peripheral corneal toricity	Corneal M	Corneal J_{180}	Corneal J_{45}
P1	43.03	40.84	2.19	2.82	41.94	−1.05	0.32
P2	45.83	42.93	2.90	5.66	44.38	−1.41	0.30
P3	45.47	43.93	1.54	0.70	44.70	−0.75	0.05
P4	43.43	40.38	3.05	3.21	41.91	−1.52	−0.13
Mean ± SD	44.44 ± 1.41	42.02 ± 1.69	2.42 ± 0.70	3.09 ± 2.03	43.23 ± 1.52	−1.18 ± 0.35	0.14 ± 0.21

Table 6-3. Baseline corneal parameters (in dioptres) for each participant and group mean ± SD.

Participant No	Refractive sphere	Refractive cylinder	Refractive cylinder axis (degrees)	Refractive M	Refractive J_{180}	Refractive J_{45}
1	−2.75	−2.50	5	−4.00	1.23	0.22
2	−4.00	−1.50	175	−4.75	0.74	−0.13
3	−3.75	−0.50	155	−4.00	0.16	−0.19
4	−3.50	−3.00	10	−5.00	1.41	0.51
Mean ± SD	−3.50 ± 0.54	−1.88 ± 1.11	–	−4.44 ± 0.52	0.88 ± 0.56	0.10 ± 0.33

Table 6-4. Baseline refractive parameters (in dioptres) for each participant and group mean ± SD.

Among all participants, participant P3 exhibited the least amount of central corneal toricity at 1.54 DC and the least amount of peripheral corneal toricity at 0.70 DC. P4 exhibited the greatest amount of central corneal toricity at 3.05 DC with 3.21 DC of peripheral toricity. P2 was unusual because although exhibiting the greatest amount of peripheral corneal toricity at 5.66 DC, central toricity measured at 2.90 DC was close to half of this amount. According to the classification of corneal toricity based on extent (Section 5.2.3.3), all participants exhibited limbus-to-limbus corneal toricity (Type-3) except participant P3, who exhibited central corneal toricity only (Type-2). All participants also had with-the-rule corneal toricity in the study eyes.

Among all participants, participant P3 exhibited the least (−0.50 DC) and participant P4 exhibited the greatest (−3.00 DC) amount of refractive astigmatism which was consistent with measured corneal toricity. In all participants refractive astigmatism was classified as with-the-rule (WTR), again consistent with what was found for corneal toricity.

6.3.1 Corneal topography changes

Figure 6-1 shows coloured refractive power difference maps (Post OK – Pre OK) derived from the Medmont E300 corneal topographer at day 1 in spherical OK lens wear (left panel), and day 1 (middle panel) and day 7 (right panel) in toric OK lens wear for all participants. Consistent with previous figures depicting corneal topography difference maps, blue colours reveal a reduction in corneal power, red colours reveal an increase in corneal power, and green reflects no change. After OK, the central blue zone in the coloured topographic difference maps indicates the TZ. From the figures it is clearly evident that after a single overnight wear of spherical OK the borders of the TZ are far less distinct in all participants than was found after toric OK lens wear. Furthermore, the TZ after toric OK appears to increase in size and become more defined by day 7, giving a visual indication of improved clinical outcome with further nights of lens wear.

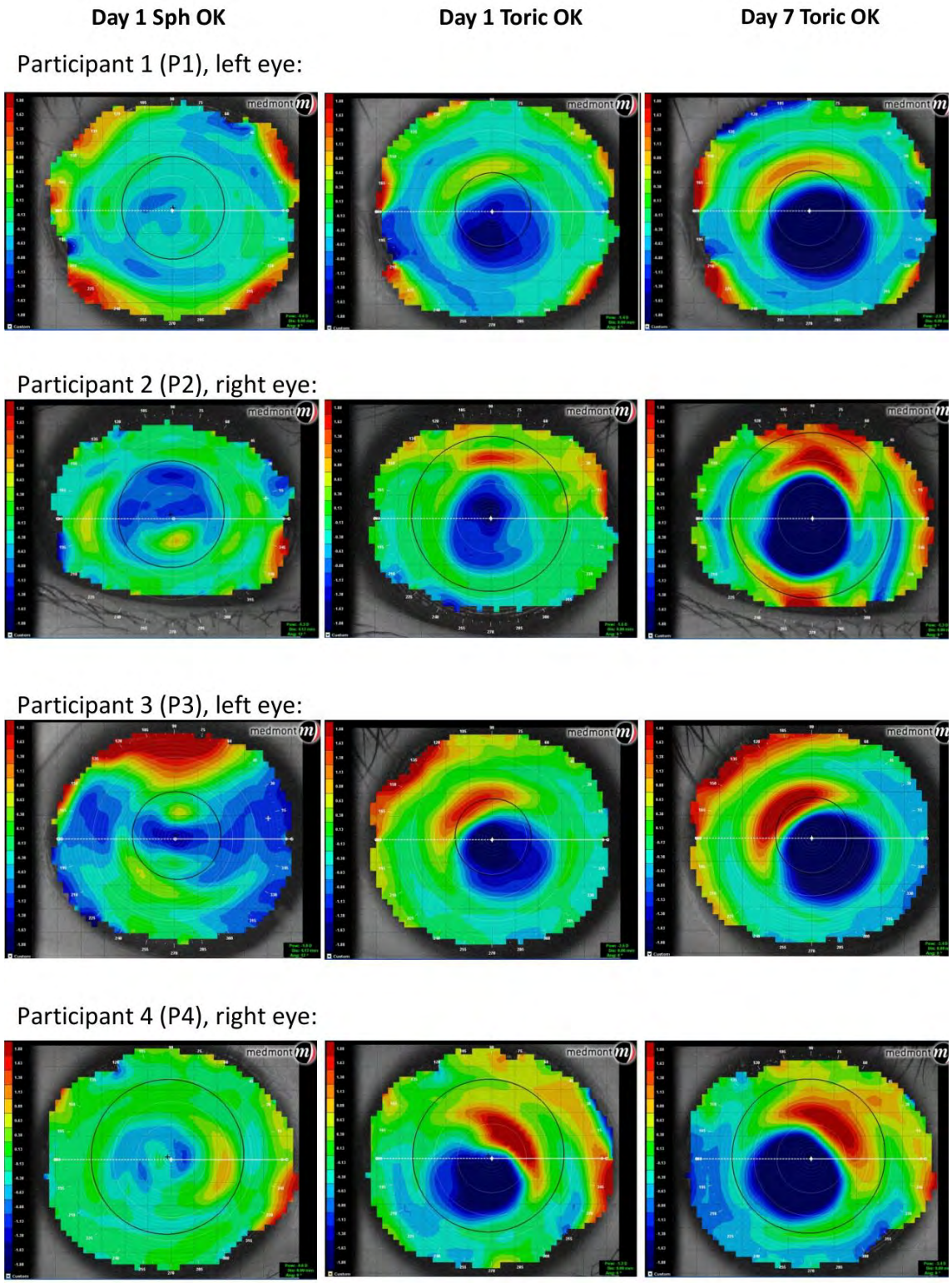

Figure 6-1. Corneal refractive power difference maps (post treatment – pre-treatment) derived from the Medmont E300 corneal topographer at day 1 after spherical orthokeratology (OK) lens wear (left panel), and day 1 (middle panel) and day 7 (right panel) after toric OK lens wear in all participants. An identical colour scale was set for all maps for comparison purposes.

6.3.2 Changes to corneal parameters

6.3.2.1 Changes in steep K and flat K

Figure 6-2 shows mean and individual changes from baseline noted in the flat and steep corneal meridians from baseline after spherical and toric OK lens wear. Participants P1 and P2 were the closest to showing the anticipated response from toric OK, with both showing similar degrees of flattening of flat K that were found with spherical OK. In these two participants similar degrees of flattening of steep K between spherical OK and toric OK were also apparent after the first night of lens wear. However by day 7 there was a much greater flattening effect for steep K which flattened by −1.48 D for P1 and by −3.18 D for P2, compared to −0.22 D and −0.57 D after spherical OK respectively. In P3, flat K showed a similar flattening response to that found with P1 and P2, however there was no apparent change in steep K. It is also interesting to note that for this subject flattening of steep K was found after spherical OK. P4 revealed a delayed response for steep K with no apparent change at day 1, but flattening apparent by day 7. The interesting outcome with this participant was that flat K flattened with spherical OK at a similar rate as the other participants, however toric OK provided the opposite profile of effect through steepening of flat K at day 1. By day 7 a similar degree of flattening to that found with spherical OK was apparent (−0.35 D in spherical OK, −0.32 D in toric OK).

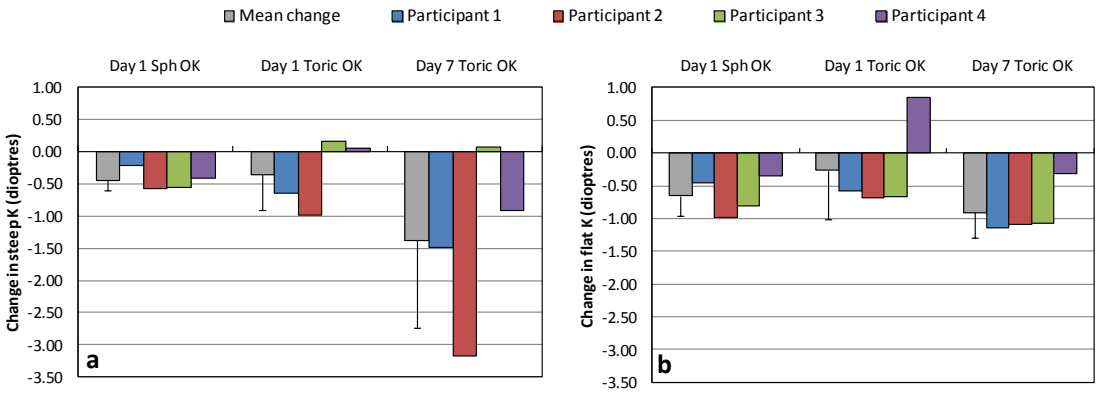

Figure 6-2. Mean and individual changes from baseline in (a) steep K and (b) flat K after one night of spherical orthokeratology lens wear (Day 1 Sph OK) and after 1 night (Day 1 Toric OK) and 7 nights (Day 7 Toric OK) of toric orthokeratology lens wear in four study participants. The error bars for the group mean represent standard deviation of the mean.

Although subject numbers were too low to perform valid statistical analysis, the average group values can be used to make some observations. Both steep and flat K showed a trend towards flattening after toric OK, with the appearance of greater flattening from day 1 to day 7. A trend towards flattening of steep and flat K was also found after one night of spherical OK, which is similar in value to that seen after one night of toric OK.

6.3.2.2 Changes in central corneal toricity

In participants P1, P2 and P3 spherical OK had the effect of inducing a small increase in corneal toricity with an average value across all participants of 0.21 ± 0.20D (Figure 6-3). The effect of changes to flat and steep K on change to corneal toricity were more varied after toric OK. In P1 and P2 there was no clinically significant change to corneal toricity at day 1 (P1 = −0.07 DC; P2 = −0.29 DC), but a reduction in corneal toricity was apparent by day 7 (P1 = −0.34 DC; P2 = −2.09 DC). These changes reflect that there was greater flattening of steep K than flat K in these two participants. In P3 there was only flattening of flat K and no clinically significant change to steep K at day 1 and day 7, which led to an increase in corneal toricity that increased from 0.82 DC at day 1 to 1.15 DC at day 7. In P4 the steepening effect of flat K at day 1 had the effect of reducing corneal toricity by −0.79 DC. By day 7 flat K instead flattened, accompanied by flattening of steep K. The difference between the meridians remained static however, leading to −0.59 DC reduction of corneal toricity, similar to that found at day 1.

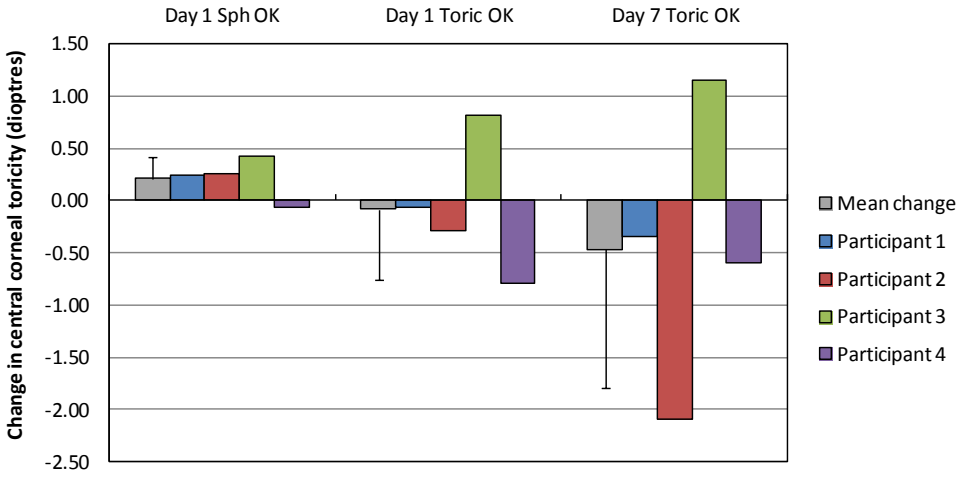

Figure 6-3. Mean and individual changes from baseline in corneal toricity after one night of spherical orthokeratology (OK) lens wear (Day 1 Sph OK) and after 1 night (Day 1 Toric OK) and 7 nights (Day 7 Toric OK) of toric OK lens wear in four study participants. The error bars for the group mean represent standard deviation of the mean.

Again, although subject numbers were too low to provide useful statistical analysis, there was a group averaged trend towards greater reduction in corneal toricity over time, with −0.08 ± 0.67 DC reduction after 1 night of lens wear and −0.47 ± 0.67 DC reduction after 7 nights of lens wear. However there were significant individual variations in response.

6.3.2.3 Changes in corneal vector components

Corneal vector components describe spherical equivalent corneal curvature, and corneal curvature in the horizontal/vertical meridians (J_{180}) and oblique 45/135° meridians (J_{45}). All participants showed similar responses in corneal M after spherical OK which, when considered as a group, averaged −0.55 ± 0.22 D (Figure 6-4). This represents a reduction in the power of the cornea, in effect creating the desired response of an hyperopic shift in refraction. There was minimal change to J_{180} in any of the participants (Figure 6-5a), but there was a noticeable though varied effect on corneal J_{45} after one night of spherical OK (Figure 6-5b). Whereas participants P2 and P3 revealed a positive dioptric shift in J_{45}, P4 instead revealed a negative dioptric shift. No change to J_{45} after spherical OK was apparent in P1.

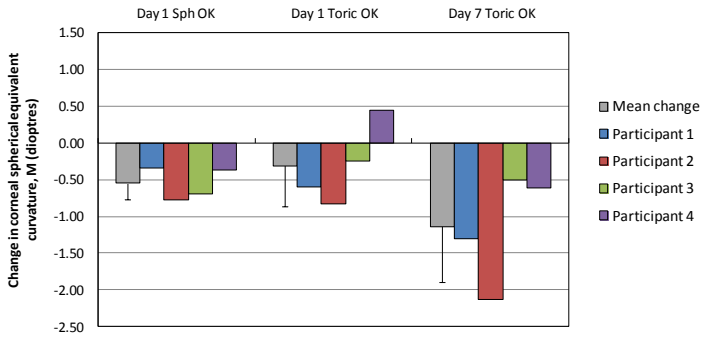

Figure 6-4. Mean and individual changes from baseline in spherical equivalent corneal curvature M after one night of spherical orthokeratology (OK) lens wear (Day 1 Sph OK) and after 1 night (Day 1 Toric OK) and 7 nights (Day 7 Toric OK) of toric OK lens wear in four study participants. The error bars for the group mean represent standard deviation of the mean.

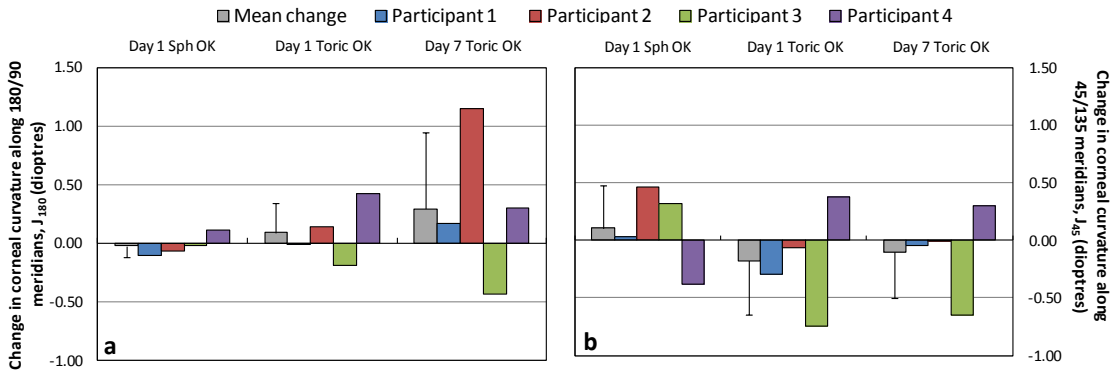

Figure 6-5. Mean and individual changes from baseline in (a) corneal J_{180} and (b) corneal J_{45} after one night of spherical orthokeratology (OK) lens wear (Day 1 Sph OK) and after 1 night (Day 1 Toric OK) and 7 nights (Day 7 Toric OK) of toric OK lens wear in four study participants. The error bars for the group mean represent standard deviation of the mean.

After one night of toric OK (Figure 6-4) participants P1, P2 and P3 showed the desired response of a negative dioptric shift in corneal M, while P4 showed the opposite response of a positive shift in corneal M. By day 7 all participants revealed a negative dioptric shift in corneal M refraction, which was greater than measured at day 1. When considering mean group values, corneal M revealed a trend towards a negative shift of −0.31 ± 0.56 D after one night of toric OK lens wear, with a trend towards a greater mean group change after 7 nights of OK lens wear (−1.14 ± 0.75D). The change between day 1 and day 7 was statistically significant (−0.83 ± 0.45 D, $p < 0.05$).

Changes to corneal J_{180} after toric OK lens wear (Figure 6-5a) followed a similar pattern of change to that reported in corneal toricity above. This is perhaps not surprising because all of the participants had with-the-rule corneal toricity, meaning that the axis orientation of their toricity would be aligned closely to the J_{180} meridian. In P1 and P2 there was no clinically significant change in corneal J_{180} at day 1 after toric OK, but a positive dioptric shift was apparent by day 7 (P1 = 0.17 D; P2 = 1.15 D). In P3 there was a negative shift in J_{180} of −0.19 D at day 1, which increased to −0.44 D by day 7. In P4 there was a similar positive shift in J_{180} at day 1 (0.42 D) and day 7 (0.30 D).

Changes to corneal J_{45} were minimal after toric OK (Figure 6-5b) in all participants except P3, who revealed a negative shift in J_{45} by −0.74 D at day 1 and −0.65 D at day 7. Realising that J_{45} represents change along the 45/135° meridians offers a possible explanation, because P3 had baseline refractive astigmatism at 155°, meaning that lens orientation along

this meridian would lead to changes to corneal curvature that were more likely to influence the closer aligned J_{45} meridian than the horizontal J_{180} meridian.

6.3.3 Changes in subjective refraction vector components

Changes in subjective refraction components were recorded only after toric OK lens wear and not with spherical OK lens wear. This is because the spherical OK data reported in this current study was gained from the study reported in Chapter 5, which had the prime purpose to investigate the influence of spherical OK on TZ decentration. Consequently there are no refraction data available for analysis.

Figure 6-6 shows group mean change and change in individual cases in subjective refractive sphere from baseline after toric OK lens wear. There were similar degrees of change to M refraction across all participants at day 1 with greater change at day 7. When described as mean group values this equates to a mean positive shift in M refraction of 1.34 ± 0.36 D after 1 night of lens wear and 3.66 ± 0.51 D after 7 nights. The change between day 1 and day 7 in refractive M was statistically significant (2.31 ± 0.84 D, $p < 0.05$).

Figure 6-7 shows group mean change and change in individual cases in refractive J_{180} and refractive J_{45} from baseline after toric OK lens wear. Minimal changes were observed in the refractive vector astigmatic J_{180} and J_{45} at day 1, but some interesting trends were seen by day 7. For J_{180}, subjects P1, P3 and P4 revealed the desired response to correct astigmatism, with approximately 0.75 - 1.00D reduction in refractive J_{180}, while P2 instead showed no clinically significant change. This reveals the complexity of the changes to corneal curvature and induced refractive effect in individual participants. For participants P1 and P4 the effect on refractive J_{180} followed that expected from the positive dioptric shift in corneal J_{180} that was measured at the same interval. However, for P2 the positive dioptric shift in corneal J_{180} that was measured at Day 7, which was larger than that measured for P1 and P4, failed to translate to any noticeable effect on refractive J_{180}. The negative shift in change in refractive J_{180} is not consistent with the negative shift in change in corneal J_{180}. A possible factor here is that participant P3 had the smallest amount of corneal toricity (1.54 D), and this may be too low to gain any benefit from toric periphery OK lens designs.

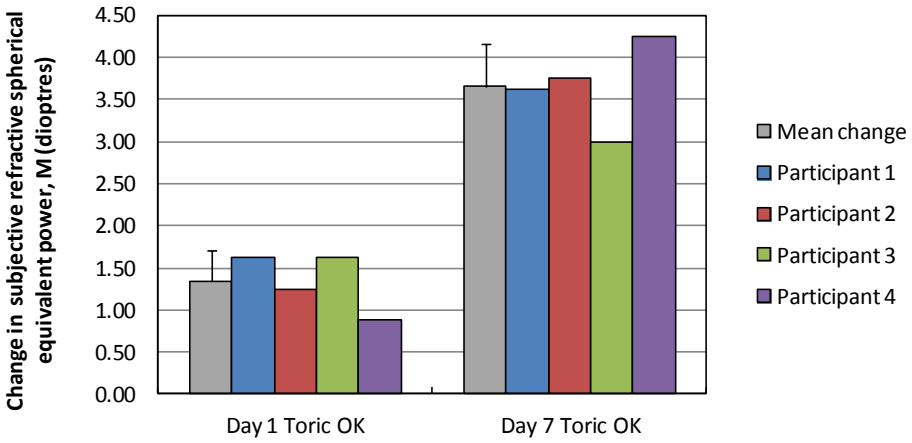

Figure 6-6. Mean and individual changes from baseline in refractive mean sphere M after 1 night (Day 1 Toric OK) and 7 nights (Day 7 Toric OK) of toric orthokeratology lens wear in four study participants. The error bars for group mean represent standard deviation of the mean.

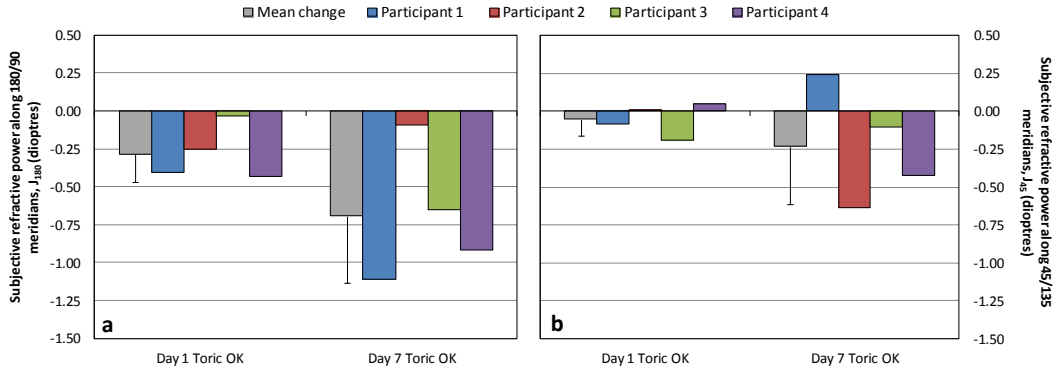

Figure 6-7. Mean and individual changes from baseline in (a) refractive J_{180} and (b) refractive J_{45} after one night (Day 1 Toric OK) and 7 nights (Day 7 Toric OK) of toric orthokeratology lens wear in all four study participants. The error bars for group mean represent standard deviation of the mean.

At day 7, participants P1 and P3 revealed minimal change to refractive J_{45} whereas P2 and P4 revealed a clinically significant induction of around −0.50D in J_{45} at Day 7. For P4 this reflected the change that was seen in corneal J_{45} astigmatism, but for P2 there had been no change in corneal J_{45} astigmatism. P2 differed from the other participants in having a larger amount of peripheral corneal toricity relative to central corneal toricity, which raises the question whether this factor could be in any way be responsible for the change to J_{45} that was induced by toric OK lens wear.

6.3.4 Changes to unaided logMAR visual acuity

All four participants reached similar levels of unaided logMAR acuity after 7 nights of toric OK lens wear, with P3 reaching logMAR 0.10 (Snellen equivalent = 6/7.5) and P1, P2 and P4 reaching around 0.20 log MAR (Snellen equivalent = 6/9.5) (Figure 6-8). These outcomes give confidence that the toric OK lenses were effective in reducing refractive astigmatism, particularly in P1 and P4 who had the largest baseline astigmatism, which if considered in isolation by correcting spherical error alone, would be expected to retain blur to the equivalent of approximately logMAR 0.40 (Snellen equivalent = 6/15) (Wolffsohn et al. 2011).

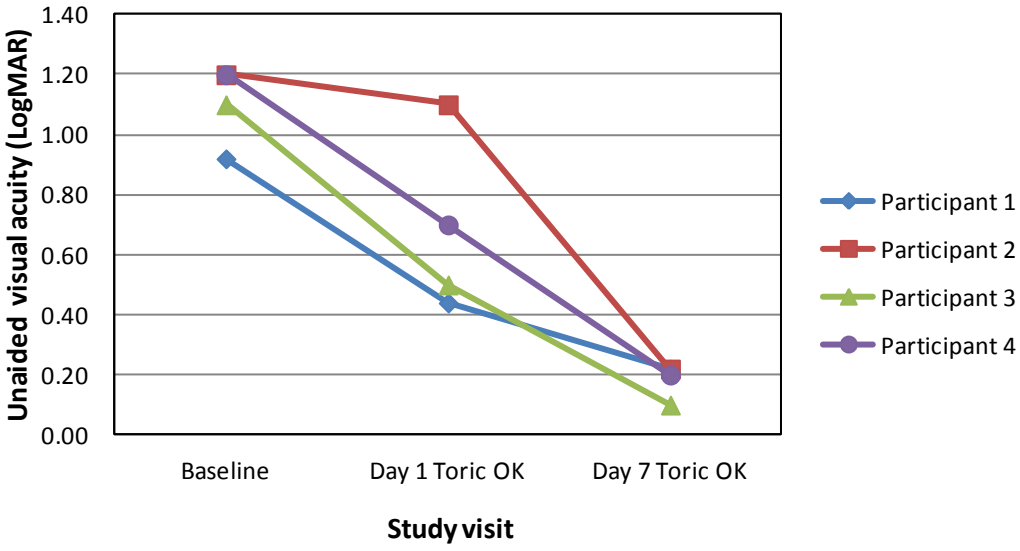

Figure 6-8. Unaided logarithm of minimum angle of resolution (LogMAR) visual acuity at baseline, after one night of toric orthokeratology (OK) lens wear (Day 1 Toric OK), and after 7 nights (Day 7 Toric OK) of toric OK lens wear in four study participants.

6.3.5 Treatment zone variables

6.3.5.1 Horizontal TZ diameter

The horizontal TZ diameter was not assessed at the day 1 visit after spherical OK lens wear because in all cases the TZ margins could not be reliably identified. The horizontal TZ diameters induced by toric OK in all four participants at day 1 and day 7 are presented in Figure 6-9. In participant P1, the magnitude of horizontal TZ diameter was almost the same day 1 (4.89 mm) and day 7 (4.88 mm). In P2, the horizontal TZ diameter reduced over time from 4.69 mm at day 1 to 4.33 mm by day 7. P3 and P4 followed the opposite profile of an increase over time, in P3 from 3.71 to 4.35 mm and in P4 from 3.34 to 4.20 mm.

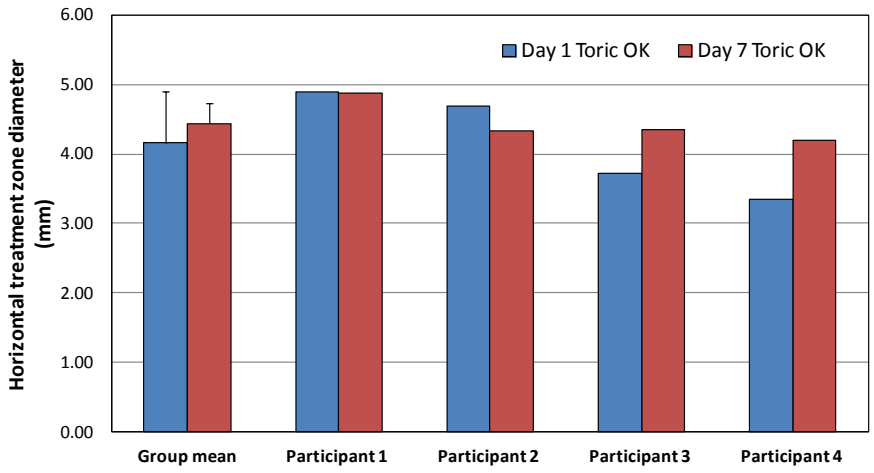

Figure 6-9. Magnitude of horizontal treatment zone diameter, after one night (Day 1 Toric OK), and after 7 nights (Day 7 Toric OK)of toric orthokeratology (OK) lens wear in four study participants. The error bars for group mean represent standard deviation of the mean.

6.3.5.2 TZ decentration

The polar magnitude and angle of TZ decentration, and horizontal (X) and vertical (Y) decentration, at day 1 and day 7 with toric OK lens wear are given in Table 6-5 and also presented in Figure 6-10. A paired t-test on the magnitude of TZ decentration at day 1 between spherical OK lens wear and toric OK lens wear revealed a significant increase in TZ decentration (0.42 ± 0.15 mm, $p < 0.05$) in eyes with moderate corneal toricity fitted with toric OK lenses. During spherical OK lens wear for one night, participants P1, P3 and P4 showed a magnitude of TZ decentration close to 1 mm and only in participant P2 the magnitude of TZ decentration was minimal at 0.18 mm. During toric OK lens wear, at day 1 all participants except participant P2 showed TZ decentration that was greater than 1.00 mm. Participant P2 showed the least amount of decentration (0.55 mm). There was no clinically appreciable

difference in the magnitude of TZ decentration between day 1 and day 7 of toric OK lens wear for all participants.

Participant	Polar decentration		X decentration (mm)	Y decentration (mm)
	Magnitude (mm)	Angle (degrees)		
	Day 1 Sph OK			
P1	0.86	325*	0.70*	−0.50
P2	0.18	144	−0.15	0.11
P3	1.03	231*	−0.65*	−0.80
P4	1.04	190	−1.03	−0.17
Mean ± SD	0.78 ± 0.41	-	−0.28 ± 0.75	−0.34 ± 0.40
	Day 1 Toric OK			
P1	1.44	250*	−0.48*	−1.36
P2	0.55	309	0.35	−0.43
P3	1.27	237*	−0.70*	−1.07
P4	1.54	229	−1.00	−1.17
Mean ± SD	1.20 ± 0.45	-	−0.46 ± 0.58	−1.01± 0.40
	Day 7 Toric OK			
P1	1.47	252*	−0.45*	−1.39
P2	0.47	238	−0.25	−0.40
P3	1.31	229*	−0.87*	−0.99
P4	1.25	223	−0.92	−0.85
Mean ± SD	1.13 ± 0.45	-	−0.62 ± 0.33	−0.91 ± 0.41

Table 6-5. Magnitude of treatment zone parameters after 1 night of spherical orthokeratology (OK) lens wear (Day 1 Sph OK), and after 1 night (Day 1 Toric OK) and 7 nights (Day 7 Toric OK) of toric OK lens wear in four study participants. '*' indicates that the decentration direction for left eyes were presented as if they were right eyes.

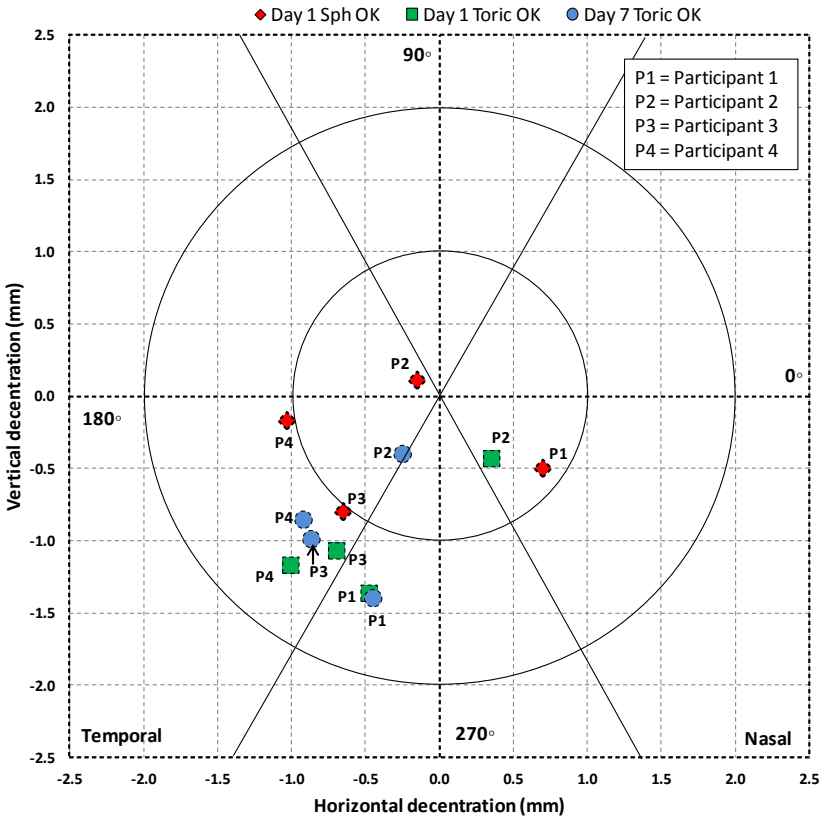

Figure 6-10. Decentration of treatment zone from the vertex normal after 1 night of spherical orthokeratology (OK) lens wear (Day 1 Sph OK), and 1 night (Day 1 Toric OK) and 7 nights (Day 7 Toric OK) of toric OK lens wear in four study participants. Note that the decentration for left eyes was presented as if they were right eyes.

6.3.6 Relationship between corneal parameters and TZ decentration

6.3.6.1 Baseline central corneal toricity and magnitude of TZ decentration

Figure 6-11a shows the relationship between baseline central corneal toricity and the magnitude of TZ decentration in all four participants at day 1 after spherical OK lens wear and at day 1 and day 7 after toric OK lens wear. It is apparent from these observations that there is considerable variability in the relationship between baseline central corneal toricity and TZ decentration after 1 night of spherical OK lens wear, with no obvious relationship between these factors. There is a tendency towards TZ decentration increasing with baseline corneal toricity after 1 night of toric OK in participants P1, P3 and P4, although this trend does not remain by day 7. Furthermore participant P2 reveals a completely different outcome by having the one of the highest levels of central corneal toricity among the four participants, yet the lowest amount of TZ decentration after spherical as well as toric OK.

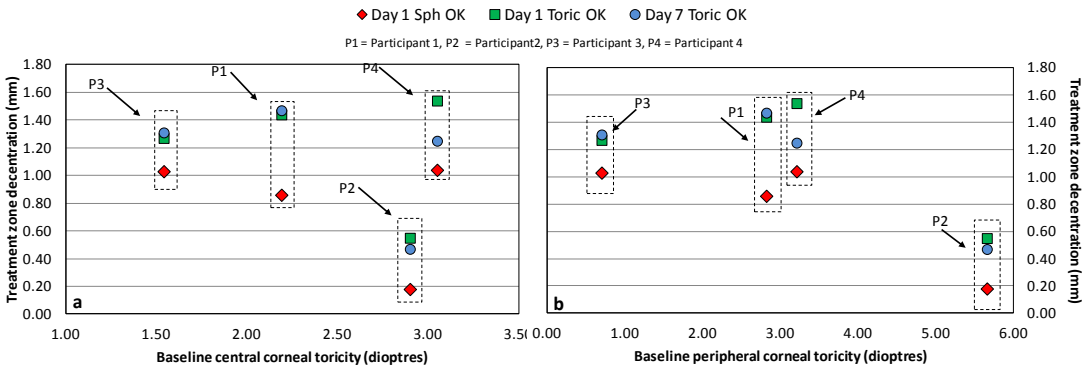

Figure 6-11. Relationship between baseline (a) central and (b) peripheral corneal toricity and the magnitude of treatment zone decentration at day 1 with spherical orthokeratology (OK) lens (Day 1 Sph OK), at day 1 (Day 1 Toric OK) and at day 7 (Day 7 Toric OK) with toric OK lens wear in four study participants.

6.3.6.2 Baseline peripheral corneal toricity and the magnitude of TZ decentration

Figure 6-11b shows the relationship between baseline peripheral corneal toricity and the magnitude of TZ decentration in all four participants at day 1 after spherical OK lens wear and at day 1 and day 7 after toric OK lens wear. Participants P1, P3 and P4 show similar amounts of TZ decentration regardless of the amount of peripheral corneal toricity measured at baseline. Participant P2 was the exception who revealed the smallest amount of TZ decentration regardless of wearing spherical or toric OK lenses. The excellent centration in this participant with high central and peripheral toricity may represent a success for the concept of peripheral toric OK lenses. However this case is particularly interesting because good centration was also found with spherical OK lenses. It may be that other factors that can

influence lens centration such as eyelid pressure may have played an important role in this particular case, and this highlights the complexity of the relationships between corneal shape, OK lens design and other influences on lens centration.

6.4 DISCUSSION

This study has shown that when comparing OK-induced changes to corneal topography between spherical OK lenses and toric OK lenses fitted to moderately toric corneas, toric OK lenses create a more consistent treatment zone area after 1 night of lens wear, which retains its definition after 7 nights of lens wear. Changes to corneal curvature, refraction and treatment zone parameters were investigated, and although only four subjects were included in the analysis, some interesting observations were made. When considered alongside the previous work that has been presented in this thesis, these observations provide useful insight into how toric OK lens designs differ from spherical OK lenses in their influence on clinical outcomes in eyes with moderate corneal toricity.

Changes to corneal curvature were measured along the principal flat and steep corneal meridians, with these then converted to vector components to allow more accurate comparisons to be made across the participant cohort. Spherical OK caused flattening of both the flat and steep corneal meridians after a single night of lens wear. Greater flattening was found in the flat meridian, leading to a greater disparity between the two meridians and consequent increase in corneal toricity. This outcome is consistent with previous studies that have been reported in Chapter 5 of this thesis. After one night of toric OK, three of the four participants (P1, P2, P4) revealed a similar response to that found with spherical OK, however by day 7 greater flattening to the steep meridian relative to the flat meridian was achieved in these three participants, leading to the desired response of an overall reduction in corneal toricity. A positive observation from toric OK is that the increased change to corneal curvature with longer periods of overnight wear is consistent with what has been reported for spherical OK on minimally toric corneas (Soni et al. 2003, Sorbara et al. 2005).

Participant P3 was the exception in this cohort, by showing just over 1.00 D of flattening of the flat meridian but no apparent clinically significant change in the steep meridian, which in combination led to the undesirable response of an increase to corneal toricity. An interesting factor here is that P3 had the least amount of central corneal toricity (1.54 D) and peripheral toricity (0.70D) of all four participants. Given that the aim of toric OK lens designs is to improve the peripheral lens fit alignment, the absence of significant corneal

toricity in this participant may indicate a limiting factor for use of these lens designs, with a certain minimum level of peripheral corneal toricity required to provide clinically significant outcomes.

The vector component M describes the spherical equivalent component of corneal curvature. When considered as group mean values there was a negative dioptric shift in M after one night of toric OK which was similar to that found with spherical OK. A negative dioptric shift indicates a reduction in corneal power, which is the equivalent of inducing a myopic correction effect. Increasing toric OK lens wear to seven nights led to greater negative dioptric shift that was found to be statistically significant even with just the four participants that were included in this study. When considered as individual cases, participant P4 had the opposite effect of a positive dioptric shift in M after one night of toric OK, but this changed to the more desirable negative shift by 7 nights of lens wear. Participant P3 followed the group mean response of greater effect by Day 7, but by a reduced amount than was found for P1 and P2. As already discussed, toric OK induced minimal changes to the steep corneal meridian in P3 when compared to the other participants, which may explain the reduced response that was found for the refractive M component.

Vector components J_{180} and J_{45} describe corneal toricity in the horizontal/vertical and oblique 45/135° axes respectively. J_{180} showed no apparent change in any participant after spherical OK and only a minimal change of +0.49 D in P4 after one night of toric OK. By day 7 of toric OK lens wear there was a trend towards a positive dioptric shift in J_{180} for the group, with P2 showing the greatest response of +1.15 D and P3 the opposite response of −0.44 D. This observation helps explain the failure of P3 to show a good response to flattening of the steep corneal meridian and a change to M refraction when compared to the other participants. The low amount of baseline peripheral corneal toricity found in P3 is suggested as a possible explanation for the reduced effect on flattening of the steep corneal meridian. This is based on the concept that toric OK offers no real benefit over spherical OK if the primary purpose of toric OK is to improve alignment between the lens back surface and cornea. This same reasoning may also explain the increased response of J_{180} that was found in participant P2, because this participant had the greatest amount of peripheral corneal toricity in the cohort, meaning that they achieved the most benefit from the improved alignment that the toric periphery OK lens design would offer.

Overall, corneal J_{45} showed no apparent change with any lens type and visit combination when considered as mean group values. However, there were some interesting individual responses with respect in spherical as well as toric OK lens wear. After spherical OK, participants P2 and P3 showed a positive dioptric shift and P4 a negative dioptric shift in J_{45}. With toric OK, clinically significant changes were found only for P3 and P4, with P3 revealing a negative dioptric shift of approximately −0.50 D after 1 and 7 nights of lens wear, and P4 the opposite response of a positive dioptric shift at both measurement intervals. A negative shift in corneal J_{45} suggests steepening of the corneal meridian close to 45° or flattening of the corneal meridian close to 135°. Since participant P3 had a baseline refractive astigmatism with minus cylinder axis located at 155°, any reduction to corneal toricity would have a greater influence on the closer aligned J_{45} meridian than the horizontal J_{180} meridian. This offers an explanation for the change in J_{45} that was found for participant P3, while at the same time offering an explanation for the reduced effect on corneal J_{180} that was also found.

In the current study it was hypothesised that TZ decentration during toric OK on moderately toric corneas would be reduced in comparison to the decentration during spherical OK in corneas with similar amounts of toricity. In Chapter 5 it was shown that increasing amounts of baseline central corneal toricity would lead to an increase in TZ decentration. This tendency for TZ decentration was attributed to increasing misalignment between the toric corneal shape and spherical back surface of the OK lens, leading to poor stability of lens fit. The toric OK lenses used in the study reported here have toroidal peripheral curves which were designed to closely align with the toroidal corneal periphery and hence should lead to a more stable fit and an improved lens centration. However, this study revealed unexpected outcomes in showing that TZ decentration noted during toric OK lens wear on eyes with moderately toric corneas was in fact greater than noted during spherical OK on the same corneas.

Another important finding is that the TZ decentration at day 7 was found to be similar to the values measured at day 1 for all participants, meaning that measurements of TZ decentration at day 1 can be used reliably predict TZ centration with increased lens wear. Observations from larger samples are required to support this suggestion.

With toric OK lens wear, the TZ diameter with toric OK lenses ranged between 3.34 to 4.89 mm with uniform refractive effect across the TZ. After 1 week of toric OK lens wear the TZ diameter remained almost the same at day 1 in participant P1, but was reduced in P2 and increased in P3 and P4. It has been shown that during myopic OK the TZ diameter increases with longer duration of lens wear (Owens et al. 2004, Lu et al. 2007b). Thus the response

noted in participants P3 and P4 followed a typical response that is generally observed during spherical OK on minimally toric corneas.

It is also very encouraging to note that even at day 1 the TZ with toric OK was well defined when it is known that on day 1 the TZ margins are poorly defined during spherical OK lens wear (Owens et al. 2004). Further the TZ margins were clearly defined after toric OK lens wear compared with spherical OK lens wear, indicating that the TZ during spherical OK lens wear is more likely to suffer some degree of variability. A possible reason for the more defined TZ after toric OK is the generation of higher tear film fluid forces with these more complex lens designs. It has been proposed that the improved peripheral alignment of toric OK lenses compared to spherical OK lenses when fitted to toric corneas would help to trap tears behind the lens allowing more efficacious post-lens tear film forces to be generated (Caroline and Andre 2009). It is equally feasible that closer alignment between the lens and cornea in the periphery would improve lens centration and movement, because the direct compressive moulding forces from the lens would be more consistently concentrated at the corneal apex.

The purpose of altering corneal shape during spherical OK is to reduce spherical refractive error and during toric OK is to reduce both spherical and astigmatic components of refractive error. This response is required to ultimately provide good visual acuity for the wearer. For this reason it is realistic to expect changes to corneal shape to be reflected in refractive parameters. Refractive measurements in this study were available only from toric OK lens wear and not from spherical OK lens wear due to differences in the original study protocols. Changes in refractive M were consistent with changes observed in corneal M. Thus a greater change in corneal M led to a greater change in refractive M with increasing time of toric OK lens wear.

Refractive J_{180} showed some inconsistent responses relative to corneal J_{180}. One would expect that, a positive change in corneal J_{180} should lead to a negative change in refractive J_{180} and vice versa. For participants P1 and P4 the effect on J_{180} followed the expected trend. It is interesting to note that participant P2 showed a pronounced positive shift in corneal J_{180} measured at day 7, which failed to translate into an equivalent negative shift in refractive J_{180}. Participant P3 who showed a negative shift in corneal J_{180}, demonstrated a negative shift in refractive J_{180} instead of a positive shift.

Refractive J_{45} revealed approximately 0.50 D of negative shift in participants P2 and P4 at day 7, suggesting the induction of oblique astigmatism with minus cylinder axis located close to 135 degrees. It is reasonable to expect that this change in refractive astigmatism in these participants should have been accompanied by a positive shift in corneal J_{45}. But only participant P4 showed this expected positive shift in corneal J_{45}. Surprisingly, P2 who was expected to reveal greater amounts of positive shift in corneal J_{45} showed no change in corneal J_{45}. Participant P3 who revealed a greater amount of negative shift in corneal J_{45} did not show any noticeable effect on refractive J_{45}. It is interesting to note that participant P2 had a greater amount of peripheral corneal toricity relative to central corneal toricity at baseline, whereas participant P3 had a lesser amount of peripheral corneal toricity relative to central corneal toricity at baseline. One might therefore speculate that this distribution of toricity in the corneal centre versus periphery at baseline may have an effect on changes in refractive J_{45}.

The disagreement between changes in corneal topography and refraction was also shown during spherical orthokeratology on minimally toric corneas by Cheung and Cho (2004) previously. A possible reason for inconsistencies between corneal and refractive outcomes is that corneal measurements are performed over a 3 mm annular zone (Sim K) whereas subjective refraction components reflect refraction characteristics of a bundle of light rays entering through a corneal region overlying the pupillary area rather restricted it to a specific annular zone. Given that the pupil diameter (as shown in Figure 6-1) is larger in participants P2 and P4 may mean that the para-central steeper zone falls within the pupillary zone, and this may contribute to this inconsistency. The failure to observe consistencies between refractive J_{180} and J_{45} with respect to changes in corneal J_{180} and J_{45} reveals the complexity of the relationship between changes to corneal curvature and induced refractive effect. A more feasible way to investigate agreement between corneal and refractive changes is to consider all the regions overlying the pupillary zone. Hiraoka et al. (2004a, 2006) employed Fourier harmonic analysis and Zernike polynomials, and measured regular and irregular astigmatism and higher order irregularities in corneal shape. They correlated these changes to the amount of myopic correction achieved after spherical OK lens wear on eyes with minimum refractive astigmatism. If a similar type of analysis was applied to corneal changes after toric OK, this may reveal better agreement between corneal and refractive outcomes.

The outcomes in terms of improvements in unaided visual acuity during toric OK lens wear are very encouraging. All four participants reached similar levels of unaided logMAR visual acuity by day 7, with P3 reaching the equivalent of 6/7.5 (95%) and the other

participants achieving an equivalent of 6/9.5 (90%). This demonstrates that toric OK lenses may be effective in reducing visual blur due to astigmatism. This was apparent particularly in participants P1 and P4, who had the largest baseline refractive astigmatism that would have blurred visual acuity to at least approximately 6/15 (or 20/50) if only baseline spherical error had been corrected.

The alignment between the sag height of the OK lens and cornea is critical to the success of myopic OK. This is an important consideration in this current study which relied on empirical lens fitting of toric OK lenses. During spherical OK lens fitting. Corneal topographic maps are generally viewed after the first night of lens wear to assess if the lens sag is appropriate for the reduction of myopic refractive error. Of all participants in the current study only participant P2 revealed a bulls eye pattern at both post wear visits which is considered as a desirable outcome after spherical OK on minimally toric corneas. The other participants showed possible errors in alignment between the OK lens back surface and the toric cornea, leading to a superior arc of steepening at day 1 which became more defined by day 7. This is a vertically reversed image of what would be described as a smiley pattern, which indicates a flat fitting of OK lenses as a result of insufficient lens sag height. Because of this apparent flat fitting alignment the upper eyelid pulls the lens in a superior direction, leading to superior TZ decentration. Alternatively the inferior decentration noted for participants P1, P3 and P4 during toric OK lens wear may be related to the nature of the alignment of the lens with the toric corneal periphery, which may have caused the lens to decentre inferiorly.

It is reasonable to speculate that an improved outcome may have been achieved by manipulating lens sag height (employing a diagnostic method of fitting) for P1, P3 and P4, leading to possible improvements in TZ centration in these participants.

A limitation of this study is the observational nature of the study which used only four participants. Nevertheless this study revealed some interesting outcomes that can help guide future studies. Post-hoc analysis revealed study power to be 94% to detect a difference more than 0.40 mm in the TZ decentration between spherical and toric OK lenses. A sample size of 32 would be required to detect a minimum of 0.50 DC difference in toricity between eyes fitted with spherical and toric OK lenses with an estimated variance of 0.70 D.

6.5 CONCLUSIONS

From the observations made on a very limited number of participants, this study reveals that toric OK lenses may show enhanced performance over spherical OK lenses in

terms of inducing a TZ with well-defined edges, despite showing a greater amount of TZ decentration. The study supports the speculation that toric OK lenses may achieve a more defined TZ by locking up fluid forces underneath the OK lens but this proposal of mechanism requires further investigation.

CHAPTER 7 OVERALL SUMMARY AND CONCLUSIONS

7.1 SUMMARY

During overnight orthokeratology lens wear for myopic correction, the OK lens is expected to centre well over the cornea consequently producing a uniform central flattening and para-central annular steepening. The flattened central zone overlying the pupillary area is responsible for myopic reduction. However, if the lens is decentred during OK lens wear, the central flattened zone will be displaced causing the area of para-central annular steepening to fall within the pupillary area. Clinically, this is an undesired outcome. Because the OK lens is in close proximity with the cornea during OK lens wear, it is reasonable to speculate that the lens dynamics, including centration, are to some extent dependent on the contour of the cornea. This raises the question of what constitutes normal corneal shape.

7.1.1 Normal corneal shape in eyes with minimally toric corneas

It is well known that the normal anterior corneal surface can be represented by a conicoid model (Kiely et al. 1982), which describes the surface is close to rotationally symmetrical and prolate in shape, meaning that the surface gradually flattens from the centre towards the periphery. When considered at a more detailed level however, the normal cornea has been shown to flatten towards the periphery at different rates between meridians (Mandell and St Helen 1971, Kiely et al. 1982, Sheridan and Douthwaite 1989). Although useful to give a better description of corneal shape, an understanding of meridional differences is not sufficient to relate to OK lens centration because the OK lens is likely to come in contact with the anterior corneal surface over a region (or zone) rather than just along isolated meridians. Therefore it is important to understand corneal shape at a regional level by dividing the cornea into zones or sectors. Unfortunately no published reports exist investigating corneal shape at a zonal or sectorial level while taking the rate of corneal flattening into account. Therefore the first study I undertook as a part of this thesis was to investigate corneal shape across different sectors.

Normal corneal shape in eyes with minimal corneal toricity (< 1.50 DC) was investigated in Chapter 2 The study revealed a significant variation in corneal asphericity across different corneal sectors when ethnicity was not taken into consideration. Along the central horizontal meridian temporal corneal sectors were revealed to be less prolate than nasal corneal sectors. This indicates that the rate of corneal flattening towards the temporal region is slower than in the nasal region. When considering the central vertical corneal

meridian no significant asymmetry was noted. This significant horizontal asymmetry was considered a likely influencing factor for OK lens decentration during overnight wear and hence was worthy of investigating in more detail.

Previous studies have suggested that corneal shape is different between different ethnicities (Section 1.3.6.2) and that eyelid pressure, position, and shape have an influence on corneal shape (Section 1.3.6.3). It was found in Chapter 2 that eyelid shape was different between East Asians and non-East Asians. Although some studies have shown that eyelid shape affects corneal topography (Read et al. 2007a), the information about how East Asian eyelid shape influences corneal shape in contrast to non- East Asian eyelids has not been reported. Therefore a further analysis was made in Chapter 2 to investigate differences in sectorial corneal shape and eyelid morphometry between East Asians and non-East Asians, and the influence of eyelid morphometry on corneal shape. The study showed that the superior, superior-nasal, supero-temporal and infero-temporal corneal sectors were significantly different between the two ethnic groups. Several eyelid morphometry features were also shown to be different between East Asians and non-East Asians, the most relevant differences being in upper eyelid position, curvature and slope.

When correlations were tested between individual eyelid and corneal shape components, the relationship between upper eyelid curvature and spherical equivalent corneal power was the only factor that was significantly different between the two ethnicities, with a stronger association in non-East Asians than East Asians. The remaining eyelid shape features did not exhibit a difference in association with corneal sectorial shape. This implies that there are factors beyond eyelid shape, such as eyelid pressure, that could be responsible for the differences in corneal shape that were observed between non-East Asians and East Asians. Eyelid pressure was not investigated in the current study because the primary purpose of the research presented in this thesis was to identify corneal factors responsible for OK lens or TZ decentration and not eyelid factors.

7.1.2 Effect of baseline corneal shape of minimally toric corneas on treatment zone decentration

Having shown significant variation in normal corneal shape in Chapter 2, further interest was generated to see if this variation in normal corneal shape at baseline would influence treatment zone (TZ) centration. The study showed that after a single night of spherical OK lens wear on eyes with minimally toric corneas, the TZ decentred towards the temporal side of the cornea in 76% of cases (38% supero-temporal and 38% infero-temporal).

When the cohort was considered as a whole, in the majority of cases the least prolate region of the cornea was on the temporal side. However, despite this there was no association found between the location of least prolate corneal sectors and the sectors to which the TZ was decentred.

Instead, a high negative association was found between the location of most prolate corneal sectors and sectors where the TZ was centred, indicating that the lenses moved away from the most prolate corneal region after a single night of spherical OK lens wear. At day 14 a high proportion of eyes (67%) still showed a tendency for temporal TZ decentration. However, at this visit there were differences in the associations between TZ centration and sectoral curvature, with a significant positive association noted between the baseline least prolate corneal location and the sector to which the TZ was decentred. This needs to be considered with caution, because the baseline corneal shape would have already altered at day 1 and thus the lens decentration at subsequent visits and would be more dependent on the altered corneal shape rather than baseline corneal shape. This led to further analysis to investigate the role of post OK lens wear corneal shape after one night of lens wear on TZ centration after further nights of lens wear.

7.1.3 Effect of spherical OK lens on corneal topography in minimally toric corneas

The relationship found between baseline corneal sectorial shape and TZ decentration at day 14 was not helpful because OK-induced changes to corneal shape after the first night of lens wear would have had a greater influence on decentration than baseline corneal shape. In Chapter 3, regional corneal shape was used to define baseline corneal shape and this was then related to TZ decentration. However, corneal asphericity could not be accurately determined after 1 night of wear because asphericity formulas are less robust in representing post-OK corneal shapes. One way to overcome this problem is to instead analyse changes to corneal curvature rather than asphericity, and relate these changes in curvature to subsequent TZ centration. This was achieved by investigating corneal tangential curvature changes with spherical OK lenses in the same cohort described in Chapter 3. The cornea was divided into a central circular zone and a para-central annular zone, which were further subdivided into four sectors (nasal, superior, temporal and inferior) to allow analysis of horizontal and vertical asymmetry. The results of the study showed a significant nasal versus temporal asymmetry at day 1 and also at day 14.

After OK lens wear at day 1, there was greater temporal central flattening with a simultaneous greater temporal para-central steepening than the nasal cornea. This is consistent with the temporal TZ decentration that has already been described. A temporally decentred OK lens would cause the central compressive effect from the lens to be concentrated in the temporal sector, which would explain the greater degree of central corneal flattening that was measured on the temporal side. In OK, central corneal flattening is typically surrounded by an annulus of corneal steepening, which in this scenario of temporal decentration would be more pronounced in the temporal than nasal para-central sector, explaining the greater amount of steepening that was observed in the temporal para-central sector relative to the nasal para-central sector. On the other hand, temporal TZ decentration would move this zone of para-central steepening into the nasal central zone, giving on average less central flattening.

After OK lens wear at day 14, the cornea continued to show greater temporal flattening in the central zone and also greater para-central temporal steepening, which suggests that the OK lens returned to a similar location on the eye on subsequent nights of lens wear. So rather than the least or most prolate sector at baseline being the influential factor on TZ centration after day 1, it is the shape change that has been made to the cornea after the first night of lens wear that acts as an anchor for further nights of lens wear, akin to the way in which a mould, if reapplied, will naturally return to the same position on a shape that it helped make. This repeated positioning and continued overnight wear helps to solidify the corneal shape that the OK lens has initially created.

7.1.4 Effect of baseline corneal toricity of moderately toric corneas on treatment zone decentration

Attempting to fit spherical OK lenses to corneas with increasingly greater amounts of corneal toricity would result in greater misalignment between the back surface of the lens and corneal surface. If this misalignment is a factor in TZ centration, then a greater amount of TZ decentration would be expected with increasing corneal toricity. To investigate this hypothesis, a comparison study was conducted and reported in Chapter 5. The study confirmed this hypothesis by showing a greater amount of TZ decentration in eyes with moderate amounts of corneal toricity than in eyes with minimal amounts of corneal toricity when fitted with spherical OK lenses using an empirical method. With this finding this study scientifically endorsed a major limitation of fitting spherical OK lenses to corneas with moderate corneal toricity, which was until this point only the subject of clinical anecdote.

When fitting conventional RGP contact lenses on moderately toric corneas, practitioners generally employ a rule of thumb involving steepening of the back optic zone radius (BOZR) in order to control lens decentration. The BOZR is generally fitted steeper than flat K by one third of the difference between the corneal curvatures along the principal corneal meridians. It was our further interest to understand if a similar rule of thumb could be used to control OK lens decentration in moderately toric corneas.

The study was conducted by fitting one eye with a spherical OK lens in a conventional manner (matching lens sag height with corneal sag height along the flatter corneal meridian) and the fellow eye with an adjusted fitting method. The adjusted fitting method employed a lens fitting with sag height that was deeper than that measured along the flatter corneal meridian by one third of the difference in sag heights along the principal corneal meridians. The adjusted fitting protocol showed no improvement in arresting TZ decentration, however lens wear was only conducted for one night due to the ethical dilemma of inducing visual distortion had the lens wear been continued for longer duration. Having failed to achieve a better TZ centration with spherical OK lenses the next attempt was to fit toric OK lenses on moderately toric corneas.

7.1.5 Effect of fitting toric OK lenses on eyes with moderate amounts of corneal toricity.

Clinical experience of failures when fitting spherical OK lenses on highly toric corneas has generated the need for more complex OK lens designs such as toric OK lenses. Recent publications claim to overcome the problem of lens instability on moderately toric corneas, achieving better correction of refractive astigmatism (Section 1.9.2). However these early reports did not analyse TZ decentration as a part of their investigation. In this thesis I performed an explorative research on the performance of toric OK lens wear in comparison to the outcomes of spherical OK lens wear with a specific emphasis on TZ decentration.

The observations made on a small sample of participants led to the conclusion that the magnitude of TZ decentration is greater in comparison to the magnitude of TZ decentration observed when the same eyes were fitted using spherical OK lenses. A further important observation was that the TZ produced after toric OK lens wear was more uniform with distinct edges. This is certainly a step forward in improving TZ effects on toric corneas compared to spherical OK using conventional fitting methods.

There are some other important observations made from the study reported in Chapter 6. Aspects which are encouraging towards toric OK lens wear were reductions in refractive error and improvement in unaided visual acuity. There was a dramatic reduction in the group mean corneal M with a simultaneous reduction in myopic refractive error. The reduction was more pronounced with longer duration of OK lens wear, and was comparable with outcomes of conventional spherical OK lens wear on minimally toric corneas (Nichols et al. 2000, Mika et al. 2007). All participants exhibited reasonably good unaided visual acuity by the end of the treatment period despite the presence of high amounts of TZ decentration. The well-defined TZ could possibly explain the reason for good visual outcome.

7.2 A POSSIBLE THEORY OF TREATMENT ZONE DECENTRATION DURING ORTHOKERATOLOGY

Based on the observations made from the series of experiments summarised in the Section 7.1 it is possible to generate a possible model by which the TZ is decentred towards a specific region during spherical OK lens fitting on minimally toric corneas. The model takes into consideration only horizontal and not vertical corneal asymmetry because it was shown that in general the cornea is more asymmetric in the horizontal than vertical meridian in terms of asphericity (Chapter 2). In addition it was also noted that TZ decentration was predominantly towards the temporal cornea than in minimally toric corneas.

7.2.1 Direct compression theory

A prediction of how the OK lens would behave if corneal shape were perfectly spherical will help explain how corneal asymmetry might cause OK lens decentration leading to TZ decentration. Figure 7-1 shows the alignment relationship between an OK lens and a hypothetical rotationally symmetrical corneal profile. Upon initial application the OK lens is likely to gain perfect stability due to the symmetric corneal shape. If fitted correctly the OK lens will align well at the corneal apex and also land in a symmetric manner towards the corneal periphery. This lens-to-cornea relationship is likely to lead to a uniform central flattening and uniform para-central corneal steepening after a single overnight wear, thus generating the desired bull's eye pattern on the coloured topographic difference map. This kind of topographic appearance is what is clinically desirable during myopic spherical OK and this leads to the reduction of myopia without induction of corneal toricity.

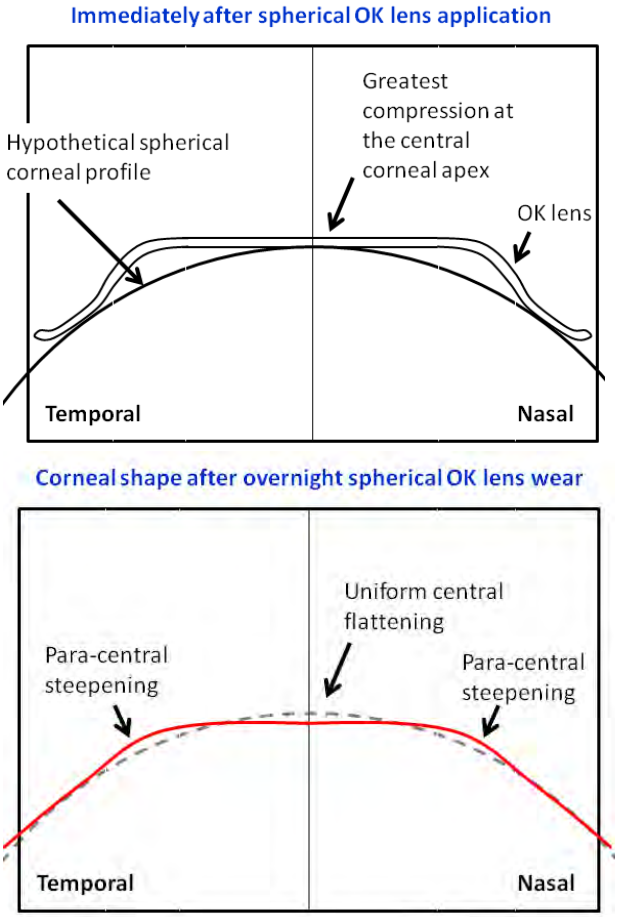

Figure 7-1. Illustration showing the effect of spherical orthokeratology (OK) lens on corneal shape. Top figure: scenario representing relationship between spherical OK lens and hypothetical spherical corneal surface, immediately after the application of a spherical OK lens. Note the OK lens back surface aligns well with the corneal surface at the apex and the peripheral alignment curves symmetrically land over the peripheral cornea. Bottom figure: scenario representing change in corneal shape (red line) after overnight wear of OK lens, after lens. The dotted line represents pre-lens wear corneal shape. Note the uniform central flattening and symmetric para-central steepening.

Figure 7-2a. illustrates how an asymmetric prolate corneal profile varies its shape from the centre towards the periphery in comparison to a spherical corneal profile. It shows that the nasal cornea flattens at a faster rate than the temporal cornea.

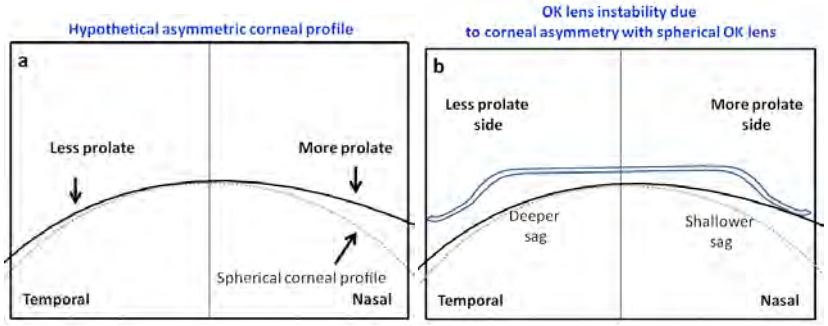

Figure 7-2. (a) Illustration comparing a horizontally asymmetric hypothetical corneal profile with a spherical corneal profile. Note the nasal cornea tends to flatter at a faster rate (more prolate) than the temporal cornea (less prolate). (b) spherical OK lens placed on a cornea with asymmetric corneal profile. Note the asymmetric alignment of the peripheral parts of the OK lens with the peripheral cornea which may cause lens instability.

When a spherical OK lens is applied to an asymmetric corneal profile there is increasing disparity towards the temporal periphery between the back surface of the lens and the cornea due to the underlying asymmetry (Figure 7-2b). The outcomes found in the studies presented in this thesis indicate that the lens decentres away from the more prolate corneal region as an initial response (Figure 7-3). This response can be explained through recognising that the alignment of the OK lens is not even on the nasal and temporal sides. A perfect alignment would require a lens with shallow sag on the nasal more prolate corneal side and deeper sag on the temporal less prolate corneal side. Since a spherical OK lens has a uniform rotationally symmetric single lens sag height at a common chord, when placed over this hypothetical asymmetric cornea it tends to tilt away from the most prolate corneal region. This tilting effect would result in the closest proximity between the lens and cornea. There would now be greater compressive bearing towards the less prolate temporal region than the more prolate nasal region, leading to the lens compressing more in the central temporal region than central nasal region. This mechanism explains the greater amount of central temporal flattening compared to central nasal flattening that was observed. This is likely to be accompanied by a simultaneous greater para-central steepening in the temporal region than the nasal region. As overnight wear of OK lens is continued, the lens tends to cause more compression in the central temporal region with minimal flattening on the nasal temporal region, accompanied by a greater para-central steepening in the temporal region than the nasal region.

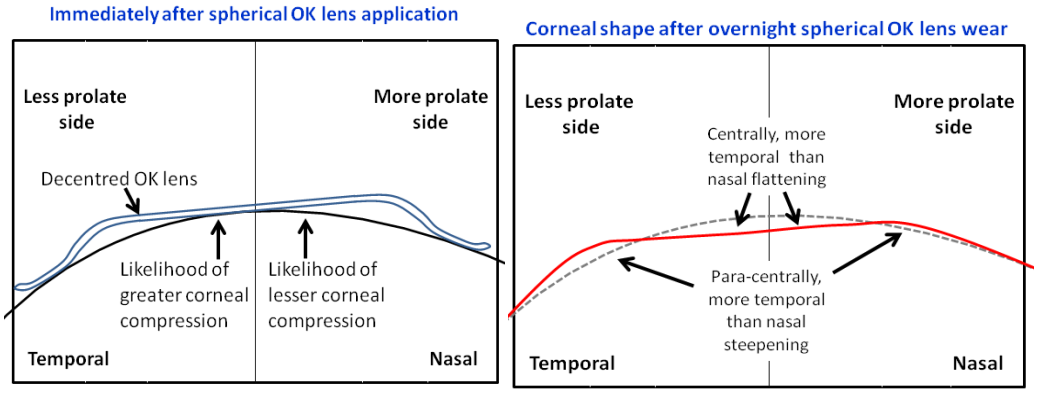

Figure 7-3. Illustration showing the effect of spherical orthokeratology (OK) lens on a hypothetical asymmetrical corneal surface. Left figure: note that immediately on spherical OK lens application the lens tended to incline towards the less prolate temporal cornea. This in effect causes more bearing in the central temporal corneal region than central nasal region. Right figure: showing central corneal flattening with asymmetry in change after of spherical OK lens wear. Post-wear corneal shape reveals more flattening in the central temporal region than the central nasal region with a simultaneous corneal asymmetry in the para-central corneal steepening.

7.2.2 Squeeze film force theory

If the original underlying mechanism of OK is not direct mechanical compression but squeeze tear film forces under the OK lens, then the proposed hypothesis differs slightly.

Squeeze film forces are forces generated by the tear fluid trapped between the lens and cornea to help retain lenses on the cornea between and during blinks (Allaire and Flack 1980, Hayashi and Fatt 1980). When a spherical OK lens is applied on a perfectly spherical cornea the lens is in a quasi-static state with several forces acting on the lens dynamics. These forces include eyelid pressure, gravity and squeeze film forces. The tear fluid is trapped under the lens as it aligns at the periphery circumferentially. Because of the lens-cornea alignment, the tear fluid is thin in the centre and thick towards the mid-peripheral region. The squeeze film compressive force is reciprocal to the thickness of the tear film, therefore the fluid exerts greater compressive pressure over the cornea at the apex causing central corneal flattening (i.e. the TZ), with definite edges. Simultaneously the squeeze film force generates a negative suction force under the reverse curve of the OK lens causing para-central steepening.

However it was shown in Chapter 2 that the cornea exhibits nasal-temporal shape asymmetry in minimally toric corneas. This asymmetry causes the lens to rock until the closest match between lens and the cornea is attained. Because of nasal-temporal corneal asymmetry, the lens is likely to tilt away from the most prolate cornea to settle. Once the lens is settled, the squeeze film forces become operational. Since the lens in its tilted position is closest to the cornea on the temporal side than the nasal side there will be more positive compressive

squeeze film forces in the central temporal region with simultaneous greater negative squeeze film forces in the para-central temporal region. This kind of pressure distribution causes more flattening in the central temporal region and steepening in the para-central temporal region than the nasal cornea.

During spherical OK on toric corneas, there is poor alignment between the OK lens periphery and the corneal periphery, because the OK lens is rotationally symmetric whereas the cornea is not. Since the OK lens edges are lifted off along the steeper corneal meridian, they act as open channels for the tear fluid to seep off resulting in a collapse of squeeze fluid forces under the OK lens. Thus the resultant TZ is poorly defined.

During wear of toric periphery OK lenses on toric corneas, the first step is for the lens to seek a quasi-static state where all forces are acting in balance, during which the lenses tend to exhibit some decentration. At this position the peripheral toric part of the lens is in close alignment with the peripheral toric cornea, therefore sealing off the edges. This causes the tear film to be trapped under the OK lens creating greater compression in the decentred position and producing a well defined TZ.

7.3 LIMITATIONS OF THE RESEARCH

7.3.1 Measurement and interpretation of corneal shape

The reliability of measuring corneal shape towards the periphery was not determined in these studies. In various studies reported in this thesis, corneal shape was assessed and analysed towards the periphery and sometimes up to an 8 mm chord diameter (4 mm radius). Corneal raw topographic data including corneal height, tangential curvature and axial curvature (for determining corneal refractive power) exported from the Medmont E300 corneal topographer were used for these purposes. For Placido disc-based corneal topographers it is generally known that repeatability progressively worsens towards the corneal periphery from the centre (Zadnik et al. 1995). The repeatability of the Medmont E300 has been assessed in the previous studies on human corneas, although, only a few corneal parameters were considered. These parameters were apical radius, eccentricity for central region, and elevation at a 9 mm chord diameter in the horizontal meridian (Cho et al. 2002). The repeatability of these values across other meridians is not known. Further, all studies related to repeatability of corneal topographers were conducted in eyes with minimally toric corneas. To date no study has investigated the repeatability of the Medmont E300 corneal

topographers in highly toric corneas and also in eyes after corneal reshaping procedures such as OK.

Some previous studies have investigated the repeatability of the Placido disc-based TMS-1 corneal topographer (manufacturer, city etc), in measuring corneal power and the angles of steep and flat K after post-penetrating keratoplasty (Karabatsas et al. 1998a, Karabatsas et al. 1998b), and other corneal indices in keratoconus (McMahon et al. 2005). The results show that the agreement between measurements in these distorted corneas was poorer than in normal corneas.

Except where retrospective data were used, this potential problem of measurement error was partly overcome in the studies conducted in this thesis by taking multiple corneal topographic maps. Cho et al. (2002) determined that an average of at least 2 topographic measurements with the Medmont E300 are required to achieve precise measurements, although the study did not state the magnitude of a corneal toricity was not taken into consideration. The number of topographic measurements to be taken to give acceptable precision of Medmont E300 measurements in the eyes with moderate corneal toricity and in post OK corneas is not known.

Analysing corneal data in most studies reported in this research required extrapolation towards the corneal periphery as the corneal area captured by the Medmont E300 topographer used in these studies was often limited due to obstruction from the ocular adnexa. In Chapter 4, a cut-off value was applied when analysing corneal changes if any corneal sector contained < 70% of data points. Since the para-central superior region was frequently affected due to the upper eyelid interfering with topography capture, after applying the cut-off value the sample size was reduced from 21 to 12, in this sector resulting in some loss of study power.

The validity of determination of peripheral corneal toricity is dependent on the validity of the eccentricity e value along the principal meridians derived from the Medmont E300 topographer. Further it was assumed that the central corneal principal meridians would continue to maintain their orientation even in the periphery, but this may not be true as the principal corneal meridians towards may change towards the corneal periphery showing some misalignment with principal meridians in the central region.

The corneal topographic information gained from analysing changes after OK using Sim K values is limited. Such topographic information includes steep K, flat K, corneal M, corneal J_{180} and corneal J_{45}. The limitation of Sim K values to determine the effect of OK lens wear is that Sim K values represent only regular corneal toricity when the principal corneal powers are orthogonal, but not as valid in assessing changes after OK, because after OK, corneal shape may distorted leading to an irregular corneal surface. Other evaluation methods such as Fourier analysis or Zernike polynomials would be useful to quantify corneal irregularity resulting from OK-induced corneal shape changes. Although some papers (Hiraoka et al. 2004a,Hiraoka et al. 2006) are available related to this, information is not specifically available pertaining to happening to toric corneas after spherical and toric OK.

7.3.2 Choice of reference centre

A possible argument could be raised regarding the choice of reference centre used for calculating TZ decentration. The magnitude of TZ decentration in all studies that form this research was measured relative to the corneal vertex normal (VN, along the videokeratoscopic axis) as oppose to the centre of the entrance pupil or corneal sighting centre (CSC). The reason why VN was used as a reference centre was that OK practitioners generally make clinical decisions based on the observations made from topographic maps which by default are referenced to the VN. Considering that the TZ affects the quality of vision, the TZ measurements should ideally be measured relative to CSC or alternatively the entrance pupil centre (see Section 1.8.4). Otherwise it is possible that the TZ decentration observed relative to the VN could simply be an artefact, as the CSC itself is decentred from the VN by a mean of 0.38 mm in any direction (Mandell et al. 1995). To counter this argument, a further analysis was performed to compare the magnitude of TZ decentration relative to VN and relative to the entrance pupil centre. For each map the pupil horizontal and vertical offsets relative to corneal vertex normal were extracted from the corneal topographer. Then using already known polar TZ decentration values from the VN, the distance from the centre of the entrance pupil to the TZ centre was determined using trigonometric formulas. The analysis revealed no significant difference in decentration (Table 7-1), giving confidence that referencing TZ to the VN had minimal impact on conclusions.

Chapter (visit)	Corneal toricity (dioptres cylinder)	VN to entrance pupil centre distance (mm)	TZ decentration distance relative to VN (mm)	TZ decentration relative to entrance pupil centre (mm)	*p*-value (Student t-test)
Chapter 3 (day 1)	≤ 1.50 Diagnostic fitting	0.24 ± 0.13	0.44 ± 0.25	0.46 ± 0.20	0.707
Chapter 3 (day 14)		0.21 ± 0.12	0.62 ± 0.27	0.57 ± 0.28	0.191
Chapter 5 (day 1)	≤ 1.50 Conventional fitting	0.21 ± 0.11	0.57 ± 0.29	0.54 ± 0.33	0.306
Chapter 5 (day 1)	1.50 to 3.50 Conventional fitting	0.19 ± 0.09	1.06 ± 0.57	1.03 ± 0.51	0.395
Chapter 5 (day 1)	1.50 to 3.50 Adjusted fitting	0.21 ± 0.09	0.95 ± 0.44	0.93 ± 0.33	0.763

Table 7-1. Comparison of the magnitude of treatment zone (TZ) decentration (mean ± SD) assessed from the vertex normal (VN) and the magnitude assessed from the centre of the entrance pupil.

7.3.1 OK lens fitting

Another potential limiting factor is that only an empirical method of OK lens fitting was employed in all studies except in Chapter 3. While this is completely a valid criticism, it must be emphasised that the purpose of this research was to identify corneal factors responsible for TZ decentration and not to attempt to minimise TZ decentration through altering lens fit. Had it been the case that diagnostic fitting was employed rather than empirical fitting, the factors which are truly responsible for TZ decentration could have been obscured because the fitting approach could have deliberately over-ridden all these factors.

7.3.2 Influence of eyelids and eye movements

It should be borne in mind that the lens decentration and thus TZ decentration could have been governed by various factors other than non-uniform corneal shape, including pressure from the upper eyelid, altered position of the eye ball during sleep due to Bell's phenomenon (Wilkins and Brody 1969) and onset of rapid eye movements (REM) during sleep (Mahowald and Schenck 1998). These factors may affect the TZ decentration in isolation or in combination and thus may act as confounders to the results found in this study. Further

studies are needed to understand the effect of these non-corneal factors on TZ decentration in OK.

7.3.3 MATLAB software

There are some limitations in the scope of the software that was developed for measuring TZ decentration. The program performed well to define TZ location in minimally toric corneas but failed to identify edges accurately after spherical OK lens wear on moderately toric corneas. The limitation did not relate to the program itself but related to the clinical outcomes of TZ decentration. The edges of the TZ were indistinct after one night wear of spherical OK lenses on moderately toric corneas. Interestingly the software did not pose any problem when analysing TZ in moderately toric corneas fitted with toric periphery OK lenses because of the more clearly defined TZ margins even after single night of lens wear.

7.3.4 Generalising the study results

The results of studies reported in this thesis cannot be generalised to populations with different ocular characteristics such as children, high myopes, or the elderly. For example eighty percent of the study participants in Chapter 3 had with-the-rule (WTR) corneal toricity and all participants in Chapter 5 with moderately toric corneal toricity had WTR corneal toricity. The outcomes may be different in eyes with against-the-rule and oblique corneal toricity as the baseline corneal shape in these eyes would tend be different. Similarly, older people who wear OK lenses may exhibit a reduced or slower response (Jayakumar and Swarbrick 2005), which could affect the sectorial corneal change and TZ decentration after OK. Further, lid pressure may reduced in older people due to more flaccid eyelids, and there is also greater propensity towards against-the-rule corneal astigmatism with age (Read et al. 2007b).

7.4 FUTURE RECOMMENDATIONS

The original intention at the commencement of this PhD project was to investigate correction of astigmatism during spherical and toric OK in eyes with a range of astigmatism. However, early recognition of the complete lack of knowledge in all aspects of response to toric OK lens wear caused the project to focus on TZ decentration during spherical and toric OK on eyes with minimal and moderate amounts of corneal toricity. The research questions thus left unanswered require further study, not only to evaluate the effects of spherical OK on higher amounts of refractive astigmatism but also outcomes in terms of visual acuity, contrast sensitivity and aberrations.

One factor that is likely to affect TZ decentration but was not analysed in this current research was eyelid pressure particularly in the closed eye. Recent studies highlight the effect of eyelid pressure on corneal shape in the open eye in primary and downward gaze (Sections 1.3.6.3 and 1.3.6.4). Studies pertaining to eyelid pressure in the closed eye with and without OK lenses in place will address some unanswered questions in this thesis. Similarly, questions are remain about the involvement of other factors affecting TZ centration in the closed eye such as Bell's phenomenon and REM, which may affect the lens position during sleep and hence influence TZ centration.

This research showed that the TZ decentration during spherical OK was instigated by non-uniform baseline corneal shape variation. This understanding will assist in the development of new OK lens designs that have the capability to more closely match non-uniform corneal profiles, in the process promoting higher degrees of first lens success when using empirical fitting methods. Due to tremendous advancements in contact lens manufacturing, the industry may be able to produce custom OK lens designs, especially with non-rotationally symmetric designs that match with the non-rotationally symmetrical corneal surface. This will allow OK lenses to produce uniform central flattening and para-central corneal steepening in eyes with spherical refractive error without induction of astigmatism, and desired corneal shape changes in eyes with minimal or moderate refractive astigmatism.

By describing four cases of fitting toric OK lenses to moderately toric corneas this research has shown that toric periphery OK lenses show some positive findings with respect to quality of TZ centration. Some manufacturers are also producing lenses with full toric OK lens designs that have toric back surfaces in the centre and also in the periphery. Research into clinical outcomes from these novel lens designs is needed to understand whether these complex lens designs create more uniform and predictable flattening to the cornea and correction of residual refractive astigmatism.

This research explored corneal factors responsible for TZ decentration. It was identified that spherical OK lenses have a tendency to decentre away from the most prolate corneal area. Further, lens decentration itself seems to generate non-uniform corneal shape changes particularly inducing nasal-versus temporal corneal asymmetry. This research also indicated that spherical OK lenses tend to decentre more in eyes with moderately toric corneas than minimally toric corneas when conventional fitting approaches are used. It was also revealed that alternative fitting methods such as deepening the lens sag did not provide any benefit in controlling TZ decentration. Observations of fitting toric periphery OK lens

designs in comparison to spherical OK lenses also showed some interesting results. Although toric OK lenses were shown to decentre more on moderately toric corneas than spherical OK lenses on minimally toric corneas, the quality of TZ achieved with the toric OK lenses was superior resulting in improvement in visual acuity. This research will help in understanding the effects of baseline corneal shape of minimally and moderately toric corneas on TZ parameters during spherical OK and also the effect of toric OK lenses on moderately toric corneas. This knowledge will take forward our current understanding on spherical OK lens fitting and the limitations in fitting moderately toric corneas. The research also underlines the point that toric OK lenses may not achieve best results when fitted empirically, thus emphasising the need for fitting these lenses using diagnostic fitting methods.

REFERENCES

Alharbi A, Swarbrick HA (2003). The effects of overnight orthokeratology lens wear on corneal thickness. Invest Ophthalmol Vis Sci 44: 2518-23.

Allaire P, Flack R (1980). Squeeze forces in contact lenses with a steep base curve radius. Am J Optom Phys Opt 57: 219.

Alpins NA (1993). A new method of analyzing vectors for changes in astigmatism. J Cataract Refract Surg 19: 524-33.

Anstice J (1971). Astigmatism: Its components and their changes with age. Am J Optom Arch Am Acad Optom 12: 1001-6.

Applegate RA, Howland HC (1995). Noninvasive measurement of corneal topography. IEEE Eng Med Biol Mag 14: 30-42.

Asbell PA, Chiang B, Somers ME, Morgan KS (1990). Keratometry in children. Eye Contact Lens 16: 99-102.

Atkinson T (1984). A re-appraisal of the concept of fitting rigid hard lenses by the tear layer thickness and edge clearance technique. J Br Contact Lens Assoc 7: 106-10.

Atkinson T (1985). A computer assisted and clinical assessment of current trends in gas permeable lens design. Optician 189: 16-22.

Auffarth GU, Wang L, Völcker HE (2000). Keratoconus evaluation using the Orbscan topography system. J Cataract Refract Surg 26: 222-8.

Baertschi M, Wyss M (2010). Correction of high amounts of astigmatism through orthokeratology. A case report. J Optom 3: 182-4.

Bailey IL, Carney LG (1970). Analyzing contact lens induced changes of the corneal curvature. Am J Optom Arch Am Acad Optom 47: 761-8.

Baker TY (1943). Ray tracing through non-spherical surfaces. Proc Phys Soc 55: 361-4.

Baldwin W, Mills D (1981). A longitudinal study of corneal astigmatism and total astigmatism. Am J Optom Physiol Opt 58: 206-11.

Barr J, Schoessler J (1980). Corneal endothelial response to rigid contact lenses. Am J Optom Physiol Opt 57: 267-74.

Belin MW, Ratliff CD (1996). Evaluating data acquisition and smoothing functions of currently available videokeratoscopes. J Cataract Refract Surg 22: 421-6.

Benjamin W, Hill R (1985). Human cornea: oxygen uptake immediately following graded deprivation. Graefe's Arch Clin Exp Ophthalmol 223: 47-9.

Benjamin W, Hill R (1988). Human cornea: individual responses to hypoxic environments. Graefe's Arch Clin Exp Ophthalmol 226: 45-8.

Benjamin WJ, Cappelli QA (2002). Oxygen permeability (Dk) of thirty-seven rigid contact lens materials. Optom Vis Sci 79: 103-11.

Bennett ES, Sorbara L (2009). Lens design, fitting and evaluation In: Bennett ES, Henry VA (eds), Clinical Manual of Contact Lenses. London: Lippincott Williams & Wilkins: 99-138.

Berntsen DA, Barr JT, Mitchell GL (2005). The effect of overnight contact lens corneal reshaping on higher-order aberrations and best-corrected visual acuity. Optom Vis Sci 82: 490-7.

Bibby M (1979a). Factors affecting peripheral curve design. Am J Optom Physiol Opt 56: 2-9.

Bibby M (1979b). Factors affecting peripheral curve design. Part II: Specifying for reproducible performance. Am J Optom Physiol Opt 56: 618-27.

Binder PS, May CH, Grant SC (1980). An evaluation of orthokeratology. Ophthalmology 87: 729-44.

Borish IM (1975). Astigmatism.(eds), Clinical Refraction. 3rd Edition, Chicago: The Professional Press, Inc.: 123-141.

Brand RJ, Polse KA, Schwalbe JS (1983). The Berkeley Orthokeratology Study, Part I: General conduct of the study. Am J Optom Physiol Opt 60: 175-86.

Brennan NA, Efron N, Carney LG (1987). Critical oxygen requirements to avoid oedema of the central and peripheral cornea. Acta Ophthalmol 65: 556-64.

Budak K, Khater TT, Friedman NJ, Holladay JT, Koch DD (1999). Evaluation of relationships among refractive and topographic parameters. J Cataract Refract Surg 25: 814-20.

Buehren T, Collins MJ, Carney L (2003). Corneal aberrations and reading. Optom Vis Sci 80: 159-66.

Burek H, Douthwaite W (1993). Mathematical models of the general corneal surface. Ophthalmic Physiol Opt 13: 68-72.

Cano D, Barbero S, Marcos S (2004). Comparison of real and computer-simulated outcomes of LASIK refractive surgery. J Opt Soc Am A 21: 926-36.

Carney LG (1975). Effect of hypoxia on central and peripheral corneal thickness and corneal topography. Aust J Optom 58: 61-5.

Carney LG, Liubinas J, Bowman KJ (1981). The role of corneal distortion in the occurrence of monocular diplopia. Acta Ophthalmol 59: 271-4.

Caroline PJ (2001). Contemporary orthokeratology. Contact Lens Ant Eye 24: 41-6.

Caroline PJ, Andre MP (2009). Orthokeratology for astigmats. Contact Lens Spectrum 24: 56.

Chan B, Cho P, Cheung SW (2008a). Orthokeratology practice in children in a university clinic in Hong Kong. Clin Exp Optom 91: 453-60.

Chan B, Cho P, de Vecht A (2009). Toric orthokeratology: a case report. Clin Exp Optom 92: 387-91.

Chan B, Cho P, Mountford J (2008b). The validity of the Jessen formula in overnight orthokeratology: a retrospective study. Ophthalmic Physiol Opt 28: 265-8.

Chan JS, Mandell RB, Burger DS, Fusaro RE (1995). Accuracy of videokeratography for instantaneous radius in keratoconus. Optom Vis Sci 72: 793-9.

Charman WN (1991). Optics of the human eye. In: Cronly Dillon J (eds), Visual Optics and Instrumentation. Boca Raton: CRC Press: 1-26.

Charman WN, Mountford J, Atchison DA, Markwell EL (2006). Peripheral refraction in orthokeratology patients. Optom Vis Sci 83: 641-8.

Chen C, Cheung SW, Cho P (2012). Toric orthokeratology for highly astigmatic children. Optom Vis Sci 89: 849-55.

Chen C, Cho P (2012). Toric orthokeratology for high myopic and astigmatic subjects for myopic control. Clin Exp Optom 95: 103-8.

Chen D, Lam AKC (2009). Reliability and repeatability of the Pentacam on corneal curvatures. Clin Exp Optom 92: 110-8.

Cheung SW, Cho P (2004). Subjective and objective assessments of the effect of orthokeratology-a cross-sectional study. Curr Eye Res 28: 121-7.

Cheung SW, Cho P, Chan B (2009). Astigmatic changes in orthokeratology. Optom Vis Sci 86: 1352-8.

Cheung SW, Cho P, Chui WS, Woo GC (2007). Refractive error and visual acuity changes in orthokeratology patients. Optom Vis Sci 84: 410-6.

Cheung SW, Cho P, Douthwaite W (2000). Corneal shape of Hong Kong-Chinese. Ophthalmic Physiol Opt 20: 119-25.

Cho P, Chan B, Cheung SW, Mountford J (2012). Do fenestrations affect the performance of orthokeratology lenses? Optom Vis Sci 89: 401-10.

Cho P, Cheung SW, Edwards M (2005). The longitudinal orthokeratology research in children (LORIC) in Hong Kong: a pilot study on refractive changes and myopic control. Curr Eye Res 30: 71-80.

Cho P, Cheung SW, Edwards MH, Fung J (2003). An assessment of consecutively presenting orthokeratology patients in a Hong Kong based private practice. Clin Exp Optom 86: 331-8.

Cho P, Lam AK, Mountford J, Ng L (2002). The performance of four different corneal topographers on normal human corneas and its impact on orthokeratology lens fitting. Optom Vis Sci 79: 175-83.

Chui WS, Cho P (2003). Recurrent lens binding and central island formations in a fast-responding orthokeratology lens wearer. Optom Vis Sci 80: 490-4.

Collins MJ, Buehren T, Bece A, Voetz SC (2006). Corneal optics after reading, microscopy and computer work. Acta Ophthalmol Scand 84: 216-24.

Coon LJ (1982). Orthokeratology. Part I: Historical perspective. J Am Optom Assoc 53: 187-95.

Coon LJ (1984). Orthokeratology. Part II: Evaluating the Tabb method. J Am Optom Assoc 55: 409-18.

Coorpender SJ, Klyce SD, McDonald MB, Doubrava MW, Kim CK, Tan AL, Srivannaboon S (1999). Corneal topography of small-beam tracking excimer laser photorefractive keratectomy. J Cataract Refract Surg 25: 675-84.

Cutler SI (2001). Fitting challenging corneas. Contact Lens Spectrum 16: 22-31.

Davis WR, Raasch TW, Mitchell GL, Mutti DO, Zadnik K (2005). Corneal asphericity and apical curvature in children: a cross-sectional and longitudinal evaluation. Invest Ophthalmol Vis Sci 46: 1899-906.

Denis D, Burguiere O, Oudahi F, Scheiner C (1995). Measurement of facial growth in the human fetus. Graefe's Arch Clin Exp Ophthalmol 233: 756-65.

Dingeldein SA, Klyce SD (1988). Imaging of the cornea. Cornea 7: 170-82.

Dingeldein SA, Klyce SD (1989). The topography of normal corneas. Arch Ophthalmol 107: 512-8.

Dobson V, Miller JM, Harvey EM (1999). Corneal and refractive astigmatism in a sample of 3- to 5-year-old children with a high prevalence of astigmatism. Optom Vis Sci 76: 855-60.

Douthwaite WA (1995). EyeSys corneal topography measurement applied to calibrated ellipsoidal convex surfaces. Br Journal of Ophthalmology 79: 797-801.

Douthwaite WA (2003). The asphericity, curvature and tilt of the human cornea measured using a videokeratoscope. Ophthalmic Physiol Opt 23: 141-50.

Douthwaite WA, Hough T, Edwards K, Notay H (1999). The EyeSys videokeratoscopic assessment of apical radius and p-value in the normal human cornea. Ophthalmic Physiol Opt 19: 467-74.

Douthwaite WA, Matilla MT (1996). The TMS-1 corneal topography measurement applied to calibrated ellipsoidal convex surfaces. Cornea 15: 147-53.

Efron N, Carney LG (1982). Response of the human cornea to anoxic stress. Aust J Optom 65: 56-7.

Eghbali F, Yeung KK, Maloney RK (1995). Topographic determination of corneal asphericity and its lack of effect on the refractive outcome of radial keratotomy. Am J Ophthalmol 119: 275-80.

Ehrmann K, Francis I, Stapleton F (2001). A novel instrument to quantify the tension of upper and lower eyelids. Contact Lens Ant Eye 24: 65-72.

El Hage S, Leach NE (1999). Tangential or sagittal dioptric plots : Is there a difference? Int Contact Lens Clin 26: 39-45.

Elliott M, Callender MG, Elliott DB (1994). Accuracy of Javal's rule in the determination of spectacle astigmatism. Optom Vis Sci 71: 23-6.

Emsley HH (1953). Optical system of the eye, Visual Optics. London: Hatton Press: 38-78.

Fan DS, Rao SK, Cheung EY, Islam M, Chew S, Lam DS (2004). Astigmatism in Chinese preschool children: prevalence, change, and effect on refractive development. Br J Ophthalmol 88: 938-41.

Fan L, Jun J, Jia Q, Wangqing J, Xinjie M, Yi S (1999). Clinical study of orthokeratology in young myopic adolescents. Int Contact Lens Clin 26: 113-6.

Fatt I (1978). Gas transmission properties of soft contact lenses In: Ruben M (eds), Soft Contact Lenses. New York: John Wiley & Sons: 83-110.

Fonn D, Holden B (1988). Rigid gas-permeable vs. hydrogel contact lenses for extended wear. Am J Optom Physiol Opt 65: 536-44.

Fontana A (1972). Orthokeratology using the onepiece bifocal. Contacto 16: 45-7.

Ford JG, Davis RM, Reed JW, Weaver RG, Craven TE, Tyler ME (1997). Bilateral monocular diplopia associated with lid position during near work. Cornea 16: 525-30.

Franklin RJ, Morelande MR, Iskander DR, Collins MJ, Davis BA (2006). Combining central and peripheral videokeratoscope maps to investigate total corneal topography. Eye Contact Lens 32: 27-32.

Freeman R (1978). Predicting stable changes in orthokeratology. Contact Lens Forum 3: 21-31.

Friling R, Weinberger D, Kremer I, Avisar R, Sirota L, Snir M (2004). Keratometry measurements in preterm and full term newborn infants. Br Journal of Ophthalmology 88: 8-10.

Gifford P, Swarbrick HA (2008). Time course of corneal topographic changes in the first week of overnight hyperopic orthokeratology. Optom Vis Sci 85: 1165-71.

Gleason W, Albright RA (2003). Menicon Z 30-day continuous wear lenses: a clinical comparison to Acuvue 7-day extended wear lenses. Eye Contact Lens 29: S149-52.

Golnik KC, Eggenberger E (2001). Symptomatic corneal topographic change induced by reading in downgaze. J Neuro Ophthalmol 21: 199-204.

Gonzalez-Meijome JM, Villa-Collar C, Montes-Mico R, Gomes A (2007). Asphericity of the anterior human cornea with different corneal diameters. J Cataract Refract Surg 33: 465-73.

Gordon RA, Donzis PB (1985). Refractive development of the human eye. Arch Ophthalmol 103: 785-9.

Grant SC (1980). Orthokeratology. I. A safe and effective treatment for a disabling problem. Surv Ophthalmol 24: 291-7.

Grant SC (1992). Orthokeratology – night therapy and night retention. Contact Lens Spectrum 7: 28-33.

Grey C, Yap M (1986). Influence of lid position on astigmatism. Am J Optom Physiol Opt 63: 966-9.

Grosvenor T (1978). Etiology of astigmatism. Am J Optom Physiol Opt 55: 214-8.

Grosvenor T (1994). Fitting the astigmatic patient with rigid contact lenses In: Guillon M, Ruben M (eds), Contact Lens Practice. London: Chapman & Hall: 623-47.

Grosvenor T (1978). Etiology of astigmatism. Am J Optom Physiol Opt 55: 214-8.

Grosvenor T, Quintero S, Perrigin DM (1988). Predicting refractive astigmatism: a suggested simplification of Javal's rule. Am J Optom Physiol Opt 65: 292-7.

Guillon M (1994). Basic contact lens fitting In: Guillon M, Ruben M (eds), Contact Lens Practice. London: Chapman & Hall: 587-622.

Guillon M, Lydon DP, Sammons WA (1983). Designing rigid gas permeable contact lenses using the edge clearance technique. J Br Contact Lens Assoc 6: 19-26.

Guillon M, Lydon DP, Wilson C (1986). Corneal topography: a clinical model. Ophthalmic Physiol Opt 6: 47-56.

Harris DH, Stoyan N (1992). A new approach to orthokeratology. Contact Lens Spectrum 7: 37-9.

Harvitt DM, Bonanno JA (1999). Re-evaluation of the oxygen diffusion model for predicting minimum contact lens Dk/t values needed to avoid corneal anoxia. Optom Vis Sci 76: 712-9.

Hayashi K, Hayashi H, Hayashi F (1995). Topographic analysis of the changes in corneal shape due to aging. Cornea 14: 527-32.

Hayashi TT, Fatt I (1980). Forces retaining a contact lens on the eye between blinks. Am J Optom Phys Opt 57: 485.

Henry V, Bennett E, Forrest J (1987). Clinical investigation of the Paraperm EW rigid gas-permeable contact lens. Am J Optom Physiol Opt 64: 313-20.

Hiraoka T, Furuya A, Matsumoto Y, Okamoto F, Sakata N, Hiratsuka K, Kakita T, Oshika T (2004a). Quantitative evaluation of regular and irregular corneal astigmatism in patients having overnight orthokeratology. J Cataract Refract Surg 30: 1425-9.

Hiraoka T, Furuya A, Matsumoto Y, Okamoto F, Kakita T, Oshika T (2004b). Influence of overnight orthokeratology on corneal endothelium. Cornea 23: S82-6.

Hiraoka T, Matsumoto Y, Okamoto F, Yamaguchi T, Hirohara Y, Mihashi T, Oshika T (2005). Corneal higher-order aberrations induced by overnight orthokeratology. Am J Ophthalmol 139: 429-36.

Hiraoka T, Mihashi T, Okamoto C, Okamoto F, Hirohara Y, Oshika T (2009). Influence of induced decentered orthokeratology lens on ocular higher-order wavefront aberrations and contrast sensitivity function. J Cataract Refract Surg 35: 1918-26.

Hiraoka T, Okamoto C, Ishii Y, Takahira T, Kakita T, Oshika T (2008). Mesopic contrast sensitivity and ocular higher-order aberrations after overnight orthokeratology. Am J Ophthalmol 145: 645-55.

Hiraoka T, Okamoto F, Kaji Y, Oshika T (2006). Optical quality of the cornea after overnight orthokeratology. Cornea 25: S59-63.

Hjortdal JØ, Erdmann L, Bek T (1995). Fourier analysis of video-keratographic data. A tool for separation of spherical, regular astigmatic and irregular astigmatic corneal power components. Ophthalmic Physiol Opt 15: 171-85.

Holden BA, Mertz GW (1984). Critical oxygen levels to avoid corneal edema for daily and extended wear contact lenses. Invest Ophthalmol Vis Sci 25: 1161-7.

Hough T, Edwards K (1999). The reproducibility of videokeratoscope measurements as applied to the human cornea. Contact Lens Ant Eye 22: 91-9.

Howland HC, Sayles N (1985). Photokeratometric and photorefractive measurements of astigmatism in infants and young children. Vision Res 25: 73-81.

Isenberg SJ, Del Signore M, Chen A, Wei J, Christenson PD (2004). Corneal topography of neonates and infants. Arch Ophthalmol 122: 1767-71.

Iskander DR, Collins MJ, Read SA (2007). Extrapolation of central corneal topography into the periphery. Eye Contact Lens 33: 293-9.

Iskander DR, Morelande MR, Collins MJ, Davis B (2002). Modeling of corneal surfaces with radial polynomials. IEEETrans Biomed Eng 49: 320-8.

Jayakumar J, Swarbrick HA (2005). The effect of age on short-term orthokeratology. Optom Vis Sci 82: 505-11.

Jessen GN (1964). Contact lenses as a therapeutic device. Am J Optom Arch Am Acad Optom 41: 429-35.

Jessen GN (1962). Orthofocus techniques. Contacto 6: 200-4.

Joslin CE, Wu SM, McMahon TT, Shahidi M (2003). Higher-order wavefront aberrations in corneal refractive therapy. Optom Vis Sci 80: 805-11.

Kakita T, Hiraoka T, Oshika T (2011). Influence of overnight orthokeratology on axial elongation in childhood myopia. Invest Ophthalmol Vis Sci 52: 2170-4.

Kang P, Swarbrick H (2011). Peripheral refraction in myopic children wearing orthokeratology and gas-permeable lenses. Optom Vis Sci 88: 476-82.

Kang P, Swarbrick HA (2012). Time course of the effects of orthokeratology on peripheral refraction and corneal topography. Invest Ophthalmol Vis Sci 53: E-Abstract 4713.

Karabatsas CH, Cook SD, Papaefthymiou J, Turner P, Sparrow JM (1998a). Clinical evaluation of keratometry and computerised videokeratography: intraobserver and interobserver variability on normal and astigmatic corneas. Br J Ophthalmol 82: 637-42.

Karabatsas CH, Cook SD, Powell K, Sparrow JM (1998b). Comparison of keratometry and videokeratography after penetrating keratoplasty. J Refract Surg 14: 420-6.

Kawamorita T, Nakayama N, Uozato H (2009). Repeatability and reproducibility of corneal curvature measurements using the Pentacam and Keratron topography systems. J Refract Surg 25: 539-44.

Keller PR, McGhee CNJ, Weed KH (1998). Fourier analysis of corneal topography data after photorefractive keratectomy. J Cataract Refract Surg 24: 1447-55.

Kerns RL (1976a). Research in orthokeratology. Part I: Introduction and background. J Am Optom Assoc 47: 1047-51.

Kerns RL (1976b). Research in orthokeratology. Part II: Experimental design, protocol and method. J Am Optom Assoc 47: 1275-85.

Kerns RL (1976c). Research in orthokeratology. Part III: Results and observations. J Am Optom Assoc 47: 1505-15.

Kerns RL (1977a). Research in orthokeratology. Part IV: Results and observations. J Am Optom Assoc 48: 227-38.

Kerns RL (1977b). Research in orthokeratology. Part V: Results and observations--recovery aspects. J Am Optom Assoc 48: 345-59.

Kerns RL (1977c). Research in orthokeratology. Part VI: Statistical and clinical analyses. J Am Optom Assoc 48: 1134-47.

Kerns RL (1977d). Research in orthokeratology. Part VII: examination of techniques, procedures and control. J Am Optom Assoc 48: 1541-53.

Kerns RL (1978). Research in orthokeratology. Part VIII: results, conclusions and discussion of techniques. J Am Optom Assoc 49: 308-14.

Kiely PM, Smith G, Carney LG (1982). The mean shape of the human cornea. Optica Acta 29: 1027-40.

Kiely PM, Smith G, Carney LG (1984). Meridional variations of corneal shape. Am J Optom Physiol Opt 61: 619-26.

Klein SA (1992). A corneal topography algorithm that produces continuous curvature. Optom Vis Sci 69: 829-34.

Klein SA (1997). Axial curvature and the skew ray error in corneal topography. Optom Vis Sci 74: 931-44.

Klein SA, Mandell RB (1995a). Shape and refractive powers in corneal topography. Invest Ophthalmol Vis Sci 36: 2096-109.

Klein SA, Mandell RB (1995b). Axial and instantaneous power conversion in corneal topography. Invest Ophthalmol Vis Sci 36: 2155-9.

Kline L, DeLuca T, Fishberg G (1979). Corneal staining relating to contact lens wear. J Am Optom Assoc 50: 353-7.

Klyce SD (1984). Computer-assisted corneal topography. High-resolution graphic presentation and analysis of keratoscopy. Invest Ophthalmol Vis Sci 25: 1426-35.

Knappe S, Stachs O, Guthoff R (2007). Corneal changes after wearing orthokeratology contact lenses. Ophthalmologe 104: 681-7.

Kunjur J, Sabesan T, Ilankovan V (2006). Anthropometric analysis of eyebrows and eyelids: an inter-racial study. Br J Oral Maxillofac Surg 44: 89-93.

La Hood D, Sweeney D, Holden B (1988). Overnight corneal edema with hydrogel, rigid gas-permeable and silicone elastomer contact lenses. Int Contact Lens Clin 15: 149-54.

Lam AKC, Douthwaite WA (1996). Application of a modified keratometer in the study of corneal topography on Chinese subjects. Ophthalmic Physiol Opt 16: 130-4.

Lam BL, Lam S, Walls RC (1995). Prevalence of palpebral fissure asymmetry in white persons. Am J Ophthalmol 120: 518-22.

Lam CSY, Loran DFC (1991). Designing contact lenses for oriental eyes. J Br Contact Lens Assoc 14: 109-14.

Larson R, Hostetler RP (2007). Precalculus with limits. In: Larson R (eds), Topics in Analytic Geometry. Pacific Grove, Calif. : Brooks/Cole: 727-809.

Levene JR (1965). The true inventors of the kerato-scope and photo-keratoscope. Br J Hist Sci 2: 324-42.

Lieberman DM, Grierson JW (2000). The lids influence on corneal shape. Cornea 19: 336-42.

Lindsay R, Smith G, Atchison D (1998). Descriptors of corneal shape. Optom Vis Sci 75: 156-8.

Loper LR (1959). The relationship between angle lambda and the residual astigmatism of the eye. Am J Optom Arch Am Acad Optom 36: 365-77.

Lorente-Velázquez A, Nieto-Bona A, Collar CV, Mesa AG (2011). Straylight and contrast sensitivity after Corneal Refractive Therapy. Optom Vis Sci 88: 1245-51.

Lu C, Smith G (1990). The aspherizing of intra-ocular lenses. Ophthalmic Physiol Opt 10: 54-66.

Lu F, Simpson T, Sorbara L, Fonn D (2007a). Corneal refractive therapy with different lens materials, part 2: effect of oxygen transmissibility on corneal shape and optical characteristics. Optom Vis Sci 84: 349-56.

Lu F, Simpson T, Sorbara L, Fonn D (2007b). The relationship between the treatment zone diameter and visual, optical and subjective performance in Corneal Refractive Therapy lens wearers. Ophthalmic Physiol Opt 27: 568-78.

Ludlam WM, Wittenberg S, Rosenthal J, Harris G (1967). Photographic analysis of the ocular dioptric components. 3. The acquisition, storage, retrieval and utilization of primary data in photokeratoscopy. Am J Optom Arch Am Acad Optom 44: 276-96.

Lui WO, Edwards MH (2000). Orthokeratology in low myopia. Part 2: corneal topographic changes and safety over 100 days. Contact Lens Ant Eye 23: 90-9.

Lum E, Swarbrick HA (2011). Lens Dk/t influences the clinical response in overnight orthokeratology. Optom Vis Sci 88: 469-75.

Maguire LJ, Singer DE, Klyce SD (1987). Graphic presentation of computer-analyzed keratoscope photographs. Arch Ophthalmol 105: 223-30.

Mahowald MW, Schenck CH (1998). Dissociated states of wakefulness and sleep. Handbook of Behavioral State Control: Cellular and Molecular Mechanisms 143.

Maldonado-Codina C, Efron S, Morgan P, Hough T, Efron N (2005). Empirical versus trial set fitting systems for accelerated orthokeratology. Eye Contact Lens 31: 137-47.

Maloney RK, Bogan SJ, Waring GO, 3rd (1993). Determination of corneal image-forming properties from corneal topography. Am J Ophthalmol 115: 31-41.

Mandell R (1995). Locating the corneal sighting center from videokeratography. J Refract Surg 11: 253-9.

Mandell R, Farrell R (1980). Corneal swelling at low atmospheric oxygen pressures. Invest Ophthalmol Vis Sci 19: 697-702.

Mandell R, Polse K (1971). Corneal thickness changes accompanying central corneal clouding. Am J Optom Arch Am Acad Optom 48: 129-32.

Mandell R, St Helen R (1969). Position and curvature of the corneal apex. Am J Optom Arch Am Acad Optom 46: 25-9.

Mandell RB (1994). Apparent pupil displacement in videokeratography. CLAO J 20: 123-7.

Mandell RB (1996). A guide to videokeratography. Int Contact Lens Clin 23: 205-28.

Mandell RB (1966). Reflection point ophthalmometry: a method to measure corneal contour. Am J Optom Arch Am Acad Optom 39: 513-37.

Mandell RB, Chiang CS, Klein SA (1995). Location of the major corneal reference points. Optom Vis Sci 72: 776-84.

Mandell RB, St Helen R (1971). Mathematical model of the corneal contour. Br J Physiol Opt 26: 183-97.

Mattioli R, Tripoli NK (1997). Corneal geometry reconstruction with the Keratron videokeratographer. Optom Vis Sci 74: 881-94.

McAlinden C, Khadka J, Pesudovs K (2011). A comprehensive evaluation of the precision (repeatability and reproducibility) of the Oculus Pentacam HR. Invest Ophthalmol Vis Sci 52: 7731-7.

McMahon TT, Anderson RJ, Roberts C, Mahmoud AM, Szczotka-Flynn LB, Raasch TW, Friedman NE, Davis LJ (2005). Repeatability of corneal topography measurement in keratoconus with the TMS-1. Optom Vis Sci 82: 405-15.

Menassa N, Kaufmann C, Goggin M, Job OM, Bachmann LM, Thiel MA (2008). Comparison and reproducibility of corneal thickness and curvature readings obtained by the Galilei and the Orbscan II analysis systems. J Cataract Refract Surg 34: 1742-7.

Menchaca C, Malacara D (1984). Directional curvatures in a conic surface. Applied Optics 23: 3258-60.

Mika R, Morgan B, Cron M, Lotoczky J, Pole J (2007). Safety and efficacy of overnight orthokeratology in myopic children. Optometry 78: 225-31.

Millodot M (1978). Effect of long-term wear of hard contact lenses on corneal sensitivity. Arch Ophthalmol 96: 1225-7.

Montalbán R, Piñero DP, Javaloy J, Alió JL (2012). Intrasubject repeatability of corneal morphology measurements obtained with a new Scheimpflug photography–based system. J Cataract Refract Surg 38: 971-7.

Mountford J (1997a). Orthokeratology. In: Phillips AJ, Speedwell L (eds), Contact Lenses. 4th Edition, Oxford: Butterworth-Heinemann: 653-92.

Mountford J (1997b). An analysis of the changes in corneal shape and refractive error induced by accelerated orthokeratology. Int Contact Lens Clin 24: 128-44.

Mountford J (1998). Retention and regression of orthokeratology with time. Int Contact Lens Clin 25: 59-64.

Mountford J (2004a). Design variables and fitting philosophies of reverse geometry lenses. In: Mountford J, Ruston D, Dave T (eds), Orthokeratology. Principles and Practice. London: Butterworth-Heinemann: 69-107.

Mountford J (2004b). Corneal and refractive changes due to orthokeratology In: Mountford J, Ruston D, Dave T (eds), Orthokeratology. Principles and Practice. London: Butterworth-Heinemann: 175-203.

Mountford J (2004c). Trial lens fitting. In: Mountford J, Ruston D, Dave T (eds), Orthokeratology. Principles and Practice. London: Butterworth-Heinemann: 139-173.

Mountford J, Noack D (2002). Corneal topography and orthokeratology: post-fit assessment. Contact Lens Spectrum 17: 25-31.

Mountford J, Pesudovs K (2002). An analysis of the astigmatic changes induced by accelerated orthokeratology. Clin Exp Optom 85: 284-93.

Nichols JJ, Marsich MM, Nguyen M, Barr JT, Bullimore MA (2000). Overnight orthokeratology. Optom Vis Sci 77: 252-9.

Nieto-Bona A, Lorente-Velázquez A, Mòntes-Micó R (2009). Relationship between anterior corneal asphericity and refractive variables. Graefe's Arch Clin Exp Ophthalmol 247: 815-20.

Nolan JA (1972). Orthokeratology with steep lenses. Contacto 16: 31-7.

O'Leary D, Millodot M (1981). Abnormal epithelial fragility in diabetes and in contact lens wear. Acta Ophthalmol 59: 827-33.

Owens H, Garner LF, Craig JP, Gamble G (2004). Posterior corneal changes with orthokeratology. Optom Vis Sci 81: 421-6.

Park D, Song Han K, Kang J (1990). Anthropometry of normal Korean eyelids. J Korean Soc Plast Reconst Surg 17: 822-34.

Park DH, Choi WS, Yoon SH, Song CH (2008). Anthropometry of Asian eyelids by age. Plastic Reconst Surg 121: 1405-13.

Patil SB, Kale SM, Math M, Khare N, Sumeet J (2011). Anthropometry of the eyelid and palpebral fissure in an Indian population. Aesthet Surg J 31: 290-4.

Pauné J, Cardona G, Quevedo L (2012). Toric double tear reservoir contact lens in orthokeratology for astigmatism. Eye Contact Lens 38: 245-51.

Phillips AJ (1997). Rigid gas permeable contact lens fitting. In: Phillips AJ, Speedwell L (eds), Contact Lenses. London: Butterworth-Heinemann: 313-55.

Polse K, Rivera R, Bonanno J (1988). Ocular effects of hard gas-permeable-lens extended wear. Am J Optom Physiol Opt 65: 358-64.

Polse KA, Brand RJ, Keener RJ, Schwalbe JS, Vastine DW (1983a). The Berkeley orthokeratology study, part III: Safety. Am J Optom Physiol Opt 60: 321-8.

Polse KA, Brand RJ, Schwalbe JS, Vastine DW, Keener RJ (1983b). The Berkeley orthokeratology study, Part II: Efficacy and duration. Am J Optom Physiol Opt 60: 187-98.

Potts AV (1997). Orthokeratological reduction of astigmatism. Contact Lens Spectrum 12: 26-32.

Price KM, Gupta PK, Woodward JA, Stinnett SS, Murchison AP (2009). Eyebrow and eyelid dimensions: an anthropometric analysis of African Americans and Caucasians. Plastic Reconst Surg 124: 615-23.

Queiros A, Gonzalez-Meijome JM, Jorge J, Villa-Collar C, Gutierrez AR (2010a). Peripheral refraction in myopic patients after orthokeratology. Optom Vis Sci 87: 323-9.

Queiros A, Gonzalez-Meijome JM, Villa-Collar C, Gutierrez AR, Jorge J (2010b). Local steepening in peripheral corneal curvature after Corneal Refractive Therapy and LASIK. Optom Vis Sci 87: 432-9.

Raasch TW (1995). Corneal topography and irregular astigmatism. Optom Vis Sci 72: 809-15.

Rabbetts RB (2007). Astigmatism. In: Rabbetts RB (eds), Clinical Visual Optics. 4th Edition, London: Butterworth Heinemann Elsevier: 85-101.

Rabbetts RB, Edward AHM (2007). Measurement of ocular dimensions. In: Rabbetts RB (eds), Clinical Visual Optics. 4th Edition, London: Butterworth Heinemann Elsevier: 395-419.

Rah MJ, Jackson JM, Jones LA, Marsden HJ, Bailey MD, Barr JT (2002). Overnight orthokeratology: preliminary results of the Lenses and Overnight Orthokeratology (LOOK) study. Optom Vis Sci 79: 598-605.

Read SA, Collins MJ, Carney LG (2007a). The influence of eyelid morphology on normal corneal shape. Invest Ophthalmol Vis Sci 48: 112-9.

Read SA, Collins MJ, Carney LG (2007b). A review of astigmatism and its possible genesis. Clin Exp Optom 90: 5-19.

Read SA, Collins MJ, Carney LG, Franklin RJ (2006). The topography of the central and peripheral cornea. Invest Ophthalmol Vis Sci 47: 1404-15.

Read SA, Collins MJ, Iskander DR, Davis BA (2009). Corneal topography with Scheimpflug imaging and videokeratography: comparative study of normal eyes. J Cataract Refract Surg 35: 1072-81.

Reddy T, Szczotka LB, Roberts C (2000). Peripheral corneal contour measured by topography influences soft toric contact lens fitting success. CLAO J 26: 180-5.

Roberts C (1994a). Characterization of the inherent error in a spherically-biased corneal topography system in mapping a radially aspheric surface. J Refract Corneal Surg 10: 103-11.

Roberts C (1994b). The accuracy of 'power' maps to display curvature data in corneal topography systems. Invest Ophthalmol Vis Sci 35: 3525-32.

Salmon TO, Horner DG (1995). Comparison of elevation, curvature, and power descriptors for corneal topographic mapping. Optom Vis Sci 72: 800-8.

Sanaty M, Temel A (1996). Corneal curvature changes in soft and rigid gas permeable contact lens wearers after two years of lens wear. Eye Contact Lens 22: 186-8.

Savini G, Barboni P, Carbonelli M, Hoffer KJ (2009). Agreement between Pentacam and videokeratography in corneal power assessment. J Refract Surg 25: 534-8.

Savini G, Barboni P, Carbonelli M, Hoffer KJ (2011a). Repeatability of automatic measurements by a new Scheimpflug camera combined with Placido topography. J Cataract Refract Surg 37: 1809-16.

Savini G, Carbonelli M, Barboni P, Hoffer KJ (2011b). Repeatability of automatic measurements performed by a dual Scheimpflug analyzer in unoperated and post-refractive surgery eyes. J Cataract Refract Surg 37: 302-9.

Savini G, Carbonelli M, Sbreglia A, Barboni P, Deluigi G, Hoffer KJ (2011c). Comparison of anterior segment measurements by 3 Scheimpflug tomographers and 1 Placido corneal topographer. J Cataract Refract Surg 37: 1679-85.

Schoessler J, Woloschak M (1981). Corneal endothelium in veteran PMMA contact lens wearers. Int Contact Lens Clin 8: 19-25.

Shankar S, Bobier WR (2004). Corneal and lenticular components of total astigmatism in a preschool sample. Optom Vis Sci 81: 536-42.

Shaw AJ, Collins MJ, Davis BA, Carney LG (2009). Eyelid pressure: inferences from corneal topographic changes. Cornea 28: 181-8.

Shaw AJ, Collins MJ, Davis BA, Carney LG (2010). Eyelid pressure and contact with the ocular surface. Invest Ophthalmol Vis Sci 51: 1911-7.

Shaw AJ, Collins MJ, Davis BA, Carney LG (2008). Corneal refractive changes due to short-term eyelid pressure in downward gaze. J Cataract Refract Surg 34: 1546-53.

Sheridan M, Douthwaite WA (1989). Corneal asphericity and refractive error. Ophthalmic Physiol Opt 9: 235-8.

Shirayama M, Wang L, Weikert MP, Koch DD (2009). Comparison of corneal powers obtained from 4 different devices. Am J Ophthalmol 148: 528-35.

Sivak J (1977). A simple photokeratoscope. Am J Optom Physiol Opt 54: 241-3.

Smith EL, Kee CS, Ramamirtham R, Qiao-Grider Y, Hung LF (2005). Peripheral vision can influence eye growth and refractive development in infant monkeys. Invest Ophthalmol Vis Sci 46: 3965-72.

Smolek MK, Klyce SD, Hovis JK (2002a). The Universal Standard Scale: Proposed improvements to the American National Standards Institute (ANSI) scale for corneal topography. Ophthalmology 109: 361-9.

Smolek MK, Klyce SD, Sarver EJ (2002b). Inattention to nonsuperimposable midline symmetry causes wavefront analysis error. Arch Ophthalmol 120: 439-47.

Soni PS, Nguyen TT (2006). Overnight orthokeratology experience with XO material. Eye Contact Lens 32: 39-45.

Soni PS, Nguyen TT, Bonanno JA (2003). Overnight orthokeratology: visual and corneal changes. Eye Contact Lens 29: 137-45.

Soper JW, Sampson WG, Girard LJ (1962). Corneal topography, keratometry and contact lenses. Arch Ophthalmol 67: 753-60.

Sorbara L, Fonn D, Simpson T, Lu F, Kort R (2005). Reduction of myopia from Corneal Refractive Therapy. Optom Vis Sci 82: 512-8.

Sridharan R, Swarbrick H (2003). Corneal response to short-term orthokeratology lens wear. Optom Vis Sci 80: 200-6.

Stillitano I, Chalita M, Schor P, Maidana E, Lui M, Lipener C, Hofling-Lima AL (2007). Corneal changes and wavefront analysis after orthokeratology fitting test. Am J Ophthalmol 144: 378-86.

Swarbrick H (2004b). The e's, p's and Q's of corneal shape. Refractive Eyecare for Ophthalmologists 8: 5-8.

Swarbrick HA (2004a). Orthokeratology (corneal refractive therapy): what is it and how does it work? Eye Contact Lens 30: 181-5; discussion 205-6.

Swarbrick HA (2006). Orthokeratology review and update. Clin Exp Optom 89: 124-43.

Sweeney DF (2003). Clinical signs of hypoxia with high-Dk soft lens extended wear: Is the cornea convinced? Eye Contact Lens 29: S22-5.

Sweeney DF, Holden BA (1983). The closed eye swelling response of the cornea to Polycon and Menicon O2 gas permeable hard lenses. Aust J Optom 66: 186-9.

Tahhan N, Du Toit R, Papas E, Chung H, La Hood D, Holden BA (2003a). Comparison of reverse-geometry lens designs for overnight orthokeratology. Optom Vis Sci 80: 796-804.

Tahhan N, Sarfraz F, Raad N, Raad C, Weber T, Du Toit R, Papas E (2003b). Orthokeratology and the eyelid. Invest Ophthalmol Vis Sci 44: E-Abstract 3714.

Tang W, Collins MJ, Carney L, Davis B (2000). The accuracy and precision performance of four videokeratoscopes in measuring test surfaces. Optom Vis Sci 77: 483-91.

Taubin G (1991). Estimation of planar curves, surfaces, and nonplanar space-curves defined by implicit equations with applications to edge and range image segmentation. IEEE Trans Patt Analysis Machine Intell 13: 1115-38.

Thibos LN, Wheeler W, Horner D (1997). Power vectors: an application of Fourier analysis to the description and statistical analysis of refractive error. Optom Vis Sci 74: 367-75.

Tomlinson A, Schwartz C (1979). The position of the corneal apex in the normal eye. Am J Optom Physiol Opt 56: 236-40.

Townsley MG (1970). New knowledge of the corneal contour. Contacto 14: 38-43.

Twelker JD, Mitchell GL, Messer DH, Bhakta R, Jones LA, Mutti DO, Cotter SA, Klenstein RN, Manny RE, Zadnik K (2009). Children's ocular components and age, gender, and ethnicity. Optom Vis Sci 86: 918-35.

Uozato H, Guyton DL (1987). Centering corneal surgical procedures. Am J Ophthalmol 103: 264-75.

Vihlen FS, Wilson G (1983). The relation between eyelid tension, corneal toricity, and age. Invest Ophthalmol Vis Sci 24: 1367-73.

Villa-Collar C, Gonzalez-Meijome JM, Queiros A, Jorge J (2009). Short-term corneal response to Corneal Refractive Therapy for different refractive targets. Cornea 28: 311-6.

Walline JJ, Jones LA, Sinnott LT (2009). Corneal reshaping and myopia progression. Br J Ophthalmol 93: 1181-5.

Walline JJ, Rah MJ, Jones LA (2004). The Children's Overnight Orthokeratology Investigation (COOKI) pilot study. Optom Vis Sci 81: 407-13.

Wilkins RH, Brody IA (1969). Bell's palsy and Bell's phenomenon. Arch Neurology 21: 661-2.

Wilson G, Bell C, Chotai S (1982). The effect of lifting the lids on corneal astigmatism. Am J Optom Physiol Opt 59: 670-4.

Wilson SE, Klyce SD (1991). Advances in the analysis of corneal topography. Surv Ophthalmol 35: 269-77.

Wlodyga RJ, Bryla C (1989). Corneal molding: the easy way. Contact Lens Spectrum 4: 58-65.

Wolffsohn JS, Bhogal G, Shah S (2011). Effect of uncorrected astigmatism on vision. J Cataract Refract Surg 37: 454-60.

Wu R, Stapleton F, Swarbrick HA (2009). Residual corneal flattening after discontinuation of long-term orthokeratology lens wear in asian children. Eye Contact Lens 35: 333-7.

Yang X, Zhong X, Gong X, Zeng J (2005). [Topographical evaluation of the decentration of orthokeratology lenses]. [Chinese] Yan Ke Xue Bao 21: 132-5.

Yoshida T, Miyata K, Tokunaga T, Tanabe T, Oshika T (2003). Difference map or single elevation map in the evaluation of corneal forward shift after LASIK. Ophthalmology 110: 1926-30.

Young G, Port M (1992). Rigid gas-permeable extended wear: a comparative clinical study. Optom Vis Sci 69: 214-26.

Young G, Sulley A, Hunt C (2011). Prevalence of astigmatism in relation to soft contact lens fitting. Eye Contact Lens 37: 20-5.

Zadnik K, Friedman NE, Mutti DO (1995). Repeatability of corneal topography: the "corneal field". J Refract Surg 11: 119-25.

Zhang Z, Wang J, Niu W, Ma M, Jiang K, Zhu P, Ke B (2011). Corneal asphericity and its related factors in 1052 Chinese subjects. Optom Vis Sci 88: 1232-9.

Zhong X, Chen X, Xie RZ, Yang J, Li S, Yang X, Gong X (2009). Differences between overnight and long-term wear of orthokeratology contact lenses in corneal contour, thickness, and cell density. Cornea 28: 271-9.

APPENDIX A

APPENDIX A.1

Mathematical steps involved in determination of meridional asphericity1

Ellipse

An ellipse is the locus of all points such that sum of distances to each focus is constant. It has two standard forms:

$\frac{x^2}{a^2} + \frac{y^2}{b^2} = 1$; foci on *x-axis* (major axis)

$\frac{x^2}{b^2} + \frac{y^2}{a^2} = 1$; foci on *y-axis* (major axis)

The length of major radius =a; the length of minor radius = b; with a > b. The foci are located at ±*c* units from the centre where

$$a^2 - b^2 = c^2$$

The eccentricity of an ellipse is $e = c/a$ and takes values between 0 (circle) and 1 (parabola).

Hyperbola

A hyperbola is the locus of all points such that difference of distances to each focus is constant. It has two standard forms:

$\frac{x^2}{a^2} - \frac{y^2}{b^2} = 1$; foci on *x-axis* (major axis)

$\frac{y^2}{a^2} - \frac{x^2}{b^2} = 1$; foci on *y-axis* (major axis)

where a > b. Like ellipse, the foci are located at ±*c* units from the centre, but in this conic :

[1] The series of mathematical steps are adapted from the description given by Stephen R. Schmitt, Determining type of conic given the general conic equation at http://mysite.verizon.net/res148h4j/javascript/script_conic_equation_type.html.

$$a^2 + b^2 = c^2$$

The eccentricity of a hyperbola is *e = c/a* and takes values greater than 1.

Determination of conic type

Determination of conic type from the general conic equation form:

$$Ax^2 + Bxy + Cy^2 + Dx + Ey + F = 0$$

The type of conic section can be found by evaluating the determinant and two of the minors of the symmetric matrix:

$$M = \begin{vmatrix} F & \frac{1}{2}D & \frac{1}{2}E \\ \frac{1}{2}D & A & \frac{1}{2}B \\ \frac{1}{2}E & \frac{1}{2}B & C \end{vmatrix}$$

Thus determinant $|M|$ and minors *M1* and *M2* can be determined as follows:

$$|M| = ACF + \frac{1}{4}(BDE - BBF - CCD - AEE)$$

$$M1 = AC - \frac{1}{4}BB$$

$$M2 = \frac{1}{4}DE - \frac{1}{2}BF$$

The type of conic can be determined using the following logical steps

If $|M| \neq 0$ & $A|M| < 0$ & $M1 > 0$ & $A \neq 0$ & $B \neq 0$ Conic is an ellipse

If $|M| \neq 0$ & $M1 < 0$ Conic is a hyperbola

Transformation to a standard form:

The general conic equation may represent a standard conic section that has been translated and rotated. To convert the general equation to a standard form , a rotation and a translation are applied to give a new set of coefficients for the equation the conic section does not change its shape.

Rotation

When the coefficient B of the general conic equation is non-zero; a rotational transformation to remove xy term will align the conic with the axes of the Cartesian plane giving a new equation:

$$A'^{x^2} + C'^{y^2} + D'x + E'y + F' = 0$$

From this new equation, a co-ordinate translation can be found by completing the squares in x and y that will convert the general equation into a standard form. The rotation angle determined from:

$\theta = \frac{\pi}{4}$ if $A = C$

Otherwise $\theta = 0.5\ tan^{-1}\frac{B}{A-C}$

The new coefficients are therefore are

$$A' = A\cos\theta\ cos\theta + B\sin\theta\ cos\theta + C\ sin\theta\sin\theta$$

$$C' = A\sin\theta\ sin - B\sin\theta\ cos\theta + C\cos\theta\cos\theta$$

$$D' = D\cos\theta + E\sin\theta$$

$$E' = -D\sin\theta + E\cos\theta$$

$$F' = F$$

Translation

When the equation for a conic section is in the form of:

$$A'^{x^2} + C'^{y^2} + D'x + E'y + F' = 0$$

It can be changed by a translation that moves the center from the point (x_o, y_o) to the origin. The origin depends on the form of the standard conic equation. For a circle, ellipse, or hyperbola; the standard form is

$$A''x^2 \pm C''y^2 - 1 = 0$$

Thus the centre is computed from

$x_o = \frac{-D\prime}{2A\prime}$ $\quad$ $y_o = \frac{-E\prime}{2C\prime}$

Then the coefficients for the standard conic can be calculated using:

$$A'' = \frac{A'}{A'x_o^2 + C'y_o^2 - F'}$$

$$C'' = \frac{C'}{A'x_o^2 + C'y_o^2 - F'}$$

Determining the asphericity

If the conic is either an ellipse or hyperbola the orientation of the major axis is determined by the values of A'' and C''. The table below indicates how the location of the foci and the eccentricity are calculated.

For ellipse

Condition	Form	Foci
$\|A''\| < \|C''\|$	$\frac{x^2}{a^2} + \frac{y^2}{b^2} = 1$	$[\pm c, 0]$
$\|C''\| < \|A''\|$	$\frac{y^2}{a^2} + \frac{x^2}{b^2} = 1$	$[0, \pm c]$

$$a^2 = \frac{1}{min(|A''|, |C''|)}$$

$$b^2 = \frac{1}{max(|A''|, |C''|)}$$

where $c^2 = a^2 - b^2$ so that $a^2 > b^2$. The shape factor, $p = b^2/a^2$ and the asphericity $Q = p - 1$

For hyperbola

Condition	Form	Foci
$\|A''\| < \|C''\|$	$\frac{x^2}{a^2} - \frac{y^2}{b^2} = 1$	$[\pm c, 0]$
$\|C''\| < \|A''\|$	$\frac{y^2}{a^2} - \frac{x^2}{b^2} = 1$	$[0, \pm c]$

where $c^2 = a^2 + b^2$ so that $a^2 > b^2$. The eccentricity, $e = c/a$ which is always greater than 1. The asphericity (Q) value for hyperbola can be determined as $Q = -e^2$

APPENDIX A.2

The regression analysis plots and the Bland-Altman plots for two different measurements of eyelid variables that are not presented in Chapter 2.

1. Vertical palpebral fissure height

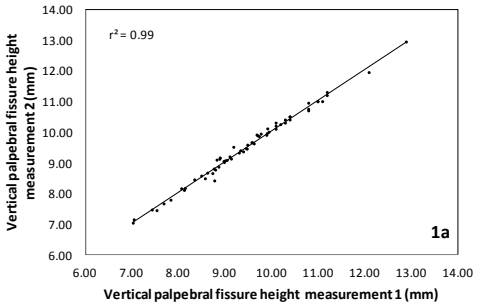

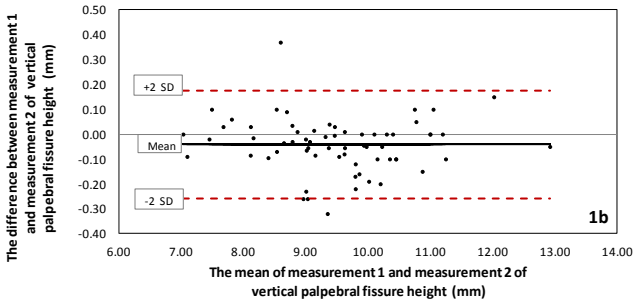

2. Horizontal eyelid fissure

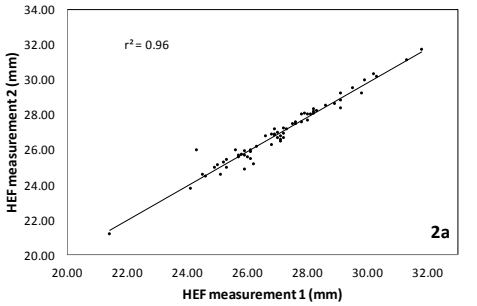

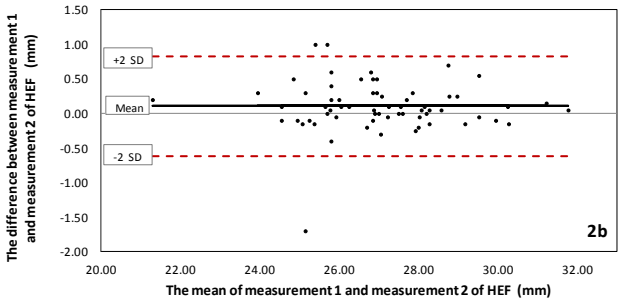

3. Upper eyelid angle

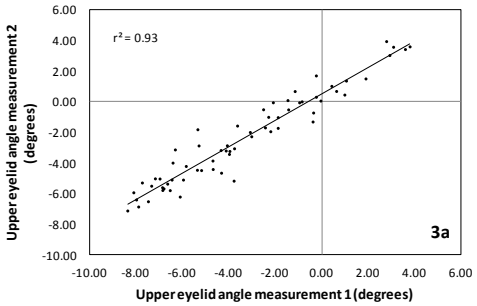

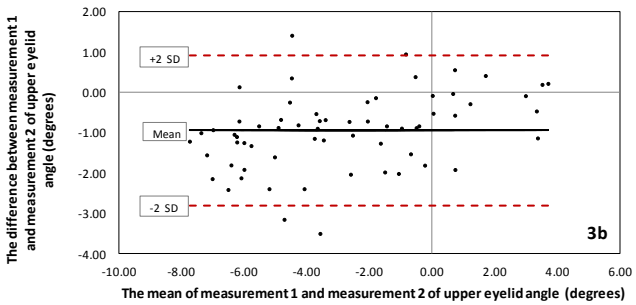

4. Lower eyelid angle

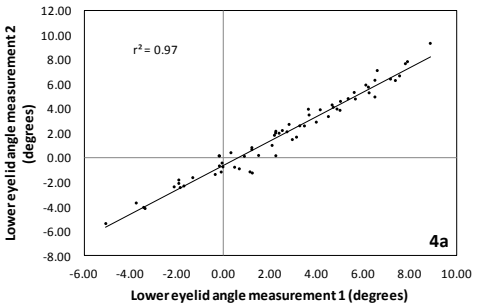

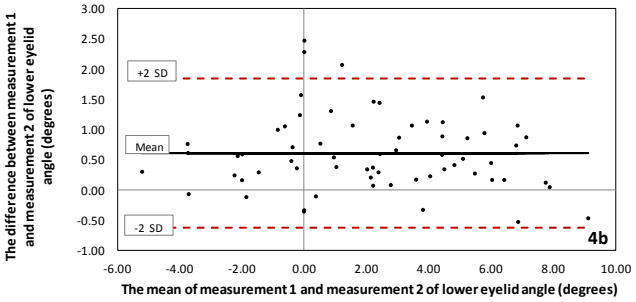

5. Upper eyelid position

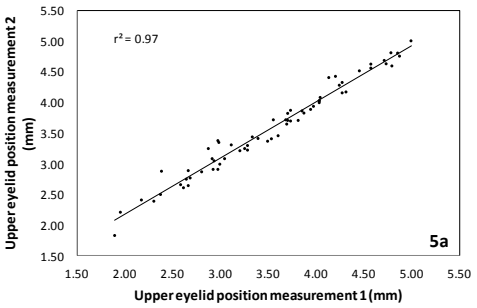

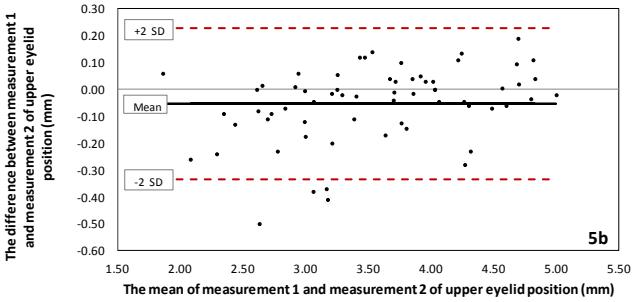

6. Upper eyelid slope

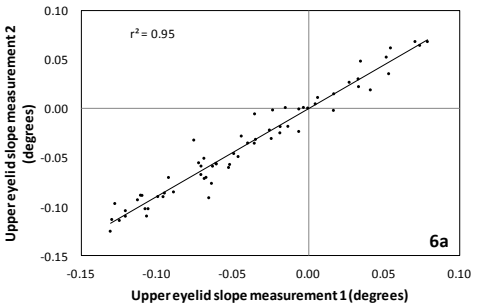

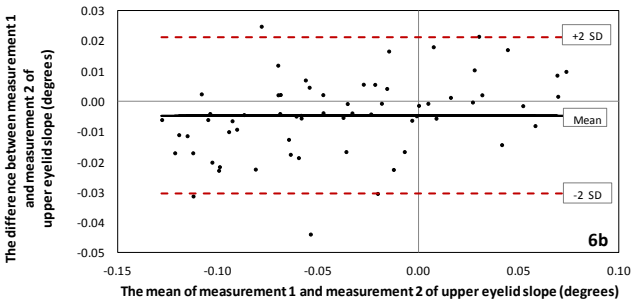

7. Upper eyelid curvature

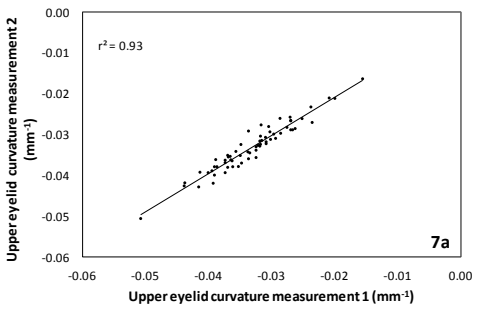

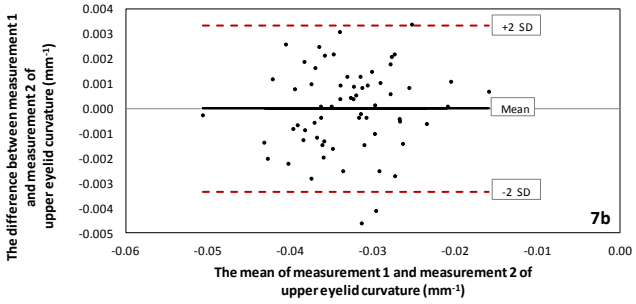

8. Upper eyelid curvature

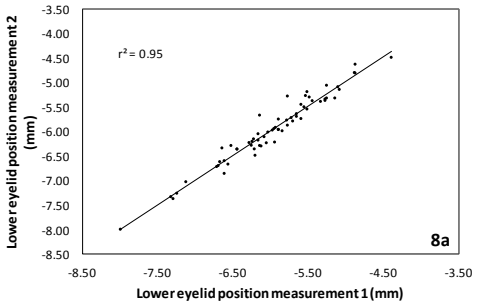

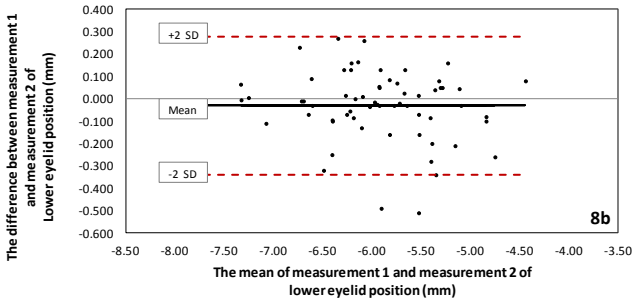

9. Lower eyelid slope

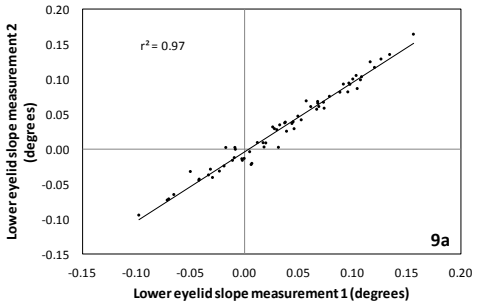

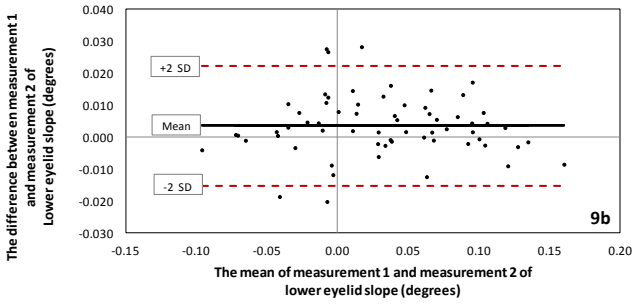

10. Lower eyelid curvature

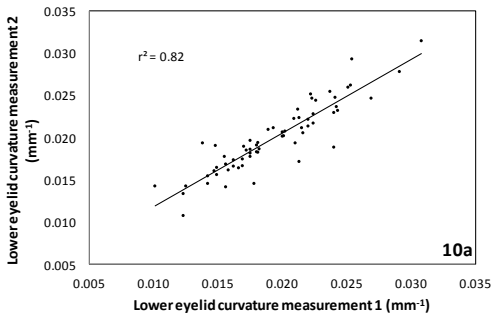

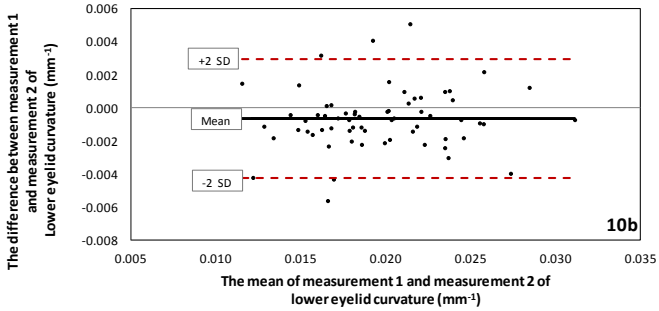

APPENDIX A.3

MATLAB functions used to determine meridional asphericity Q in Chapters 2, 3 and 5

```
function [RosOnly,QsOnly,meanRMSE] =  DetermineQ_FAp
warning off all

dst_fnames =( uigetfile('*dst','Select file with *dst ext','MultiSelect','On'))'; %Select files
xlsxfile =uigetfile('*xlsx','Choose xlsx file that has ref centres Centres');
refcentres = xlsread(xlsxfile,-1);% Choose refcentres from the excel sheet

      prompt = {'Enter step interval (0.05 to 0.5)','Chord diameter to which Q and Ro must be determined',
'CONIC FIT TYPE. (1- for Taubin method of fitting conics, 2- for Direct method of fitting ellipses '};
      dlg_title = 'Specify the following:';
num_lines = 1;
Variables = inputdlg(prompt,dlg_title,num_lines);
StepIntvl=str2double(Variables{1,1});
ChordDiameter = str2double(Variables{2,1});
ConicFittingType=str2double(Variables{3,1});
DecentVals=refcentres(:,10:11);

      if ConicFittingType>2
                  h = warndlg('Program stopped running because conic fit type can only be 1 or 2', 'Wrong
entry');
                  return
      end

      %% Read Filenames Dst and Hgt
      if ischar(dst_fnames);
                  dst_fnames=cellstr(dst_fnames');
```

```
        end

        [rc,~]=size(dst_fnames);
        for ic = 1:rc
              [~,dst_names,~]=fileparts(dst_fnames{ic,1});
              hgt_fnames{ic,1} =  strcat(dst_names,'.hgt');
        end

    %% Make Pt Blocks
        [r1,c1]=size(refcentres);
              for fileNos=1:r1
                    DstPtBlock(fileNos,1)={dst_fnames(refcentres(fileNos,13):refcentres(fileNos,14),1)};
                    HgtPtBlock(fileNos,1)={hgt_fnames(refcentres(fileNos,13):refcentres(fileNos,14),1)};

                    %% Read Individuals Pt Block and from that each map separately and Centre to the RC with
              required step intvl


                     IndividualPtDstFileNames  =  DstPtBlock{fileNos,1};  % get individual radial distance file
names
                     IndividualPtHgtFileNames = HgtPtBlock{fileNos,1};% get individual height file names
                    [r3,~]=size(IndividualPtDstFileNames);
                           for i3=1:1:r3

                                 EachDstMap(1,1)={dlmread(IndividualPtDstFileNames{i3,1})};   %   read   individual
                          radial distance files of a given participant
                                 EachHgtMap(1,1)={dlmread(IndividualPtHgtFileNames{i3,1})};   %   read   individual
                          height files of a given participant

                          [AllInterpHgt{i3,1},AllInterpDst{i3,1},~]=CentertoRefCent_FAp(EachHgtMap,EachDstMap,De
                          centVals(fileNos,1),DecentVals(fileNos,2),StepIntvl);
                                 % the above step centres the data to a given reference
                                 % centre, which can be entrance pupil centre,
                                 % geometric centre or vertex normal.
```

```
                end
            AllInterpHgt2{1,1}=AllInterpHgt;
            AllInterpDst2{1,1}=AllInterpDst;
            AvgHgtMap = AverageSelectedMap_FAp(AllInterpHgt2); % average each participants height data
            AvgDstMap  =  AverageSelectedMap_FAp(AllInterpDst2)  ;%  average  each  participants  radial
        distance data
            clearvars AllInterpHgt AllInterpDst

            [Coeffs{fileNos,1},meanRMSE(fileNos,1),~                                                    ]=
        ExtrapHgtFindCoeffs(AvgHgtMap,AvgDstMap,ChordDiameter,ConicFittingType);

            CoeffData(fileNos,:) = {IndividualPtHgtFileNames(1,1),Coeffs{fileNos,1}};
            %the above step extrapolates the height data and finds the
            %coefficients of the conic section using Taubins method
             RoQs(fileNos,1) = IndividualPtHgtFileNames(1,1);
             RoQs(fileNos,2) = {CoeffsToRoQVals_FAp(CoeffData{fileNos,2})};
             % the above step finds Ros and Qs of individual participant

         end

[RosOnly,QsOnly]=GetRosandQsOnly_FAp(RoQs);

end
```

Sub functions

CentertoRefCent_FAp

```
% CenterRawMedmontFileToGC centres the given curvature data data to the
% reference centre
```

```
function [DesiredZ,WantedDstData,EffecRad]=CentertoRefCent_FAp(HgtData,DstData,DecX,DecY,StepIntvl);

HgtData=[zeros(300,1) HgtData{1,1}]; %add extra line of zeros so interpolate knows that centre val is zero
DstData=[zeros(300,1) DstData{1,1}]; %add extra line of zeros so interpolate knows that centre val is zero
[~ ,cAXL]=size(HgtData);
EffecRad=4.80;  %This is range for interpolate grid

%% Creating Theta matrix
theta = deg2rad([0:1.2:358.8]');
thetaMatrixinradians=repmat(theta,1,cAXL);



%%
hgtnonzero = ~isnan(HgtData);
[x,y,z]=pol2cart(thetaMatrixinradians,DstData,HgtData); % finding cartesian coordinates from the polar data
X=x(hgtnonzero);
Y=y(hgtnonzero);
Z=z(hgtnonzero);
%%
F = TriScatteredInterp(X,Y,Z,'linear'); % Interpolation

%% create new distance grid with uniform 0.15 mm spacing
SpokeLength = 0.15:StepIntvl:EffecRad;
WantedDstData = [];

      for i=1:1:length(0:1.2:358.8),
                  WantedDstData = [WantedDstData;SpokeLength;];
      end

%% convert distance data to radial data

      thetaMatrixinradians(:,1) = [];
```

```
[xDst,yDst] = pol2cart(thetaMatrixinradians, WantedDstData);

%% shift grid by decentration amount as per the reference centres
ShiftX = xDst + DecX;
ShiftY = yDst + DecY;

%% find new height values for shifted data points
DesiredZ = F(ShiftX,ShiftY);

 end
```

AverageSelectedMap_FAp

```
function AvgMap = AverageSelectedMap_FAp(Maps)
   [numberofmaps,~]=size(Maps{1,1});
   Maps2=Maps{1,1}';


      if numberofmaps>10
            h = errordlg('Hey this program can do averaging of 10 maps only, May be you need to rewrite the
      program!!! ','OOPS!')
      end
        if numberofmaps==1
            AvgMap=(Maps2{1,1});
        end


        if numberofmaps==2
        AvgMap=(Maps2{1,1}+Maps2{1,2})/numberofmaps;
        end
```

```
        if numberofmaps==3
            AvgMap=(Maps2{1,1}+Maps2{1,2}+Maps2{1,3})/numberofmaps;
        end

        if numberofmaps==4
            AvgMap=(Maps2{1,1}+Maps2{1,2}+Maps2{1,3}+Maps2{1,4})/numberofmaps;
        end


        if numberofmaps==5
             AvgMap=(Maps2{1,1}+Maps2{1,2}+Maps2{1,3}+Maps2{1,4}+Maps2{1,5})/numberofmaps;
        end

        if numberofmaps==6
            AvgMap=(Maps2{1,1}+Maps2{1,2}+Maps2{1,3}+Maps2{1,4}+Maps2{1,5}+Maps2{1,6})/numberofmaps;
        end


        if numberofmaps==7

AvgMap=(Maps2{1,1}+Maps2{1,2}+Maps2{1,3}+Maps2{1,4}+Maps2{1,5}+Maps2{1,6}+Maps2{1,7})/numberofmaps;
        end

        if numberofmaps==8

      AvgMap=(Maps2{1,1}+Maps2{1,2}+Maps2{1,3}+Maps2{1,4}+Maps2{1,5}+Maps2{1,6}+Maps2{1,7}+Maps2{1,8})/numbero
      fmaps;
        end

        if numberofmaps==9

      AvgMap=(Maps2{1,1}+Maps2{1,2}+Maps2{1,3}+Maps2{1,4}+Maps2{1,5}+Maps2{1,6}+Maps2{1,7}+Maps2{1,8}+Maps2{1,
      9})/numberofmaps;
```

```
        end

        if numberofmaps==10

      AvgMap=(Maps2{1,1}+Maps2{1,2}+Maps2{1,3}+Maps2{1,4}+Maps2{1,5}+Maps2{1,6}+Maps2{1,7}+Maps2{1,8}+Maps2{1,
      9}+Maps2{1,10})/numberofmaps;
        end
end
```

ExtrapHgtFindCoeffs_FAp

```
function [Coeffs,meanRMSE,RMSEc ]= ExtrapHgtFindCoeffs_FAp(AvgHGT,AvgDST,ChordDiameter,ConicFittingType)
 [r,c]=size(AvgHGT);
for i=1:1:r
            [NewY,meanRMSE,RMSEc]= ExtrapHgt_FAp(AvgHGT,AvgDST,ChordDiameter);
            if ConicFittingType ==1
                  Coeffs=TaubinConicCoeff_MirrorFM(NewY(:,1:end),AvgDST(:,1:end),ChordDiameter);
            elseif ConicFittingType==2
                  Coeffs=DirectConicCoeff_MirrorFM(NewY(:,1:end),AvgDST(:,1:end),ChordDiameter);
            end
end
end
```

TaubinConicCoeff_MirrorFM

```
%Determines conic section coefficients of general equation

function A=TaubinConicCoeff_MirrorFM(HgtData,DstData,ChordDiameter)
      %
      rowlength = round(((ChordDiameter)/2)/0.15); % row length as per chord dia
            %%

            [row,~]=size(HgtData);

            for ijk=1:1:row
                  x(1,:) = DstData(ijk,1:rowlength);
                  xf(1,:)=-fliplr(DstData(ijk,1:rowlength));
```

```
            y(1,:)=HgtData(ijk,1:rowlength);
            yf(1,:)=fliplr(HgtData(ijk,1:rowlength));

            X = [xf,x];
            Y = [yf,y];

            xy=[X',Y'];

            A(ijk,1)= {EllipseFitByTaubin(xy)};

        end
end
```

EllipseFitByTaubin(

```
function A = EllipseFitByTaubin(XY);
%
%   Ellipse fit by Taubin's Method published in
%      G. Taubin, "Estimation Of Planar Curves, Surfaces And Nonplanar
%                  Space Curves Defined By Implicit Equations, With
%                  Applications To Edge And Range Image Segmentation",
%      IEEE Trans. PAMI, Vol. 13, pages 1115-1138, (1991)
%
%     Input:  XY(n,2) is the array of coordinates of n points x(i)=XY(i,1),
      y(i)=XY(i,2)
%
%     Output: A = [a b c d e f]' is the vector of algebraic
%             parameters of the fitting ellipse:
%             ax^2 + bxy + cy^2 +dx + ey + f = 0
%             the vector A is normed, so that ||A||=1
%
%     Among fast non-iterative ellipse fitting methods,
%     this is perhaps the most accurate and robust
%
%     Note: this method fits a quadratic curve (conic) to a set of points;
```

```
%     if points are better approximated by a hyperbola, this fit will
%     return a hyperbola. To fit ellipses only, use "Direct Ellipse Fit".
%     centroid = mean(XY);   % the centroid of the data set
      Z   =   [(XY(:,1)-centroid(1)).^2,   (XY(:,1)-centroid(1)).*(XY(:,2)-
centroid(2)),(XY(:,2)-centroid(2)).^2,    XY(:,1)-centroid(1),    XY(:,2)-
centroid(2), ones(size(XY,1),1)];
M = Z'*Z/size(XY,1);
      P  =  [M(1,1)-M(1,6)^2,  M(1,2)-M(1,6)*M(2,6),  M(1,3)-M(1,6)*M(3,6),
M(1,4),    M(1,5);    M(1,2)-M(1,6)*M(2,6),    M(2,2)-M(2,6)^2,    M(2,3)-
M(2,6)*M(3,6), M(2,4), M(2,5); M(1,3)-M(1,6)*M(3,6), M(2,3)-M(2,6)*M(3,6),
M(3,3)-M(3,6)^2, M(3,4), M(3,5); M(1,4), M(2,4), M(3,4), M(4,4), M(4,5);
M(1,5), M(2,5), M(3,5), M(4,5), M(5,5)];
Q = [4*M(1,6), 2*M(2,6), 0, 0, 0;
      2*M(2,6), M(1,6)+M(3,6), 2*M(2,6), 0, 0;
      0, 2*M(2,6), 4*M(3,6), 0, 0;
      0, 0, 0, 1, 0;
      0, 0, 0, 0, 1];
[V,D] = eig(P,Q);
      [Dsort,ID] = sort(diag(D));
      A = V(:,ID(1));
A = [A; -A(1:3)'*M(1:3,6)];
A4 = A(4)-2*A(1)*centroid(1)-A(2)*centroid(2);
A5 = A(5)-2*A(3)*centroid(2)-A(2)*centroid(1);
A6 = A(6)+A(1)*centroid(1)^2+A(3)*centroid(2)^2+...
      A(2)*centroid(1)*centroid(2)-A(4)*centroid(1)-A(5)*centroid(2);
A(4) = A4;  A(5) = A5;  A(6) = A6;
A = A/norm(A);

end
```

Copyright (c) 2009, Nikolai Chernov
All rights reserved.

Redistribution and use in source and binary forms, with or without
modification, are permitted provided that the following conditions are
met:

Redistributions of source code must retain the above copyright
notice, this list of conditions and the following disclaimer.
Redistributions in binary form must reproduce the above copyright
notice, this list of conditions and the following disclaimer in
the documentation and/or other materials provided with the distribution
1. Neither the name of the University of Alabama at Birmingham nor the
names
of its contributors may be used to endorse or promote products derived
from this software without specific prior written permission.

THIS SOFTWARE IS PROVIDED BY THE COPYRIGHT HOLDERS AND CONTRIBUTORS "AS IS"
AND ANY EXPRESS OR IMPLIED WARRANTIES, INCLUDING, BUT NOT LIMITED TO, THE
IMPLIED WARRANTIES OF MERCHANTABILITY AND FITNESS FOR A PARTICULAR PURPOSE
ARE DISCLAIMED. IN NO EVENT SHALL THE COPYRIGHT OWNER OR CONTRIBUTORS BE
LIABLE FOR ANY DIRECT, INDIRECT, INCIDENTAL, SPECIAL, EXEMPLARY, OR
CONSEQUENTIAL DAMAGES (INCLUDING, BUT NOT LIMITED TO, PROCUREMENT OF
SUBSTITUTE GOODS OR SERVICES; LOSS OF USE, DATA, OR PROFITS; OR BUSINESS
INTERRUPTION) HOWEVER CAUSED AND ON ANY THEORY OF LIABILITY, WHETHER IN
CONTRACT, STRICT LIABILITY, OR TORT (INCLUDING NEGLIGENCE OR OTHERWISE)
ARISING IN ANY WAY OUT OF THE USE OF THIS SOFTWARE, EVEN IF ADVISED OF THE
POSSIBILITY OF SUCH DAMAGE.

CoeffsToRoQVals_FAp

```
function RoQs = CoeffsToRoQVals_FAp(CoeffData)

[rv,cv]=size(CoeffData);
for j=1:1:rv
            Coeffs2=cell2mat(CoeffData(j,1));
            [ Ro(j,:),Q(j,:) ] = QvalueFromCoeffs_FAp( Coeffs2 );
            RoQs=[Ro,Q];
end
end
```

```
function [ Ro,Qvals ] = QvalueFromCoeffs_FAp( Coeffs )
      %%

tol = 1e-15;
A=Coeffs(1,1);
B=Coeffs(2,1);
C=Coeffs(3,1);
D=Coeffs(4,1);
E=Coeffs(5,1);
F=Coeffs(6,1);
det = (A*C*F +(((B*D*E)-(B*B*F)-(C*D*D)-(A*E*E))/4));

M11=(A*C)-(B*B/4);
M23=(D*(E/4))-(B*(F/2));

                        if det ~=tol && A*det<tol && M11 > tol && A ~=C && B ~=0 %
                    Conic = 1;          %ellipse

             elseif det ~=tol  &&  M11<-tol
                   Conic = 2 ;  %hyperbola
             end

      %%Find standard conic equation corresponding to general equation by
      %%removing rotation and then removing translation.

      if A==C
                   theta = pi/4;
      else theta = 0.5*atan(B/(A-C));
      end
      Sa = sin(theta);
Ca = cos(theta);
Ar=(A*Ca*Ca)+(B*Sa*Ca)+(C*Sa*Sa);
Cr = (A*Sa*Sa)-(B*Sa*Ca)+(C*Ca*Ca);
Dr = (D*Ca)+(E*Sa);
```

```
Er = (-D*Sa)+(E*Ca);
Fr = F;

Rotation = (180*theta)/pi;

      if Conic ==1
                  Xo = -Dr/(2*Ar);
                  Yo = -Er/(2*Cr);
                  TranslationValue = [Xo,Yo];
                  R(1,1) = Ar/((Ar*Xo*Xo)+(Cr*Yo*Yo) -Fr);
                  R(3,1)=Cr/((Ar*Xo*Xo)+(Cr*Yo*Yo) -Fr);
                  R(6,1) = 0;
            %foci on x-axis
                  semiminor = sqrt(abs(1/R(1,1)));
                  semimajor = sqrt(abs(1/R(3,1)));

                  p = (semiminor^2)/(semimajor^2);
                  Ro = semiminor^2/semimajor;
                  Qvals = p-1;

      elseif Conic ==2
                  Xo = -Dr/(2*Ar);
                  Yo = -Er/(2*Cr);
                  TranslationValue = [Xo,Yo];
                  R(1,1) = Ar/((Ar*Xo*Xo)+(Cr*Yo*Yo) -Fr);
                  R(3,1)=Cr/((Ar*Xo*Xo)+(Cr*Yo*Yo) -Fr);
                  R(6,1) = 0.0;

                        if R(1,1) > R(3,1)
                                    a2 = abs(1/R(1,1));
                                    b2 = abs(1/R(3,1));

                                    c = sqrt(a2+b2);
                                    Foci = [c,0];
```

```
            ecc = c / sqrt(a2);
            Ro = b2/sqrt(a2);
            Qvals = -(ecc^2);
      else a2 =abs(1/(R(3,1)));
            b2 = abs(1/R(1,1));
            c = sqrt(a2+b2);
            Foci = [0,c];
            ecc = c / sqrt(a2);
            Ro = b2/sqrt(a2);
             Qvals = -(ecc^2);

      end



end


    end
    Copyright &copy; 2004, Stephen R. Schmitt, the source code is available at
http://mysite.verizon.net/res148h4j/javascript/script_conic_equation_type.html#top
```

GetRosandQsOnly_FAp

```
function [RosOnly,QsOnly]=GetRosandQsOnly_FAp(RoQs)

[r,c]=size(RoQs);

    for i=1:r
    A = RoQs(i,2);
    B = cell2mat(A(1,1));
    RosOnly(i,:)=(B(:,1))';
```

```
    A2 = RoQs(i,2);
    B2 = cell2mat(A(1,1));
    QsOnly(i,:)=(B(:,2))';

    end
end
```

APPENDIX B

MATLAB functions used to determine the treatment zone decentration between Chapters 3 and 5

```
function[DecentParams,eye]=
Decentparams(BL_RefPwr,PostOK_RefPwr,DistanceMat,type,filename,RefCentVals,eye,figoption)
% BL_RefPwr = Baseline refractive power data
% PostOK_RefPwr = Post OKrefractive power data
% RefCentVals = reference centre values
% eye = eye
% figoption = figure option(1= yes, 2 = no)

DiffCurv=PostOK_RefPwr-BL_RefPwr;

SplitDiffCurv=DiffCurv(:,2:end);

switch type
    case{'axlCurv','tglCurv'}

          NegVals=SplitDiffCurv<0;

    case{'axlPwr','tglPwr','refPwr'}
            NegVals=SplitDiffCurv>0;
end
 SplitDiffCurv(NegVals)=NaN;

NaN_Indices=isnan(SplitDiffCurv);

FirstNaN = findfirst(NaN_Indices, 2);
 [~,minInd]=min(SplitDiffCurv,[],2);
```

```
[M,N]=size(SplitDiffCurv);
for i=1:1:M
    if FirstNaN(i,1)==0
        FirstNaN(i,1)=minInd(i,1);

    end
end

ColNums=FirstNaN+(InnermostCell-1);

[r,~]= size (minInd);
DistVals=[];
for i=1:1:r
DistVals(i,1)=DistanceMat(1,ColNums(i,1));

end
theta=[deg2rad(0:1.2:358.8)]';

[X,Y]=pol2cart(theta,DistVals);% Co-ordinate points of the actual decentration

[ActualGeom]=polygeom(X,Y); % gives parameters area, decentration (x-dec, y-dec)and perimeter)
XDec=ActualGeom(1,2); % actual x-decentration
YDec=ActualGeom(1,3); % actual y-decentration

ActualArea=ActualGeom(1,1);
ActualPerimeter=ActualGeom(1,4);


if eye==1
    ActualDecent=[XDec,YDec];
elseif eye==2
    ActualDecent=[(-1*XDec),YDec];
elseif eye>2
```

```
        errordlg('You have entered a wrong value for EYE! enter 1 for RE, 2 for LE, Please check your input XL
sheet ')
    elseif isempty(eye)
        errordlg('You did not enter EYE for one or more pts')
    end

    %%
    [ActlHzTZDiameter,ActlMaxDia,ActlMaxDiaAngle]= Diams(X,Y,eye);
    ActlDecParams = [ActualDecent,ActlHzTZDiameter,ActlMaxDia,ActlMaxDiaAngle,ActualArea];
    ellipse_t = fit ellipse(X,Y); % gets the parameters of the best-fit ellipse.
     % model ellipse x,y coorinates will be given by x=a *cos t and y = b*sint

    a=ellipse_t.a; % getting the 1/2major
    b=ellipse_t.b; % 1/2minor of the ellipse

    % from half major and half minor of the ellipse getting the co-ordinates of
    % the best fit ellipse.

    phi=(ellipse_t.phi)+deg2rad(90);
    %theta2=theta+EllipseTheta;
    x=(a*cos(theta)*cos(phi))-(b*sin(theta)*sin(phi)); %
    y=(a*cos(theta)*sin(phi)) + (b*sin(theta)*cos(phi));
    %[MaxDia,Theta]=MaxDiaTheta(x,y)

    % ellipse X and Y decentration from ellipse_t
    Ellip_Xdec=ellipse_t.X0_in;
    Ellip_Ydec=ellipse_t.Y0_in;

    if eye==1
        EllipDecent=[Ellip_Xdec,Ellip_Ydec];
    elseif eye==2
        EllipDecent=[(-1*Ellip_Xdec),Ellip_Ydec];
    end
```

```
      Dec_ellipse_Xcoord=x+Ellip_Xdec;
      Dec_ellipse_Ycoord=y+Ellip_Ydec;


      [EllipseHzTZDiameter,EllipseMaxDia,EllipseMaxDiaAngle]= Diams(Dec_ellipse_Xcoord,Dec_ellipse_Ycoord,eye);
      [EllipGeom]=polygeom(Dec_ellipse_Xcoord,Dec_ellipse_Ycoord);
      [EllipArea]=EllipGeom(1,1);
      [EllipPerimeter]=EllipGeom(1,4);

      EllipseDecParams = [EllipDecent,EllipseHzTZDiameter,EllipseMaxDia,EllipseMaxDiaAngle,EllipArea];

      if figoption ==1
      createfigure5(X,      Y,      Dec_ellipse_Xcoord,      Dec_ellipse_Ycoord,      XDec,      YDec,      Ellip_Xdec,
Ellip_Ydec,filename,RefCentVals,EllipDecent,eye)
      saveas(gcf,filename,'png');
      end

      DecentParams=[EllipseDecParams];
      end
```

Sub functions

```
function [ geom, iner, cpmo ] = polygeom( x, y )
%POLYGEOM Geometry of a planar polygon
%
%   POLYGEOM( X, Y ) returns area, X centroid,
%   Y centroid and perimeter for the planar polygon
%   specified by vertices in vectors X and Y.
%
%   [ GEOM, INER, CPMO ] = POLYGEOM( X, Y ) returns
%   area, centroid, perimeter and area moments of
%   inertia for the polygon.
%   GEOM = [ area   X_cen  Y_cen  perimeter ]
%   INER = [ Ixx    Iyy    Ixy    Iuu    Ivv    Iuv ]
```

```
%     u,v are centroidal axes parallel to x,y axes.
%   CPMO = [ I1     ang1   I2     ang2   J ]
%     I1,I2 are centroidal principal moments about axes
%         at angles ang1,ang2.
%     ang1 and ang2 are in radians.
%     J is centroidal polar moment.  J = I1 + I2 = Iuu + Ivv

% H.J. Sommer III - 02.05.14 - tested under MATLAB v5.2
%
% sample data
% x = [ 2.000  0.500  4.830  6.330 ]';
% y = [ 4.000  6.598  9.098  6.500 ]';
% 3x5 test rectangle with long axis at 30 degrees
% area=15, x_cen=3.415, y_cen=6.549, perimeter=16
% Ixx=659.561, Iyy=201.173, Ixy=344.117
% Iuu=16.249, Ivv=26.247, Iuv=8.660
% I1=11.249, ang1=30deg, I2=31.247, ang2=120deg, J=42.496
%
% H.J. Sommer III, Ph.D., Professor of Mechanical Engineering, 337 Leonhard Bldg
% The Pennsylvania State University, University Park, PA  16802
% (814)863-8997  FAX (814)865-9693  hjs1@psu.edu  www.me.psu.edu/sommer/

% begin function POLYGEOM

% check if inputs are same size
if ~isequal( size(x), size(y) ),
  error( 'X and Y must be the same size');
end

% number of vertices
[ x, ns ] = shiftdim( x );
[ y, ns ] = shiftdim( y );
[ n, c ] = size( x );
```

```
% temporarily shift data to mean of vertices for improved accuracy
xm = mean(x);
ym = mean(y);
x = x - xm*ones(n,1);
y = y - ym*ones(n,1);

% delta x and delta y
dx = x( [ 2:n 1 ] ) - x;
dy = y( [ 2:n 1 ] ) - y;

% summations for CW boundary integrals
A = sum( y.*dx - x.*dy )/2;
Axc = sum( 6*x.*y.*dx -3*x.*x.*dy +3*y.*dx.*dx +dx.*dx.*dy )/12;
Ayc = sum( 3*y.*y.*dx -6*x.*y.*dy -3*x.*dy.*dy -dx.*dy.*dy )/12;
Ixx = sum( 2*y.*y.*y.*dx -6*x.*y.*y.*dy -6*x.*y.*dy.*dy ...
          -2*x.*dy.*dy.*dy -2*y.*dx.*dy.*dy -dx.*dy.*dy.*dy )/12;
Iyy = sum( 6*x.*x.*y.*dx -2*x.*x.*x.*dy +6*x.*y.*dx.*dx ...
          +2*y.*dx.*dx.*dx +2*x.*dx.*dx.*dy +dx.*dx.*dx.*dy )/12;
Ixy = sum( 6*x.*y.*y.*dx -6*x.*x.*y.*dy +3*y.*y.*dx.*dx ...
          -3*x.*x.*dy.*dy +2*y.*dx.*dx.*dy -2*x.*dx.*dy.*dy )/24;
P = sum( sqrt( dx.*dx +dy.*dy ) );

% check for CCW versus CW boundary
if A < 0,
  A = -A;
  Axc = -Axc;
  Ayc = -Ayc;
  Ixx = -Ixx;
  Iyy = -Iyy;
  Ixy = -Ixy;
end

% centroidal moments
xc = Axc / A;
```

```
yc = Ayc / A;
Iuu = Ixx - A*yc*yc;
Ivv = Iyy - A*xc*xc;
Iuv = Ixy - A*xc*yc;
J = Iuu + Ivv;

% replace mean of vertices
x_cen = xc + xm;
y_cen = yc + ym;
Ixx = Iuu + A*y_cen*y_cen;
Iyy = Ivv + A*x_cen*x_cen;
Ixy = Iuv + A*x_cen*y_cen;

% principal moments and orientation
I = [ Iuu  -Iuv ;
     -Iuv   Ivv ];
[ eig_vec, eig_val ] = eig(I);
I1 = eig_val(1,1);
I2 = eig_val(2,2);
ang1 = atan2( eig_vec(2,1), eig_vec(1,1) );
ang2 = atan2( eig_vec(2,2), eig_vec(1,2) );

% return values
geom = [ A  x_cen  y_cen  P ];
iner = [ Ixx  Iyy  Ixy  Iuu  Ivv  Iuv ];
cpmo = [ I1  ang1  I2  ang2  J ];

% end of function POLYGEOM
Copyright (c) 1998, H.J. Sommer
All rights reserved.

Redistribution and use in source and binary forms, with or without
modification, are permitted provided that the following conditions are
met:
```

```
    * Redistributions of source code must retain the above copyright
      notice, this list of conditions and the following disclaimer.
    * Redistributions in binary form must reproduce the above copyright
      notice, this list of conditions and the following disclaimer in
      the documentation and/or other materials provided with the distribution
    * Neither the name of the Penn State University nor the names
      of its contributors may be used to endorse or promote products derived
      from this software without specific prior written permission.

THIS SOFTWARE IS PROVIDED BY THE COPYRIGHT HOLDERS AND CONTRIBUTORS "AS IS"
AND ANY EXPRESS OR IMPLIED WARRANTIES, INCLUDING, BUT NOT LIMITED TO, THE
IMPLIED WARRANTIES OF MERCHANTABILITY AND FITNESS FOR A PARTICULAR PURPOSE
ARE DISCLAIMED. IN NO EVENT SHALL THE COPYRIGHT OWNER OR CONTRIBUTORS BE
LIABLE FOR ANY DIRECT, INDIRECT, INCIDENTAL, SPECIAL, EXEMPLARY, OR
CONSEQUENTIAL DAMAGES (INCLUDING, BUT NOT LIMITED TO, PROCUREMENT OF
SUBSTITUTE GOODS OR SERVICES; LOSS OF USE, DATA, OR PROFITS; OR BUSINESS
INTERRUPTION) HOWEVER CAUSED AND ON ANY THEORY OF LIABILITY, WHETHER IN
CONTRACT, STRICT LIABILITY, OR TORT (INCLUDING NEGLIGENCE OR OTHERWISE)
ARISING IN ANY WAY OUT OF THE USE OF THIS SOFTWARE, EVEN IF ADVISED OF THE
POSSIBILITY OF SUCH DAMAGE.
```

```
function B = findfirst(A, dim, count, firstlast)
% B = FINDFIRST(A)
%
% Look for the row-indices of a first non-zero element(s) for all columns
% in the array. It is equivalent to doing:
%
%       B=zeros(1,size(A,1));
%       for j=1:size(A,2)
%           Bj = find(A(:,j), 1, 'first');
%           if ~isempty(Bj); B(j)=Bj; end
%       end
%
% B = FINDFIRST(A, DIM): operate along the dimension DIM
% B = FINDFIRST(A, DIM, COUNT): look for the most COUNT non-zeros elements
%                               (by default COUNT is 1)
% B = FINDFIRST(A, DIM, COUNT, 'LAST'): returns most last non-zero indices
%
% INPUTS:
%       A: array of dimension (N1 x N2 x ...x Nd x ... Nn)
%          A can be any numerical class
% OUTPUT:
%       B: same dimension than A, but only Nd is contracted to COUNT
%          where d is the dimension specified by the second input (DIM)
%          and COUNT is specified by the third input
%       B dimension is (N1 x N2 x ... x COUNT x ... Nn)
%       B contains indices non-zero elements of A along DIM
%       B is filled when it's possible, the rest is filles with zeros if A
%         contains less than COUNT non-zero elements.
%
% NOTES: - Sparse matrix is not suuported
%        - Inplace engine, i.e., no duplicated temporary array is created
%
% USAGE EXAMPLES:
```

```
%
%    A = [ 0   1   1
%          1   0   1
%          0   0   0
%          0   0   1
%          1   1   1 ]
%
% OPERATE ALONG COLUMNS: > B = FINDFIRST(A) % returns [2 1 1]
%
% OPERATE ALONG ROWS: > B=FINDFIRST(A,2) % returns [2 1 0 3 1]'
%
% > B=FINDFIRST(A,1,2) % returns two indexes for each column [2 1 1
%                                                            5 5 2]
%
% > B=FINDFIRST(A,1,2, 'last') % returns two last indexes [5 5 5
%                                                          2 1 4]
%
% See also: find, nonzeros
%
% AUTHOR: Bruno Luong <brunoluong@yahoo.com>
% HISTORY
%   Original: 05-Jul-2009
%

% Default working dimension
if nargin<2 || isempty(dim)
    dim = 1;
end
% Check if it's correct
if ~isscalar(dim)
    error('FINDFIRST: dim must be a scalar');
end
dim = round(dim);
if dim<=0
    error('FINDFIRST: dim must be positive number');
```

```
end

% Default count
if nargin<3 || isempty(count)
    count = 1;
end
% Check if it's correct
if ~isscalar(count)
    error('FINDFIRST: count must be a scalar');
end
count = round(double(count));

% Default 'first' 'last flag
if nargin<4 || isempty(firstlast)
    firstlast = 'first';
end
if ~ischar(firstlast) || isempty(strmatch(firstlast,{'first' 'last'}))
    error('FINDFIRST: Fourth argument must be ''first'' or ''last''');
end

if issparse(A)
    error('FINDFIRST: A must be full matrix')
end

% Extend trailing singleton dimension if needed
szA = size(A);
szA(end+1:dim) = 1;

% Reshape A in 3D arrays, working dimension is the middle
% That is the form the FIND1DMEX
k = prod(szA(1:dim-1)); % return 1 if empty
m = szA(dim);
n = prod(szA(dim+1:end)); % return 1 if empty
A = reshape(A,[k m n]);
```

```
% Call mex engine
if strcmpi(firstlast, 'first')
    B = find1dmex(A, count);
else
    B = find1dmex(A, -count);
end

% Dimension of the output
szB = szA;
szB(dim) = count;
B = reshape(B,szB);

end

Copyright (c) 2009, Bruno Luong
All rights reserved.

Redistribution and use in source and binary forms, with or without
modification, are permitted provided that the following conditions are
met:

    * Redistributions of source code must retain the above copyright
      notice, this list of conditions and the following disclaimer.
    * Redistributions in binary form must reproduce the above copyright
      notice, this list of conditions and the following disclaimer in
      the documentation and/or other materials provided with the distribution

THIS SOFTWARE IS PROVIDED BY THE COPYRIGHT HOLDERS AND CONTRIBUTORS "AS IS"
AND ANY EXPRESS OR IMPLIED WARRANTIES, INCLUDING, BUT NOT LIMITED TO, THE
IMPLIED WARRANTIES OF MERCHANTABILITY AND FITNESS FOR A PARTICULAR PURPOSE
ARE DISCLAIMED. IN NO EVENT SHALL THE COPYRIGHT OWNER OR CONTRIBUTORS BE
LIABLE FOR ANY DIRECT, INDIRECT, INCIDENTAL, SPECIAL, EXEMPLARY, OR
CONSEQUENTIAL DAMAGES (INCLUDING, BUT NOT LIMITED TO, PROCUREMENT OF
```

```
SUBSTITUTE GOODS OR SERVICES; LOSS OF USE, DATA, OR PROFITS; OR BUSINESS
INTERRUPTION) HOWEVER CAUSED AND ON ANY THEORY OF LIABILITY, WHETHER IN
CONTRACT, STRICT LIABILITY, OR TORT (INCLUDING NEGLIGENCE OR OTHERWISE)
ARISING IN ANY WAY OUT OF THE USE OF THIS SOFTWARE, EVEN IF ADVISED OF THE
POSSIBILITY OF SUCH DAMAGE.

function ellipse_t = fit_ellipse( x,y,axis_handle )
%
% fit_ellipse - finds the best fit to an ellipse for the given set of points.
%
% Format:   ellipse_t = fit_ellipse( x,y,axis_handle )
%
% Input:    x,y         - a set of points in 2 column vectors. AT LEAST 5 points are needed !
%           axis_handle - optional. a handle to an axis, at which the estimated ellipse
%                         will be drawn along with it's axes
%
% Output:   ellipse_t - structure that defines the best fit to an ellipse
%                       a           - sub axis (radius) of the X axis of the non-tilt ellipse
%                       b           - sub axis (radius) of the Y axis of the non-tilt ellipse
%                       phi         - orientation in radians of the ellipse (tilt)
%                       X0          - center at the X axis of the non-tilt ellipse
%                       Y0          - center at the Y axis of the non-tilt ellipse
%                       X0_in       - center at the X axis of the tilted ellipse
%                       Y0_in       - center at the Y axis of the tilted ellipse
%                       long_axis   - size of the long axis of the ellipse
%                       short_axis  - size of the short axis of the ellipse
%                       status      - status of detection of an ellipse
%
% Note:     if an ellipse was not detected (but a parabola or hyperbola), then
%           an empty structure is returned

% ================================================================================
%                   Ellipse Fit using Least Squares criterion
% ================================================================================
% We will try to fit the best ellipse to the given measurements. the mathematical
```

```
% representation of use will be the CONIC Equation of the Ellipse which is:
%
%    Ellipse = a*x^2 + b*x*y + c*y^2 + d*x + e*y + f = 0
%
% The fit-estimation method of use is the Least Squares method (without any weights)
% The estimator is extracted from the following equations:
%
%    g(x,y;A) := a*x^2 + b*x*y + c*y^2 + d*x + e*y = f
%
%    where:
%       A   - is the vector of parameters to be estimated (a,b,c,d,e)
%       x,y - is a single measurement
%
% We will define the cost function to be:
%
%   Cost(A) := (g_c(x_c,y_c;A)-f_c)'*(g_c(x_c,y_c;A)-f_c)
%            = (X*A+f_c)'*(X*A+f_c)
%            = A'*X'*X*A + 2*f_c'*X*A + N*f^2
%
%   where:
%       g_c(x_c,y_c;A) - vector function of ALL the measurements
%                        each element of g_c() is g(x,y;A)
%       X              - a matrix of the form: [x_c.^2, x_c.*y_c, y_c.^2, x_c, y_c ]
%       f_c            - is actually defined as ones(length(f),1)*f
%
% Derivation of the Cost function with respect to the vector of parameters "A" yields:
%
%   A'*X'*X = -f_c'*X = -f*ones(1,length(f_c))*X = -f*sum(X)
%
% Which yields the estimator:
%
%       ~~~~~~~~~~~~~~~~~~~~~~~~~~~~~~~~~~~~~~~~~~~~~~~~~~~~~~~~~~~~~~~~~~~~~~~~~~~
%       |  A_least_squares = -f*sum(X)/(X'*X) ->(normalize by -f) = sum(X)/(X'*X)  |
%       ~~~~~~~~~~~~~~~~~~~~~~~~~~~~~~~~~~~~~~~~~~~~~~~~~~~~~~~~~~~~~~~~~~~~~~~~~~~
%
```

```
% (We will normalize the variables by (-f) since "f" is unknown and can be accounted for later on)
%
% NOW, all that is left to do is to extract the parameters from the Conic Equation.
% We will deal the vector A into the variables: (A,B,C,D,E) and assume F = -1;
%
%    Recall the conic representation of an ellipse:
%
%       A*x^2 + B*x*y + C*y^2 + D*x + E*y + F = 0
%
% We will check if the ellipse has a tilt (=orientation). The orientation is present
% if the coefficient of the term "x*y" is not zero. If so, we first need to remove the
% tilt of the ellipse.
%
% If the parameter "B" is not equal to zero, then we have an orientation (tilt) to the ellipse.
% we will remove the tilt of the ellipse so as to remain with a conic representation of an
% ellipse without a tilt, for which the math is more simple:
%
% Non tilt conic rep.:  A`*x^2 + C`*y^2 + D`*x + E`*y + F` = 0
%
% We will remove the orientation using the following substitution:
%
%   Replace x with cx+sy and y with -sx+cy such that the conic representation is:
%
%   A(cx+sy)^2 + B(cx+sy)(-sx+cy) + C(-sx+cy)^2 + D(cx+sy) + E(-sx+cy) + F = 0
%
%   where:      c = cos(phi)    ,   s = sin(phi)
%
%   and simplify...
%
%       x^2(A*c^2 - Bcs + Cs^2) + xy(2A*cs +(c^2-s^2)B -2Ccs) + ...
%           y^2(As^2 + Bcs + Cc^2) + x(Dc-Es) + y(Ds+Ec) + F = 0
%
%   The orientation is easily found by the condition of (B_new=0) which results in:
%
%   2A*cs +(c^2-s^2)B -2Ccs = 0  ==> phi = 1/2 * atan( b/(c-a) )
```

```
%
%   Now the constants   c=cos(phi)  and  s=sin(phi)  can be found, and from them
%   all the other constants A`,C`,D`,E` can be found.
%
%   A` = A*c^2 - B*c*s + C*s^2                  D` = D*c-E*s
%   B` = 2*A*c*s +(c^2-s^2)*B -2*C*c*s = 0      E` = D*s+E*c
%   C` = A*s^2 + B*c*s + C*c^2
%
% Next, we want the representation of the non-tilted ellipse to be as:
%
%       Ellipse = ( (X-X0)/a )^2 + ( (Y-Y0)/b )^2 = 1
%
%       where:  (X0,Y0) is the center of the ellipse
%               a,b     are the ellipse "radiuses" (or sub-axis)
%
% Using a square completion method we will define:
%
%       F`` = -F` + (D`^2)/(4*A`) + (E`^2)/(4*C`)
%
%       Such that:    a`*(X-X0)^2 = A`(X^2 + X*D`/A` + (D`/(2*A`))^2 )
%                     c`*(Y-Y0)^2 = C`(Y^2 + Y*E`/C` + (E`/(2*C`))^2 )
%
%       which yields the transformations:
%
%           X0  =   -D`/(2*A`)
%           Y0  =   -E`/(2*C`)
%           a   =   sqrt( abs( F``/A` ) )
%           b   =   sqrt( abs( F``/C` ) )
%
% And finally we can define the remaining parameters:
%
%   long_axis   = 2 * max( a,b )
%   short_axis  = 2 * min( a,b )
%   Orientation = phi
%
```

```
%

% initialize
orientation_tolerance = 1e-3;

% empty warning stack
warning( '' );

% prepare vectors, must be column vectors
x = x(:);
y = y(:);

% remove bias of the ellipse - to make matrix inversion more accurate. (will be added later on).
mean_x = mean(x);
mean_y = mean(y);
x = x-mean_x;
y = y-mean_y;

% the estimation for the conic equation of the ellipse
X = [x.^2, x.*y, y.^2, x, y ];
a = sum(X)/(X'*X);

% check for warnings
if ~isempty( lastwarn )
    disp( 'stopped because of a warning regarding matrix inversion' );
    ellipse_t = [];
    return
end

% extract parameters from the conic equation
[a,b,c,d,e] = deal( a(1),a(2),a(3),a(4),a(5) );

% remove the orientation from the ellipse
```

```
if ( min(abs(b/a),abs(b/c)) > orientation_tolerance )

    orientation_rad = 1/2 * atan( b/(c-a) );
    cos_phi = cos( orientation_rad );
    sin_phi = sin( orientation_rad );
    [a,b,c,d,e] = deal(...
        a*cos_phi^2 - b*cos_phi*sin_phi + c*sin_phi^2,...
        0,...
        a*sin_phi^2 + b*cos_phi*sin_phi + c*cos_phi^2,...
        d*cos_phi - e*sin_phi,...
        d*sin_phi + e*cos_phi );
    [mean_x,mean_y] = deal( ...
        cos_phi*mean_x - sin_phi*mean_y,...
        sin_phi*mean_x + cos_phi*mean_y );
else
    orientation_rad = 0;
    cos_phi = cos( orientation_rad );
    sin_phi = sin( orientation_rad );
end

% check if conic equation represents an ellipse
test = a*c;
switch (1)
case (test>0),  status = '';
case (test==0), status = 'Parabola found';  warning( 'fit_ellipse: Did not locate an ellipse' );
case (test<0),  status = 'Hyperbola found'; warning( 'fit_ellipse: Did not locate an ellipse' );
end

% if we found an ellipse return it's data
if (test>0)

    % make sure coefficients are positive as required
    if (a<0), [a,c,d,e] = deal( -a,-c,-d,-e ); end
```

```
    % final ellipse parameters
    X0          = mean_x - d/2/a;
    Y0          = mean_y - e/2/c;
    F           = 1 + (d^2)/(4*a) + (e^2)/(4*c);
    [a,b]       = deal( sqrt( F/a ),sqrt( F/c ) );
    long_axis   = 2*max(a,b);
    short_axis  = 2*min(a,b);

    % rotate the axes backwards to find the center point of the original TILTED ellipse
    R           = [ cos_phi sin_phi; -sin_phi cos_phi ];
    P_in        = R * [X0;Y0];
    X0_in       = P_in(1);
    Y0_in       = P_in(2);

    % pack ellipse into a structure
    ellipse_t = struct( ...
        'a',a,...
        'b',b,...
        'phi',orientation_rad,...
        'X0',X0,...
        'Y0',Y0,...
        'X0_in',X0_in,...
        'Y0_in',Y0_in,...
        'long_axis',long_axis,...
        'short_axis',short_axis,...
        'status','' );
else
    % report an empty structure
    ellipse_t = struct( ...
        'a',[],...
        'b',[],...
        'phi',[],...
        'X0',[],...
        'Y0',[],...
        'X0_in',[],...
```

```
        'Y0_in',[],...
        'long_axis',[],...
        'short_axis',[],...
        'status',status );
end

% check if we need to plot an ellipse with it's axes.
if (nargin>2) & ~isempty( axis_handle ) & (test>0)

    % rotation matrix to rotate the axes with respect to an angle phi
    R = [ cos_phi sin_phi; -sin_phi cos_phi ];

    % the axes
    ver_line        = [ [X0 X0]; Y0+b*[-1 1] ];
    horz_line       = [ X0+a*[-1 1]; [Y0 Y0] ];
    new_ver_line    = R*ver_line;
    new_horz_line   = R*horz_line;

    % the ellipse
    theta_r         = linspace(0,2*pi);
    ellipse_x_r     = X0 + a*cos( theta_r );
    ellipse_y_r     = Y0 + b*sin( theta_r );
    rotated_ellipse = R * [ellipse_x_r;ellipse_y_r];

    % draw
    hold_state = get( axis_handle,'NextPlot' );
    set( axis_handle,'NextPlot','add' );
    plot( new_ver_line(1,:),new_ver_line(2,:),'r' );
    plot( new_horz_line(1,:),new_horz_line(2,:),'r' );
    plot( rotated_ellipse(1,:),rotated_ellipse(2,:),'r' );
    set( axis_handle,'NextPlot',hold_state );
end

Copyright (c) 2003, Ohad Gal
```

All rights reserved.

Redistribution and use in source and binary forms, with or without
modification, are permitted provided that the following conditions are
met:

    * Redistributions of source code must retain the above copyright
      notice, this list of conditions and the following disclaimer.
    * Redistributions in binary form must reproduce the above copyright
      notice, this list of conditions and the following disclaimer in
      the documentation and/or other materials provided with the distribution

THIS SOFTWARE IS PROVIDED BY THE COPYRIGHT HOLDERS AND CONTRIBUTORS "AS IS"
AND ANY EXPRESS OR IMPLIED WARRANTIES, INCLUDING, BUT NOT LIMITED TO, THE
IMPLIED WARRANTIES OF MERCHANTABILITY AND FITNESS FOR A PARTICULAR PURPOSE
ARE DISCLAIMED. IN NO EVENT SHALL THE COPYRIGHT OWNER OR CONTRIBUTORS BE
LIABLE FOR ANY DIRECT, INDIRECT, INCIDENTAL, SPECIAL, EXEMPLARY, OR
CONSEQUENTIAL DAMAGES (INCLUDING, BUT NOT LIMITED TO, PROCUREMENT OF
SUBSTITUTE GOODS OR SERVICES; LOSS OF USE, DATA, OR PROFITS; OR BUSINESS
INTERRUPTION) HOWEVER CAUSED AND ON ANY THEORY OF LIABILITY, WHETHER IN
CONTRACT, STRICT LIABILITY, OR TORT (INCLUDING NEGLIGENCE OR OTHERWISE)
ARISING IN ANY WAY OUT OF THE USE OF THIS SOFTWARE, EVEN IF ADVISED OF THE
POSSIBILITY OF SUCH DAMAGE.

APPENDIX C

MATLAB functions used to determine sectorial tangential curvature and refractive power in Chapter 4

```
function [ Sectorial_AxlPwr,Sectorial_TglPwr,Sectorial_RefPwr ] = NonCyclic_Sectors3( Axl,Tgl,Dst,Hgt,Eye,StepIntvl,
RefCentXdec, RefCentYdec,InterpMethod)
   EffecRad = 4.8;
warning off all


            BLaxlNaN=ReplaceWithNans(0,Axl(:,1:32));

            %tgl
            BLtglNaN=ReplaceWithNans(0,Tgl(:,1:32));

            BLdistNaN=ReplaceWithNans(0,Dst(:,1:32));

            BLhgtNaN=ReplaceWithNans(0,Hgt(:,1:32));


            %{

            %}

            [InterpAxl,InterpDsta,EffecRad]= CentertoRefCent_FAp(
(BLaxlNaN,BLdistNaN,RefCentXdec,RefCentYdec,StepIntvl);
            [InterpTgl,InterpDstt,EffecRad]=CentertoRefCent_FAp
(BLtglNaN,BLdistNaN,RefCentXdec,RefCentYdec,StepIntvl);
            [InterpHgt,InterpDsth,EffecRad]= CentertoRefCent_FAp
(BLhgtNaN,BLdistNaN,RefCentXdec,RefCentYdec,StepIntvl);
```

```
BL_Final_AXL_Pwr_Data=ParaxPwrCal( InterpAxl,InterpDsta,InterpHgt, 'axl' );
BL_Final_TGL_Pwr_Data=ParaxPwrCal( InterpTgl,InterpDstt,InterpHgt, 'tgl' );
BL_Final_REF_Pwr_Data=ParaxPwrCal( InterpAxl,InterpDsth,InterpHgt, 'ref' );

        [ BL_Final_AXL_Pwr_Data_NaNs_SF ] = MakeItSectorialEase( BL_Final_AXL_Pwr_Data );

         [ BL_Final_TGL_Pwr_Data_NaNs_SF ] = MakeItSectorialEase( BL_Final_TGL_Pwr_Data );

         [ BL_Final_REF_Pwr_Data_NaNs_SF ] = MakeItSectorialEase( BL_Final_REF_Pwr_Data );

        [ InterpDsta_SF ] = MakeItSectorialEase( InterpDsta );

%%
%%%%%%%%%%%%%%%%%%%%%%%%%%%%%%%%%%%%%%%%%%%%%%%%%%%%%%%%%%%%%%%%%%%%%%%%%%%%%%%%%%%%%%%%%%%%%%%%%%%%%%%%%%%%%%%%%%%
%%%%%%%%%%%%%%%%%%%%%%%%%%%%%%%%%%%%%%%%
% O V E R A L L   C O R N E A L    D E S C R I P T O R S %%%%%%%%%%%%%%%%%

%%%%%%%%%%%%%%%%%%%%%%%%%%%%%%%%%%%%%%%%%%%%%%%%%%%%%%%%%%%%%%%%%%%%%%%%%%%%%%%%%%%%%%%%%%%%%%%%%%%%%%%%%%%%%%%%%%%
%%%%%%%%%%%%%%%%%%%%%%%%%%%%%%%%%%%%%%%%%%%%%%%%%

% BL Tgl,Ref, Cur power descriptors
[BLAxlpwrNumel_WC,BLAxlNaN_Count_WC,BLAxl_NaN_Percent_WC,BLAxl_ZoneMean_WC] =
AnnularZoneMean2(BL_Final_AXL_Pwr_Data,InterpDsta,0,5);
[BLTglpwrNumel_WC,BLTglNaN_Count_WC,BLTgl_NaN_Percent_WC,BLTgl_ZoneMean_WC] =
AnnularZoneMean2(BL_Final_TGL_Pwr_Data,InterpDsta,0,5);
[BLRefpwrNumel_WC,BLRefNaN_Count_WC,BLRef_NaN_Percent_WC,BLRef_ZoneMean_WC] =
AnnularZoneMean2(BL_Final_REF_Pwr_Data,InterpDsta,0,5);

%
```

```
%%%%%%%%%%%%%%%%%%%%%%%%%%%%%%%%%%%%%%%%%%%%%%%%%%%%%%%%%%%%%%%%%%%%%%%%%%%%%%%%%%%%%%%%%%%%%%%%%%%%%%%%%%%%%%%%%%%%%%%%
%%%%%%%%%%%%%%%%%%%%%%%%%%%%%%%%%
%%%%%%%%%%%%%%%%%%%%%%%%%%%%%%%%%%%%%%%%%%%%%%%%%%%%%%%%%%%%%%%%%%%%%%%%%%%%%%%%%%%%%%%%%%%%%%%%%%%%%%%%%%%%%%%%%%%%%%%%
%%%%%%%%%%%%%%%%%%%%%%%%%%%%%%%%%
%%%%%%%%%%%%%%%%%%%%%%%%%%%%%%%%%%%%%%%%%%%      A N N U L A R   Z O N E
%%%%%%%%%%%%%%%%%%%%%%%%%%%%%%%%%%%%%%%%%%%      D E S C R I P T O R S
%%%%%%%%%%%%%%%%%%%%%%%%%%%%%%%%%%%%%%%%%%%               R S
%%%%%%%%%%%%%%%%%%%%%%%%%%%%%%%%%%%%%%%%%%%%%%%%%%%%%%%%%%%%%%%%%%%%%%%%%%%%%%%%%%%%%%%%%%%%%%%%%%%%%%%%%%%%%%%%%%%%%%%%
%%%%%%%%%%%%%%%%%%%%%%%%%%%%%%%


 [ BLAxlpwrNumel_CC,BLAxlNaN_Count_CC,BLAxl_NaN_Percent_CC,BLAxl_ZoneMean_CC ] = AnnularZoneMean2(
BL_Final_AXL_Pwr_Data_NaNs_SF,InterpDsta,0,2.5 );
[ BLTglpwrNumel_CC,BLTglNaN_Count_CC,BLTgl_NaN_Percent_CC,BLTgl_ZoneMean_CC ] = AnnularZoneMean2(
BL_Final_TGL_Pwr_Data_NaNs_SF,InterpDsta,0,2.5 );
[ BLRefpwrNumel_CC,BLRefNaN_Count_CC,BLRef_NaN_Percent_CC,BLRef_ZoneMean_CC ] = AnnularZoneMean2(
BL_Final_REF_Pwr_Data_NaNs_SF,InterpDsta,0,2.5 );

%% Para-CentralZone  Descriptors ( Num of elements, Count Nan, NaN Percent, Zonal Mean)

% BL Tgl an Ref power descriptors

[ BLAxlpwrNumel_PC,BLAxlNaN_Count_PC,BLAxl_NaN_Percent_PC,BLAxl_ZoneMean_PC ] = AnnularZoneMean2(
BL_Final_AXL_Pwr_Data_NaNs_SF,InterpDsta,2.5,4 );
[ BLTglpwrNumel_PC,BLTglNaN_Count_PC,BLTgl_NaN_Percent_PC,BLTgl_ZoneMean_PC ] = AnnularZoneMean2(
BL_Final_TGL_Pwr_Data_NaNs_SF,InterpDsta,2.5,4 );
[ BLRefpwrNumel_PC,BLRefNaN_Count_PC,BLRef_NaN_Percent_PC,BLRef_ZoneMean_PC ] = AnnularZoneMean2(
BL_Final_REF_Pwr_Data_NaNs_SF,InterpDsta,2.5,4 );
```

```
[ BLAxlpwrNumel_Peri,BLAxlNaN_Count_Peri,BLAxl_NaN_Percent_Peri,BLAxl_ZoneMean_Peri ] = AnnularZoneMean2(
BL_Final_AXL_Pwr_Data_NaNs_SF,InterpDsta,4,5 );
[ BLTglpwrNumel_Peri,BLTglNaN_Count_Peri,BLTgl_NaN_Percent_Peri,BLTgl_ZoneMean_Peri ] = AnnularZoneMean2(
BL_Final_TGL_Pwr_Data_NaNs_SF,InterpDsta,4,5 );
[ BLRefpwrNumel_Peri,BLRefNaN_Count_Peri,BLRef_NaN_Percent_Peri,BLRef_ZoneMean_Peri ] = AnnularZoneMean2(
BL_Final_REF_Pwr_Data_NaNs_SF,InterpDsta,4,5);

%%%%%%%%%%%%%%%%%%%%%%%%%%%%%%%%%%%%%%%%%%%%%%%%%%%%%%%%%%%%%%%%%%%%%%%%%%%%%%%


[ BLAxlpwrNumel_CN,BLAxlNaN_Count_CN,BLAxl_NaN_Percent_CN,BLAxl_ZoneMean_CN ] = SectorialMean2(
BL_Final_AXL_Pwr_Data_NaNs_SF,InterpDsta_SF,0,2.5,264,338 );
[ BLTglpwrNumel_CN,BLTglNaN_Count_CN,BLTgl_NaN_Percent_CN,BLTgl_ZoneMean_CN ] = SectorialMean2(
BL_Final_TGL_Pwr_Data_NaNs_SF,InterpDsta_SF,0,2.5,264,338 );
[ BLRefpwrNumel_CN,BLRefNaN_Count_CN,BLRef_NaN_Percent_CN,BLRef_ZoneMean_CN ] = SectorialMean2(
BL_Final_REF_Pwr_Data_NaNs_SF,InterpDsta_SF,0,2.5,264,338 );

%% Central Superior Sector Descriptors

% BL Tgl an Ref power descriptors
[ BLAxlpwrNumel_CS,BLAxlNaN_Count_CS,BLAxl_NaN_Percent_CS,BLAxl_ZoneMean_CS ] = SectorialMean2(
BL_Final_AXL_Pwr_Data_NaNs_SF,InterpDsta_SF,0,2.5,39,113 );
[ BLTglpwrNumel_CS,BLTglNaN_Count_CS,BLTgl_NaN_Percent_CS,BLTgl_ZoneMean_CS ] = SectorialMean2(
BL_Final_TGL_Pwr_Data_NaNs_SF,InterpDsta_SF,0,2.5,39,113 );
[ BLRefpwrNumel_CS,BLRefNaN_Count_CS,BLRef_NaN_Percent_CS,BLRef_ZoneMean_CS ] = SectorialMean2(
BL_Final_REF_Pwr_Data_NaNs_SF,InterpDsta_SF,0,2.5,39,113 );


%% Central Temporal Sector Descriptors

% BL Tgl an Ref power descriptors
```

```
[ BLAxlpwrNumel_CT,BLAxlNaN_Count_CT,BLAxl_NaN_Percent_CT,BLAxl_ZoneMean_CT ] = SectorialMean2(
BL_Final_AXL_Pwr_Data_NaNs_SF,InterpDsta_SF,0,2.5,114,188 );
[ BLTglpwrNumel_CT,BLTglNaN_Count_CT,BLTgl_NaN_Percent_CT,BLTgl_ZoneMean_CT ] = SectorialMean2(
BL_Final_TGL_Pwr_Data_NaNs_SF,InterpDsta_SF,0,2.5,114,188 );
[ BLRefpwrNumel_CT,BLRefNaN_Count_CT,BLRef_NaN_Percent_CT,BLRef_ZoneMean_CT ] = SectorialMean2(
BL_Final_REF_Pwr_Data_NaNs_SF,InterpDsta_SF,0,2.5,114,188 );


%% Central Inferior Sector Descriptors

% BL Tgl an Ref power descriptors

[ BLAxlpwrNumel_CI,BLAxlNaN_Count_CI,BLAxl_NaN_Percent_CI,BLAxl_ZoneMean_CI ] = SectorialMean2(
BL_Final_AXL_Pwr_Data_NaNs_SF,InterpDsta_SF,0,2.5,189,263 );
[ BLTglpwrNumel_CI,BLTglNaN_Count_CI,BLTgl_NaN_Percent_CI,BLTgl_ZoneMean_CI ] = SectorialMean2(
BL_Final_TGL_Pwr_Data_NaNs_SF,InterpDsta_SF,0,2.5,189,263 );
[ BLRefpwrNumel_CI,BLRefNaN_Count_CI,BLRef_NaN_Percent_CI,BLRef_ZoneMean_CI ] = SectorialMean2(
BL_Final_REF_Pwr_Data_NaNs_SF,InterpDsta_SF,0,2.5,189,263 );



%%%%%%%%%%%%%%%%%%%%%%%%%%%%%%%%%%%%%%%%%%%%%%%%%%%%%%%%%%%%%%%%%%%%%%%%%%%%%%%%%%%%%%%%%%%%%%%%%%%%%%%%%%%%%%%%%%%%
%%%%%%%%%%%%%%%%%%%%%%%%%%%%%%%%%%%%%%%%%%%%%%%%%%%%%%%%%%%%%%%



%% Para-CentralNasalSector Descriptors

% BL Tgl an Ref power descriptors
```

```
[ BLAxlpwrNumel_PCN,BLAxlNaN_Count_PCN,BLAxl_NaN_Percent_PCN,BLAxl_ZoneMean_PCN ] = SectorialMean2(
BL_Final_AXL_Pwr_Data_NaNs_SF,InterpDsta_SF,2.5,4,264,338 );
[ BLTglpwrNumel_PCN,BLTglNaN_Count_PCN,BLTgl_NaN_Percent_PCN,BLTgl_ZoneMean_PCN ] = SectorialMean2(
BL_Final_TGL_Pwr_Data_NaNs_SF,InterpDsta_SF,2.5,4,264,338 );
[ BLRefpwrNumel_PCN,BLRefNaN_Count_PCN,BLRef_NaN_Percent_PCN,BLRef_ZoneMean_PCN ] = SectorialMean2(
BL_Final_REF_Pwr_Data_NaNs_SF,InterpDsta_SF,2.5,4,264,338 );

%% Para-Central Superior Sector Descriptors

% BL Tgl an Ref power descriptors

[ BLAxlpwrNumel_PCS,BLAxlNaN_Count_PCS,BLAxl_NaN_Percent_PCS,BLAxl_ZoneMean_PCS ] = SectorialMean2(
BL_Final_AXL_Pwr_Data_NaNs_SF,InterpDsta_SF,2.5,4,39,113 );
[ BLTglpwrNumel_PCS,BLTglNaN_Count_PCS,BLTgl_NaN_Percent_PCS,BLTgl_ZoneMean_PCS ] = SectorialMean2(
BL_Final_TGL_Pwr_Data_NaNs_SF,InterpDsta_SF,2.5,4,39,113 );
[ BLRefpwrNumel_PCS,BLRefNaN_Count_PCS,BLRef_NaN_Percent_PCS,BLRef_ZoneMean_PCS ] = SectorialMean2(
BL_Final_REF_Pwr_Data_NaNs_SF,InterpDsta_SF,2.5,4,39,113 );

%% Para-Central Temporal Sector Descriptors

% BL Tgl an Ref power descriptors

[ BLAxlpwrNumel_PCT,BLAxlNaN_Count_PCT,BLAxl_NaN_Percent_PCT,BLAxl_ZoneMean_PCT ] = SectorialMean2(
BL_Final_AXL_Pwr_Data_NaNs_SF,InterpDsta_SF,2.5,4,114,188 );
[ BLTglpwrNumel_PCT,BLTglNaN_Count_PCT,BLTgl_NaN_Percent_PCT,BLTgl_ZoneMean_PCT ] = SectorialMean2(
BL_Final_TGL_Pwr_Data_NaNs_SF,InterpDsta_SF,2.5,4,114,188 );
[ BLRefpwrNumel_PCT,BLRefNaN_Count_PCT,BLRef_NaN_Percent_PCT,BLRef_ZoneMean_PCT ] = SectorialMean2(
BL_Final_REF_Pwr_Data_NaNs_SF,InterpDsta_SF,2.5,4,114,188 );

%% Para-Central Inferior Sector Descriptors

% BL Tgl an Ref power descriptors
```

```
[ BLAxlpwrNumel_PCI,BLAxlNaN_Count_PCI,BLAxl_NaN_Percent_PCI,BLAxl_ZoneMean_PCI ] = SectorialMean2(
BL_Final_AXL_Pwr_Data_NaNs_SF,InterpDsta_SF,2.5,4,189,263 );
[ BLTglpwrNumel_PCI,BLTglNaN_Count_PCI,BLTgl_NaN_Percent_PCI,BLTgl_ZoneMean_PCI ] = SectorialMean2(
BL_Final_TGL_Pwr_Data_NaNs_SF,InterpDsta_SF,2.5,4,189,263 );
[ BLRefpwrNumel_PCI,BLRefNaN_Count_PCI,BLRef_NaN_Percent_PCI,BLRef_ZoneMean_PCI ] = SectorialMean2(
BL_Final_REF_Pwr_Data_NaNs_SF,InterpDsta_SF,2.5,4,189,263 );

%%%%%%%%%%%%%%%%%%%%%%%%%%%%%%%%%%%%%%%%%%%%%%%%%%%%%%%%%%%%%%%%%%%%%%%%%%%%%%%%%%%%%%%%%%%%%%%%%%%%%%%%%%%%%%%%%%%%%
%%%%%%%%%%%%%%%%%%%%%%%%%%%%%%%%%%%%%%%%%%%%%%%%%%%%%%%%%%%%%%%



%% Peripheral NasalSector Descriptors

% BL Tgl an Ref power descriptors

[ BLAxlpwrNumel_PN,BLAxlNaN_Count_PN,BLAxl_NaN_Percent_PN,BLAxl_ZoneMean_PN ] = SectorialMean2(
BL_Final_AXL_Pwr_Data_NaNs_SF,InterpDsta_SF,4,5,264,338 );
[ BLTglpwrNumel_PN,BLTglNaN_Count_PN,BLTgl_NaN_Percent_PN,BLTgl_ZoneMean_PN ] = SectorialMean2(
BL_Final_TGL_Pwr_Data_NaNs_SF,InterpDsta_SF,4,5,264,338 );
[ BLRefpwrNumel_PN,BLRefNaN_Count_PN,BLRef_NaN_Percent_PN,BLRef_ZoneMean_PN ] = SectorialMean2(
BL_Final_REF_Pwr_Data_NaNs_SF,InterpDsta_SF,4,5,264,338 );


%% Peripheral Superior Sector Descriptors

% BL Tgl an Ref power descriptors
[ BLAxlpwrNumel_PS,BLAxlNaN_Count_PS,BLAxl_NaN_Percent_PS,BLAxl_ZoneMean_PS ] = SectorialMean2(
BL_Final_AXL_Pwr_Data_NaNs_SF,InterpDsta_SF,4,5,39,113 );
[ BLTglpwrNumel_PS,BLTglNaN_Count_PS,BLTgl_NaN_Percent_PS,BLTgl_ZoneMean_PS ] = SectorialMean2(
BL_Final_TGL_Pwr_Data_NaNs_SF,InterpDsta_SF,4,5,39,113 );
[ BLRefpwrNumel_PS,BLRefNaN_Count_PS,BLRef_NaN_Percent_PS,BLRef_ZoneMean_PS ] = SectorialMean2(
BL_Final_REF_Pwr_Data_NaNs_SF,InterpDsta_SF,4,5,39,113 );
```

```
%% Peripheral Temporal Sector Descriptors

% BL Tgl an Ref power descriptors
[ BLAxlpwrNumel_PT,BLAxlNaN_Count_PT,BLAxl_NaN_Percent_PT,BLAxl_ZoneMean_PT ] = SectorialMean2(
BL_Final_AXL_Pwr_Data_NaNs_SF,InterpDsta_SF,4,5,114,188 );
[ BLTglpwrNumel_PT,BLTglNaN_Count_PT,BLTgl_NaN_Percent_PT,BLTgl_ZoneMean_PT ] = SectorialMean2(
BL_Final_TGL_Pwr_Data_NaNs_SF,InterpDsta_SF,4,5,114,188 );
[ BLRefpwrNumel_PT,BLRefNaN_Count_PT,BLRef_NaN_Percent_PT,BLRef_ZoneMean_PT ] = SectorialMean2(
BL_Final_REF_Pwr_Data_NaNs_SF,InterpDsta_SF,4,5,114,188 );


%% Peripheral Inferior Sector Descriptors

% BL Tgl an Ref power descriptors
[ BLAxlpwrNumel_PI,BLAxlNaN_Count_PI,BLAxl_NaN_Percent_PI,BLAxl_ZoneMean_PI ] = SectorialMean2(
BL_Final_AXL_Pwr_Data_NaNs_SF,InterpDsta_SF,4,5,189,263 );
[ BLTglpwrNumel_PI,BLTglNaN_Count_PI,BLTgl_NaN_Percent_PI,BLTgl_ZoneMean_PI ] = SectorialMean2(
BL_Final_TGL_Pwr_Data_NaNs_SF,InterpDsta_SF,4,5,189,263 );
[ BLRefpwrNumel_PI,BLRefNaN_Count_PI,BLRef_NaN_Percent_PI,BLRef_ZoneMean_PI ] = SectorialMean2(
BL_Final_REF_Pwr_Data_NaNs_SF,InterpDsta_SF,4,5,189,263 );


% ************************************************** F  O  R  M  I  N  G
% ************************************************  M  A  T  R  I  C  E  S
%
*****************************************************************************************************************
****************************************

%% FORMING MATRICES

%%  WHOLE CORNEA : FORMING MATRICES
```

```
% BL WHOLE CORNEA
BL_AXLpwrDesc_Mat_WC=[BLAxlpwrNumel_WC,BLAxlNaN_Count_WC,BLAxl_NaN_Percent_WC,BLAxl_ZoneMean_WC] ;
BL_TGLpwrDesc_Mat_WC=[BLTglpwrNumel_WC,BLTglNaN_Count_WC,BLTgl_NaN_Percent_WC,BLTgl_ZoneMean_WC] ;
BL_REFpwrDesc_Mat_WC=[BLRefpwrNumel_WC,BLRefNaN_Count_WC,BLRef_NaN_Percent_WC,BLRef_ZoneMean_WC] ;

%% CENTRAL CORNEAL ZONE : FORMING MATRICES

% BL CENTRAL CORNEA

BL_AXLpwrDesc_Mat_CC=[ BLAxlpwrNumel_CC,BLAxlNaN_Count_CC,BLAxl_NaN_Percent_CC,BLAxl_ZoneMean_CC ] ;
BL_TGLpwrDesc_Mat_CC=[ BLTglpwrNumel_CC,BLTglNaN_Count_CC,BLTgl_NaN_Percent_CC,BLTgl_ZoneMean_CC ] ;
BL_REFpwrDesc_Mat_CC=[ BLRefpwrNumel_CC,BLRefNaN_Count_CC,BLRef_NaN_Percent_CC,BLRef_ZoneMean_CC ] ;

%% PARA-CENTRAL CORNEAL ZONE : FORMING MATRICES

% BL PARA-CENTRAL CORNEA

BL_AXLpwrDesc_Mat_PC=[ BLAxlpwrNumel_PC,BLAxlNaN_Count_PC,BLAxl_NaN_Percent_PC,BLAxl_ZoneMean_PC ] ;
BL_TGLpwrDesc_Mat_PC=[ BLTglpwrNumel_PC,BLTglNaN_Count_PC,BLTgl_NaN_Percent_PC,BLTgl_ZoneMean_PC ] ;
BL_REFpwrDesc_Mat_PC=[ BLRefpwrNumel_PC,BLRefNaN_Count_PC,BLRef_NaN_Percent_PC,BLRef_ZoneMean_PC ] ;


%% PERIPHERAL CORNEAL ZONE : FORMING MATRICES

% BL PERIPHERAL CORNEA
BL_AXLpwrDesc_Mat_Peri=[ BLAxlpwrNumel_Peri,BLAxlNaN_Count_Peri,BLAxl_NaN_Percent_Peri,BLAxl_ZoneMean_Peri ] ;
BL_TGLpwrDesc_Mat_Peri=[ BLTglpwrNumel_Peri,BLTglNaN_Count_Peri,BLTgl_NaN_Percent_Peri,BLTgl_ZoneMean_Peri ] ;
BL_REFpwrDesc_Mat_Peri=[ BLRefpwrNumel_Peri,BLRefNaN_Count_Peri,BLRef_NaN_Percent_Peri,BLRef_ZoneMean_Peri ] ;

%

%% SECTORIAL CORNEA : FORMING MATRICES
%% Central Nasal : FORMING MATRICES
```

```
% BL Tgl an Ref power descriptors

BL_AXLpwrDesc_Mat_CN=[ BLAxlpwrNumel_CN,BLAxlNaN_Count_CN,BLAxl_NaN_Percent_CN,BLAxl_ZoneMean_CN ] ;
BL_TGLpwrDesc_Mat_CN=[ BLTglpwrNumel_CN,BLTglNaN_Count_CN,BLTgl_NaN_Percent_CN,BLTgl_ZoneMean_CN ] ;
BL_REFpwrDesc_Mat_CN=[ BLRefpwrNumel_CN,BLRefNaN_Count_CN,BLRef_NaN_Percent_CN,BLRef_ZoneMean_CN ] ;


%% Central Superior : FORMING MATRICES
% BL Tgl an Ref power descriptors
BL_AXLpwrDesc_Mat_CS=[ BLAxlpwrNumel_CS,BLAxlNaN_Count_CS,BLAxl_NaN_Percent_CS,BLAxl_ZoneMean_CS ] ;
BL_TGLpwrDesc_Mat_CS=[ BLTglpwrNumel_CS,BLTglNaN_Count_CS,BLTgl_NaN_Percent_CS,BLTgl_ZoneMean_CS ] ;
BL_REFpwrDesc_Mat_CS=[ BLRefpwrNumel_CS,BLRefNaN_Count_CS,BLRef_NaN_Percent_CS,BLRef_ZoneMean_CS ] ;

%% Central Temporal : FORMING MATRICES
% BL Tgl an Ref power descriptors
BL_AXLpwrDesc_Mat_CT=[ BLAxlpwrNumel_CT,BLAxlNaN_Count_CT,BLAxl_NaN_Percent_CT,BLAxl_ZoneMean_CT ] ;
BL_TGLpwrDesc_Mat_CT=[ BLTglpwrNumel_CT,BLTglNaN_Count_CT,BLTgl_NaN_Percent_CT,BLTgl_ZoneMean_CT ] ;
BL_REFpwrDesc_Mat_CT=[ BLRefpwrNumel_CT,BLRefNaN_Count_CT,BLRef_NaN_Percent_CT,BLRef_ZoneMean_CT ] ;

%% Central Inferior : FORMING MATRICES
% BL Tgl an Ref power descriptors
BL_AXLpwrDesc_Mat_CI=[ BLAxlpwrNumel_CI,BLAxlNaN_Count_CI,BLAxl_NaN_Percent_CI,BLAxl_ZoneMean_CI ] ;
BL_TGLpwrDesc_Mat_CI=[ BLTglpwrNumel_CI,BLTglNaN_Count_CI,BLTgl_NaN_Percent_CI,BLTgl_ZoneMean_CI ] ;
BL_REFpwrDesc_Mat_CI=[ BLRefpwrNumel_CI,BLRefNaN_Count_CI,BLRef_NaN_Percent_CI,BLRef_ZoneMean_CI ] ;

%% Para-Central Nasal : FORMING MATRICES
% BL Tgl an Ref power descriptors
BL_AXLpwrDesc_Mat_PCN=[ BLAxlpwrNumel_PCN,BLAxlNaN_Count_PCN,BLAxl_NaN_Percent_PCN,BLAxl_ZoneMean_PCN ] ;
BL_TGLpwrDesc_Mat_PCN=[ BLTglpwrNumel_PCN,BLTglNaN_Count_PCN,BLTgl_NaN_Percent_PCN,BLTgl_ZoneMean_PCN ] ;
BL_REFpwrDesc_Mat_PCN=[ BLRefpwrNumel_PCN,BLRefNaN_Count_PCN,BLRef_NaN_Percent_PCN,BLRef_ZoneMean_PCN ] ;
```

```
%% Para-Central Superior : FORMING MATRICES
% BL Tgl an Ref power descriptors
BL_AXLpwrDesc_Mat_PCS=[ BLAxlpwrNumel_PCS,BLAxlNaN_Count_PCS,BLAxl_NaN_Percent_PCS,BLAxl_ZoneMean_PCS ] ;
BL_TGLpwrDesc_Mat_PCS=[ BLTglpwrNumel_PCS,BLTglNaN_Count_PCS,BLTgl_NaN_Percent_PCS,BLTgl_ZoneMean_PCS ] ;
BL_REFpwrDesc_Mat_PCS=[ BLRefpwrNumel_PCS,BLRefNaN_Count_PCS,BLRef_NaN_Percent_PCS,BLRef_ZoneMean_PCS ] ;


%% Para-Central Temporal : FORMING MATRICES
% BL Tgl an Ref power descriptors
BL_AXLpwrDesc_Mat_PCT=[ BLAxlpwrNumel_PCT,BLAxlNaN_Count_PCT,BLAxl_NaN_Percent_PCT,BLAxl_ZoneMean_PCT ] ;
BL_TGLpwrDesc_Mat_PCT=[ BLTglpwrNumel_PCT,BLTglNaN_Count_PCT,BLTgl_NaN_Percent_PCT,BLTgl_ZoneMean_PCT ] ;
BL_REFpwrDesc_Mat_PCT=[ BLRefpwrNumel_PCT,BLRefNaN_Count_PCT,BLRef_NaN_Percent_PCT,BLRef_ZoneMean_PCT ] ;



%% Para-Central Inferior : FORMING MATRICES
% BL Tgl an Ref power descriptors
BL_AXLpwrDesc_Mat_PCI=[ BLAxlpwrNumel_PCI,BLAxlNaN_Count_PCI,BLAxl_NaN_Percent_PCI,BLAxl_ZoneMean_PCI ] ;
BL_TGLpwrDesc_Mat_PCI=[ BLTglpwrNumel_PCI,BLTglNaN_Count_PCI,BLTgl_NaN_Percent_PCI,BLTgl_ZoneMean_PCI ] ;
BL_REFpwrDesc_Mat_PCI=[ BLRefpwrNumel_PCI,BLRefNaN_Count_PCI,BLRef_NaN_Percent_PCI,BLRef_ZoneMean_PCI ] ;



%% Peripheral Nasal : FORMING MATRICES
% BL Tgl an Ref power descriptors

BL_AXLpwrDesc_Mat_PN=[ BLAxlpwrNumel_PN,BLAxlNaN_Count_PN,BLAxl_NaN_Percent_PN,BLAxl_ZoneMean_PN ] ;
BL_TGLpwrDesc_Mat_PN=[ BLTglpwrNumel_PN,BLTglNaN_Count_PN,BLTgl_NaN_Percent_PN,BLTgl_ZoneMean_PN ] ;
BL_REFpwrDesc_Mat_PN=[ BLRefpwrNumel_PN,BLRefNaN_Count_PN,BLRef_NaN_Percent_PN,BLRef_ZoneMean_PN ] ;



%% Peripheral Superior : FORMING MATRICES
```

```
% BL Tgl an Ref power descriptors
BL_AXLpwrDesc_Mat_PS=[ BLAxlpwrNumel_PS,BLAxlNaN_Count_PS,BLAxl_NaN_Percent_PS,BLAxl_ZoneMean_PS ] ;
BL_TGLpwrDesc_Mat_PS=[ BLTglpwrNumel_PS,BLTglNaN_Count_PS,BLTgl_NaN_Percent_PS,BLTgl_ZoneMean_PS ] ;
BL_REFpwrDesc_Mat_PS=[ BLRefpwrNumel_PS,BLRefNaN_Count_PS,BLRef_NaN_Percent_PS,BLRef_ZoneMean_PS ] ;


%% Peripheral Temporal : FORMING MATRICES
% BL Tgl an Ref power descriptors
BL_AXLpwrDesc_Mat_PT=[ BLAxlpwrNumel_PT,BLAxlNaN_Count_PT,BLAxl_NaN_Percent_PT,BLAxl_ZoneMean_PT ] ;
BL_TGLpwrDesc_Mat_PT=[ BLTglpwrNumel_PT,BLTglNaN_Count_PT,BLTgl_NaN_Percent_PT,BLTgl_ZoneMean_PT ] ;
BL_REFpwrDesc_Mat_PT=[ BLRefpwrNumel_PT,BLRefNaN_Count_PT,BLRef_NaN_Percent_PT,BLRef_ZoneMean_PT ] ;



%% Peripheral Inferior : FORMING MATRICES
% BL Tgl an Ref power descriptors
BL_AXLpwrDesc_Mat_PI=[ BLAxlpwrNumel_PI,BLAxlNaN_Count_PI,BLAxl_NaN_Percent_PI,BLAxl_ZoneMean_PI ] ;
BL_TGLpwrDesc_Mat_PI=[ BLTglpwrNumel_PI,BLTglNaN_Count_PI,BLTgl_NaN_Percent_PI,BLTgl_ZoneMean_PI ] ;
BL_REFpwrDesc_Mat_PI=[ BLRefpwrNumel_PI,BLRefNaN_Count_PI,BLRef_NaN_Percent_PI,BLRef_ZoneMean_PI ] ;

    %%

   if Eye == 1


BL_AllinOneMat_AxlPwr=[BL_AXLpwrDesc_Mat_WC,BL_AXLpwrDesc_Mat_CC,BL_AXLpwrDesc_Mat_PC,BL_AXLpwrDesc_Mat_Peri,BL_AXLp
wrDesc_Mat_CN,BL_AXLpwrDesc_Mat_CS,BL_AXLpwrDesc_Mat_CT,BL_AXLpwrDesc_Mat_CI,...

BL_AXLpwrDesc_Mat_PCN,BL_AXLpwrDesc_Mat_PCS,BL_AXLpwrDesc_Mat_PCT,BL_AXLpwrDesc_Mat_PCI,BL_AXLpwrDesc_Mat_PN,BL_AXLp
wrDesc_Mat_PS,BL_AXLpwrDesc_Mat_PT,BL_AXLpwrDesc_Mat_PI];
```

```
BL_AllinOneMat_TglPwr=[BL_TGLpwrDesc_Mat_WC,BL_TGLpwrDesc_Mat_CC,BL_TGLpwrDesc_Mat_PC,BL_TGLpwrDesc_Mat_Peri,BL_TGLp
wrDesc_Mat_CN,BL_TGLpwrDesc_Mat_CS,BL_TGLpwrDesc_Mat_CT,BL_TGLpwrDesc_Mat_CI,...

BL_TGLpwrDesc_Mat_PCN,BL_TGLpwrDesc_Mat_PCS,BL_TGLpwrDesc_Mat_PCT,BL_TGLpwrDesc_Mat_PCI,BL_TGLpwrDesc_Mat_PN,BL_TGLp
wrDesc_Mat_PS,BL_TGLpwrDesc_Mat_PT,BL_TGLpwrDesc_Mat_PI];




BL_AllinOneMat_RefPwr=[BL_REFpwrDesc_Mat_WC,BL_REFpwrDesc_Mat_CC,BL_REFpwrDesc_Mat_PC,BL_REFpwrDesc_Mat_Peri,BL_REFp
wrDesc_Mat_CN,BL_REFpwrDesc_Mat_CS,BL_REFpwrDesc_Mat_CT,BL_REFpwrDesc_Mat_CI,...

BL_REFpwrDesc_Mat_PCN,BL_REFpwrDesc_Mat_PCS,BL_REFpwrDesc_Mat_PCT,BL_REFpwrDesc_Mat_PCI,BL_REFpwrDesc_Mat_PN,BL_REFp
wrDesc_Mat_PS,BL_REFpwrDesc_Mat_PT,BL_REFpwrDesc_Mat_PI];
   elseif Eye == 2


BL_AllinOneMat_AxlPwr=[BL_AXLpwrDesc_Mat_WC,BL_AXLpwrDesc_Mat_CC,BL_AXLpwrDesc_Mat_PC,BL_AXLpwrDesc_Mat_Peri,BL_AXLp
wrDesc_Mat_CT,BL_AXLpwrDesc_Mat_CS,BL_AXLpwrDesc_Mat_CN,BL_AXLpwrDesc_Mat_CI,...

BL_AXLpwrDesc_Mat_PCT,BL_AXLpwrDesc_Mat_PCS,BL_AXLpwrDesc_Mat_PCN,BL_AXLpwrDesc_Mat_PCI,BL_AXLpwrDesc_Mat_PT,BL_AXLp
wrDesc_Mat_PS,BL_AXLpwrDesc_Mat_PN,BL_AXLpwrDesc_Mat_PI];



BL_AllinOneMat_TglPwr=[BL_TGLpwrDesc_Mat_WC,BL_TGLpwrDesc_Mat_CC,BL_TGLpwrDesc_Mat_PC,BL_TGLpwrDesc_Mat_Peri,BL_TGLp
wrDesc_Mat_CT,BL_TGLpwrDesc_Mat_CS,BL_TGLpwrDesc_Mat_CN,BL_TGLpwrDesc_Mat_CI,...

BL_TGLpwrDesc_Mat_PCT,BL_TGLpwrDesc_Mat_PCS,BL_TGLpwrDesc_Mat_PCN,BL_TGLpwrDesc_Mat_PCI,BL_TGLpwrDesc_Mat_PT,BL_TGLp
wrDesc_Mat_PS,BL_TGLpwrDesc_Mat_PN,BL_TGLpwrDesc_Mat_PI];
```

```
            %% All visits Ref Pwr Mats


BL_AllinOneMat_RefPwr=[BL_REFpwrDesc_Mat_WC,BL_REFpwrDesc_Mat_CC,BL_REFpwrDesc_Mat_PC,BL_REFpwrDesc_Mat_Peri,BL_REFp
wrDesc_Mat_CT,BL_REFpwrDesc_Mat_CS,BL_REFpwrDesc_Mat_CN,BL_REFpwrDesc_Mat_CI,...

BL_REFpwrDesc_Mat_PCT,BL_REFpwrDesc_Mat_PCS,BL_REFpwrDesc_Mat_PCN,BL_REFpwrDesc_Mat_PCI,BL_REFpwrDesc_Mat_PT,BL_REFp
wrDesc_Mat_PS,BL_REFpwrDesc_Mat_PN,BL_REFpwrDesc_Mat_PI];

   end
  %% Apply 70% Rule and get only sectorial mean values.

  [Sectorial_AxlPwr_Descriptors] = Apply70PercentRule(BL_AllinOneMat_AxlPwr);
  [Sectorial_TglPwr_Descriptors] = Apply70PercentRule(BL_AllinOneMat_TglPwr);
  [Sectorial_RefPwr_Descriptors] = Apply70PercentRule(BL_AllinOneMat_RefPwr);

  Sectorial_AxlPwr=Sectorial_AxlPwr_Descriptors(1,2:4:46);
  Sectorial_TglPwr=Sectorial_TglPwr_Descriptors(1,2:4:46);
  Sectorial_RefPwr=Sectorial_RefPwr_Descriptors(1,2:4:46);

end
```

Sub functions

```
function [ M ] = ReplaceWithNans(a,M )
%replace value 'a' with NaNs in the Matrix 'M'
[r,c]=size(M);
for i=1:1:r,
    for j = 1:1:c,
        tval =M(i,j);
        if (tval==a),
```

```
            M(i,j)=NaN;
        end

    end
end

end
```

```
function [ ExpData ] = MakeItSectorialEase( Data )
%Makes a matrix bigger (expands), means a 300 * 32 matrix will become a 338 * 32
%matrix, which makes it easier for us to do sectorial calculations
IntendedTail_Data=Data(1:38,:);
ExpData=[Data;IntendedTail_Data];


end
```

```
function [ pwrNumel,NaN_Count,NaN_Percent,ZoneMean ] = AnnularZoneMean2( pwr_SF,dst_NL,radStart,radEnd )
Actual_Pwrdata=pwr_SF(1:300,:);
Actual_Distdata=dst_NL(1:300,:);
%zone selected
DefinedDist=Actual_Distdata>radStart & Actual_Distdata<=radEnd;
%getting out the corresponsing pwr values
zonalpwr_SF=Actual_Pwrdata(DefinedDist);

pwrNumel=numel(zonalpwr_SF);
NaN_Count=nancount(zonalpwr_SF);
NaN_Percent=nanpercent(zonalpwr_SF);
ZoneMean=nanmean(zonalpwr_SF);
```

```
end


function [ pwrNumel,NaN_Count,NaN_Percent,SecMean  ] = SectorialMean2(
pwr_SF,dst_NL,radStart,radEnd,MeridianStart,MeridianEnd )
EntireSectorPwr=pwr_SF(MeridianStart:MeridianEnd,:);
EntireSectorDst=dst_NL(MeridianStart:MeridianEnd,:);
DefinedSectorLogicals=EntireSectorDst>radStart & EntireSectorDst<=radEnd;
DefinedSectorPwr=EntireSectorPwr(DefinedSectorLogicals);

pwrNumel=numel(DefinedSectorPwr);
NaN_Count=nancount(DefinedSectorPwr);
NaN_Percent=nanpercent(DefinedSectorPwr);
SecMean=nanmean(DefinedSectorPwr);

end
```

APPENDIX D

Participation information statements and consent forms used in the studies described in this thesis received approval from the University of New South Wales Ethics Advisory Panel.

D1 CHAPTER 2 STUDY

Approval No (090031)

THE UNIVERSITY OF NEW SOUTH WALES

PARTICIPANT INFORMATION STATEMENT AND CONSENT FORM

Meridional and hemi-meridional differences in normal corneal topography of South Asians, East Asians and Europeans

You are invited to participate in a study that is investigating the shape (topography) of the anterior eye surface called the 'cornea' which is the transparent window of the eye. We hope to learn whether differences exist in different meridians in corneal topography in various ethnic groups. You were selected as a possible participant in this study because you belong to a specific ethnic group (East Asian, South Asian or European), and meet our study inclusion criteria.

If you decide to participate, we will assess your vision, spectacle power, photograph your eyes and take corneal shape images using a corneal topographer. While the initial two procedures do not require any contact with the eye the latter requires using a lid retractor that widens your eye, which may stop your normal blinking for a minute or so, allowing the capturing of topography images.

You may experience slight discomfort from the placement of the lid retractor. You may also feel some dryness as a result of arresting the eye lids. This procedure will be completed in less than 2 minutes per eye; the similar procedure will be repeated for the other eye, so the whole procedure including visual acuity assessment and refraction will take approximately 20 minutes.

Rarely some people may develop slight corneal drying as a result of placement of the lid retractor, but this usually resolves in a few minutes. In case of severe corneal drying resulting in superficial damage (that is quite rare) arrangements have been made for immediate referring of the participants to an appropriate medical practitioner.

Any information that is obtained in connection with this study and that can be identified with you will remain confidential and will be disclosed only with your permission, except as required by law. If you give us your permission by signing this document, we plan to present the results in scientific conferences or scientific journals. The information to be presented will be mean group data and individual responses of interest, and in the latter case these will be presented in such a way that your identity will not be disclosed.

We cannot and do not guarantee or promise that you will receive any benefits from this study.

Complaints may be directed to the Ethics Secretariat, The University of New South Wales, SYDNEY 2052 AUSTRALIA (phone 9385 4234, fax 9385 6648, email ethics.sec@unsw.edu.au). Any complaint you make will be investigated promptly and you will be informed out the outcome.

As a feed back to you a short summary of the study results will be displayed in our website *http://www.optom.unsw.edu.au/research/rokindex.html.* after the completion of the study.

Your decision whether or not to participate will not prejudice your future relations with the University of New South Wales. If you decide to participate, you are free to withdraw your consent and to discontinue participation at any time without prejudice.

If you have any questions, please feel free to ask us. If you have any additional questions later, Prof. Helen Swarbrick (Ph - 93854373 / email- h.swarbrick@unsw.edu.au) will be happy to answer them.

You will be given a copy of this form to keep.

You are making a decision whether or not to participate. Your signature indicates that, having read the information provided above, you have decided to participate.

……
……

Signature of Research Participant | Signature of Witness

……
……

(Please PRINT name) | (Please PRINT name)

……
……

Date | Nature of Witness

THE UNIVERSITY OF NEW SOUTH WALES

PARTICIPANT INFORMATION STATEMENT AND CONSENT FORM
(continued)

REVOCATION OF CONSENT

Meridional and hemi-meridional differences in normal corneal topography of South Asians, East Asians and Europeans

I hereby wish to **WITHDRAW** my consent to participate in the research proposal described above and understand that such withdrawal **WILL NOT** jeopardise any treatment or my relationship with The University of New South Wales.

.....

Signature

……

Date

.....

Please PRINT Name

The section for Revocation of Consent should be forwarded to

Mr. Vinod Maseedupally
PG Room, Level-3
School of Optometry and Vision Science
RM building (North wing), Gate 14
UNSW 2052
Ph: 93854536

D2 CHAPTERS 3 & 4 STUDIES

THE UNIVERSITY OF NEW SOUTH WALES

SCHOOL OF OPTOMETRY AND VISION SCIENCE

PARTICIPANT INFORMATION STATEMENT AND CONSENT FORM
Effects of Lens Dk/t on Efficacy of Orthokeratology

Orthokeratology (OK) is a method of using contact lenses to reshape the front surface of the eye to reduce myopia (short-sightedness). You are invited to participate in a study to investigate the effect of the oxygen transmissibility (Dk/t) of contact lenses on the efficacy of OK. You are selected as a possible participant in this study because you have good ocular health, show no contra-indications for contact lens wear, have myopia and corneal curvatures within the ranges required for this study and are aged between 18 and 40 years.

If you decide to participate, we will require you to attend a preliminary session to collect baseline measurements and perform lens fitting. This session will be of approximately 1 hour duration. You will also be taught insertion, removal, care and maintenance of the lenses at this visit. You will then be required to wear the lenses on an overnight (approximately 8 hours) basis for 14 nights. You will return for follow-up measurements after the first night of lens wear (day 1) within 1 hour of eye opening wearing the lenses, and again in the evening approximately 8 hours after lens removal. This visit schedule will be repeated on days 4, 7 and 14 of lens wear. Each of these sessions will take approximately 30 minutes. Lenses and lens care solutions will be free of charge for the duration of the study.

All study measurements are non-invasive and require no contact between the instrument and your eye:

- Refraction to determine the refractive error of your eye,
- Visual acuity

- Corneal curvature, using a computerized corneal mapping instrument, and
- Corneal thickness, using an optical pachometer

None of these measurement procedures carries any risk of physical injury or discomfort. You may experience mild discomfort after lens insertion because of the interaction between the rigid lens edge and your eyelid margins. Your vision may be slightly blurry during and after lens removal, particularly after the first night of lens wear. In the event of the incomplete correction of your refractive error, disposable soft contact lenses will be provided particularly if you are required to drive. Wearing rigid lenses overnight carries a slight risk. Mild epithelial disturbances, ocular inflammation, corneal infections and temporary lens adherence to the eye have been reported with overnight lens wear. In the context of this closely monitored study, the risks of such complications are minimal. In the unlikely event that ocular or other complications occur which will require medical intervention, you will be referred immediately to an appropriate health care practitioner. A 24 hour contact phone number will be provided for emergencies. You may also contact us during working hours on 9385 4613 if you have any concerns.

We cannot and do not guarantee or promise that you will receive any benefits from this study.

Any information that is obtained in connection with this study and that can be identified with you will remain confidential and will be disclosed only with your permission, except as required by law. If you give us your permission by signing this document, we plan to present selected information obtained from this study in the scientific press or at scientific conferences. The nature of the information disclosed will be the group average and individual responses of interest. In any publication, information will be provided in such a way that you cannot be identified.

Complaints may be directed to the Ethics Secretariat, The University of New South Wales, SYDNEY 2052 AUSTRALIA (phone 9385 4234, fax 9385 6648, email ethics.sec@unsw.edu.au). All complaints will be kept confidential. You will be informed of any outcomes.

Your decision whether or not to participate will not prejudice your future relations with the University of New South Wales. If you decide to participate, you are free to withdraw your consent and to discontinue participation at any time without prejudice. If you have any questions, please feel free to ask us. If you have any additional questions later, Dr Helen Swarbrick (9385 4373) will be happy to answer them. You will be given a copy of this form to keep.

You are making a decision whether or not to participate. Your signature indicates that, having read the Participant Information Statement, you have decided to take part in the study.

……

……..……

Signature of Research Participant

Signature of Witness

……

…….

(Please PRINT name)

(Please PRINT name)

……

Date

…….

Nature of Witness

……

Signature(s) of Investigator(s)

……

Please PRINT Name

REVOCATION OF CONSENT

Effects of Lens Dk/t on Efficacy of Orthokeratology

I hereby wish to WITHDRAW my consent to participate in the research study described above and understand that such withdrawal WILL NOT jeopardise any treatment or my relationship with The University of New South Wales.

……

…….

Signature Date

……

Please PRINT Name

The section for Revocation of Consent should be forwarded to Dr Helen Swarbrick, School of Optometry and Vision Science, The University of New South Wales, Sydney NSW 2052.

D3 CHAPTER 3 & 4 STUDIES

THE UNIVERSITY OF NEW SOUTH WALES

SCHOOL OF OPTOMETRY AND VISION SCIENCE

PARTICIPANT INFORMATION STATEMENT AND CONSENT FORM
Effects of Lens Dk/t on Efficacy of Orthokeratology – 2 week study

Orthokeratology (OK) is a method of using contact lenses to reshape the front surface of the eye to reduce myopia (short-sightedness). You are invited to participate in a study to investigate the effect of the oxygen transmissibility (Dk/t) of contact lenses on the efficacy of OK. An OK lens in a well-established lens material of moderate oxygen permeability (Dk) will be worn in one eye, and a matching OK lens in a new lens material of high Dk, which has not yet been released commercially in Australia, will be worn in the other eye. You are selected as a possible participant in this study because you have good ocular health, show no contra-indications for contact lens wear, have myopia and corneal curvatures within the ranges required for this study and are aged between 18 and 40 years.

If you decide to participate, we will require you to attend a preliminary session to collect baseline measurements and perform lens fitting. This session will be of approximately 1 hour duration. You will also be taught insertion, removal, care and maintenance of the lenses at this visit. You will then be required to wear the lenses on an overnight (approximately 8 hours) basis for 15 nights. You will return for follow-up measurements after the first night of lens wear (day 1) within 1 hour of eye opening wearing the lenses, and again in the evening approximately 8 hours after lens removal. This visit schedule will be repeated on days 4, 8, and 15 of lens wear. Each of these sessions will take approximately 45 minutes. Lenses and lens care solutions will be free of charge for the duration of the study. You may also be provided with supplementary disposable soft contact lenses for daytime wear

All study measurements are non-invasive and require no contact between the instrument and your eye:

- Refraction to determine the refractive error of your eye,
- Visual acuity
- Corneal curvature, using a computerized corneal mapping instrument, and
- Corneal thickness, using an optical pachometer

None of these measurement procedures carries any risk of physical injury or discomfort. You may experience mild discomfort after lens insertion because of the interaction between the rigid lens edge and your eyelid margins. Your vision may be slightly blurry during and after lens removal, particularly after the first night of lens wear. In the event of the incomplete correction of your refractive error, disposable soft contact lenses will be provided particularly if you are required to drive. Wearing rigid lenses overnight carries a slight risk. Mild epithelial disturbances, ocular inflammation, corneal infections and temporary lens adherence to the eye have been reported with overnight lens wear. In the context of this closely monitored study, the risks of such complications are minimal. In the unlikely event that ocular or other complications occur which will require medical intervention, you will be referred immediately to an appropriate health care practitioner. A 24 hour contact phone number will be provided for emergencies. You may also contact us during working hours on 9385 4613 if you have any concerns.

We cannot and do not guarantee or promise that you will receive any benefits from this study.

Any information that is obtained in connection with this study and that can be identified with you will remain confidential and will be disclosed only with your permission, except as required by law. If you give us your permission by signing this document, we plan to present selected information obtained from this study in the scientific press or at scientific conferences. The nature of the information disclosed will be the group average and individual responses of interest. In any publication, information will be provided in such a way that you cannot be identified.

Complaints may be directed to the Ethics Secretariat, The University of New South Wales, SYDNEY 2052 AUSTRALIA (phone 9385 4234, fax 9385 6648, email ethics.sec@unsw.edu.au).

Your decision whether or not to participate will not prejudice your future relations with the University of New South Wales. If you decide to participate, you are free to withdraw your consent and to discontinue participation at any time without prejudice. If you have any questions, please feel free to ask us. If you have any additional questions later, A/Prof. Helen Swarbrick (9385 4373) will be happy to answer them. You will be given a copy of this form to keep.

You are making a decision whether or not to participate. Your signature indicates that, having read the Participant Information Statement, you have decided to take part in the study.

……

……

Signature of Research Participant

Signature of Witness

…… ……

(Please PRINT name)

(Please PRINT name)

…… ……

Date

Nature of Witness

……

Signature(s) of Investigator(s)

……

Please PRINT Name

REVOCATION OF CONSENT

Effects of Lens Dk/t on Efficacy of Orthokeratology – 2 week study

I hereby wish to WITHDRAW my consent to participate in the research study described above and understand that such withdrawal WILL NOT jeopardise any treatment or my relationship with The University of New South Wales.

……

……

Signature Date

……

Please PRINT Name

The section for Revocation of Consent should be forwarded to A/Prof Helen Swarbrick, School of Optometry and Vision Science, The University of New South Wales, Sydney NSW 2052.

D4 CHAPTER 5 STUDY

Approval No (11019)

THE UNIVERSITY OF NEW SOUTH WALES

PARTICIPANT INFORMATION STATEMENT AND CONSENT FORM

Evaluation of lens decentration on toric corneas during overnight spherical orthokeratology lens wear

You are invited to participate in a study that involves the use of orthokeratology (OK) lenses, which are specifically designed rigid contact lenses worn overnight to reshape the cornea (front surface of your eye), to reduce near sightedness during the day. The cornea is normally spherical in shape (surface shaped like a soccer ball), although it sometimes can be non-spherical (toric, surface shaped like a football) by differing amounts. Traditionally OK lenses are used on patients with moderate amounts of near sightedness and low corneal toricity. We would like to investigate the effect of short term OK lenses on moderately toric corneas. You were selected as a possible participant in this study because your cornea is non-spherical in shape, i.e.toric by a moderate amount.

If you decide to participate, you will need to attend a contact lens fitting session where baseline measurements will also be taken, and two study measurements after overnight wear of the contact lenses. The following measurements will be conducted at each visit:

- Visual acuity: Standard eye testing charts
- Objective refraction: Shin Nippon NVision K5001 autorefractor
- Contrast sensitivity function (CSF): Computer generated charts
- Corneal topography: Medmont E300 corneal topographer
- Whole eye aberrations: Innovative Visual Systems (IVS) Discovery Aberrometer

Visual acuity (a measure of the clarity of your vision) is measured by asking how far you can read down a standard eye testing letter chart. Objective refraction is a measure of the strength of your eyes akin to the prescription used to describe the strength of glasses. The Shinn Nippon autorefractor measures refraction by measuring low intensity light reflected from the back of your eye. CSF is measured using sine-wave gratings displayed on a computer monitor. These gratings are alternating dark and light bands that are reduced in intensity until you cannot detect a difference between them. Whole eye aberrations are an assessment of the way light is focussed by your eye. The IVS Discovery measures whole eye aberrations by shining a low intensity beam of light (which you will not be able to see) into your eye and measuring how it is reflected from the back of your eye. The Medmont E300 corneal topographer measures the shape of your cornea by analysing a digitally captured black and white photograph of your eye. None of the instruments require contact with your eyes.

The study OK lenses will be calculated using proprietary lens fitting software based on the captured corneal topography data. You will then be required to wear the lenses for one night while staying on the UNSW Kensington Campus. Food and drinks will be provided during the overnight stay. The same study measurements that were taken at baseline (see above) will be repeated in the morning after the lenses are removed, and in the afternoon approximately eight hours after the morning visit. Each measurement session will take approximately 30 min.

You will be informed if only one of your eyes meet our criteria. In this circumstance you will be offer the option to wear the lens on one eye only and attend the overnight study on two occasions, with a two week washout period in between these visits to allow the studied eye to return to its original shape.

If you are a soft contact lens wearer, you will be required to stop lens wear for 48 hours initial visit. If you are a rigid gas permeable lens wearer, you will be required to stop lens wear for 1 week; this is to allow your cornea to return to its normal shape prior to the study.

None of these measurement procedures carries any risk of physical injury or discomfort. You may experience mild discomfort after lens insertion because of interaction between the rigid lens edge and your eyelid margins. Your vision may be slightly blurry during and after lens removal, particularly after one night wear. If you are given OK treatment in only one eye you are advised to wear contact lens or spectacles to correct your other eye. Wearing rigid lenses overnight carries slight risk. Mild epithelial disturbances, ocular inflammation, corneal infections and temporary lens adherence to the eye have been reported with overnight lens wear. In the context of this closely monitored study, the risks of such complications are minimal. In the unlikely event that ocular or other complications occur which require medical intervention you will be referred immediately to an appropriate health care practitioner. During any emergency (24 hours) you may contact Vinod Maseedupally(0430820017). You may also contact us during working hours on 9385 4613 if you have any concerns.

OK has been proven to be a safe and effective method to reduce moderate amounts of near sightedness in patients with low corneal toricity. The side effects of 1 night OK lens wear are expected to

be minimal. Possible side effects can include mild discomfort, tearing, fluctuation of vision, glare, and night driving difficulties. In the event of an occurrence, changes are expected to return to normal within 24 hours. Rarely, some people might develop superficial damage to the cornea due to wearing of the OK lens (although these cases are very rare). Arrangements have been made for immediate referral of the participant to an appropriate medical practitioner.

We cannot and do not guarantee or promise that you will receive any benefits from this study. Any information that is obtained in connection with this study and that can be identified with you will remain confidential and will be disclosed only with your permission, except as required by law. If you give us your permission by signing this document, we plan to present the results in scientific conferences or scientific journals. The information to be presented will be mean group data and individual responses of interest. In any publication, information will be provided in such a way that you cannot be identified.

Complaints may be directed to the Ethics Secretariat, The University of New South Wales, SYDNEY 2052 AUSTRALIA (phone 9385 4234, fax 9385 6648, email ethics.sec@unsw.edu.au). Any complaint you make will be investigated promptly and you will be informed out the outcome.

If you would like to have a summary of our findings as well as any implications after the study has completed, please let us know and provide your contact details. On study completion a short summary of the study results will also be displayed in our website http://www.optom.unsw.edu.au/research/rokindex.html. after the completion of the study.

Your decision whether or not to participate will not prejudice your future relations with the University of New South Wales. If you decide to participate, you are free to withdraw your consent and to discontinue participation at any time without prejudice. If you have any questions, please feel free to ask us. If you have any additional questions later, Mr. Vinod Maseedupally (Ph-93854536/email-vinodm@student.unsw.edu.au) will be happy to answer them.

You will be given a copy of this form to keep.

THE UNIVERSITY OF NEW SOUTH WALES

PARTICIPANT INFORMATION STATEMENT AND CONSENT FORM (continued)

Evaluation of lens decentration on toric corneas during overnight spherical orthokeratology lens wear

You are making a decision whether or not to participate. Your signature indicates that, having read the information provided above, you have decided to participate.

.....
.....

Signature of Research Participant | Signature of Witness

.....
.....

(Please PRINT name) | (Please PRINT name)

.....
.....

Date | Nature of Witness

REVOCATION OF CONSENT

Evaluation of lens decentration on toric corneas during overnight spherical orthokeratology lens wear

I hereby wish to **WITHDRAW** my consent to participate in the research proposal described above and understand that such withdrawal **WILL NOT** jeopardise any treatment or my relationship with The University of New South Wales.

…… ……

Signature Date

……

Please PRINT Name

The section for Revocation of Consent should be forwarded to

Mr. Vinod Maseedupally
PG Room, Level-3
School of Optometry and Vision Science
RM building (North wing), Gate 14
UNSW 2052
Ph: 93854536

D5 CHAPTER 6 STUDY

Approval No : 11065

THE UNIVERSITY OF NEW SOUTH WALES

PARTICIPANT INFORMATION STATEMENT AND CONSENT FORM

Evaluating the performance of toric orthokeratology lenses

You (*i.e. the research participant*) are invited to participate in a study that involves the use of orthokeratology (OK) lenses, which are specifically designed rigid contact lenses worn overnight to reshape the cornea (front surface of your eye), to reduce near sightedness during the day. The cornea is normally spherical in shape (surface shaped like a soccer ball), although it sometimes can be non-spherical (toric, surface shaped like a rugby ball) by differing amounts. Traditionally OK lenses are used on patients with moderate amounts of near sightedness and low corneal toricity. We (*i.e. the investigators*) would like to investigate the performance of toric OK lenses on highly toric corneas. You were selected as a possible participant in this study because your cornea is non-spherical in shape, i.e. toric. The inclusion criteria for this study are:

Age 18- 45 years,

Myopia (Near sightedness): -1.00 to -4.50 DS,

Limbus-to-limbus corneal toricity between 1.50 to 4.50 D, at least in one eye.

No ocular disease or history of ocular trauma

Good health and no medications which may influence ocular health

If you are interested to participate you will need to attend a screening test that will decide your suitability to continue in the study. The following optometric tests will be conducted to determine subject eligibility which will take approximately 20 minutes.

Slit-lamp bio-microscopy

Visual acuity: Standard eye testing charts

Objective refraction: Shin Nippon NVision K5001 autorefractor

Subjective refraction

Corneal topography: Medmont E300 corneal topographer

Whole eye aberrations: Innovative Visual Systems (IVS) Discovery Aberrometer

Slit-lamp bio-microscopy assesses your eye's health. This instrument projects a small beam of light while you rest your chin and head on a mount. This is a routine optometric procedure. Visual acuity (a measure of the clarity of your vision) is measured by asking how far you can read down a standard eye testing letter chart. Objective refraction is a measure of the strength of your eyes akin to the prescription used to describe the strength of glasses. The Shin Nippon autorefractor measures refraction by measuring low intensity light reflected from the back of your eye. Subjective refraction is a method that is routinely used in optometry practice that guides us to arrive at your final prescription based on the objective refraction values. This involves you to give verbal responses to the various combinations of lenses that are presented to you. The Medmont E300 corneal topographer measures the shape of your cornea by analysing a digitally captured black and white photograph of your eye. Whole eye aberrations are an assessment of the way light is focussed by your eye. The IVS Discovery measures whole eye aberrations by shining a low intensity beam of light (which you will not be able to see) into your eye and measuring how it is reflected from the back of your eye. None of the instruments require contact with your eyes.

If you are suitable for participation in the study you will be required to attend a contact lens fitting session which will take approximately 20 mins each session.

Lens fitting period:

This consists of at least 1visit and a maximum of 3 visits each lasting approximately 20 minutes.

Based on the information obtained in the screening visit trial, OK lenses of two different designs will be ordered. Initially one design (type 1) of OK lens will be fitted in both eyes. You will be required to wear this trial pair overnight i.efor one night. Instructions on using these lenses will be given. After an overnight wear, lens fit will be assessed on the following morning. If one or both lenses do not fit acceptably, another fit with slightly different parameters from the same design will be fitted. If both eyes show acceptable fit, a second design (type 2) of OK lens will be fitted in both eyes. Three days of

washout period (no lens wear) will be given between wearing of these two different lens designs. The same steps that were followed to fit type 1 design will be followed for fitting type 2 design. If any one or both OK lens designs cannot be fitted acceptably you will be discontinued from the study. If both lens designs are fitted acceptably then you will enter in to the next phase of the study (Data collection period).

Data collection period:

This consists of five visits each lasting approximately 20 minutes.

Visit 1 (day 0): This visit will be conducted after three days of washout (no lens wear) after the previous lens wear trial.

Baseline measurements will be taken and study lenses are dispensed. Lens designs (type 1 or type 2) dispensed based on the two scenarios explained below:

Scenario 1:

This scenario is followed only if you have sufficient refractive astigmatism in both eyes, and will be randomised to wear a type 1 lens in one eye and a type 2 lens in the fellow eye.

Lenses will be trialled overnight in both eyes

OR

Scenario 2:

This scenario is followed if you have sufficient refractive astigmatism in only one eye.

The eligible eye will be randomly allocated to wear a type 1 or type 2 lens on the first wearing schedule.

A minimum washout period of 2 weeks without lens wear will then be commenced before you wear the alternative study lens (type 1 or 2) in the same eye.

To ensure that you maintain good vision during the study period, the fellow eye will be fitted either with standard OK lenses or soft contact lenses for day time wear.

The fellow eye will not be included in the study, and the reason for fitting the eye to correct vision is purely to provide you with a comfortable vision for normal daily activities throughout the duration of the study.

Visit 2 (day 1 am): Morning visit after one single overnight wear, within 1 hour after lens removal.

Visit 3 (day 1 pm): 7 hours after the morning visit.

Visit 4 (day 7 am): Morning visit after 7 nights of study lens wear.

Visit 5 (day 7 pm): 7 hours after the morning visit.

At all these visits measurements that were conducted at the time of screening will be repeated.

At the first measurement visit after the first night of lens wear you will be required to attend the clinic while still wearing your lenses. This assists us in the measurements we will be taking, but also provides the opportunity to give you further instruction on how to remove your lenses. Thereafter you will be required to remove your lenses in the morning. You will be advised not to drive on your way to your first visit because the lenses may blur your vision while being worn.

You will be informed if only one of your eyes meet our criteria for study participation. In this circumstance you will be offered the option to wear a study lens on one eye only and attend the lens wearing study periods over two occasions, with a two week washout period between these periods to allow the studied eye to return to its original shape. In this scenario you will be given the option to have soft contact lenses, glasses or standard OK lenses fitted to correct the vision of your other (non study lens wearing) eye.

If you are a soft contact lens wearer, you will be required to stop lens wear for 48 hours before the initial visit. If you are a rigid gas permeable lens wearer, you will be required to stop lens wear for 1 week prior to commencement of the study; this is to allow your cornea to return to its normal shape prior to the study.

None of these measurement procedures carries any risk of physical injury or discomfort. You may experience mild discomfort after lens insertion because of the interaction between the rigid lens edge and your eyelid margins. Your vision may be slightly blurry during and after lens removal, particularly after the first night of lens wear. In the event of the incomplete correction of your refractive error, supplementary disposable soft contact lenses will be provided for day-time wear particularly if you are required to drive. ***Some photographs of the eye may be taken in this study. However, due to the highly magnified nature of the photographs, you will not be able to be identified.***

Wearing rigid lenses overnight carries a slight risk. Mild epithelial disturbances, ocular inflammation, corneal infections and temporary lens adherence to the eye have been reported with overnight lens wear. In the context of this closely monitored study, the risks of such complications are minimal. ***There is an exceptionally rare but possible risk of possible severe infections/blindness. The risk of adverse reactions in rigid contact lens wear is very small (0.44-2.5/10,000 patients per year of lens wear), and significantly lower than the risk posed by soft contact lens use.*** We will teach you how to identify and safely free up an adherent lens, and how to recognise warning signs of other adverse responses. In the unlikely event that ocular or other complications occur which will require medical intervention, you will be referred immediately to an appropriate health care practitioner ***at no cost to***

yourself. You may contact a 24 hour contact phone number 0430 820 017 (Vinod Maseedupally) for emergencies. You may also contact us during working hours on 9385 4613 if you have any concerns.

We cannot and do not guarantee or promise that you will receive any benefits from this study. Any information that is obtained in connection with this study and that can be identified with you will remain confidential and will be disclosed only with your permission, except as required by law. If you give us your permission by signing this document, we plan to present the results in scientific conferences or scientific journals. The information to be presented will be mean group data and individual responses of interest. In any publication, information will be provided in such a way that you cannot be identified.

For your time spent during the study you will receive $50 as compensation for out of pocket expenses, after completion of the study. The contact lens cleaning solutions, lens case and other related products will be supplied free of charge.

Complaints may be directed to the Ethics Secretariat, The University of New South Wales, SYDNEY 2052 AUSTRALIA (phone 9385 4234, fax 9385 6648, email ethics.sec@unsw.edu.au). Any complaint you make will be investigated promptly and you will be informed out the outcome.

If you would like to have a summary of our findings as well as any implications after the study has completed, please let us know and provide your contact details. On study completion a short summary of the study results will also be displayed in our website http://www.optom.unsw.edu.au/research/rokindex.html. after the completion of the study.

Your decision whether or not to participate will not prejudice your future relations with the University of New South Wales. If you decide to participate, you are free to withdraw your consent and to discontinue participation at any time without prejudice.

If you have any questions, please feel free to ask us. If you have any additional questions later, (*Dr. Paul Gifford, 93854373, email: p.gifford@unsw.edu.au)* will be happy to answer them.

You will be given a copy of this form to keep.

THE UNIVERSITY OF NEW SOUTH WALES

PARTICIPANT INFORMATION STATEMENT AND CONSENT FORM
(continued)

Evaluating the performance of toric orthokeratology lenses

You are making a decision whether or not to participate. Your signature indicates that, having read the information provided above, you have decided to participate.

.....

Signature of Research Participant | Signature of Witness

.....
.....

(Please PRINT name) | (Please PRINT name)

..... | .....

Date | Nature of Witness

REVOCATION OF CONSENT

Evaluating the performance of toric orthokeratology lenses

I hereby wish to **WITHDRAW** my consent to participate in the research proposal described above and understand that such withdrawal **WILL NOT** jeopardise any treatment or my relationship with The University of New South Wales, *(other participating organisation[s] or other professional[s])*.

....

Signature Date

.....

Please PRINT Name

The section for Revocation of Consent should be forwarded to Mr. Vinod Maseedupally (vinodm@student.unsw.edu.au).

APPENDIX E

Publications and presentations arising from this thesis

Published abstracts

Maseedupally VK, Gifford P, Swarbrick HA (2011). Hemi-meridional topographic differences in normal cornea and relationship to eyelid morphometry; 13th Scientific Meeting in Optometry and 7th Optometric Educators Meeting (SEMO). Clin Exp Optom 94: e1-e16.

Maseedupally VK, Gifford P, Swarbrick HA (2011). Hemi-meridional differences in corneal topography in relation to ethnicity and eyelid morphometry. Invest Ophthalmol Vis Sci 52: E-abstract 4191.

Gifford P, Maseedupally V, Lum E, Swarbrick HA (2011). Sectorial corneal curvature changes during myopic orthokeratology. Invest Ophthalmol Vis Sci 52: E-abstract 6550.

Gifford P, Maseedupally V, Lum E, Swarbrick HA (2011). Regional changes to corneal curvature in myopic orthokeratology. Contact Lens Ant Eye 34;Supplement 1:S24-25.

Maseedupally VK, Gifford P, Lum E, Naidu R, Sidawi D, Wang B, Swarbrick HA (2012). Treatment zone decentration during orthokeratology on eyes with low and moderate amounts of corneal toricity. Invest Ophthalmol Vis Sci 53: E-abstract 4714.

Presentations

Maseedupally V, Gifford P, Swarbrick HA (2010). Eye shape and eyelid morphometry. The Eighth Congress of the Orthokeratology Society of Oceania, Gold Coast, Australia

Maseedupally VK, Gifford P, Lum E, Naidu R, Sidawi D, Wang B, Swarbrick HA (2012). Spherical orthokeratology, corneal toricity and treatment zone decentration effects.The Tenth Congress of the Orthokeratology Society of Oceania, Gold Coast, Australia

Maseedupally VK, Gifford P, Lum E, Naidu R, Sidawi D, Wang B, Swarbrick HA (2012). Treatment zone decentration during spherical orthokeratology on moderately toric corneas. 14th Scientific Meeting in Optometry and 8th Optometric Educators Meeting (SEMO), Melbourne, Australia.

Maseedupally VK, Gifford P, Lum E, Naidu R, Sidawi D, Wang B, Swarbrick HA (2012). Treatment zone decentration during spherical orthokeratology on moderately toric corneas. 14th International Cornea and Contact Lens Congress, Sydney, Australia (presented as an electronic poster).